The Role of Adipocytes in the Breast Cancer Tumour Microenvironment

Soofiyah Parveen Ayaani

MB ChB BMedSc MRCSEd

A Thesis submitted to The University of Warwick in partial fulfilment of the requirements for the degree of

Doctor of Medicine

Warwick Medical School

August 2020

CONTENTS

List of Figures ..... **viii**

List of Tables ..... **xi**

Acknowledgements ..... **xii**

Declaration ..... **xiv**

Abstract ..... **xv**

Abbreviations ..... **xvi**

Chapter One: Introduction

1.1	**Introduction……...**	**4**
1.2	**The Breast……...**	**4**
1.2.1	Embryology and Anatomy of the Breast……...	5
1.2.2	Structure of the Adult Female Breast……	5
1.2.3	Vasculature and Lymphatics of the Breast……	7
1.2.4	Histology of the Breast…….	7
1.3	**Assessment of Patients with Breast Symptoms…….**	**9**
1.4	**Cancer……**	**10**
1.4.1	Theories of the Development of Sporadic Cancers……...	10
1.4.1.1	Somatic Mutation Theory…….	11
1.4.1.2	Tissue Organisation Field Theory…….	14
1.5	**Breast Cancer……**	**15**
1.5.1	Statistics of Breast Cancer……	15
1.5.2	Risk Factors for Breast Cancer…….	16
1.5.3	The Pathology of Breast Cancer……...	17
1.5.3.1	Histological Subtypes of Breast Cancer……	17
1.5.3.2	Grading of Breast Cancer…….	18
1.5.3.3	Oestrogen Receptors……	18
1.5.3.4	HER2 Receptors……..	20
1.5.3.5	Molecular Subclassifications of Breast Cancer……..	21
1.5.3.6	Signalling Pathways in Breast Cancer……	21

1.5.4 The Management of Breast Cancer……... 24
1.6 The Breast Cancer Tumour Microenvironment……. 24
1.6.1 Adipose Tissue……. 26
1.6.1.1 Adipogenesis…… 26
1.6.1.2 Types and Functions of Adipose Tissue……... 28
1.6.1.3 Adipose Tissue as an Endocrine Organ…… 28
1.6.1.4 Abnormal Adipose Tissue in Obesity……... 29
1.6.2 The Mammary Fat Pad……. 31
1.6.3 Adipocytes in the Tumour Microenvironment…….. 32
1.6.4 Adipokines in the Breast Tumour Microenvironment……... 34
1.6.4.1 Adipokines……... 34
1.6.4.2 Common Adipokines of the Breast Tumour Microenvironment ….. 34
1.7 Aim of the Study…… 36
1.8 Ethical Approval…… 37

Chapter Two: Materials and Methods

2.1 Materials…… 41
2.1.1 Cell Lines……. 41
2.1.2 Cell Line and Explant Culture Chemicals……. 41
2.1.3 Media Formulations……. 42
2.1.4 General Chemicals and Reagents…….. 43
2.1.5 Primers……. 44
2.1.6 Kit…… 44
2.1.7 Miscellaneous……... 45
2.2 Methods…….. 46
2.2.1 Fresh Tissue……. 46
2.2.1.2 Explant Culture…… 46
2.2.2 Cell Lines……. 47
2.2.2.1 MCF-7 Cells……. 47
2.2.2.2 MCF-7 Cell Retrieval…… 49
2.2.2.3 MCF-7 Cell Subculture……. 49
2.2.2.4 MCF-7 Cell Cryopreservation……... 49

2.2.2.5 MDA-MB-231 Cells……. 50
2.2.2.6 MDA-MB-231 Cell Retrieval, Subculture, and Cryopreservation….. 50
2.2.2.7 SGBS Cells……... 50
2.2.2.8 SGBS Cell Recovery……. 51
2.2.2.9 SGBS Cell Subculture..……. 51
2.2.2.10 SGBS Cell Differentiation…… 52
2.2.3 Cell Lysis…….. 54
2.2.4 RNA Extraction……... 54
2.2.5 Cell Co-Culture…… 55
2.2.5.1 Cell Co-Culture for Media Harvesting ……. 55
2.2.5.2 Cell Co-Culture for RNA Extraction…… 57
2.2.6 Proteome Profiler™ Human XL Cytokine Array Kit…… 57
2.2.7 xCELLigence® RTCA™ DP Cell Proliferation Assay……... 59
2.2.7.1 xCELLigence® Optimisation…… 59
2.2.7.2 Co-Culture xCELLigence® Experiment…… 61
2.2.8 Chitinase 3 Like-1 Stimulation of MCF-7 and MDA-MB-231 Cells.. 64
2.2.9 Staining of Adipocytes with Oil Red O……. 64
2.2.10 Reverse Transcription and Polymerase Chain Reaction…… 65
2.2.11 Reverse Transcription……... 65
2.2.12 Polymerase Chain Reaction…….. 66
2.2.13 Statistical Analysis…… 68
2.2.13.1 Student's t-Test…… 68
2.2.13.2 Wilcoxon Matched-Pairs Signed-Ranks Test……. 69
2.2.13.4 ANOVA……... 69
2.2.13.5 Post Hoc Tests……. 70

Chapter Three: The Effect of Pre-Differentiated and Mature SGBS Adipocytes on the Rate of Proliferation of MCF-7 and MDA-MB-231 Cancer Cells

3.1 Introduction…… 73
3.2 Selecting Appropriate Cell Types for Experimentation…….. 73
3.2.1 Breast Cancer Cell Lines……... 74
3.2.1.1 MCF-7 Cells……. 74

3.2.1.2 MDA-MB-231 Cells…… 74
3.2.2 SGBS Cells…….. 77
3.3 Aims of this Chapter…… 77
3.4 Optimal Seeding Density of Breast Cancer Cell Lines…….. 78
3.4.1 Optimal Seeding Density of MCF-7 Cells…… 79
3.4.2 Optimal Seeding Density of MDA-MBA-231 Cells…….. 79
3.5 The Effects of SGBS Cells on Cancer Cell Proliferation…… 79
3.5.1 Co-Culture: MCF-7 Cells with Pre-Differentiated SGBS Cells……. 81
3.5.2 Co-Culture: MCF-7 Cells with Mature SGBS Cells…….. 81
3.5.3 Co-Culture: MDA-MB-231 Cells with Pre-Differentiated SGBS Cells.. 84
3.5.4 Co-Culture: MDA-MB-231 Cells with Mature SGBS Cells……... 84
3.6 Discussion…… 87
3.7 Conclusion…… 89

Chapter Four: Differences in Cytokine Secretion and Gene Expression of Adipose Tissue and Adipocytes, Dependent upon Proximity to Cancer

4.1 Introduction…… 93
4.1.1 Cytokines in the Tumour Microenvironment ……..... 93
4.2 Aims of the Chapter……..... 93
4.3 Explant Culture and Proteome Array Analysis…… 94
4.3.1 Differences in Cytokine Secretory Profile of Peri-Tumoural Adipose Tissue Compared to Resection Margin Tissue, in Patients with ER^+ Breast Cancer ……..... 95
4.3.2 Differences in Cytokine Secretory Profile of Peri-Tumoural Adipose Tissue Compared to Resection Margin Tissue, in Patients with Triple Negative Breast Cancer……. 100
4.3.3 Combined ER^+ and Triple Negative Breast Cancer Data……..…. 109
4.4 SGBS and MCF-7 Cell Co-Culture Media Cytokine and Gene Analysis……..... 109
4.4.1 SGBS and MCF-7 Cell Co-Culture Media Cytokine Analysis……..…. 109
4.4.2 SGBS Select Cytokine Gene Expression Analysis……..…. 113

4.4.2.1 SGBS Select Cytokine Gene Expression Time Course……..….. 113
4.4.2.2 Gene Expression Profile of SGBS Co (MCF-7) Adipocytes Compared to SGBS Alone Adipocytes…….….. 119
4.4.2.3 Gene Expression Profile of SGBS Co (MDA-MB-231) Adipocytes Compared to SGBS Alone Adipocytes…….……. 119
4.5 Discussion…….. 123
4.6 Conclusion……..... 125

CHAPTER FIVE: CHI3L1 Stimulation of Breast Cancer Cells

5.1 Introduction…… 128
5.2 CHI3L1 - An Overview…….. 128
5.2.1 Functions of CHI3L1……..... 128
5.2.2 CHI3L1 in Cancer and in the Tumour Microenvironment ……..... 129
5.2.3 CHI3L1 in the Breast and Breast Cancer……..... 131
5.3 Aims of this Chapter…….. 132
5.4 CHI3L1 Stimulation of Breast Cancer Cells…….…… 132
5.4.1 MCF-7……..….. 133
5.4.2 MDA-MB-231……..….. 133
5.5 Discussion……..... 136
5.6 Conclusion…….. 136

CHAPTER SIX: DISCUSSION

6.1 General Discussion…….. 139
6.1.1 General Comments: Proliferation of ER^+ and Triple Negative Breast Cancer Cell Lines in the Presence and Absence of Pre-Differentiated and Mature SGBS Adipocytes…… 140
6.1.2 General Comments: The Influence of ER^+ and Triple Negative Breast Cancer on Adipose Tissue and Adipocyte Cytokine Secretion…… 141
6.1.3 General Comments: CHI3L1 Stimulation of MCF-7 and MDA-MB-231 Cells…… 143

6.2 Conclusion……..…. 144

6.3 Future Work…….... 145

6.4 Clinical Implications……..……. 145

Appendix A:

SGBS - Cancer Co-Culture (Additional Data)……. 147

Appendix B:

Proteome Profiler™ Human XL Cytokines List……. 156

Appendix C:

Differences in Cytokine Secretion Profiles of:

- Peri-Tumoural and Resection Margin Breast Tissue Explants
- SGBS Co and SGBS Alone…… 161

Appendix D:

CHI3L1 Stimulation of MCF and MDA-MB-231 Cells

(Additional Data)……..……. 171

References……. 176

LIST OF FIGURES

1.1	Anatomy and Vasculature of the Adult Female Breast……..	6
1.2	Histology of the Adult Female Breast……...	8
1.3	Hallmarks of Cancer…….....	13
1.4	Nottingham Grading Score for Breast Cancer……..	19
1.5	The PI3K/AKT/mTOR Signalling Pathway…….....	23
1.6	Breast Cancer and its Proximity to Adipose Tissue……...	25
1.7	The Breast Cancer Tumour Microenvironment…….....	25
2.1	Human Breast Tissue Explants…….....	48
2.2	SGBS Cell Differentiation Protocol……..	53
2.3	SGBS and Breast Cancer Cells Co-Culture Construct…….....	56
2.4	Light Microscopy of Breast Cancer Cells Cultured in a Corning® Transwell® Insert……..	56
2.5	xCELLigence® E-Plate® 16……...	60
2.6	Flow of Electrons in a Media-Containing xCELLigence® E-Plate® Well……..	60
2.7	Light Microscopy of Freshly Seeded MCF-7 Cells in a Single Well of an xCELLigence® E-Plate® View 16……...	62
2.8	xCELLigence® Co-Culture Experiment Layout…….	63
2.9	xCELLigence® Insert…….	63
3.1	The Molecular Profile and Characteristics of MCF-7 Cells…….....	76
3.2	MCF-7 Seeding Density Optimisation…….....	80
3.3	MDA-MB-231 Seeding Density Optimisation…….....	80
3.4	MCF-7 Proliferation when Co-Cultured with Pre-Differentiated SGBS (Representative Experiment)…….……..	82
3.5	MCF-7 Proliferation when Co-Cultured with Mature SGBS (Representative Experiment)……..	83
3.6	MDA-MB-231 Proliferation when Co-Cultured with Pre-Differentiated SGBS (Representative Experiment)…….....	85

3.7 MDA-MB-231 Proliferation when Co-Cultured with Mature SGBS (Representative Experiment)…….. 86

4.1 Haematoxylin & Eosin Stained Slide of Human Breast Adipose Tissue Post 24 h Culture……..……..…... 97
4.2 Log_2 Fold Change of Cytokines in ER^+ Explant Media: Peri-Tumoural Tissue Compared to Resection Margin Tissue……..…… 98
4.3 Log_2 Fold Change of Select Cytokines in ER^+ Explant Media: Peri-Tumoural Tissue Compared to Resection Margin Tissue……... 99
4.4 Select Cytokine Secretion by Resection Margin and Peri-Tumoural Breast Tissue in Patients with ER^+ Breast Cancer……. 102
4.5 Log_2 Fold Change of Cytokines in Triple Negative Explant Media: Peri-Tumoural Tissue Compared to Resection Margin Tissue…….. 103
4.6 Log_2 Fold Change of Select Cytokines in Triple Negative Explant Media: Peri-Tumoural Tissue Compared to Resection Margin Tissue……. 104
4.7 Select Cytokine Secretion by Resection Margin and Peri-Tumoural Breast Tissue in Patients with Triple Negative Breast Cancer……..... 107
4.8 Log_2 Fold Change of Cytokines in ER^+ and Triple Negative Explant Media: Peri-Tumoural Tissue Compared to Resection Margin Tissue. 110
4.9 Log_2 Fold Change of Select Cytokines in ER^+ and Triple Negative Explant Media: Peri-Tumoural Tissue Compared to Resection Margin Tissue……. 111
4.10 Select Cytokine Secretion by Resection Margin and Peri-Tumoural Breast Tissue: Combined Data for ER^+ and TN Samples……..... 112
4.11 Log_2 Fold Change of Cytokines in Cell Co-Culture Media: SGBS MCF-7 Co-Culture Media Compared to SGBS Alone Media…….. 114
4.12 Select Cytokine Secretion by SGBS Cells Cultured Alone and in Co-Culture with MCF-7 Cells……... 117
4.13 Expression of Select Genes in SGBS Adipocytes at Different Stages of Differentiation……... 120
4.14 Expression of Select Genes in SGBS Adipocytes Cultured Alone and in Co-Culture with MCF-7 Cells……. 121

4.15 Expression of Select Genes in SGBS Adipocytes Cultured Alone and in Co-Culture with MDA-MB-231 Cells…….. 122

5.1 Chitinase 3-Like 1 in Cancer Progression…… 130
5.2 MCF-7 Proliferation when Cultured in the Absence and Presence of Chitinase 3-Like 1……... 134
5.3 MDA-MB-231 Proliferation when Cultured in the Presence and Absence of Chitinase 3-Like 1…… 135

LIST OF TABLES

1.1	Molecular Subclassification of Breast Cancer……	22
1.2	Select Regulators of Adipose Tissue Function……..	27
2.1	Primer Sequences (Human Genes)……	44
2.2	Media for SGBS Cell Differentiation…….	53
3.1	Molecular Subclassification of Breast Cancers and Cell Lines….	75
4.1	Human Breast Adipose Tissue Samples Processed…….	96
4.2	Cytokines Increased in Peri-Tumoural ER^+ Explant Media…...	101
4.3	Ten Most Increased Cytokines in Peri-Tumoural Triple Negative Explant Media…….	105
4.4	Ten Most Increased Cytokines in SGBS Co Media…….	115

ACKNOWLEDGEMENTS

This research period has been a journey of countless highs and lows, and I am indebted to so many for their help along this sometimes very rocky road.

I am extremely grateful to my Supervisory team for their continued guidance and support. Four years after meeting Professor Shervanthi Homer-Vanniasinkam, I remain in awe of her. Her commitment and drive, her energy, and her extraordinary knowledge on vast topic areas are an inspiration. Our chats have been fascinating and thought-provoking. I would like to express my gratitude for all she has done over these years, and I look forward to continuing my research journey with her. I will be forever grateful to Professor Mark Christian for joining the team and 'saving me' when the need for a new Laboratory Supervisor unexpectedly arose. I cannot thank him enough for his patience and understanding, particularly when I, as a Clinician ("…that sounds like a great idea, Mark… what does it mean?"), felt lost in the world of laboratory research, and for his guidance and invaluable input at every stage. Associate Clinical Professor Joseph Hardwicke has been incredible in his ongoing support, motivation, and insight. Always available when I needed advice, Joe has helped me more than I am sure he realises. My heartfelt thanks go to him. Mrs Abigail Tomlins is an amazing no-nonsense problem-solver. My sincerest gratitude goes to her for her time, support, guidance, motivational chats, and (near-lethal) strong coffee! I look forward to us perhaps working together again one day. My thanks also go to Dr Raghu Adya; the journey did not go quite as planned, but you have nonetheless taught me so much. Thank you also to Professor Andrew Beggs (University of Birmingham) for his time, advice, and support. It is very much appreciated.

Immense thanks go to Professor Christopher Imray and Ceri Jones of Research and Development at UHCW NHS Trust for funding the project. Without your input this research could not have happened. It was a lot to ask of you, and I am extremely grateful.

I would like to thank the patients who very kindly agreed to donating tissue to the project; the research would have been poorer had it not been for their generosity; and

the staff of the Arden Tissue Bank in obtaining and processing the samples. To the wonderful Sean James and his team (Adrian Fisk and Andrew White), thank you for always trying to accommodate me and my research needs. Your assistance, your humour, and your understanding will not be forgotten. My gratitude also to the Pathologists who processed the samples; thank you.

To my fellow (PGR student and Post-Doc) inhabitants of the CSB second floor office - I have made friends for life. Thank you for always helping when I needed it, and for bringing a little craziness to my research experience! You are an amazing group of people and I miss you.

My greatest thanks of all go to my loved ones. Thank you for your faith in me, your encouragement, your understanding, your patience, … the list is endless. I do not have sufficient words to express what it means to me to have your love and your support. Thank you.

DECLARATION

This thesis is submitted to the University of Warwick in support of my application for the degree of Doctor of Medicine. It has been composed by myself and has not been submitted in any previous application for any degree.

Soofiyah P Ayaani

ABSTRACT

Breast cancer is the commonest female malignancy worldwide. Although 10-year survival is good at over 75%, patients with more advanced or aggressive cancers have markedly poorer outcomes. Over recent years, the (benign) tissue local to a malignancy has generated considerable interest as promoting cancer progression. Within this *tumour microenvironment*, the role of the once neglected adipocyte is becoming clearer, although much work is still needed to fully understand the part it plays. This study aimed to further investigate the role of adipocytes in the breast cancer tumour microenvironment, with a view to identifying cytokines which may, with further research, be potential novel therapeutic targets and improve breast cancer outcome.

First, experiments were conducted to analyse the effects on breast cancer cell line proliferation when co-cultured with (SGBS) adipocytes. ER^+ (MCF-7) and triple negative (MDA-MB-231) cell lines were selected. Experiments demonstrated an increase in MCF-7 proliferation when co-cultured with both pre-differentiated and mature SGBS cells. Rate of proliferation of MDA-MB-231 cells was decreased when co-cultured with pre-differentiated SGBS cells but increased when grown alongside mature adipocytes.

Next, proteome profile analysis was undertaken to investigate cytokine secretion of fresh human breast tissue explants from patients with ER^+ and triple negative cancers. Peri-tumoural and distant adipose tissue was cultured. Cytokines in peri-tumoural ER^+ explant media were reduced as compared to the resection margin (control) media, whereas a greater number of cytokines were increased in triple negative peri-tumoural media. Additionally, further SGBS/MCF-7 co-cultures were undertaken, and proteome analysis conducted. Interestingly, this demonstrated an increase in a greater number of cytokines in the media of SGBS cells co-cultured as compared to media from peri-tumoural (ER^+) explant tissue. Gene expression analysis was undertaken for select cytokines and CHI3L1 identified as a cytokine of interest.

Finally, MCF-7 and MDA-MB-231 cells were cultured in media containing CHI3L1, and proliferation assessed. MCF-7 proliferation was significantly higher in stimulated cells, and MDA-MB-231 cells demonstrated some increase in proliferation also. CHI3L1 has thus been identified as a potential novel therapeutic target. More research is needed to further explore its stimulatory effects on breast cancer cells.

ABBREVIATIONS

μm	Micrometre(s)
μM	Micromolar
AB6	Array buffer 6
AKT	Protein kinase B
AMPK	Adenosine monophosphate activated protein kinase
ANOVA	Analysis of variance
AT	Adipose tissue
ATB	Arden Tissue Bank
BAT	Brown adipose tissue
BC	Breast cancer
BC	Before Christ
Bcl-2	B-cell lymphoma 2
Bcl-XL	B-cell lymphoma extra large
BMI	Body mass index
BRCA1	Breast cancer gene 1
BRCA2	Breast cancer gene 2
c.	*Circa*
C/EBP α	CCAAT/enhancer-binding protein α
C/EBP β	CCAAT/enhancer-binding protein β
CAA	Cancer associate adipocytes
CAF	Cancer associated fibroblast
c-AMP	Cyclic Adenosine Monophosphate
CC	Cancer cells
cDNA	Complementary DNA
CHI3L1	Chitinase 3-like 1
CLP	Chitinase like protein
CO_2	Carbon dioxide
CREB	cAMP-Response Element Binding Protein
CSF-1	Colony stimulating factor - 1
CSRL	Clinical Sciences Research Laboratory
DCIS	Ductal carcinoma *in situ*

DMEM	Dulbecco's modified Eagle's medium
DMSO	Dimethyl sulfoxide
DNA	Deoxyribonucleic acid
DNAse	Deoxyribonuclease
dNTP	Deoxyribonucleotide triphosphate
EC	Endothelial cells
ECACC	European Collection of Authenticated Cell Cultures
ECM	Extracellular matrix
EGF	Epidermal growth factor
eIF4E	Eukaryotic translocation initiation factor 4e
ENA-78	Epithelial cell derived neutrophil activating peptide - 78
ER	Oestrogen receptor
ER	Endoplasmic reticulum
ER^+	Oestrogen receptor positive
EV	Extracellular vesicle
FABP4	Fatty acid-binding protein 4
FBS	Foetal bovine serum
FC	Fold change
FCS	Foetal calf serum
FGFR	Fibroblast growth factor receptor
g	Gravity
G-CSF	Granulocyte colony-stimulating factor
GM	General medium
GROα	Growth regulated protein α
h	Hour(s)
H&E	Haematoxylin and Eosin
HER2	Human epidermal growth factor receptor 2
$HER2^+$	HER2 receptor positive
HIF-1α	Hypoxia-inducible factor - 1α
HRT	Hormone replacement therapy
I	Insert
IBMX	3-Isobutyl-1-methylxanthine
IDC	Invasive ductal carcinoma

IGF-1	Insulin-like growth factor 1
IGF-1R	Insulin-like growth factor 1 receptor
IGFBP-2	Insulin-like growth factor binding protein-2
IGFBP3	Insulin-like growth factor binding protein 3
IL-1β	Interleukin - 1β
IL	Interleukin
IL13Rα2	IL-13 receptor α2
ILC	Invasive lobular carcinoma
IRS1	Insulin receptor substrate 1
JAK	Janus kinase
LIF	Leukaemia inhibitory factor
LK	Lipid kinase
LKB1	Liver kinase b1
M	Medium
MAPK	Microtubule associated protein kinase
MCF-7	Michigan cancer foundation - 7
MCP-1	Monocyte chemoattractant protein - 1
MDA-MB-231	Munroe Dunaway Anderson [cancer centre] - MB - 231
MDM	Multi-disciplinary meeting
MFP	Mammary fat pad
mg	Milligram(s)
min	Minute(s)
MIP-3α	Macrophage inflammatory protein-3
ml	Millilitre(s)
mm	Millimetre(s)
mM	Millimolar
MM	Mastermix
MSC	Mesenchymal stem cells
mTOR	Mammalian target of rapamycin
mTORC2	mTOR complex 2
n	Number
NF-κB	Nuclear factor - κ-light-chain-enhancer of activated B cells
NHS	National Health Service

NHSBSP	National Health Service Breast Screening Programme
NK	Natural killer (cell)
NKT	Natural killer T (cell)
nM	Nanomolar
NST	No special type
^{O}C	Degrees Celsius
Oligo(dT)	Oligo deoxythymine
ONS	Office for National Statistics
ORO	Oil red O
P	Passage
Pantothenate	D-pantothenic acid
PBS	Phosphate buffered saline
PCR	Polymerase chain reaction
pd	Pre-differentiated
PDGF	Platelet derived growth factor
PDK1	Pyruvate dehydrogenase kinase 1
PFA	Paraformaldehyde
PI3K	Phosphoinositide 3-kinase
PI3KCA	PI3K catalytic subunit alpha
PIP2	Phosphatidylinositol 4,5-bisphosphate
PIP3	phosphatidylinositol 3,4,5-triphosphate
PKA	Protein kinase A
PKB	Protein kinase B
PPAR-γ	Peroxisome proliferator-activator receptor-γ
ppi	Pixels per inch
PR	Progesterone receptor
PR^{+}	Progesterone receptor positive
pRb	Retinoblastoma protein
PT	Peri-tumoural
PTEN	Phosphatase and tensin Homologue
QD	Quick differentiation
®	Registered trademark
Ras	Proto-oncogene protein P21

RM	Resection margin
RNA	Ribonucleic acid
RNase	Ribonuclease
ROS	Reactive oxygen species
rpm	Revolutions per minute
RR	Relative risk
RT	Reverse transcription
RTase	Reverse transcriptase
RT-qPCR	Real-time quantitative PCR
s	Second(s)
SGBS	Simpson-Golami-Behmel Syndrome
SGBS Alone	SGBS cells cultured alone
SGBS Co	SGBS cells co-cultured with cancer cells
SMT	Somatic mutation theory
SREB-1c	Sterol regulatory element binding protein - 1c
STAT3	Signal transducer and activator of transcription 3
STK11	Serine/threonine kinase 11
T3	Triiodo-L-thyronine
TGF-α	Tumour growth factor - α
TGF-β	Tumour growth factor - β
™	Trademark
TME	Tumour microenvironment
TN	Triple negative
TNF-α	Tumour necrosis factor - α
TOFT	Tissue organisation field theory
TORC1	Target of rapamycin complex 1
TP53	Tumour protein 53
Transferrin	Apo-transferrin human
Trypsin	Trypsin-EDTA solution 1X
TSC1/2	Tuberous sclerosis complex 1/2
TZD	Thiazolidinedione
UCP-1	Uncoupling protein - 1
UK	United Kingdom

v/v	Volume/volume
VEGF	Vascular endothelial growth factor
W	Well
WAT	White adipose tissue
WHO	World Health Organisation
WNT	Wingless int-1

CHAPTER ONE

Introduction

Chapter One: Introduction

Contents

1.1	**Introduction……...**	**4**
1.2	**The Breast……...**	**4**
1.2.1	Embryology and Anatomy of the Breast……...	5
1.2.2	Structure of the Adult Female Breast……	5
1.2.3	Vasculature and Lymphatics of the Breast……	7
1.2.4	Histology of the Breast…….	7
1.3	**Assessment of Patients with Breast Symptoms……..**	**9**
1.4	**Cancer……**	**10**
1.4.1	Theories of the Development of Sporadic Cancers……...	10
1.4.1.1	Somatic Mutation Theory…….	11
1.4.1.2	Tissue Organisation Field Theory…….	14
1.5	**Breast Cancer……**	**15**
1.5.1	Statistics of Breast Cancer……	15
1.5.2	Risk Factors for Breast Cancer…….	16
1.5.3	The Pathology of Breast Cancer……...	17
1.5.3.1	Histological Subtypes of Breast Cancer……	17
1.5.3.2	Grading of Breast Cancer…….	18
1.5.3.3	Oestrogen Receptors……	18
1.5.3.4	HER2 Receptors……..	20
1.5.3.5	Molecular Subclassifications of Breast Cancer……..	21
1.5.3.6	Signalling Pathways in Breast Cancer……	21
1.5.4	The Management of Breast Cancer……...	24
1.6	**The Breast Cancer Tumour Microenvironment……**	**24**
1.6.1	Adipose Tissue…….	26
1.6.1.1	Adipogenesis……	26
1.6.1.2	Types and Functions of Adipose Tissue……...	28
1.6.1.3	Adipose Tissue as an Endocrine Organ……	28
1.6.1.4	Abnormal Adipose Tissue in Obesity……...	29
1.6.2	The Mammary Fat Pad…….	31
1.6.3	Adipocytes in the Tumour Microenvironment……..	32

1.6.4 Adipokines in the Breast Tumour Microenvironment……... 34
1.6.4.1 Adipokines…… 34
1.6.4.2 Common Adipokines of the Breast Tumour Microenvironment ….. 34
1.7 Aim of the Study…… 36
1.8 Ethical Approval…… 37

1.1 Introduction

Breast cancer is the commonest female malignancy in the developing and developed world (World Health Organisation, 2020); in 2018, over two million new cases were diagnosed (Bray *et al.*, 2018). The United Kingdom (UK) ranks eighth globally, with an age-standardised rate of 93.6 per 100 000 population (World Cancer Research Fund, 2018). With an increasing incidence (Office for National Statistics [ONS], 2016), breast cancer poses a significant disease burden on individuals as well as healthcare systems. Although overall survival figures after treatment for breast cancer are good, outcomes for more advanced disease (ONS, 2019) and more aggressive cancers (Dixon and Barber, 2019) are markedly poorer.

The tumour microenvironment is the tissue immediately local to a cancer, where malignant cells recruit benign cells to, to communicate with and alter such that these non-cancerous cells promote the growth and progression of the tumour (Balkwill *et al.,* 2012). Various cell types are found in the tumour microenvironment, and adipocytes are increasingly recognised as important, dynamic components. Much remains unknown, however, about the mechanisms by which they effect change in malignancy (Park *et al.*, 2020).

This research aimed to investigate the role of adipocytes in the breast cancer tumour microenvironment with a focus on secreted cytokines.

1.2 The Breast

The breasts are paired modified apocrine glands located on the anterior thoracic wall. Prior to puberty there is no difference in breast structure between the sexes. Post-puberty, sexually dimorphic development occurs such that in the mature male, the breasts remain rudimentary and flat structures composed of a little fat with some ducts but no lobular tissue, whereas in the female they are usually prominent structures consisted of stromal adipose tissue (AT) and glandular tissue. The relative proportions

of these constituent components differ between individuals and are determined by various factors, both genetic and environmental.

1.2.1 Embryology and Anatomy of the Breast

The tissue of the breast shares its ectodermal (parenchyma) and mesodermal (stroma) origins with skin (Skandalakis, 2009). Normal development of the breast, which begins in the 4th to 6th weeks of foetal life, is dependent upon communication ('cross-talk') between epithelial and stromal cells (Inman *et al.,* 2015), in an environment of optimal oxygen content (Shao and Zhao, 2014), heavily under the influence of oestrogen (Javed and Lteif, 2013).

Breast development is not limited to the embryonic stage. There is great cellular plasticity in the breast (Rybinska *et al.*, 2020), and transformations in the female are lifelong phenomena (Macias and Hinck, 2012; Javed and Lteif, 2013). Transient differences are seen every month in females of childbearing age, and persisting histological and physiological changes occur at puberty, during pregnancy, and at the time of the menopause. These hormonally driven alterations (Choi *et al.*, 2018), controlled locally *via* complex signalling pathways which influence bidirectional epithelial-mesenchymal interactions, occur in anticipation of the breast fulfilling, or ceasing, its role as an organ of lactation (Schedin and Hovey, 2010).

1.2.2 Structure of the Adult Female Breast

Assessment of the normal adult female breast (Figure 1.1) reveals 15-20 epithelial cell-lined lactiferous ducts which developed late in foetal life, and acini-containing terminal lobules which developed at puberty (Skandalakis, 2009; Ellis and Mahadevan, 2010). Grouped milk-producing acini form alveoli which sit at the tips of ductules; alveoli-ductule clusters make up the lobules. Numerous lobules are grouped together to drain via a single lactiferous duct and this unit is collectively called a lobe. Lobes are spread in a radial pattern with their lactiferous ducts opening on to the surface of the nipple

Figure 1.1: Anatomy and Vasculature of the Adult Female Breast

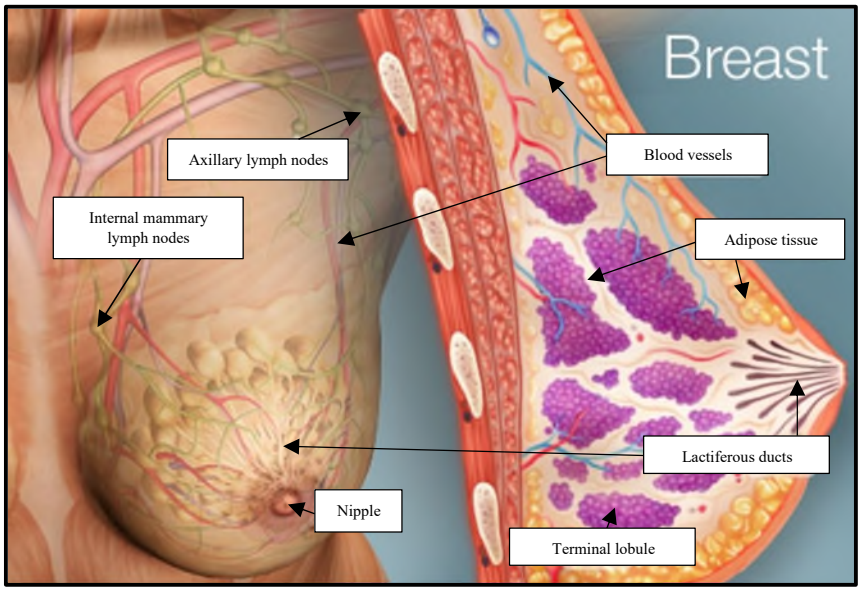

[Adapted from (https://www.webmd.com/women/picture-of-the-breasts#1); © 2016, WebMD, LLC. All rights reserved]

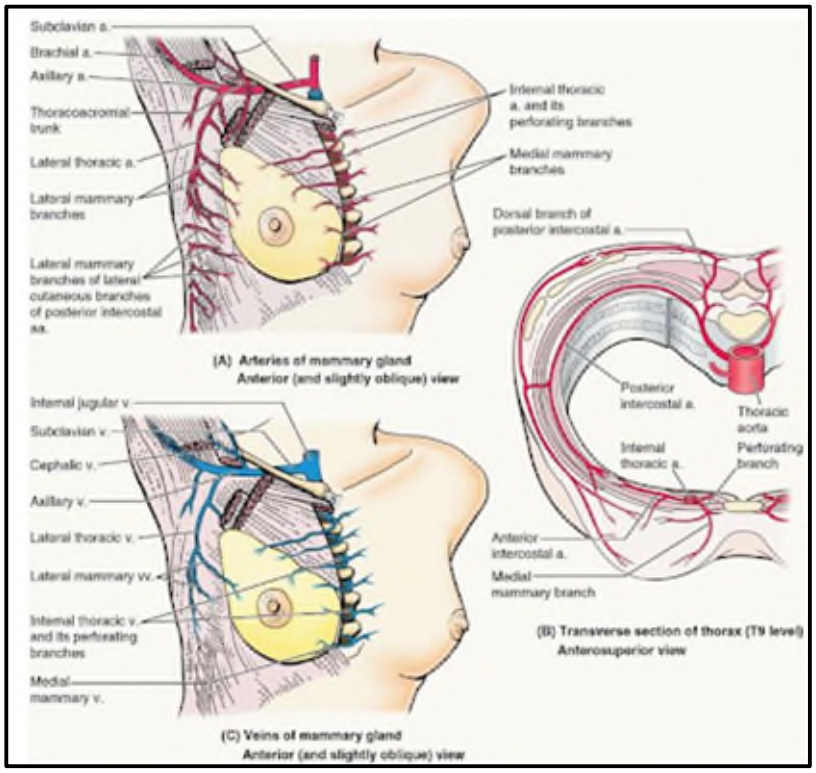

[From (Moore and Dalley, 1999); © 1999, Wolters Kluwer Health, Inc.]

which is an elevated area of specialised skin devoid of hair, fat, and sweat glands. This glandular tissue is fully enveloped in AT. Deposition of the latter increases during puberty.

1.2.3 Vasculature and Lymphatics of the Breast

Blood supply to the breast (Figure 1.1) is via the internal and lateral thoracic arteries, the thoracoacromial artery, and the posterior intercostal arteries. Most venous drainage of the breast is via the axillary vein, although a small percentage does pass to the internal thoracic vein. Lymphatic drainage of the breast occurs primarily to the axillary lymph nodes; only 10-15% of fluid drains to the internal mammary chain or to the nodes located between the pectoral muscles (Moore and Dalley, 1999). An appreciation of the vasculature and lymphatics of the breast is particularly important when considering treatment for malignant disease.

1.2.4 Histology of the Breast

The histological structure of the adult female mammary gland (Figure 1.2) consists of epithelial cells sat on a basement membrane, separated from the stroma by this collagenous layer. Tumour cells contained within this membrane form *in situ* disease; for a malignancy to be termed invasive, it must breech the basement membrane.

The epithelium lines the ducts and lobes, and is made up of two layers of three types of cells: luminal A cells which are superficial and likely produce milk, basal cells which are the most common epithelial cell type present, and myoepithelial cells which contain myofilaments and can thus contract. The stroma of the breast contains the vasculature and the lymphatics, and is intimately related to the connective tissue and adipose tissue of the breast (Dixon and Barber, 2019).

Figure 1.2: Histology of the Adult Female Breast

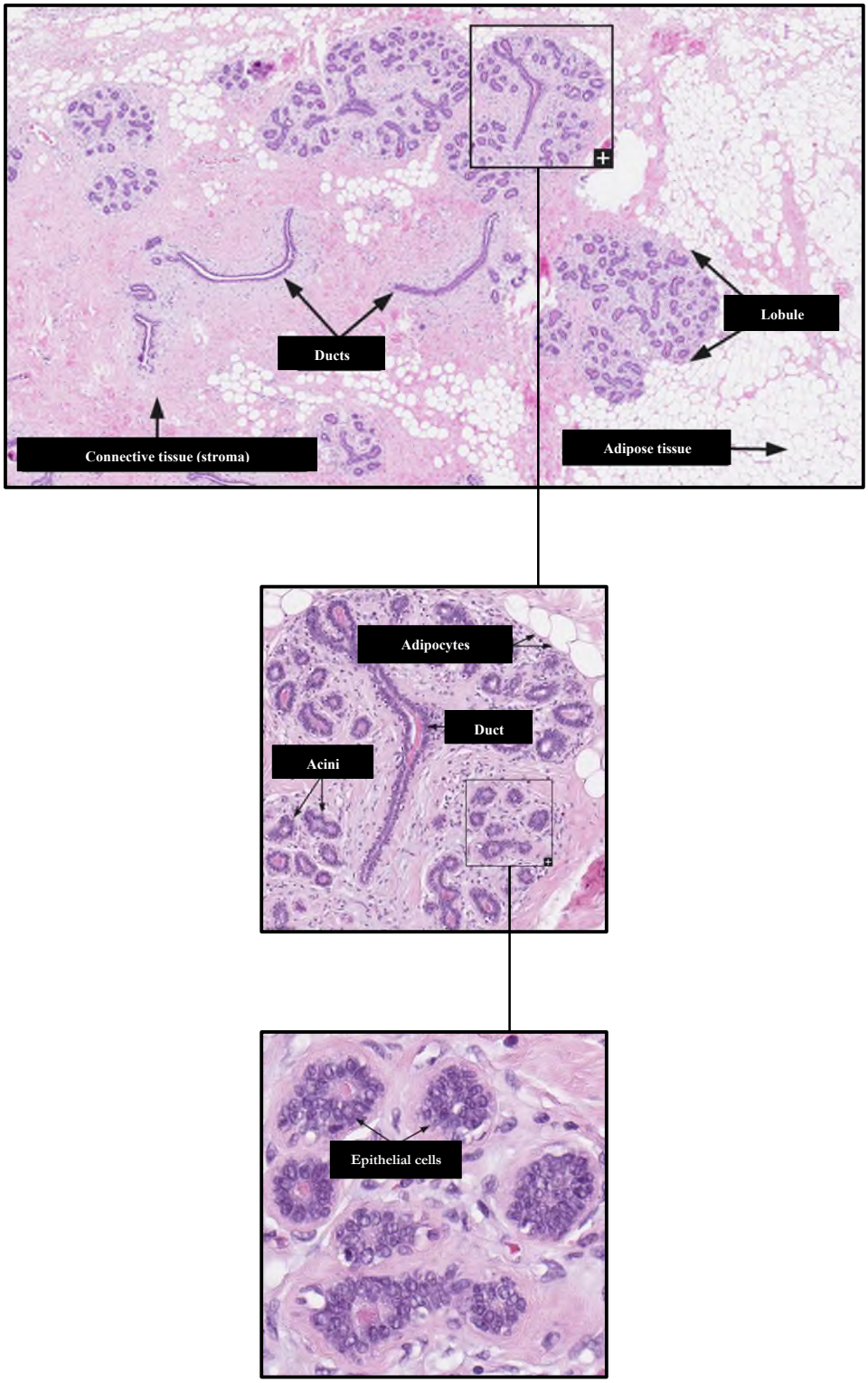

[Modified from (The Human Protein Atlas, 2020 available from https://www.proteinatlas.org/learn/dictionary/normal/breast)]

Haematoxylin and Eosin (H&E) stained slides showing histology of the adult female breast. Magnification not stated.

1.3 Assessment of Patients with Breast Symptoms

Diseases of the breast can be categorised as aberrations of normal development, benign proliferations, intermediate/uncertain entities, and malignant growths. All patients who report symptoms which cannot be managed in the Primary Care setting are referred to Secondary Care.

The Breast Department at University Hospital [University Hospitals Coventry and Warwickshire National Health Service (NHS) Trust] sees approximately 4 000 new patients annually (personal communication). Symptomatic individuals may be referred by local clinicians, including General Practitioners and other Hospital Clinicians, with issues of concern ranging from breast pain to a discrete lesion, from a rash to nipple discharge.

Alternatively, patients may be referred to the Department *via* the NHS Breast Screening Programme (NHSBSP). The latter sends invitations to females aged 50-71 years inclusive every three years, for a mammogram. In the UK, approximately two million females are sent appointments for screening every year (McGuire *et al.,* 2015), and all patients with changes warranting further investigation are sent follow-up appointments and then seen by a Breast Clinician.

In the symptomatic Breast Clinic, after having their history taken, patients are examined. Imaging of any areas of uncertainty or abnormality is arranged, and, if required, tissue sampling is undertaken. The results of this *triple assessment* are discussed at the local bi-weekly Multi-Disciplinary Meeting (MDM). Members of the MD team include Breast Surgeons, Radiologists, Pathologists, Oncologists, and Specialist Nurses. Together they formulate a patient and diagnosis-appropriate management recommendation, to be offered to and discussed with the patient at a follow-up clinic visit. Patients found to have benign disease may or may not undergo treatment. All patients with malignancy are assessed with a view to intervention, if medically fit to proceed.

1.4 Cancer

Cancer is a disease entity whereby sustained unregulated cell growth and division result in *malignant* cells having the ability to proliferate in an uncontrolled, often haphazard, manner invading local tissues and structures, as well as having the potential to spread (*metastasise*) to distant sites of the body. A complex set of processes encompassing genetic aberration(s), selective proliferation with clonal expansion, and immortality, carcinogenesis remains largely incompletely understood. This is true for breast cancer; although animal models have shown irradiation (Barcellos-Hoff and Ravani, 2000) to the mammary fat pad or inoculation with carcinogenic chemicals (Maffini *et al.,* 2003) to trigger malignancy, much remains unknown about carcinogenesis without such an obvious insult (Esquivel-Velazquez *et al.,* 2015).

1.4.1 Theories of the Development of Sporadic Cancers

Theories of the causes of cancer have progressed over the centuries. The 'Edwin Smith' and 'George Ebers' papyri, dated to 1600 BC with sources as early as 2500 BC, contain cancer descriptions (National Cancer Institute, undated). The former outlines surgical management and the latter mechanical, pharmacological, and magical. It is known from the study of papyri and hieroglyphics that the ancient Egyptians were able to distinguish between benign and malignant lesions. The Father of Medicine, Hippocrates (c. 460 BC - c. 375 BC) named the disease *karkinoma* (Greek: crab), referencing the body of the crustacean as the central body of the tumour and the legs as the malignant extensions. The Romans later introduced the use of the word *cancer* (Latin: crab). Gendron (1663 - 1750), the French physician, put forward the idea of cancer being a growing hard mass, but it was not until the late 19th Century, when improved microscopes allowed better visualisation of cancerous tissue, that the focus of cancer theory shifted to (the origin of) cells and cell behaviour. Currently, the two main approaches to understanding carcinogenesis are the longer established Somatic Mutation Theory and the more recent Tissue Organisation Field Theory.

1.4.1.1 Somatic Mutation Theory

In 1914, the German zoologist Boveri published his book *On the Origin of Malignant Tumours*. He was clear in his stance that cancerous tumours were "…a cell problem…"; specifically, a problem of cellular proliferation and a consequence of aberrations of chromosomal arrangement (Soto and Sonnenschein, 2013). Although his writing preceded discovery of the cell cycle by decades, Boveri's principle is accepted as the primary expression of the later named Somatic Mutation Theory (SMT). The SMT proposes that carcinogenesis occurs as a consequence of (multiple) DNA mutation(s) in genes encoding cell-cycle control mechanisms and cellular proliferation in *one* somatic cell (Soto and Sonnenschein, 2014). Over 700 cancer-driving genes are now recognised (Sondka *et al.*, 2018), with over 40 identified for breast cancer (BC) (Stephens *et al.*, 2012).

Between the original proposition in 1914 and current times, the SMT umbrella has been added to by various researchers; any 'new' theory pertaining to carcinogenesis which relies at its core on deoxyribonucleic acid (DNA) mutation would still be categorised as part of the SMT.

The most significant review in the understanding of the SMT and carcinogenesis came two decades ago, by Hanahan and Weinberg (2000). In their seminal article on the six hallmarks of the neoplastic process, they outlined the functional capabilities that "…most if not all cancers…" acquire during development. The timings of these changes vary between malignancies, and do not necessarily occur simultaneously:

- Growth signal self-sufficiency, for example:
  Tumour growth factor (TGF-) α from sarcomas, platelet derived growth factor (PDGF) from glioblastomas, and overexpression of human epidermal receptor 2 (HER2) in breast cancer.

- A lack of sensitivity to anti-growth signals, for example:
  TGF-β acts to inactivate retinoblastoma protein (pRb) by preventing its phosphorylation. Phosphorylated pRb stimulates cell progression through the cell

cycle, through the G1 (growth) phase to the S (DNA synthesis) phase. Loss of sensitivity to TGF-β, which may occur as a result of downregulation of receptors or the production of abnormal receptors, thus allows the cell cycle to continue (Hocevar and Howe, 1998).

- Continuous angiogenesis, for example:
  Via production of vascular endothelial growth factor (VEGF) inducer.

- Invasion of tissue and metastasis to distant locations, for example:
  The loss of the e-cadherin cell-cell adhesion molecule.

- Ability to evade apoptosis, for example:
  Inactivation of the *p53* tumour suppressor gene's protein p53 has been identified in over half of human malignancies. Its loss results in impairment of the check system which identifies DNA damage and would normally trigger activation of apoptosis when anomalous genetic material was found.

- Unlimited potential for replication:
  A consequence of growth signal self-sufficiency, a lack of sensitivity to anti-growth signals, and the ability to evade apoptosis.

Underlying these processes are the enabling characteristics of genomic instability and inflammation which expedite occurrence of the six hallmarks.

Over a decade later, Hanahan and Weinberg (2011) revised their hallmarks of cancer to also include two further concepts (Figure 1.3):

- Energy metabolism reprogramming:
  In the 1920s, it was observed that cancerous tumours, when compared to normal local tissue, take up and utilise vast amounts of glucose (Warburg, 1925). In this *Warburg Effect*, a metabolic switch occurs whereby 'aerobic glycolysis' occurs as opposed to the normal oxidative phosphorylation, even in the presence of sufficient oxygen. Although the exact reason for this switch remains unknown, it

Figure 1.3: Hallmarks of Cancer

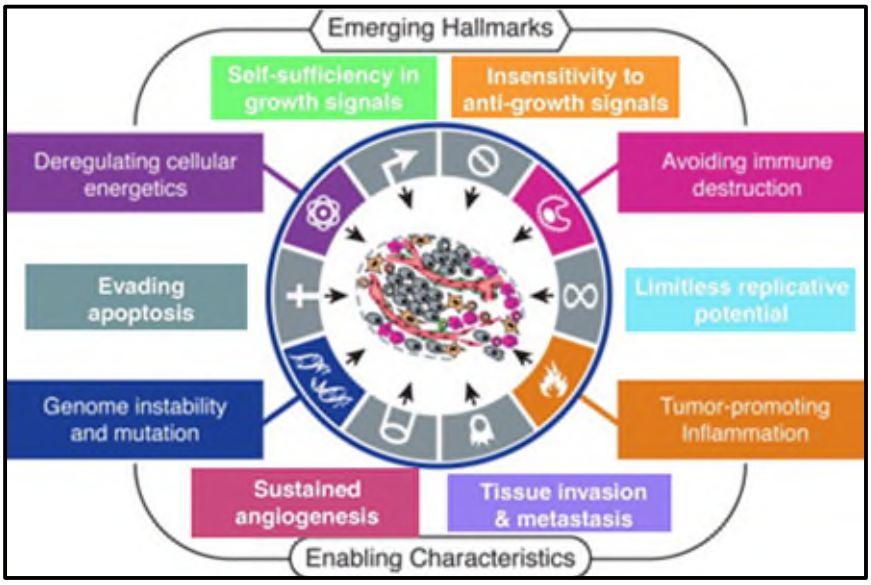

[Adapted, with permission from Elsevier©, from (Hanahan and Weinberg, 2000) and (Hanahan and Weinberg, 2011)]

has been postulated that the aerobic glycolysis better supports biosynthesis on a larger scale, as is seen with rapid cell proliferation (Liberti and Locasale, 2016).

- Evasion of immune destruction:
  The competent immune system has long been recognised as a major defence against malignancy where a viral insult is a necessary trigger. More recently, its role in non-viral cancers is becoming clearer. Interestingly, it is an observed phenomenon that some transplant patients develop malignancy derived from the donor. This would suggest that this cancer was suppressed in the immune competent donor but could take hold in the suppressed recipient.

The SMT has dominated scientific research for decades but has faced criticism, not least that benign tumours have five of the six hallmarks of cancer described by Hanahan and Weinberg (2000), with the only additional feature of malignancy being invasion and metastasis (Lazebnik, 2010). One of the greatest challenges of the SMT came from Sonnenschein and Soto (2000) when they put forward their markedly different Tissue Organisation Field Theory of carcinogenesis.

1.4.1.2 Tissue Organisation Field Theory

In 2000, Soto and Sonnenschein published their paper *Somatic mutation theory of carcinogenesis; Why it should be dropped and replaced.* In it, they outlined their *tissue-based* theory of cancer - the 'Tissue Organisation Field Theory' (TOFT). They described cancer as a reversible defect of tissue architecture with malignant transformation being a consequence of chronic, abnormal interactions between a tissue parenchyma and its stroma. These chronic insults from *carcinogens* result in loss of the normal restraints on cell motility and proliferation, leading to epithelial hyperplasia, metaplasia, dysplasia, and eventually malignant transformation. The DNA damage seen in the resulting cancerous cells is a *consequence* of abnormal interaction and the initiation of the malignant process, and not the cause.

Carcinogenesis is multifactorial and complex, and some researchers have postulated that components of both the SMT and TOFT may play roles (Rosenfeld, 2013). In 2009, Colcotta *et al.* proposed cancer related inflammation as an additional hallmark of malignancy, and not just an enabling characteristic as Hanahan and Weinberg (2000) had done. They suggested an intrinsic component whereby oncogenes drive processes related to inflammation, and an extrinsic component where cancer development is promoted by local inflammatory conditions, combing the SMT and TOFT, with transcription factors, chemo- and cytokines, and infiltrating leucocytes being essential in this model.

1.5 Breast Cancer

The extensive remodelling seen in the post-pubertal female breast increases its vulnerability to malignant transformation (Javed and Lteif, 2013).

1.5.1 Statistics of Breast Cancer

BC is the commonest female malignancy worldwide (WHO, 2020). In 2015, in the UK, over 55 000 invasive BC diagnoses were made; these made up 15% of all malignancies identified that year (Cancer Research UK, undated). Only 1% of new cases were seen in males. Of every 1 000 females screened through the NHSBSP, eight are ultimately diagnosed with cancer (Public Health England, 2018). In 2016, over 11 500 deaths were attributed to the disease (Cancer Research UK, 2017). Since the early 1970s, the BC mortality rate has fallen by almost 40%; in the late-1980s, the NHSBSP was introduced and it is calculated to decrease the number of deaths per year by approximately 1 300 (Cancer Research UK, undated).

1.5.2 Risk Factors for Breast Cancer

A risk factor for malignancy is that which increases an individual's chance of developing cancer. With the ongoing investment and drive to continue research into BC, many risk factors have been identified:

- Age and Sex:

  Age and female sex are the two greatest risk factors for the development of BC. Age related risk of breast malignancy increases from 1 in 53 at the age of <49 years, to 1 in 15 in the >70 years group (McGuire *et al.*, 2015). Females are approximately 100 times more likely to be diagnosed with the disease as males (Feng *et al.,* 2018).

- Genetics:

  Autosomal dominant genetic mutations are identified in approximately 5-10% of all patients diagnosed with a breast malignancy (Dixon and Barber, 2019; Shah *et al.,* 2014). *BRCA1, BRCA2, TP53, PTEN,* and *STK11* are categorised as 'high-risk predisposition alleles', conferring a lifetime cancer risk between 40% and 85% (Shah *et al.*, 2014). A significant family history of breast cancer is one of the greatest risk factors for the development of malignancy and although ≤10% of patients have an identifiable genetic mutation, up to 25% have a significant family history (Dixon and Barber, 2019).

- Hormone exposure:

  Increased lifetime exposure to cycling endogenous hormone levels increases a woman's risk of BC, as does the long-term use of exogenous hormones (Shah *et al.*, 2014). Early menarche and late menopause, and fewer full-term pregnancies increase BC risk whilst breast feeding confers a risk-reducing effect. Studies have indicated combined hormone replacement therapy (HRT), which is known to result in persistence of breast epithelium, also increases the risk of breast malignancy (Travis and Key, 2003).

- Other:

  Environmental and lifestyle factors important in breast carcinogenesis include smoking, alcohol consumption, physical inactivity, radiation exposure, and obesity. The latter is associated with disease of a higher grade in BC (Toren *et al.*, 2013), with a high body mass index ('BMI' ≥30) being intimately linked to the role of inflammation in cancer (Siriwardhana *et al.*, 2012). Both local and systemic inflammation are recognised as important in the pathogenesis of many malignancies; over the last few years, local inflammation in the tissue in which a cancer develops and progresses - the *tumour microenvironment* - has increasingly become a focus for research.

1.5.3 The Pathology of Breast Cancer

The histological assessment of a BC is performed by a Pathologist at the time of initial (diagnostic) tissue analysis and is revised when the (therapeutic) resection specimen is available. At the time of this analysis, the Pathologist will report, amongst other features, the histological subtype of malignancy, the size of the tumour, the grade, and the receptor status.

1.5.3.1 Histological Subtypes of Breast Cancer

BC is widely accepted as a heterogenous group of diseases; considerable histopathological, and biomolecular differences are seen between different tumour types, and both clinical course and prognosis can vary greatly. Although the specific mechanism of BC development has not been fully elucidated, predisposing conditions have been identified: proliferative disease without atypia results in a relative risk (RR) of future BC of 1.3-1.9, atypical hyperplasia a RR of 3.5-5.3, and ductal carcinoma *in situ* (DCIS) a RR of 10-11 (Cichon *et al.*, 2010).

Most invasive malignancies are glandular in origin and thus classified as adenocarcinoma (Dixon and Barber, 2019). Over 75% of all invasive disease is ductal

(invasive ductal cancer; 'IDC'), whilst 8% is lobular (ILC) (Li and Uribe, 2005; Makki, 2015). Historically thought to differ based on their structural site of origin, it is now understood that the histological variation seen between IDC and ILC malignancies is because of differences in cell biology as opposed to site (Dixon and Barber, 2019; Makki, 2015). ILC, for example, loses expression of the cell adhesion molecule e-cadherin.

IDC can be further sub-categorised based on special features the tumour may or may not display. Criteria for sub-categorisation include type of cell predominating (such as apocrine), architectural features (tubular, papillary, micropapillary), secretions (mucinous), and immunohistochemical profile (neuroendocrine) (Makki, 2015). If there are no particular features of note, the cancer is labelled as invasive ductal cancer NST (no special type). IDC NST constitutes up to 75% of all IDC.

1.5.3.2 Grading of Breast Cancer

Grading of BC has significant implications for treatment modalities employed and is also an important prognostic indicator. The grade of BC can be determined *via* several scoring techniques, with all designed to determine how aggressive a tumour is. The Nottingham Score gives a value of 1, 2, or 3 based on tubule formation, nuclear pleomorphism, and mitotic activity (Figure 1.4) Grade 3 disease is more aggressive than Grade 1 and, all other factors being equal, carries a poorer prognosis (Dixon and Barber, 2019).

1.5.3.3 Oestrogen Receptors

The oestrogen receptor (ER), like the progesterone receptor (PR), is a steroid receptor located both on the cell membrane and in the nucleus, and acts as a transcription factor (Carroll, 2016). It has a DNA-binding domain and a ligand-binding domain. The former allows it to directly regulate events pertaining to gene expression when the latter is activated by oestrogen. The nuclear ER pathway is incredibly complex; the

Figure 1.4: Nottingham Grading Score for Breast Cancer

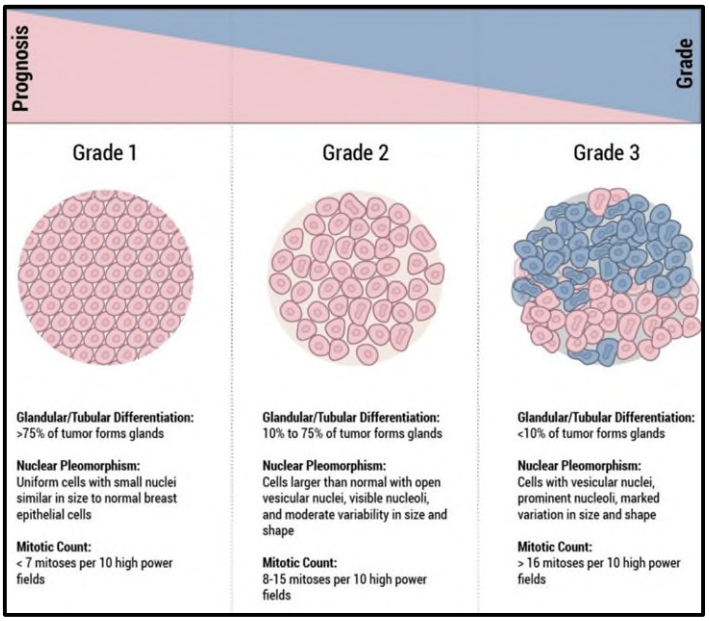

[Reproduced, with permission, from (John Hopkins Medicine Pathology, 2020)]

receptor associates with thousands of genome regions, via hundreds of proteins, and functions in the control of multiple genes as well as non-coding ribonucleic acids (RNAs). In normal health, ER has a critical role in breast gland development, regulating gene expression leading to cellular division. In disease, the ER transcription factor can escape control processes; oestrogen binds to its ligand as normal, but the ensuing downstream oestrogen mediated cellular division is uncontrolled, resulting in potential progression to malignant cell proliferation.

In the normal breast epithelium, ER are present in 7-17% of cells, as determined by immunohistochemistry (Badowska-Kozakiewicz *et al.* 2015), but up to 80-85% of breast cancers are found to be ER^+. In clinical practice, PR is also often checked. Likelihood of response to hormonal treatment is 73% in patients with ER^+/PR^+ disease, and 40% in those with ER^+/PR^- disease. Generally, prognosis in ER^+ disease is better.

1.5.3.4 HER2 Receptors

Human epidermal growth factor receptor 2 (HER2) is a transmembrane cell surface receptor belonging to the epidermal growth factor (EGF) group (Mitri *et al.*, 2012). It has an extracellular domain which does not have a recognised ligand; it can undergo dimerisation with other EGF receptors independently or, alternatively, it may exist in its natural state in its activated form. HER2 is overexpressed in 20-30% of breast malignancies, with up to 50 copies of the gene and up to a 100-fold increase in the protein, per cell (Iqbal and Iqbal, 2014). Ultimately, this results in 2 million cell surface receptors as opposed to the normal 20 000 (Hicks and Kulkarni, 2008). (Over)-activation of HER2 mediated pathways results in increased cell proliferation, prolonged cellular survival, angiogenesis, and acquisition of invasive characteristics (Iqbal and Iqbal, 2014). HER2 positivity confers a poorer prognosis as it is associated with disease which is more aggressive, has a higher rate of recurrence, and has a higher mortality rate. Patients who develop cancer with overexpressed HER2 receptors will be assessed for suitability for HER2 receptor blocking treatment.

1.5.3.5 Molecular Subclassification of Breast Cancer

Malignant breast tumours may be classified according to the combination of receptors they do or do not (over)express, as well as the marker of proliferation Ki67 and the basal markers CK5/6 and EGFR (Table 1.1) (Malhotra *et al.*, 2010; Dixon and Barber, 2019).

1.5.3.6 Signalling Pathways in Breast Cancer

A number of signalling pathways including PI3K/AKT/mTOR, JAK/STAT, MAPK, and WNT, have been found to be important in BC (Guille *et al.*, 2013; Harvey, 2019). One of the most significant is the PI3K/AKT/mTOR pathway (Engelman *et al.,* 2006; Park *et al.*, 2020).

The PI3K/AKT/mTOR pathway (Figure 1.5) is often implicated in breast malignancies; approximately 60% of BCs have mutations pertaining to it. The phosphoinositide 3-kinases (PI3Ks) family of lipid kinases (LKs) consists of three different classes of LKs and Class I has been the most well studied, playing a clear role in carcinogenesis (Engelman *et al.*, 2006). The commonest genetic aberration seen in the pathway is in the *PIK3CA* gene, being present in 45% of Luminal A malignancies, 39% of HER2 enriched tumours, and 30% of Luminal B cancers (Guerrero-Zotano *et al.*, 2016). The PI3K/AKT/mTOR pathway transmits extracellular stimuli signals downstream to ultimately control cell metabolism and growth, proliferation, survival, and motility (Engelman *et al.*, 2006). Genetic aberrations result in initiation of carcinogenesis as well as progression of the malignancy and may also confer drug resistance.

Table 1.1: Molecular Subclassification of Breast Cancers

Class	Descriptor	Notes
Luminal A (~ 40%)	• ER + • PR + / - • HER2 - • Low Ki67	Most common Less aggressive Good prognosis
Luminal B (~ 20%)	• ER + / - • PR + / - • HER2 + / - • High Ki67	Hormone positive Most frequently ER + PR - Poorer outcome than Luminal A
HER2 Enriched (10-15%)	• ER - • PR - • HER2 +	Highly aggressive
Triple Negative (15-20%) Basal-like	• ER - • PR - • HER2 - • CK5/6 + • EGFR +	50-75% of triple negative BC
Triple Negative (15-20%) 'Five marker negative'	• ER - • PR - • HER2 - • CK5/6 - • EGFR -	25-50% of triple negative BC

[Adapted from (Malhotra *et al.*, 2010; Dixon and Barber, 2019)]

Figure 1.5: The PI3K/AKT/mTOR Signalling Pathway

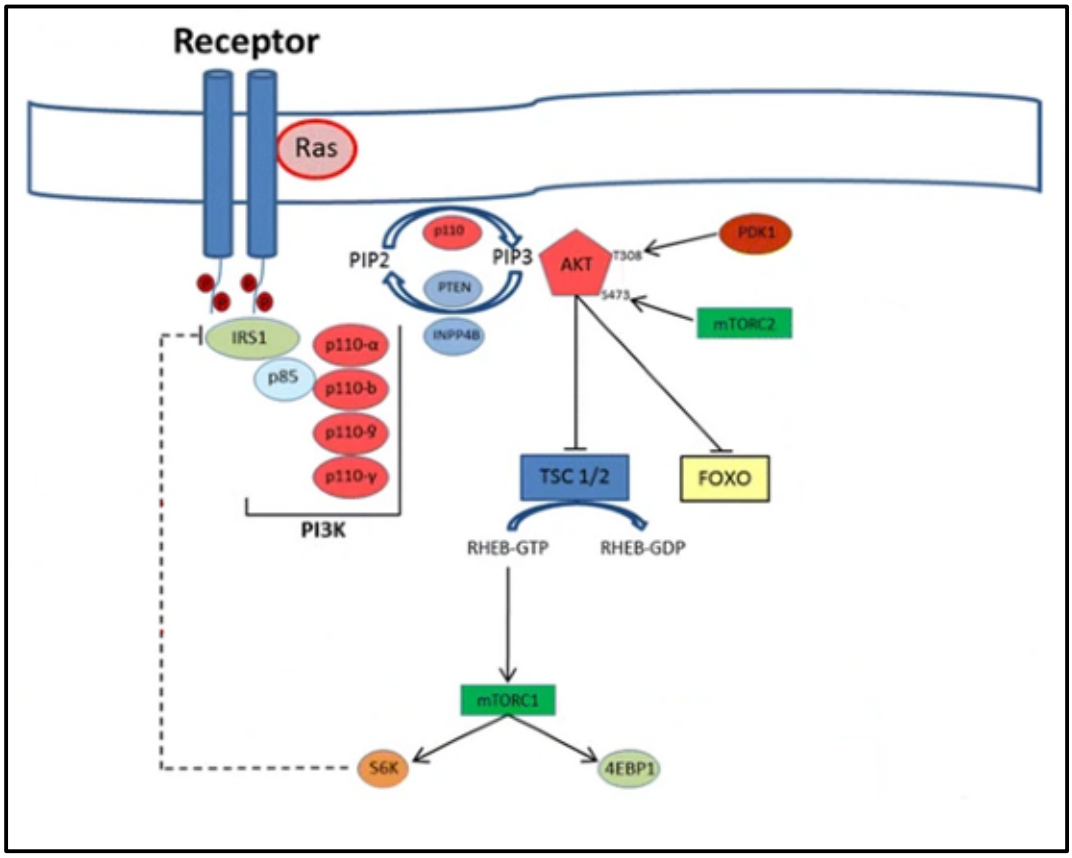

[Adapted from (Guerrero-Zotano *et al.*, 2016). Reprinted by permission from Springer Nature: Nature, Cancer and Metastasis Review. PI3K/AKT/mTOR: role in breast cancer progression, drug resistance, and treatment. Guerrero-Zotano A, Mayer IA, Arteaga CL. ©2016]

Stimulation of the normally functioning PI3K/AKT/mTOR pathway occurs via growth factor receptor kinases, for example fibroblast growth factor receptor (FGFR), insulin-like growth factor 1 receptor (IGF-1R) and ErbB receptors, as well as G-protein coupled receptors. Binding of ligands to their respective receptors results in activation of adaptor proteins (for example insulin receptor substrate 1 [IRS1]) which recruit PI3K to the plasma membrane. This leads to the conversion of phosphatidylinositol 4,5-bisphosphate (PIP2) to phosphatidylinositol 3,4,5-triphosphate (PIP3) which recruits pyruvate dehydrogenase kinase 1 (PDK1) and protein kinase B (PKB/AKT) to the cell membrane. Phosphorylation of AKT (by PDK1 and mammalian target of rapamycin complex 2 [mTORC2]) results in its full activation and allows it to inhibit the tuberous sclerosis complex 1/2 (TSC1/2) complex. This leads to activation of TORC1, and consequentially phosphorylation of S6 kinase and eukaryotic translocation initiation factor 4e (eIF4E) binding protein 1. This results in the promotion of ribonucleic acid (RNA) translation and protein synthesis, and autophagy. (Guerrero-Zotano *et al.*, 2016)

1.5.4 The Management of Breast Cancer

The management of BC is dependent upon multiple factors including the histological subtype of the malignancy and its grade, the size and position of the tumour, whether the cancer expresses the various receptors, and the presence or absence of cancer spread beyond the breast. These factors are all considered within the context of the patient's general health and the likelihood that they will tolerate treatment. Interventions are tailored to individuals and combinations may include surgery (removal of the whole breast [mastectomy], or removal of the tumour with a rim of normal tissue [wide local excision, commonly called a "lumpectomy"], with or without removal of all lymph nodes from the axilla), radiotherapy, chemotherapy, and biological and endocrine treatment. Currently, overall BC prognosis sits at over 75% survival at ten years (ONS, 2019), but prognosis of the more aggressive tumours is much poorer.

1.6 The Breast Cancer Tumour Microenvironment

"Cancers are not just masses of malignant cells but complex 'rogue' organs, to which many other cells are recruited…" (Balkwill *et al.*, 2012). Indeed, in malignancy, non-cancerous cells may form over half of the mass of a primary lesion (Balkwill *et al.*, 2012). Once recruited, the cells are corrupted to play a supportive role in the growth and progression of the cancerous cells (Zewdu *et al.,* 2020). These complex, multi-directional interactions which occur between the malignant cells and the recruited cells, within an important extracellular matrix (ECM) form a local tumour microenvironment (TME) which has marked infiltration of inflammatory cells (Gao *et al.*, 2016). Cancers create a hypoxic, acidic environment in the TME, and this results in marked repression of immune cells' anti-tumour activity and there is consequential inflammation and cancer progression (Dominiak *et al.*, 2020).

In the breast, where cancers sit intimately related to AT-rich stroma (Figure 1.6), the breast TME potentially consists of all cell populations found in AT, as well as those immune cells travelling to the site (Figure 1.7).

Figure 1.6: Breast Cancer and its Proximity to Adipose Tissue

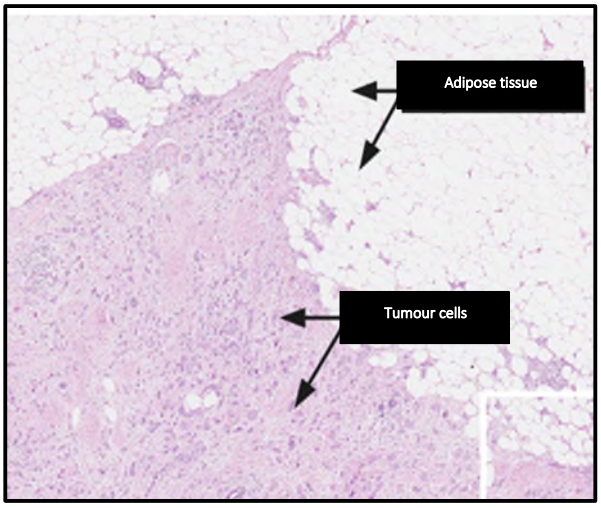

[Adapted from (Human Protein Atlas, 2020 available from https://www.proteinatlas.org/learn/dictionary/pathology/breast+cancer)]

H&E stained slide of breast cancer abutting adipocytes of the AT stroma. Scale not stated.

Figure 1.7: The Breast Cancer Tumour Microenvironment

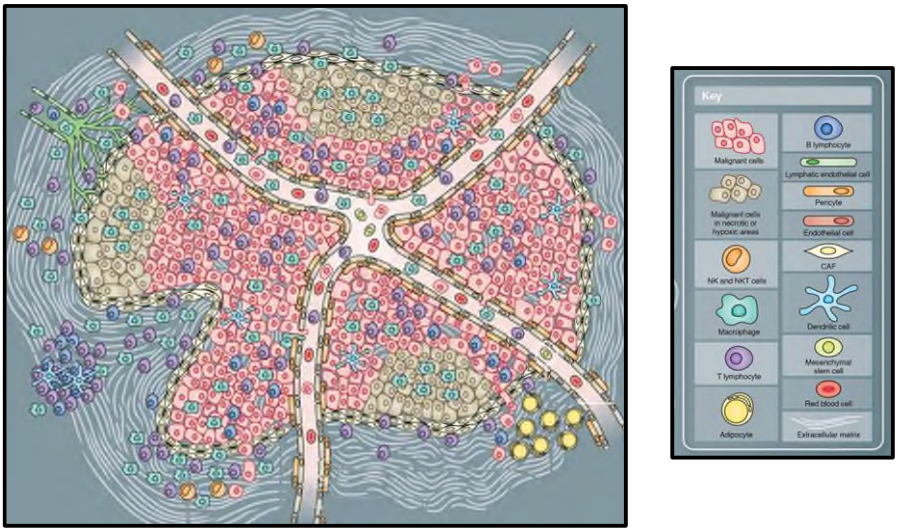

[Adapted, with permission, from (Balkwill *et al.*, 2012)]

Schematic illustraining the various cell populations of the tumour microenvironment. NK = natural killer (cell), NKT = natural killer T (cell), CAF = cancer associated fibroblast.

1.6.1 Adipose Tissue

AT is a loose connective tissue consisted of interdependent, metabolically and hormonally active cell populations within a complex extracellular matrix (ECM). In addition to supporting the cells of AT, the ECM also supports immune surveillance and rich lymphatic and vascular networks. Each component of AT has its own significant role to play in the modulation of the local environment (Schedin and Hovey, 2010). Fibroblasts, immune cells, adipocytes, and preadipocytes are all found in AT (Achari and Jain, 2017), and progenitor and stem cells are also important constituents (Rybinska *et al.*, 2020). These cells are in a constant state of dynamic equilibrium and relative proportions of each are heavily influenced by many factors including an individual's nutritional status, medication, and environmental change (Wang *et al.,* 2008). With the ongoing obesity epidemic, AT is now considered potentially the largest body organ in many individuals (Zewdu *et al.,* 2020). Factors which have been identified as external regulators of the function of AT include those outlined in Table 1.2.

1.6.1.1 Adipogenesis

Mesenchymal stem cells (MSC) are multipotent cells, with the potential to differentiate into chondroblasts, myoblasts, osteoblasts, and adipocytes (Ghaben and Scherer, 2019). At *determination*, the first stage of adipogenesis, the MSC is committed to the adipocyte line. Although previously understood to be non-reversible, this commitment is now recognised as multidirectional. These committed cells, now termed preadipocytes, enter a phase of growth arrest during which they become receptive to the stimuli of the next phase - *differentiation*. In this second phase, preadipocytes, under the influence of various inducer chemicals, progressively acquire the characteristics of mature adipocytes. The process of adipogenesis is complicated and closely regulated; peroxisome proliferator-activator receptor-γ (PPAR-γ) is a nuclear receptor essential for normal adipocyte differentiation, with other important players being the transcription coactivators CCAAT/enhancer-binding protein α (C/EBP α) and CCAAT/enhancer-binding protein β (C/EBP β) (Rybinska *et al.*, 2020).

Table 1.2: Select Regulators of Adipose Tissue Function

Factor	Action / Pathway
Catecholamines	- Stimulation of lipolysis *via* hormone-sensitive lipase activation *via* cAMP-PKA-phosphorylation
Cold exposure	- White to brown adipocytes
Warm exposure	- Brown to white adipocytes
Food intake	- Increased triglyceride delivery to AT
Free fatty acids	- Stimulation of adipocyte differentiation *via* PPAR-γ pathway
Glucocorticoids	- Stimulation of adipocyte differentiation *via* glucocorticoid receptor and maybe SREB-1c - Stimulation of lipogenesis at central nervous system level
Growth hormone	- Possible stimulation of preadipocyte proliferation - Stimulation of adipocyte differentiation - Reduce lipogenesis *via* inhibition of lipoprotein lipase activity - Increases lipolysis
Insulin and insulin-like growth factor-1 (IGF-1)	- Stimulation of differentiation *via* Ras and/or PKB - Activation of lipoprotein lipase and esterification pathways - Inhibition of hormone-sensitive lipase to inhibit lipolysis
Prolactin	- Possible promotion of adipocyte differentiation - Possible reduction of lipogenesis by inhibition of activity of lipoprotein lipase
Sex steroids	- Regulation of quantity and distribution of AT
Thiazolidinediones (TZDs)	- Stimulation of adipocyte differentiation *via* PPAR-γ pathway

[Adapted from (Wang *et al*., 2008)]

cAMP: cyclic adenosine monophosphate, PKA: phosphate kinas A, SREB-1c: sterol regulatory element-binding protein 1, Ras: proto-oncogene protein P21, PKB: protein kinase B.

1.6.1.2 Types and Functions of Adipose Tissue

The two main biologically, and thus functionally, distinct types of AT which have been identified in humans are white (WAT; the most common type in adults) and brown (BAT) (Saely *et al.,* 2012). WAT, consisting of adipocytes with a single large lipid droplet, and a peripheral nucleus and mitochondria, functions to store energy, and BAT, consisting of more highly vascularised (Hovey and Aimo, 2010) multilocular adipocytes which express uncoupling-protein 1 (UCP-1), functions to dissipate energy via non-shivering thermogenesis (Saely *et al.,* 2012) to maintain body temperature often considerably above ambient temperature (Zewdu *at al.,* 2020).

WAT, made up of <20 to 300 μm sized adipocytes (Stenkula and Erlanson-Albertsson, 2018), is the dominant fat type in the adult human body. Developing in mid-gestation in humans, depots are found in dermal, subcutaneous, intramuscular, bone marrow, and visceral (including gonadal, epiploic, omental, perirenal, and mesenteric) locations. These differing depots vary in their structure as well as their biochemical properties. Visceral WAT is known to be more metabolically active than subcutaneous AT and plays a greater role in metabolic disease (risk) when compared to subcutaneous AT (Rybinska *et al*., 2020). In humans, approximately 80% of WAT is in the subcutaneous depot. In athletes, body proportion of WAT mass may be as low as 6%, and in obesity the proportion exceeds the normal population measure of approximately 20% to at least 25% (males) or 30% (females) (Pallegar and Christian, 2020).

1.6.1.3 Adipose Tissue as an Endocrine Organ

In addition to its recognised activities as an energy depot, energy generator, and insulator, AT is now an accepted organ of metabolic regulation, having significant endocrine effects (Ouchi *et al*., 2011; Liu *et al.,* 2013; Choe *et al*., 2016; Achari *et al.,* 2017) and playing a fundamental role in whole organism homeostasis (Hovey and Aimo, 2010; Barchetta *et al*., 2019).

In 1993, TNF-α was identified as the first adipocyte-derived cytokine (Lehr *et al.*, 2012), and leptin was discovered soon after (Rybinska *et al.*, 2020). Research into the endocrine function of AT has advanced considerably since that time and now over 600 signalling molecules or hormones have been identified (Lehr *et al.,* 2012). AT has recognised endocrine roles at both local and systemic levels, with input into the modulation of, amongst others, feeding behaviour, haematopoiesis, immune function, and reproduction (Rybinska *et al.*, 2020). Recently, adipocytes have become an important focus in the research into disease states, including obesity and cancer.

1.6.1.4 Abnormal Adipose Tissue in Obesity

Obesity is "…abnormal or excessive fat accumulation that may impair health" (WHO, 2018) and is a preventable cause of numerous malignant and benign diseases. Globally, obesity prevalence almost tripled in the four decades after 1975, and now affects more than 650 million adults worldwide (WHO, 2018). Measures of obesity include waist size, waist-to-hip ratio, and BMI. The latter, the most commonly used, is calculated as $BMI = weight\ (kg) / height^2\ (m)$ and is defined as a value ≥30kg/m^2 (World Obesity Federation, 2015). Obesity is widely accepted as a significant risk factor for the development of many cancers including breast, bowel, renal, liver, ovarian, thyroid, oesophageal, pancreatic, and gallbladder (Basen-Engquist and Chang, 2011), and is associated with a poorer long-term outcome when compared to lean patients (Gallagher and LeRoith, 2015; Divella, 2016). Several causative processes have been proposed for the obesity-mediated increased breast cancer risk; these include systemic insulin imbalance and chronic inflammation of adipose tissue (Siriwardhana *et al.*, 2012).

Diabesity, the existence of obesity causing abnormal insulin signalling, has long been accepted (Matthews and Thompson, 2016). Downstream effects of raised circulating levels of insulin and IGF-1 were proposed as possible mechanisms of carcinogenesis several years ago. Postulated to act via the P13K/AKT/mTOR pathway, these hormone imbalances result in the increased expression of proteins including the cell cycle progression regulators (Alao, 2007; Miller *et al.*, 2012) cyclin D1 and c-MyC

(Matthews and Thompson, 2016). Insulin not only upregulates cell proliferation, it results in overexpression of the anti-apoptosis proteins Bcl-2 and Bcl-XL, and suppresses the pro-apoptosis protein Bax, giving a net reduction in programmed cell death (Matthews and Thompson, 2016). Elevated IGF-1 increases the risk of breast cancer in both pre- and post-menopausal females (Christopoulous *et al.*, 2015), whilst elevated insulin increases the risk in the latter group only (Gunter, 2009; Matthews and Thompson, 2016).

Both adipocyte hyperplasia and hypertrophy are seen in obesity (Rutkowski *et al.,* 2015). Larger adipocytes display aberrant behaviour including increased lipolysis and increased cell death (Matthews and Thompson, 2016; Wang *et al.*, 2017) resulting in greater cellular debris in the local environment further promoting adipocyte stress (Wensveen *et al.,* 2015). Maturation of adipocytes is reduced (Picon-Ruiz *et* al., 2016). Abnormal adipocytes have, or induce, higher levels of IL-6, TNF-α, CSF-1, and MCP-1 cytokine expression (Hajer *et al.,* 2008), and hypertrophic adipocyte populations are associated with local hypoxia (Rutkowski *et al.,* 2009; Yao-Borengasser *et al.,* 2015). This adipocyte dysfunction, in a hypoxic environment which triggers upregulation of HIF-1α, promotes AT inflammation (Lee *et al.,* 2014). Normal WAT consists of 10% macrophages (Karastergiou and Mohamed-Ali, 2010). Endoplasmic reticulum (ER) stress and increased reactive oxygen species (ROS) seen in obesity promote JNK and Nϰ-B (pro-inflammatory) pathways, recruiting more macrophages resulting in greater inflammatory cytokine release. Formation of crown-like structures, consisting of dying or dead adipocytes surrounded by macrophages, exacerbates inflammation and has been postulated as a mechanism of tumourigenesis (Choi *et al.*, 2018).

AT inflammation is compounded by a deficient anti-inflammatory response; the normal feedback mechanisms existing to produce IL-10/13/14 to dampen inflammation are compromised in obesity (Matthews and Thompson, 2016). Multiple pathways are implicated in the subsequent signalling cascades. IL-6, for example, activates STAT3 (Mauer, 2015), which has been shown to have a role in carcinogenesis (Levy and Lee, 2002). Its many actions include a stimulatory effect on the transcription of cyclin D1 and c-MyC (Banerjee and Resat, 2016). TNF-α upregulates HIF-1 and VEGF, thus stimulating angiogenesis (Matthews and Thompson, 2016). Taken in

combination, these two pro-inflammatory cytokines have marked effects on signalling pathways critical in the regulation of angiogenesis, cellular proliferation and apoptosis, and thus cause local environmental changes that predispose, encourage, and allow the malignant transformation of cells.

1.6.2 The Mammary Fat Pad

Although falling within the category of subcutaneous AT, fat of the breast - *the mammary fat pad* (MFP) - is distinct to other types of subcutaneous adipose. 56% of the radiologically assessed breast in the non-lactating female is AT, whilst it comprises 35% during lactation (Choi *et al.*, 2018). These findings are supported by analyses of mastectomy specimens which have suggested breast fat content of between 7-56% (Hovey and Aimo, 2010). With age and progression through the menopause, the relative proportion of AT increases as glandular tissue reduces (Hovey and Aimo, 2010).

Of particular importance in the MFP are the adipocytes (Hovey and Aimo, 2010). Normal breast glandular development is *dependent* upon communication with adipocytes likely at both a chemical (signalling) level as well as a physical (contact) level; in mice, in the absence of breast WAT, mammary gland development has been shown to be markedly limited, with only a few rudimentary short, distended ducts resulting (Couldrey *et al.*, 2002). Ongoing ovulation with normal serum oestradiol levels indicated that this role is independent of oestrogen exposure (Couldrey *et al.,* 2002). In humans, neonatal breast ductal structures are often seen surrounded by connective tissue stroma and have also been observed intimately located within embryonic fat islands (Hovey and Aimo, 2010).

The mature MFP has several features of distinction which set it apart from AT elsewhere in the body (Choi *et al.*, 2018), and these differences further vary over time, particularly with changes in physiological state such as moving from the non-pregnant, to the pregnant, then to the lactational states. During the latter, de-differentiation of adipocytes to fibroblast-like cells occurs, and then when lactation ceases, re-

differentiation occurs (Vasconcellos *et al.*, 2019). Involution with menopause is another important point of transformation. Differences have also been noted in different animal models (Hovey and Aimo, 2010). In humans, the relative proportions of the MFP fibroblasts and adipocytes is greater than hip AT. Also, the lipolytic response of the MFP to noradrenaline differs depending upon whether subjects are pre- or post-menopausal (being lower in the postmenopausal breast), whereas in other regions, such as the femoral area, the AT response to noradrenaline remains constant.

Perhaps the greatest transformation in the MFP is seen during pregnancy and lactation. These changes are above and beyond those seen in other fat depots in these states and are thought related to the considerable change seen in the mammary glandular tissue (Pujol *et al.,* 2006). The cross-sectional area of rats' MFP adipocytes increases by approximately 20% over time, when progressing from the non-pregnant state to pregnancy, and overall MFP weight, DNA content and protein content were observed to increase approximately two-fold by day 20 of gestation (Pujol *et al.,* 2006). These changes can be explained by an inhibition of lipolytic pathways and activity (Pujol *et al.,* 2006). MFP tissue in pregnancy has been shown to be more metabolically active than peritoneal AT, and even in the non-pregnant state, the MFP has been shown, repeatedly, to be a particularly active site of hormone synthesis (Hovey and Aimo, 2010). Epithelial cells have, via the action of lipoprotein lipase, been identified as inducing lipolysis in MFP adipocytes, during lactation (Hovey and Aimo, 2010).

1.6.3 Adipocytes in the Tumour Microenvironment

It is recognised that adipocytes and malignant cells communicate, and that this bidirectional cross-talk can lead to phenotypical and functional alterations in both cell populations with resulting shifts in the TME (Toren *et* al., 2013; Pallegar and Christian, 2020). It is now clear that adipocytes have a critical role to play in the TME (Toren *et al.*, 2013), and it has been suggested that they may alter epithelial cells phenotypically to become more aggressive (Carter and Church, 2012).

Upon histological review of peritumoural adipocytes, also called *cancer-associated adipocytes (*CAA*)*, morphological change can be seen; adipocytes are smaller, they lose lipid, they reduce in number, and they become more fibroblast-like (Toren *et* al., 2013; Rybinska *et al.*, 2020) when compared to their non-tumour associated counterparts. Also, fewer preadipocytes are present (Wang *et* al., 2014). Studying this change has revealed such dedifferentiation to be driven by tumour cells (Choi *et al.*, 2018), and can be objectively appreciated with reductions in the markers of differentiated adipocytes FABP4, PPAR-γ and C/EBP-α (Lee *et al.,* 2017). In addition to the architectural changes seen, biochemical behaviours also change. Research has also suggested that in addition to being a source of signalling molecules, adipocytes may act as an energy source for malignant cells (Toren *et al.*, 2013; Rybinska *et al.*, 2020); cancer cells become "…metabolic parasites…" (Wu *et al.*, 2019), appropriating glutamine, pyruvate, lactate, fatty acids, and ketone bodies from adipocytes (Hoy *et al.,* 2017; Wu *et al.*, 2019) and inducing lipolysis (Wang *et al.,* 2014). It is postulated that the quality and quantity of AT in a TME may influence all these changes (Toren *et al.*, 2013).

Preadipocytes are the second most common cell type in AT (Kim *et al.,* 2018) and thus form a significant proportion of the breast TME. They have been demonstrated to be active in this peritumoural location with regards to cancer behaviour; when medium taken from cultures of preadipocytes was used for sustaining DCIS, the pre-invasive disease demonstrated increased migration as well as invasive capabilities indicating the development of a more aggressive phenotype (Kim *et al.,* 2018). When differentiation in the presence of cancer cells was assessed, it was found to be hindered by the malignant cells and it is postulated that, as (potentially malignancy promoting) adipokine secretion is higher in some instances in preadipocytes when compared to adipocytes, *cancer cells impair preadipocyte differentiation* in order to maintain a more favourable TME.

1.6.4 Adipokines in the Breast Tumour Microenvironment

Adipocytes are able to secrete both free adipokines and adipokine-containing extracellular vesicles. Adipokines act in an endocrine, paracrine, or autocrine manner (Zewdu *et al.*, 2018), as messengers of intercellular communication. These bioactive proteins influence target cells where they may contribute to development of pathology.

1.6.4.1 Adipokines

Coined in the late 1990s, the term 'adipocytokines' refers to the mainly inflammatory chemical signalling molecules secreted by AT. The term *adipokine*, first used in 2004 (Trayhurn and Wood), was introduced to additionally encompass those secretory chemokines which are non-inflammatory in nature. Adipokines are a complex, heterogenous group of signalling molecules (Toren *et al.*, 2013), influencing numerous cell functions as well as homeostatic and whole-body mechanisms important in appetite control, metabolism, blood pressure control, and the immune system (Ouchi, *et al.,* 2011; Zagotta *et al.*, 2015). Research into the identification of adipokines has progressed considerably in recent years.

1.6.4.2 Common Adipokines of the Breast Tumour Microenvironment

Numerous adipokines have been identified in the breast TME. Amongst the most commonly studied are adiponectin, leptin, TNF-α, and IL-6.

- Adiponectin:
  Secreted by adipocytes, the 244 amino acid long (Christodoulatos *et al.*, 2019) anti-inflammatory (Housa *et al.*, 2006) polypeptide adiponectin is the most abundantly produced of all known (human) adipokines (Kaur and Zhang, 2005). Having endocrine functions and being involved in energy metabolism, adiponectin sensitises tissues to insulin and stimulates the catabolism of glucose and fatty acids (Wang and Yang, 2008). Serum levels of adiponectin are inversely associated with

mass of AT and confer a protective effect against diseases associated with obesity (namely diabetes, cardiovascular disease, and malignancy) (Christodoulatos *et al.*, 2019). Adiponectin acts primarily via the AMPK/LKB1 signalling pathway. It also activates AMPK which inhibits JAK/STAT3, MAPK, NF-ϰB and PI3K/Akt pathways (Christodoulatos *et al.*, 2019). Notably, the effect of adiponectin in BC appears to be dependent upon the ER status of the disease; in ER^- disease, malignancy is suppressed but in ER^+ disease, its role is less clear (Christodoulatos *et al.*, 2019).

- Leptin:

  A neuroendocrine hormone, leptin was discovered in the early 1990s (Friedman 2014). It functions in the regulation of food intake *via* appetite regulation, and additionally has roles in angiogenesis and reproduction (Kaur and Zhang, 2005). Circulating leptin levels are proportional to an individual's total mass of adipose tissue (Housa *et al.*, 2006); the majority of leptin is secreted by adipocytes. Small quantities are, however, expressed in other cell types including the epithelial cells of the breast (Kaur and Zhang, 2005). Leptin acts via activation of the ERK1/3 (Jiramongkol and Lam, 2020), JAK/STAT, JNK and MAPK signalling pathways (Housa *et al.*, 2006). Exogenous leptin stimulation of breast cells increases cellular transformation (Housa *et* al., 2006), and treatment of malignant breast cells increases their proliferative rate (Hu *et al.*, 2002).

- TNF-α:

  TNF-α has wide ranging actions and is involved in the pathophysiology of a number of disease states by way of its promotion of inflammation. It is produced and secreted by many cell types in addition to adipocytes, including AT-resident macrophages (Kaur and Zhang, 2005) and some cancer cells where it acts as an autocrine growth factor (Sethi *et al.*, 2008). Identified in the 1970s, it was initially thought to be active in fighting malignant cells by inducing cell death. Research since has discovered the role of TNF- α to be a far more complex one, stimulating cell proliferation and survival as well as migration in those malignant cells resistant to its cytotoxic properties (Wang and Yang, 2008). TNF-α acts via multiple signalling pathways including JNK, MAPK, and NF-ϰB (Sethi *et al.*, 2008). In cell

studies, TNF-α increased resistance to chemotherapy in MCF-7 cells (Esquivel-Velazquez *et al.,* 2015). In BC, serum levels of TNF-α are significantly higher in individuals with more advanced disease when compared to controls (Ma *et al*., 2017).

- Interleukin-6 (IL-6):

  Playing an important role in the regulation of the immune and inflammatory responses, IL-6 also acts to influence cancer cell biology (Kaur and Zhang, 2005), acting *via* the JAK/STAT3 pathway (Jiramongkol and Lam, 2020). Tumour overexpression of IL-6 results in an increase in the invasive capabilities of BC cells, and elevated serum levels corresponds to a poorer prognosis in individuals with the disease (Dirat *et al*., 2011), being significantly correlated with higher stage, involvement of lymph nodes, and HER2 receptor expression (Ma *et al*. 2017).

1.7 Aim of the Study

The aim of this research is to further investigate the role of adipocytes and adipokines in the breast cancer TME, with a focus on identifying a proliferation promoting adipokine of interest not previously known to directly increase rate of cancer cell growth. ER^+ and TN BC will be researched. This will be undertaken as follows:

1. Pre-differentiated and mature adipocytes will be co-cultured individually with ER^+ and TN BC cells, and proliferation assessed. Rate of proliferation will be compared to that of BC cells cultured alone to determine the influence of the adipocytes on rate of cell replication (Chapter Three).
2. Next, the cytokine profiles of media from benign human breast explant AT cultures (tissue from [1] close to and [2] distant to ER^+ and TN BC tumours) will be compared to identify potential cytokines of interest. To investigate the effects of adipocytes alone, further adipocyte and BC cell co-culture experiments will be undertaken to investigate the effects of BC cells on the cytokine secretion and gene expression profiles of select adipokines (Chapter Four).

3. Finally, novel cytokines of interest will be investigated to determine their effects on BC cell proliferation (Chapter Five), to ascertain whether they may be potential therapeutic targets.

1.8 Ethical Approval

This study was covered by the Arden Tissue Bank (ATB) *Tissue Surplus to Requirements* licence (ATB Reference: ATB18-007).

CHAPTER TWO

Materials and Methods

Chapter Two: Materials and Methods

Contents

2.1	**Materials……**	**41**
2.1.1	Cell Lines…….	41
2.1.2	Cell Line and Explant Culture Chemicals…….	41
2.1.3	Media Formulations…….	42
2.1.4	General Chemicals and Reagents……..	43
2.1.5	Primers…….	44
2.1.6	Kit……	44
2.1.7	Miscellaneous……...	45
2.2	**Methods…….**	**46**
2.2.1	Fresh Tissue…….	46
2.2.1.2	Explant Culture……	46
2.2.2	Cell Lines…….	47
2.2.2.1	MCF-7 Cells…….	47
2.2.2.2	MCF-7 Cell Retrieval……	49
2.2.2.3	MCF-7 Cell Subculture…….	49
2.2.2.4	MCF-7 Cell Cryopreservation……...	49
2.2.2.5	MDA-MB-231 Cells…….	50
2.2.2.6	MDA-MB-231 Cell Retrieval, Subculture, and Cryopreservation…..	50
2.2.2.7	SGBS Cells……...	50
2.2.2.8	SGBS Cell Recovery…….	51
2.2.2.9	SGBS Cell Subculture..…….	51
2.2.2.10	SGBS Cell Differentiation……	52
2.2.3	Cell Lysis……..	54
2.2.4	RNA Extraction……...	54
2.2.5	Cell Co-Culture……	55
2.2.5.1	Cell Co-Culture for Media Harvesting …….	55
2.2.5.2	Cell Co-Culture for RNA Extraction……	57
2.2.6	Proteome Profiler™ Human XL Cytokine Array Kit……	57
2.2.7	xCELLigence® RTCA™ DP Cell Proliferation Assay……...	59

2.2.7.1 xCELLigence® Optimisation…… 59
2.2.7.2 Co-Culture xCELLigence® Experiment…… 61
2.2.8 Chitinase 3 Like-1 Stimulation of MCF-7 and MDA-MB-231 Cells.. 64
2.2.9 Staining of Adipocytes with Oil Red O……. 64
2.2.10 Reverse Transcription and Polymerase Chain Reaction…… 65
2.2.11 Reverse Transcription……... 65
2.2.12 Polymerase Chain Reaction…….. 66
2.2.13 Statistical Analysis…… 68
2.2.13.1 Student's t-Test…… 68
2.2.13.2 Wilcoxon Matched-Pairs Signed-Ranks Test……. 69
2.2.13.4 ANOVA……... 69
2.2.13.5 Post Hoc Tests……. 70

2. 1 Materials

2.1.1 Cell Lines

MCF-7 (Public Health England, European Collection of Authenticated Cell Cultures, Salisbury, United Kingdom)
MDA-MB-231 (Public Health England, European Collection of Authenticated Cell Cultures, Salisbury, United Kingdom)
SGBS (kind gift from Professor M Wabitsch, University of Ulm, Germany)

2.1.2 Cell Line and Explant Culture Chemicals

3-Isobutyl-1-methylxanthine ('IBMX'; Sigma-Aldrich, Haverhill, United Kingdom)
apo-Transferrin human ('transferrin'; Sigma-Aldrich, Haverhill, United Kingdom)
Biotin (Sigma-Aldrich, Haverhill, United Kingdom)
Cortisol (Sigma-Aldrich, Haverhill, United Kingdom)
Dexamethasone (Sigma-Aldrich, Haverhill, United Kingdom)
Dimethyl sulfoxide ('DMSO'; Sigma-Aldrich, Haverhill, United Kingdom)
Dulbecco's Modified Engle's Medium ('DMEM'; Gibco™, Fisher Scientific, Loughborough, United Kingdom)
DMEM/F12 (Gibco™, Fisher Scientific, Loughborough, United Kingdom)
D-Pantothenic acid ('Pantothenate'; Sigma-Aldrich, Haverhill, United Kingdom)
Foetal bovine serum ('FBS'; Gibco™, Fisher Scientific, Loughborough, United Kingdom)
Gelatin from bovine skin (Sigma-Aldrich, Haverhill, United Kingdom)
Insulin 4mg/mL (Gibco™, Fisher Scientific, Loughborough, United Kingdom)
Penicillin/Streptomycin 100X (Gibco™, Fisher Scientific, Loughborough, United Kingdom)
Rosiglitazone (Cayman Chemical, Cambridge, United Kingdom)
Triiodo-L-thyronine ('T3'; Sigma-Aldrich, Haverhill, United Kingdom)
Trypan blue solution 0.4% (Sigma-Aldrich, Haverhill, United Kingdom)

Trypsin-EDTA solution 1X ('Trypsin'; Sigma-Aldrich, Haverhill, United Kingdom)

2.1.3 Media Formulations

0F Medium for SGBS Cells

DMEM/F12 with 1% *v/v* penicillin/streptomycin, 3.3 mM pantothenate, and 1.7 mM biotin

Quick Differentiation (QD) Medium for SGBS Cells

0F medium with 0.01 mg/ml apo-transferrin, 20 nM insulin, 100 nM cortisol, 0.2 nM triiodo-L-thyronine, 25 nM dexamethasone, 250 μM 3-isobutyl-1-methylxanthine, and 2 μM rosiglitazone

3FC Medium for SGBS Cells

0F medium with 0.01 mg/ml apo-transferrin, 20 nM insulin, 100 nM cortisol, and 0.2 nM triiodo-L-thyronine

General Medium for SGBS Cells (GM_{SGBS})

0F medium with 10% *v/v* foetal bovine serum

General Medium for MCF-7 Cells ($GM_{MCF\text{-}7}$)

DMEM/F12 with 10% *v/v* foetal bovine serum, and 1% *v/v* penicillin/streptomycin

General Medium for MDA-MB-231 Cells ($GM_{MDA\text{-}MB\text{-}231}$)

DMEM with 10% *v/v* foetal bovine serum, and 1% *v/v* penicillin/streptomycin

General Medium for Explanted Tissue ($GM_{Explant}$)

DMEM/F12 with 1% *v/v* penicillin/streptomycin

2.1.4 General Chemicals and Reagents

5X RevertAid reaction buffer (Thermo Scientific™, Fisher Scientific, Loughborough, United Kingdom)
10X DNase I reaction buffer (Sigma-Aldrich, Haverhill, United Kingdom)
100x ROX reference dye (Sigma-Aldrich, Haverhill, United Kingdom)
Chloroform (Sigma-Aldrich, Haverhill, United Kingdom)
DNase I amplification grade (Sigma-Aldrich, Haverhill, United Kingdom)
DNase stop solution (Sigma-Aldrich, Haverhill, United Kingdom)
dNTP mix 10 mM (Thermo Scientific™, Fisher Scientific, Loughborough, United Kingdom)
Ethanol (Sigma-Aldrich, Haverhill, United Kingdom)
Isopropanol (Fisher Scientific, Loughborough, United Kingdom)
Nuclease-free water (Fisher Scientific, Loughborough, United Kingdom)
Oil Red O (Sigma-Aldrich, Haverhill, United Kingdom)
Paraformaldehyde 4% in PBS 1X (Affymetrix, High Wycombe, United Kingdom)
Phosphate Buffered Saline ('PBS'; University of Warwick, United Kingdom)
QIAzol™ lysis reagent (QIAGEN, Manchester, United Kingdom)
Random Hexamer Primers (Thermo Scientific™, Fisher Scientific, Loughborough, United Kingdom)
RevertAid H Minus Reverse Transcriptase (Thermo Scientific™, Fisher Scientific, Loughborough, United Kingdom)
RNase OUT™ Recombinant Ribonuclease Inhibitor (Invitrogen™, Fisher Scientific, Loughborough, United Kingdom)
SYBR® Green JumpStart™ *Taq* ReadyMix™ (Sigma-Aldrich, Haverhill, United Kingdom)

2.1.5 Primers

Table 2.1: Primer Sequences (Human Genes)

Gene Name	Forward Primer	Reverse Primer
L19	GCGGAAGGGTACAGCCA	GCAGCCGGCGCAAAA
FABP4	TGTTGCAGAAATGGGATGGAAA	CAACGTTCCCTTGGCTTATGCT
IL1RL1	GCTCCGTCACTGACTCCAAG	ACACATGAGGCAGTTGGTGA
CCL2	GAAAGTCTCTGCCGCCCTT	GGTGACTGGGGCATTGATTG
CXCL8	CTGGGTGCAGAGGGTTGTG	GCTTGAAGTTTCACTGGCATCT
CHI3L1	GGTCAGGAGGATGCAAGTCC	TGCCCATCACCAGCTTACTG
SPP1	AGCAGAATCTCCTAGCCCCA	TGGTCATGGCTTTCGTTGGA
CST3	GGCACAATGACCTTGTCGAA	GGGTGGGAGGTGTGCATAAG
CXCL5	CTCCAATCTTCGCTCCTCCAA	AGGAGGCTCATAGTGGTCAAG

2.1.6 Kit

Proteome Profiler™ Human XL Cytokine Array Kit (R&D Systems, Abingdon, United Kingdom)

Array buffer 4

Array buffer 6

Chemi reagent 1

Chemi reagent 2

Detection Antibody Cocktail

Streptavidin-HRP

Wash buffer concentrate

2.1.7 Miscellaneous

Cell culture plate (Appleton Woods, Birmingham, United Kingdom)
Ministart 0.22 μm filter unit (Sartorius Stedim Biotech, Stonehouse, United Kingdom)
Netwells® 74 μm mesh size polyester membrane insert culture plate (Corning B.V. Life Sciences, Scientific Laboratory Supplies, Nottingham, United Kingdom)
RNase-free tube (Fisher Scientific, Loughborough, United Kingdom)
Transwell® 12mm 0.4 μm pore polyester membrane insert cell culture plate (Corning B.V. Life Sciences, Scientific Laboratory Supplies, Nottingham, United Kingdom)
Transwell® 24mm 0.4 μm pore polyester membrane insert cell culture plate (Corning B.V. Life Sciences, Scientific Laboratory Supplies, Nottingham, United Kingdom)
xCELLigence® DP E-plate® VIEW 16 PET (ACEA Biosciences, San Diego, United States of America)
xCELLigence® E-plate® insert 16 (ACEA Biosciences, San Diego, United States of America)

2.2 Methods

2.2.1 Fresh Tissue

Fresh breast adipose tissue (AT) samples were obtained, *via* Arden Tissue Bank (ATB), from consenting patients having surgery under the care of the Oncoplastic Breast Surgeons at University Hospital, University Hospitals Coventry and Warwickshire NHS Trust.

In theatre, the resected surgical specimen (mastectomy or wide local excision) was placed intact in a dry receptacle and the time of excision noted. ATB staff were contacted, and the sample collected and transported to the hospital's Pathology Department. Here, a Consultant Pathologist orientated, painted, and sliced the specimen as per standard protocol for processing diagnostic breast cancer (BC) resections. Following his/her macroscopic identification of the tumour, the Pathologist excised two pieces of fatty tissue (*peri-tumoural* and *distant*; each patient providing her own control specimen) and placed them in separate 50 ml centrifuge tubes. Each tube contained approximately 20 ml of room temperature DMEM/F12 medium (Gibco^{TM}, Fisher Scientific, Loughborough, United Kingdom). Peritumoural tissue was taken from within 10 mm of the tumour edge, and distant tissue taken from as far from the lesion as possible, at the resection margin; exact distances were measured and noted. The paired tissue specimens were transported to the Clinical Sciences Research Laboratory ('CSRL') adjoining the hospital on ice, and tissue processing commenced. All specimens arrived in the CSRL within 60 min of surgical excision.

2.2.1.2 Explant culture

The Pathologist provided samples were washed in phosphate buffered saline ('PBS'; University of Warwick, United Kingdom) warmed to 37^{O}C and divided into aliquots

of similar mass. Each aliquot was minced with scissors to produce fragments no larger than 2 mm x 2 mm allowing an increased surface area for gaseous exchange and decreased nutrient diffusion distance, with the aim of maintaining explant integrity and reducing tissue necrosis. Minced tissue was placed in sterile 74 μm polyester mesh Corning® Netwells® 12 mm inserts in 12-well-plates (Corning B.V. Life Sciences, Scientific Laboratory Supplies, Nottingham, United Kingdom), with 3 ml serum-free medium (DMEM/F12 + 1% penicillin/streptomycin) per well (Figure 2.1).

These plates were incubated (5% CO_2, 37^{O}C) and at 24 h, the media aspirated, centrifuged (250 *g*, room temperature, 5 min), and passed through a Ministart 0.2 μm filter unit (Sartorius Stedim Biotech, Stonehouse, United Kingdom) to remove debris. The resulting acellular media was frozen (-80^{O}C) for later cytokine content analysis. Explant tissue was passed back to ATB staff who kindly produced paraffin-embedded tissue slides to allow assessment of tissue integrity.

2.2.2 Cell Lines

2.2.2.1 MCF-7 Cells

The MCF-7 breast cancer cell line was established in 1973, at the Michigan Cancer Foundation. The epithelial-like adenocarcinoma cells were taken from a metastatic pleural effusion in a 69-year-old Caucasian female, and immortalised. The adherent cells fit a *Luminal A* molecular sub-classification pattern (Holliday and Speirs, 2011), being $ER^+/PR^+/HER2^-$.

MCF-7 cells were purchased from the European Collection of Authenticated Cell Cultures (ECACC, Salisbury, United Kingdom). Frozen passage 15 (P15) cells were received and stored in liquid nitrogen until required. All experiments used cells of P18 to P24 inclusive.

Figure 2.1: Human Breast Tissue Explants

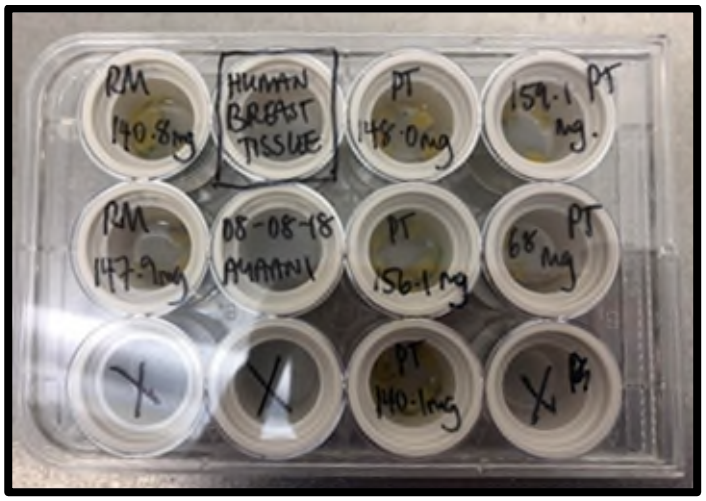

Tissue placed in sterile 74 μm polyester mesh Corning® Netwells® 12 mm inserts in a 12-well-plate.

2.2.2.2 MCF-7 Cell Retrieval

Frozen cells were partially thawed in a water bath set to 37^{O}C. 1 ml GM_{MCF-7} (DMEM/F12 + 10% FCS + 1% penicillin/streptomycin) medium was added to the cell-containing vial, and the total volume of cells and medium transferred to a 15 ml centrifuge tube containing a further 8 ml GM_{MCF-7}. The cell suspension was pipetted up and down to ensure thorough mixing. After centrifugation (250 *g*, room temperature, 5 min), the supernatant was discarded to remove the diluted freezing medium. The residual pellet was resuspended in fresh GM_{MCF-7} and the cells seeded in two T25 flasks, as per ECCAC recommendations. Medium was changed the day after thawing, and twice per week thereafter. To maintain cells in the logarithmic growth phase, they were subcultured when 80-85% confluence was reached.

2.2.2.3 MCF-7 Cell Subculture

At 80-85% cell confluence, medium was aspirated from flasks and the MCF-7 cell monolayer washed with 8 ml PBS warmed to 37^{O}C. 500 µl (T25 flask) or 1.5 ml (T75 flask) trypsin-EDTA 1X ('trypsin', Sigma-Aldrich, Haverhill, United Kingdom) were added and the vessel placed in an incubator (5% CO_2, 37^{O}C, 5 min) to ensure complete cell detachment. 5 ml (T25) or 7.5 ml (T75) GM_{MCF-7} were added as a trypsin neutraliser, and the cell/trypsin/medium mix pipetted up and down to ensure maximal cellular detachment and de-clumping. After centrifugation (250 *g*, room temperature, 5 min), the pellet was resuspended in fresh GM_{MCF-7}. Each of the initial T25 flask of cells was replated in a T75 flask. Subsequently, T75 flasks were split at a ratio appropriate to the rate of growth required (typically 1:3 or 1:4).

2.2.2.4 MCF-7 Cell Cryopreservation

Stock and surplus cells were suspended in freezing medium (90% GM_{MCF-7} + 10% DMSO [Sigma-Aldrich, Haverhill, United Kingdom]) and 1 ml pipetted into cryovials at a concentration of $1x10^6$ cells/ml. The cryovials were placed in a Mr Frosty^{TM} (Fisher

Scientific, Loughborough, United Kingdom) for controlled gradual freezing to a temperature of -80^{O}C, and then transferred for longer term storage to liquid nitrogen.

2.2.2.5 MDA-MB-231 Cells

The MDA-MB-231 BC cell line was immortalised at the MD Anderson Cancer Centre, from the pleural effusion of 51-year-old Caucasian female. The cells are TN; they lack oestrogen and progesterone receptors, and HER2 is not amplified. MDA-MB-231 is a poorly differentiated, highly aggressive cancer cell line belonging to the claudin-low TN BC molecular sub-category (ECACC, 2017).

MDA-MB-231 cells were purchased from the ECACC. Frozen P46 cells were received and stored in liquid nitrogen until required. All experiments used cells of P46 to P56 inclusive.

2.2.2.6 MDA-MB-231 Cell Retrieval, Subculture, and Cryopreservation

Cell retrieval, subculture, and cryopreservation followed the same protocols as for MCF-7 cells (2.2.2.2 - 2.2.2.4). $GM_{MDA\text{-}MB\text{-}231}$ (DMEM + 10% FBS + 1% penicillin/streptomycin + 1% pantothenate/biotin) was used. Centrifugation was at 150 *g* for 10 min (room temperature).

2.2.2.7 SGBS Cells

In 2001, Wabitsch and Brenner *et al.* published their work describing the preadipocyte cell strain they had developed from the white subcutaneous adipose tissue of an infant with Simpson-Golabi-Behmel Syndrome (SGBS). The rare SGB Syndrome is X-linked and characterised by both prenatal and postnatal overgrowth. Although the syndrome is often linked to a mutation in the *Glypican 3* gene, genetic analysis of the infant from whom the cells were harvested did not reveal this aberration.

Wabitsch and Brenner *et al.*'s (2001) work resulted in a non-immortalised cell strain which can be differentiated to >95% mature adipocytes, to at least 50 generations (Fischer-Posovszky *et al.,* 2008). Differentiated adipocytes are recognised as both functionally and biochemically comparable to primary preadipocytes (Rosenow *et al.*, 2010).

The SGBS cells used in this research were received as pre-differentiated cells, as a kind gift from Prof. Wabitsch. Cells were tested for mycoplasma contamination (negative) and cultured to produce a stock supply by fellow researchers in Prof. Christian's research laboratory. Cells were stored ($1x10^6$/ml/cryovial) in liquid nitrogen until required. All experiments used cells of P8 to P14 inclusive.

2.2.2.8 SGBS Cell Retrieval

Frozen pre-differentiated cells were partially thawed in a water bath set to 37^OC, and then suspended in 20 ml of DMEM/F12 + 10% FBS + 1% penicillin/streptomycin + 1% pantothenate/biotin (GM_{SGBS}). After centrifugation (200 *g*, room temperature, 5 min), supernatant was aspirated to remove the diluted freezing medium, and the cell pellet resuspended in fresh GM_{SGBS}. Cells were plated in a T75 flask and cultured in an incubator (5% CO_2, 37^OC) to 80% confluence. Medium was changed twice per week.

2.2.2.9 SGBS Cell Subculture

At 80% confluence, medium from the pre-differentiated cells was aspirated and the flask washed with PBS warmed to 37^OC. 750 µl trypsin were added and the vessel incubated (5% CO_2, 37^OC, 5 min) to promote cell detachment. 20 ml media were added as a trypsin-neutraliser, once cells had lifted. The cell/trypsin/medium mix was gently pipetted up and down to ensure cells were not clumped. After centrifugation (200 *g*, room temperature, 10 min), the pellet was resuspended in fresh GM_{SGBS}. Cells were split at a 1:3 ratio or plated at 1:8 T75:6-well-plates.

2.2.2.10 SGBS Cell Differentiation

In contrast to pre-differentiated cells which retain their proliferative properties, mature adipocytes do not multiply; they have lost their capacity for mitotic activity. For the purposes of laboratory work therefore, preadipocytes are first expanded in number, and then differentiation is induced to obtain mature lipid-containing cells.

For differentiation, SGBS cells were plated in gelatin-coated 6- or 12-well-plates in $GM_{SGBS,}$ at a density of $2x10^5$ cells/cm^2. They were cultured to 100% confluence and then left for a further 48 h before the differentiation process was started. A two day pause allows cells to move out of the proliferative phase of cell growth, making them more responsive to the chemical stimuli of differentiation. Two cocktails are required to differentiate SGBS cells: quick differentiation (QD) and 3-FC media (Table 2.2). Base medium is DMEM/F12 with 1% penicillin/streptomycin and 1% pantothenate/biotin.

In the absence of serum, transferrin is added as a donor of the essential trace element iron. It is necessary for optimal cellular function, including adipogenesis. Insulin, an anabolic peptide hormone produced by the β-cells of the pancreas, has several functions. Here, its ability to induce adipogenesis is exploited. By acting synergistically with insulin, dexamethasone - a synthetic glucocorticoid - promotes adipogenesis *via* activation of its glucocorticoid receptors. T3, by acting on its nuclear receptors, increases the expression of genes of adipogenesis. IBMX exerts its effect by increasing intracellular levels of cAMP *via* its inhibition of phosphodiesterases. Rosiglitazone belongs to the thiazolidinedione (TZD) family of drugs. It, along with other TZDs, is recognised as a stimulator of adipogenesis *via* its activation of PPARγ.

From the addition of QD (Day 0), cells require 14 days to differentiate into fully mature adipocytes ready for experimentation (Figure 2.2).

Table 2.2: Media for SGBS Cell Differentiation

Compound	QD	3-FC
Transferrin	0.01 mg/ml	0.01 mg/ml
Insulin	20 nM	20 nM
Cortisol	100 nM	100 nM
T3	0.2 nM	-
Dexamethasone	25 nM	-
IBMX	250 µM	-
Rosiglitazone	2 µM	-

T3: triiodo-L-thyronine, IBMX: 3-Isobutyl-1-methylxanthine.

Figure 2.2: SGBS Cell Differentiation Protocol

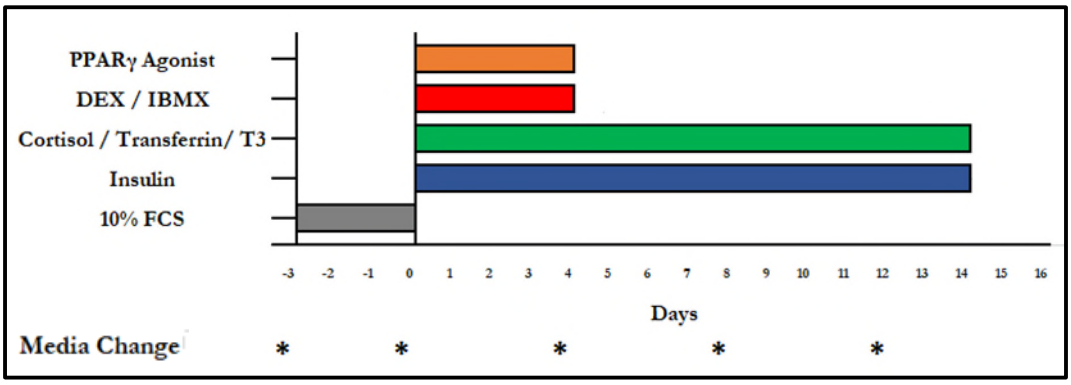

[Taken from (Fischer-Posovszky *et al.,* 2008), ©2008 Karger Publishers, Basel, Switzerland]

Graph to illustrate media used and media change points for SGBS differentiation.

DEX: dexamethasone, FCS: foetal calf serum.

At Day 0, when QD replaces GM_{SGBS}, pre-differentiated cells are washed twice with warmed PBS to ensure complete removal of foetal bovine serum (FBS) as cells will not differentiate in its presence. On Day 4, the medium is switched from QD to 3-FC, with the latter being changed on Days 8 and 12. In this research, cells were only used if ≥90% of the plated population achieved differentiation to maturity (differentiation was deemed successful if cells contained lipid droplets, as visually assessed using Oil Red O staining [2.2.9]).

2.2.3 Cell Lysis

Medium was aspirated and cells washed with PBS warmed to 37^{O}C. After PBS removal, 500 µl (12mm well/insert) or 1 ml (24mm well/insert) QIAzol® (QIAGEN, Manchester, United Kingdom) was added. A scraper was used to ensure complete cell detachment and lysis. After incubation (room temperature, 5 min), the lysate was transferred to an RNAse-free tube.

2.2.4 RNA Extraction

All steps were carried out on ice, unless otherwise specified. Chloroform (Sigma-Aldrich, Haverhill, United Kingdom) was added to the lysate at a ratio of QIAZOL® : chloroform 5:1 *v/v*. Samples were shaken vigorously for 30 s, incubated (room temperature, 3 min), and then centrifuged (15 000 *g*, 4^{O}C, 30 min). During centrifugation, phase separation occurs resulting in a pink lower phenol-chloroform organic phase, a white intermediate DNA-containing phase, and a clear upper RNA-containing aqueous phase. The latter was aspirated and transferred to a new RNAse-free tube. Isopropanol (Fisher Scientific, Loughborough, United Kingdom) was added (QIAzol® : isopropanol 2:1 *v/v*), and samples incubated (room temperature, 10 min) to allow for the precipitation of RNA. Centrifugation (15 000 *g*, 4^{O}C, 30 min) was followed by supernatant aspiration. 1 ml ethanol (Sigma-Aldrich, Haverhill, United

Kingdom) was added to the residual RNA pellet. After centrifugation (15 000 *g*, 4^{O}C, 30 min), again supernatant was aspirated and discarded. The RNA pellet was left to air dry (maximum 10 min), and then 8-15 µl of RNAse-free water (Fisher Scientific, Loughborough, United Kingdom) added, as appropriate. A final incubation of 20 min followed, to allow complete solubilisation of RNA. The concentration of extracted RNA was measured using a NanoDrop™ 1000 Spectrophotometer (ThermoFisher Scientific, Altrincham, United Kingdom). If not immediately reverse transcribed to complementary DNA (cDNA), RNA samples were stored at -80^{O}C.

2.2.5 Cell Co-Culture

MCF-7 and MDA-MB-231 cells were, separately, co-cultured with pre-differentiated and mature SGBS cells to investigate the effects of cancer cells on adipocyte inflammatory cytokine secretion and gene expression.

2.2.5.1 Cell Co-Culture for Media Harvesting

Pre-differentiated SGBS cells were differentiated to maturity as described (2.2.2.10), in 6-well plates. On Day 14, their 3-FC medium was aspirated and 2.5 ml GM_{SGBS} added to each well. Simultaneously, six 24 mm Corning® Transwell® inserts with 0.4 µm pore polyester membranes (Corning B.V. Life Sciences, Scientific Laboratory Supplies, Nottingham, United Kingdom) were incubated (5% CO_2, 37^{O}C, 1 h) with 2 ml GM_{SGBS}, as per manufacturer's instruction, to allow for greater membrane permeability. Post-incubation, media was aspirated from the inserts, and cancer cells seeded in six inserts, at a density of 40 000/cm^2. Three cancer cell containing inserts were placed in SGBS-containing wells to commence the co-culture, and three media-only containing inserts were placed in wells containing SGBS (SGBS controls). Each insert had a total of 1.5 ml GM_{SGBS}, and each well contained 2.5 ml of medium (Figures 2.3 and 2.4).

Figure 2.3: SGBS and Breast Cancer Cells Co-Culture Construct

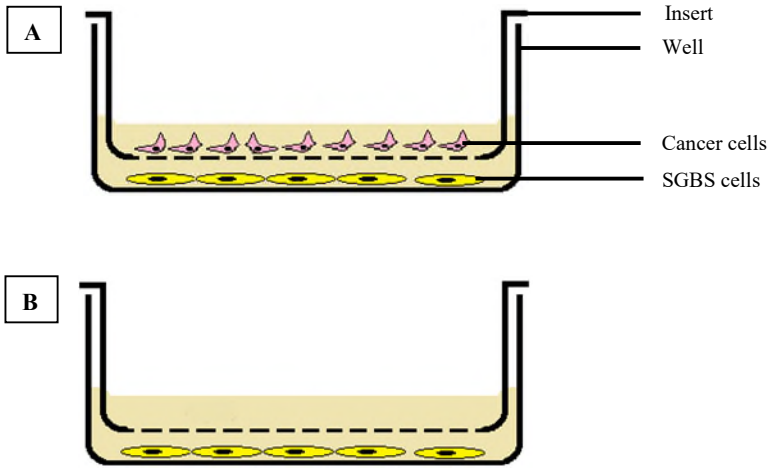

A: SGBS / cancer cell co-culture (SGBS Co). **B**: SGBS alone (SGBS control).

Figure 2.4: Light Microscopy Images of Breast Cancer Cells cultured in a Corning® Transwell® Insert

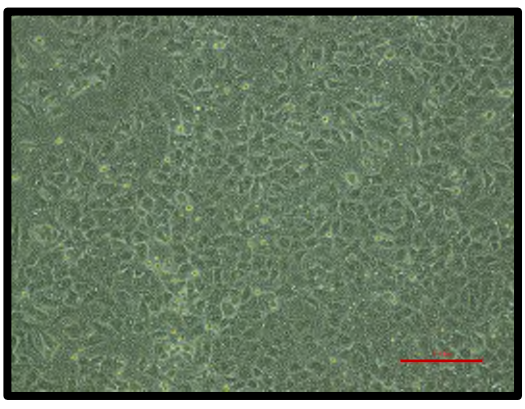

A: MCF-7 cells (pores just visible).
Scale bar: 0.1 mm.

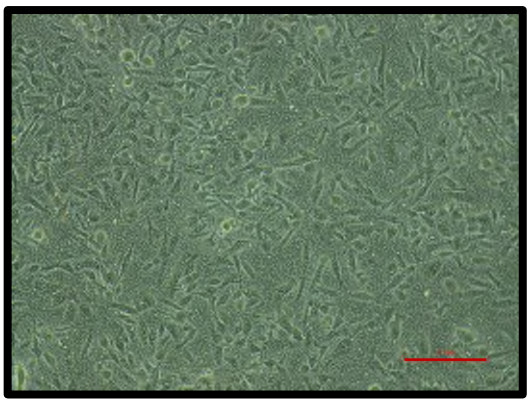

B: MDA-MB-231 cells (pores just visible).
Scale bar: 0.1 mm.

At 48 h, media were aspirated and discarded. Cells were washed twice with warmed PBS to remove all FBS, and the co-culture deconstructed. 1.5 ml (inserts) or 2.5 ml (wells) fresh 0F (serum-free) media were added. Cells were cultured for a further 24 h.

At 72 h media were aspirated, centrifuged (250 *g*, room temperature, 5 min), and passed through a 0.2 μM filter unit to remove cellular debris. The resulting acellular media was frozen (-80^{O}C) for later proteome array analysis.

2.2.5.2 Cell Co-Culture for RNA Extraction

Pre-differentiated SGBS cells were differentiated to maturity, as described (2.2.2.10), in gelatin-coated 12-well plates. On Day 14, their 3-FC media were aspirated and 2 ml GM_{SGBS} added to each well. Simultaneously, twelve 12 mm Corning® Transwell® Inserts with 0.4 μm pore polyester membranes (Corning B.V. Life Sciences, Scientific Laboratory Supplies, Nottingham, United Kingdom) were incubated (5% CO_2, 37^{O}C, 1 h) with 1 ml GM_{SGBS}, as per manufacturer's instruction, to allow for greater membrane permeability. Post-incubation, medium was aspirated from the inserts, and cancer cells seeded in eight inserts, at a density of 40 000/cm^2. Four cancer cell containing inserts were placed in SGBS-containing wells to commence the co-culture, and four media-only containing inserts were placed in wells containing SGBS (SGBS controls). At 72 h, media were aspirated, and the cells washed and lysed as described above. The co-culture experiment was repeated three times.

2.2.6 Proteome Profiler™ Human XL Cytokine Array Kit

The Proteome Profiler™ Human XL Cytokine Array Kit (R&D Systems, Abingdon, United Kingdom) allows for the simultaneous assessment of 105 cytokines, chemokines, growth factors, and acute phase proteins from cell and tissue lysates, culture supernatants, saliva, human milk, and plasma. Nitrocellulose membranes are spotted, in duplicate, with capture antibodies that bind target proteins. Detection of these bound cytokines is *via* detection antibodies, and visualisation is *via* luminescent

detection chemicals. Signals produced are proportional to the quantity of target protein bound, and observations can be made comparing cytokine quantities in different samples. The kit was used to identify and compare cytokines secreted by SGBS cells cultured both alone and alongside MCF-7 cells, as well as cytokines secreted by breast adipose tissue, both peritumoural and distant.

Frozen paired media samples harvested from cell culture and explant culture were thawed on ice and processed as per the kit's protocol (R&D Systems, 2017). Briefly, reagents were brought to room temperature before use and all incubation steps were carried out on a Stuart® mini gyro-rocker SSM3 (Stuart, Stone, United Kingdom) set to 28 rpm, at room temperature, unless otherwise specified. 2 ml of Array Buffer 6 ('AB6', a block buffer) were pipetted into each of two wells of a multi-well dish. One membrane was incubated (60 min) in each well. After this 1 h incubation, AB6 was aspirated and a 1 ml media sample / AB6 mixture (media : AB6 2:1 *v/v*) added to each membrane. Further incubation (4^{O}C, overnight) was commenced. The following morning, each membrane was moved to a petri dish and 20 ml of Wash Buffer added. Following a 10 min incubation, the Wash Buffer was replaced. This was repeated once more to give a total of three washes. Next, the membranes were placed in separate wells of the multi-well dish (previously washed in deionised water and dried), and 1.5 ml of diluted Detection Antibody Cocktail added to each. After a 60 min incubation, the membranes were washed three times, as described. Next, the membranes were incubated with 2 ml of Streptavidin-HRP for 30 mins, and then washed three times. After removal from the Wash Buffer, with excess liquid blotted off, the membranes were placed on a plastic sheet and 1 ml of Chemi Reagent Mix pipetted on to each. After covering with a top plastic sheet protector, air bubbles were smoothed out and the membranes incubated in the dark (1 min). Excess Chemi Reagent Mix was blotted away and the membranes, in their plastic sleeve, placed in a GeneGnome XRQ Imaging System (Syngene, Cambridge, United Kingdom). Images were captured at 10 s, 30 s, 1 min, 5 min, 30 min, and 60 min, and analysed with ImageQuantTL 8.1 (GE Healthcare Life Sciences, Little Chalfont, United Kingdom) software.

2.2.7 xCELLigence® RTCA™ DP Cell Proliferation Assay

The xCELLigence® RTCA™ DP instrument (ACEA Biosciences Inc., San Diego, United States of America) quantifies cellular proliferation using electrical impedance. Cells suspended in culture medium, a conductive solution, are seeded in 16-well plates ('E-Plate® VIEW 16') which have gold microelectrodes fused to their bottom surface (Figure 2.5). When an electrical potential is applied across the electrodes, electrons pass through the solution from the negative terminal to the positive. In a well containing medium but devoid of cells, the electron flow is unimpeded. Adherent cells hinder electron flow, with the magnitude of this impedance being determined by the number of adherent cells, the quality of their attachment, and their size and shape (Figure 2.6). When all other factors are equal, a greater number of adherent cells results in greater impedance. Changes in impedance over time can be used as a measure of the proliferative rate of the cell population being studied. Up to three 16-well plates may be processed at any one time, and they may be assessed as individual experiments or as one whole.

The unit housing the plates sits within a standard cell culture incubator, with an external bench-top laptop used to control the experiment. Company provided software allows for real-time interpretation of impedance data.

2.2.7.1 xCELLigence® Optimisation

For xCELLigence® experimentation, optimal cell seeding density must be determined. Density must allow enough cell-cell communication such that proliferation is not hindered, but cells must not be so dense that 100% confluence is achieved too rapidly, before enough experimentation time has elapsed.

Figure 2.5: xCELLigence® E-Plate® 16

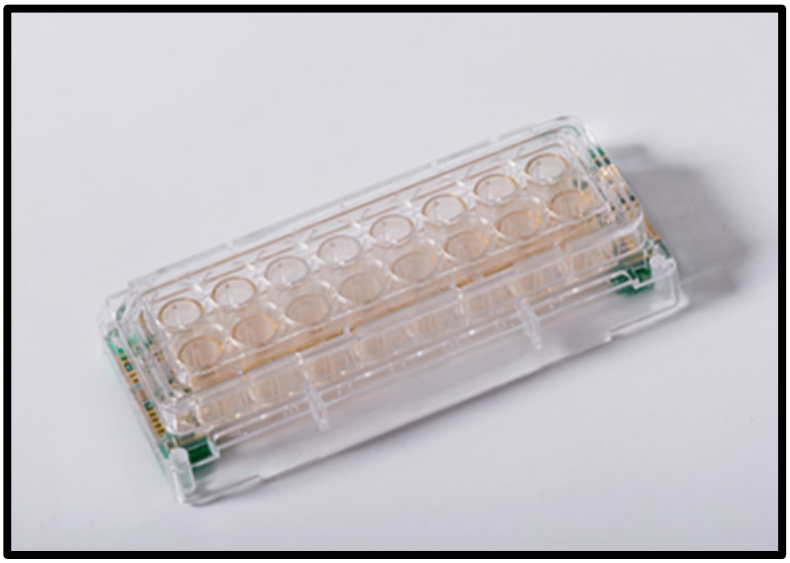

(From [https://www.aceabio.com.cn/products/rtca-systems/consumables/e-plate-16])

Figure 2.6: Flow of Electrons in a Media-Containing xCELLigence® E-Plate® Well

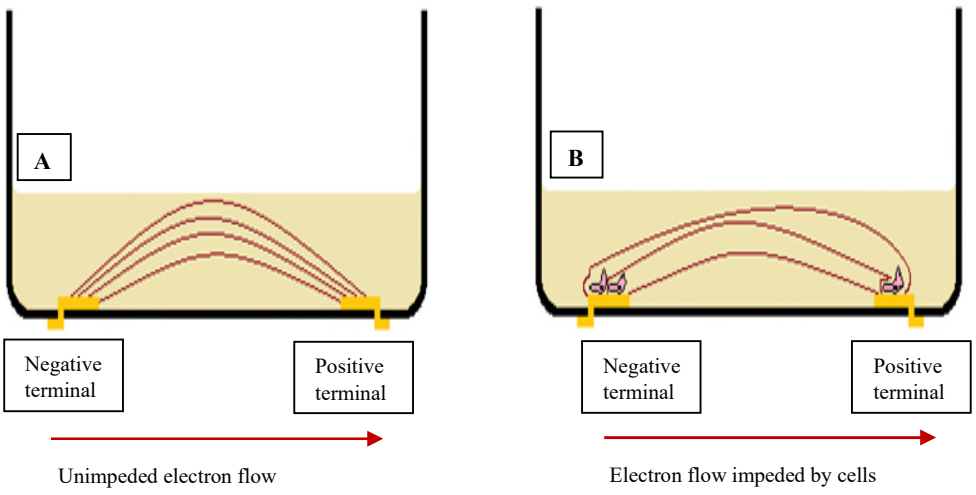

(A) Absence of, and **(B)** presence of cells. Not to scale. Gold electrodes cover 70-80% of a plate's surface area. Here, only two have been shown.

Separately, MCF-7 and MDA-MB-231 cells were seeded, in duplicate, at concentrations of 10 000, 20 000, 30 000, 35 000, 40 000, 50 000, and 60 000 cells per well (Figure 2.7). GM_{SGBS} medium was used. Proliferation was measured for 24 h and an optimal cell seeding density of 30 000 cells per well identified.

2.2.7.2 Co-Culture xCELLigence® Experiment

To assess the effect of SGBS cells on cancer cell line proliferation, co-culture experiments were undertaken using the xCELLigence® RTCA® DP system. MCF-7 cells and MDA-MB-231 cells were each co-cultured separately with both pre-differentiated SGBS cells and mature SGBS cells (Figure 2.8):

Co-culture one:	MCF-7 cells with pre-differentiated SGBS cells
Co-culture two:	MCF-7 cells with mature SGBS cells
Co-culture three:	MDA-MB-231 cells with pre-differentiated SGBS cells
Co-culture four:	MDA-MB-231 cells with mature SGBS cells

Each co-culture experiment was performed with four technical and three biological repeats.

50 µl of GM_{SGBS} were pipetted in to each well of the E-Plate® VIEW 16, the plate incubated for 30 min (room temperature), and a background impedance measurement taken. Cancer cells were trypsinised and counted. 30 000 cells suspended in 100 µl of GM_{SGBS} were added to each well. To allow for even distribution of cells within the wells, plates were incubated for 30 min (room temperature). After incubation, plates were placed in the system's housing unit and the xCELLigence® experiment started. Impedance measurements were taken every 15 min.

60 µl of trypsin were added to two wells of a 6-well plate containing SGBS cells, and the plate incubated (5% CO_2, 37^{O}C, 5 min). Next, 300 µl of GM_{SGBS} were added to each of the two wells, and the cells gently pipetted to ensure detachment. Trypsinised cells from both wells were combined. In quadruplicate, SGBS cells were pipetted into

Figure 2.7: Light Microscopy of Freshly Seeded MCF-7 Cells in a Single Well of an xCELLigence® E-Plate® VIEW 16

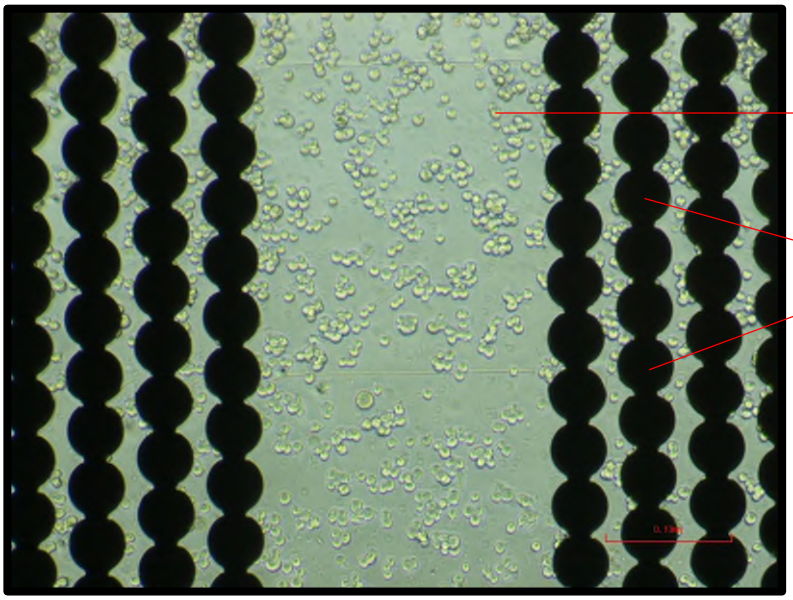

Electrode free area measures approximately 400 μm wide and allows greater visualisation of cells. x10 magnification.

Figure 2.8: xCELLigence® Co-Culture Experiment Layout

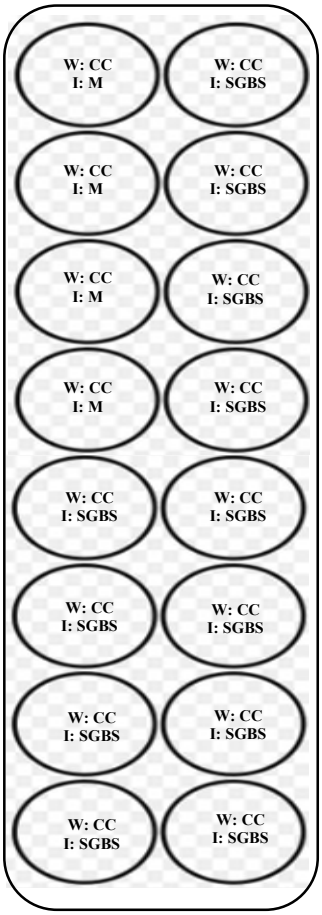

W: well, I: insert, CC: cancer cells, SGBS: SGSB cells, M: medium.

Figure 2.9: xCELLigence® Insert

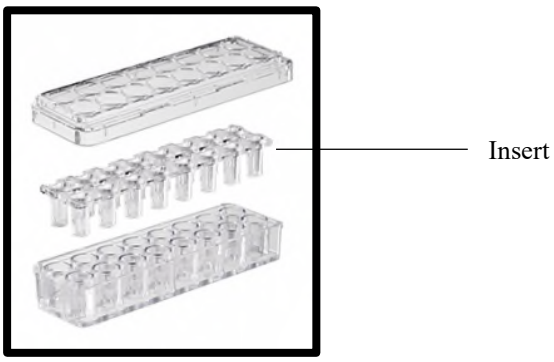

[Image taken from (https://www.ols-bio.de/en/accessories/cell-culture-cell-analysis/cell-analysis-xcelligence/59/e-plate-insert)]

gelatin pre-coated E-Plate® Inserts 16 (Figure 2.9) wells at concentrations of 25 000, 31 250, and 41 750 cells. Where needed, further GM_{SGBS} was added to the inserts to make up to a final volume of 60 µl. 12 of 16 insert wells contained SGBS cells. 60 µl of GM_{SGBS} were added to the four wells devoid of cells, and the inserts incubated (5% CO_2, 37^{O}C) for 4-6 h to allow the cells to settle and attach.

At 4-6 h, the xCELLigence® experiment was paused and the cancer cell containing E-Plate® 16 removed from the housing unit. SGBS containing inserts were transferred in to the xCELLigence® plate to commence the co-culture. The plate, which now contained four wells of cancer cells alone and 12 wells of cancer cells co-cultured with three different concentrations of SGBS cells, was returned to the housing unit in the incubator. The experiment was restarted and run for a minimum of 24 h.

2.2.8 Chitinase 3-Like 1 Stimulation of MCF-7 and MDA-MB-231 Cells

The inflammatory cytokine Chitinase 3-like 1 (CHI3L1) was identified as a cytokine of interest. To assess its effect, if any, on BC cell proliferation, xCELLigence® experiments were conducted with MCF-7 and MDA-MB-231 cells in the presence of three concentrations of CHI3L1. 30 000 cells were seeded in each E-Plate® VIEW 16 well. Media were prepared with concentrations of 250 ng/ml, 500 ng/ml, and 750 ng/ml of CHI3L1 and the experiments run (four technical and three biological repeats for each), for at least 24 h.

2.2.9 Staining of Adipocytes with Oil Red O

Oil Red O (ORO) is a lysochrome which stains lipid material, including adipocyte lipid droplets, an orange-red colour. Stock was produced by dissolving 500 mg of powdered ORO (Sigma-Aldrich, Haverhill, United Kingdom) in 100 ml 100% isopropanol. After overnight stirring, the solution was diluted at 3:2 stock : distilled water *v/v*, and stirred for a further 10 min. Finally, this working solution was passed through a 0.22 µm filter and immediately used.

After aspiration of medium, adipocytes were washed with warmed PBS, and cell fixation was performed with 4% paraformaldehyde ('PFA', Affymetrix, High Wycombe, United Kingdom) for a minimum 15 min. After PFA aspiration and further PBS washing, 500 µl of ORO working solution were left to incubate (room temperature, 60 min) in each 24 mm well. At the end of the incubation period, ORO was removed, and cells washed initially with 60% isopropanol, and then with PBS.

2.2.10 Reverse Transcription and Polymerase Chain Reaction

To ascertain gene expression in a cell population or tissue of interest, polymerase chain reactions (PCRs) are performed. PCR can be a one-step or two-step process. Here, the latter was undertaken; first, RNA previously extracted from samples was converted to complementary DNA (cDNA), and then the DNA amplified.

2.2.11 Reverse Transcription

Reverse transcription (RT) is the process by which RNA, acting as a template, is converted to cDNA by the RNA-dependent DNA polymerase enzyme reverse transcriptase (RTase). This process is dependent on (random hexamer, oligo(dT), or gene specific) primers which anneal to the extracted RNA and function as starting points for RTase, and nucleotides (dNTPs) which are incorporated to form the new cDNA strands. RTase thus produces a hybrid RNA-DNA product; half of the newly formed double stranded structure is the original RNA template, and the other half is the newly added material.

For each specimen, nuclease-free water was added to a tube containing 1 µg extracted RNA to make up to a volume of 4 µl. To remove any DNA contamination, 0.5 µl DNAse I (Sigma-Aldrich, Haverhill, United Kingdom) with 0.5 µl DNAse I x10 buffer (Sigma-Aldrich, Haverhill, United Kingdom) were added to the dissolved RNA, and the mixture incubated (room temperature, 15 min). Next, incubation (65^{O}C, 10 min)

with 0.5 µl stop solution (Sigma-Aldrich, Haverhill, United Kingdom) deactivated the DNAse I, thereby preventing product DNA breakdown later in the process. Tubes were placed on ice.

A master mix (MM) of 1 µl random hexamer primers (Thermo Scientific™, Fisher Scientific, Loughborough, United Kingdom), 1 µl dNTPs (Thermo Scientific™, Fisher Scientific, Loughborough, United Kingdom) and 4.5 µl nuclease-free water per sample was prepared at a volume of *n samples + 10%*. 6.5 µl MM were added to each tube, and samples incubated (70^{O}C, 10 min) and then cooled (on ice, 2 min), allowing for efficient primer annealing to single stranded RNA.

A second MM was prepared, again at a volume of *n samples + 10%*. This MM consisted of 4 µl 5X RevertAid reaction buffer (Thermo Scientific™, Fisher Scientific, Loughborough, United Kingdom), 1 µl RevertAid H Minus Reverse Transcriptase (Thermo Scientific™, Fisher Scientific, Loughborough, United Kingdom), 0.5 µl RNAse OUT RNase inhibitor (Thermo Scientific™, Fisher Scientific, Loughborough, United Kingdom) and 4.5 µl nuclease-free water per sample. 8 µl were added to each tube, and the mixture incubated (25^{O}C 10min, 37^{O}C 50 min, 80^{O}C 10 min). This completed the RT process, and to this newly formed cDNA, 180 µl nuclease-free water were added. Samples were stored at -20^{O}C.

2.2.12 Polymerase Chain Reaction

The real-time quantitative PCR (RT-qPCR) process results in the rapid amplification and fluorescence mediated quantification of DNA and can be used to determine gene expression. It requires a DNA template, primers, DNA polymerase, nucleotides, and a fluorescent dye.

To begin, double stranded DNA is heated to allow strand separation, or denaturing. Next, specially designed paired forward and reverse primers anneal to the now single

DNA strands, flanking the genetic region of interest. Finally, the enzyme DNA polymerase extends each primer, from its 3' end, by adding nucleotides complementing the template DNA strand. Multiple cycles of these three steps are programmed to occur, and an exponential production of DNA ensues. The amount of final DNA is proportional to the quantity of relevant cDNA initially.

In contrast to RT where whole RNA sequences are to be transcribed into cDNA and thus random primers may be used, PCR is used to assess the expression of specific genes located within longer genomic sequences. Targeted amplification with primers tailored to the region of interest on the DNA strand is thus undertaken. Specific primers are required and must be designed to minimise homology to DNA sequences outside the region of interest. For this study, primers were designed using Ensemble Genome Browser Primers (accessed at http://www.ensembl.org/index.html), and those with exon-exon junction overlap were preferentially selected (Table 2.1). Important characteristics included product size between 70 and 150 nucleotides, a melting temperature of 60^{O}C, and a GC content of 55%. Primers were checked using USCS Genome In-silico PCR (accessed at http://genome.ucsc.edu/cgi-bin/hgPCR), and ordered from Sigma-Aldrich (Haverhill, United Kingdom). Upon receipt, after dissolving in nuclease-free water as per manufacturer instructions to achieve a stock concentration of 100 μM, primers were stored at -20^{O}C. Just prior to use, primers were diluted to a working concentration of 20 μM.

For this study, SYBR® Green JumpStart™ *Taq* ReadyMix™ (Sigma-Aldrich, Haverhill, United Kingdom) was used. This mix contains SYBR® Green I dye, DNA polymerase, deoxynucleotides and reaction buffer. SYBR® Green I is a fluorescent cyanine dye used in PCR to measure, at the end of each cycle, the amount of double-stranded DNA product amplified; SYBR® Green I inserts between double stranded DNA bases and, once bound, alters structurally. This physical change results in reduced mobility and a release of energy as fluorescence. As more DNA is amplified and more dye binding occurs, fluorescence increases.

A MM of 7.5 µl SYBR® Green JumpStart™ *Taq* ReadyMix™, 0.15 µl diluted 100x ROX reference dye (Sigma-Aldrich, Haverhill, United Kingdom), 0.15 µl forward and reverse primers, and 9.2 µl of nuclease-free water per sample was produced at a volume of *n samples + 10%* for each gene of interest. 12 µl of MM were added to each well of a 96-well-plate, and 3 µl of sample DNA (or no template control; NTC) also added. Samples/no template controls were plated in duplicate. Post-pipetting, air bubbles were dispelled, and plates sealed and centrifuged (1 000 *g,* 3 min). Following an initial denaturing step (2 min, 95^{O}C), the PCR experiment was run for 40 cycles (94^{O}C 34 s, 60 ^{O}C 34 s, 72^{O}C 30 s). Raw data were extracted and analysed using the $2^{\Delta\Delta CT}$ method.

2.2.13 Statistical Analysis

To interpret experiments and draw conclusions from data obtained, statistical analyses of results were undertaken. When selecting the most appropriate statistical test to use, several factors must be considered; the nature of the data (such as nominal, ordinal, interval, and continuous), the number of samples (one, two, more than two), the distribution of the data (normal), and the relationship to be tested.

2.2.13.1 Student's t-Test

The Student's t-test is a parametric test used to compare the means of two normally distributed groups displaying equal variance. When a group is compared to a population with a known mean which may be specified in the hypothesis (for example comparison of a sample's age of retirement to the population mean of 65 years), the one-sample t-test is employed. When the two groups are independent of each other and data points are unpaired, the independent t-test is utilised (for example comparison of males' and females' mean test scores). Finally, if the two groups of data are linked or dependent upon one another (for example comparison of mean exam scores before and after extra tuition), the paired t-test is appropriate.

T-tests can be computed as one-tailed or two-tailed. Both test the same null hypothesis that there is no true difference between the means of the two groups being studied. A one-tailed test is employed where one of the groups is specified as likely having the larger mean, if a difference exists. A one-tailed test is only to be used where the prediction is made prior to data being obtained (or seen), and where, if the other group is shown to have the larger of the two means, this finding can be wholly attributed to chance. A two-tailed test is employed where either group may have the larger mean.

2.2.13.2 Wilcoxon Matched-Pairs Signed Ranks Test

The Wilcoxon Matched-Pairs Signed Ranks Test is used for paired, non-parametric data. As it analyses ranks of data as opposed to data values, the test does not compare means but can be considered to analyse changes in group median values.

2.2.13.4 ANOVA

The ANOVA – *Analysis of Variance* – statistical test is used when more than two samples are to be compared. It is a parametric test and avoids the risk of increasing the Type I error that would result from running multiple t-tests between groups. When two groups are compared with the Student t-test, the experiment error rate is the significance level of 0.05. When four groups are compared (six comparisons), this error rate increases to 0.26.

In order to satisfy the prerequisites for running an ANOVA, data must be normally distributed with the same variance between all groups. When only one factor is changed between sample groups, for example differing concentrations of a treatment, the one-way ANOVA is employed. When an additional factor is modified, such as time, a two-way ANOVA is appropriate. An ANOVA reports the presence or absence

of one or more statistically significant differences between the means of the groups. It does not indicate the groups between which the difference exists.

2.2.13.5 Post Hoc Tests

When an ANOVA test identifies the existence of (a) significant difference(s) between groups, further analyses must be performed to identify where the difference sits. In order to determine this 'location', post hoc tests are run. When groups are compared to one control group, Dunnett's test is utilised. When comparison between all groups is to be undertaken, Tukey's test is to be employed. Because the latter performs a higher number of comparisons, the point at which significance is achieved is set at a tighter level per comparison than in a Dunnett's analysis, in order to lower the risk of falsely rejecting the null hypothesis. Consequently, Tukey may falsely accept the null hypothesis following a significant ANOVA result.

CHAPTER THREE

The Effect of Pre-Differentiated and Mature SGBS Adipocytes on the Rate of Proliferation of MCF-7 and MDA-MB-231 Cancer Cells

Chapter Three: The Effect of Pre-Differentiated and Mature SGBS Adipocytes on the Rate of Proliferation of MCF-7 and MDA-MB-231 Cancer Cells

Contents

3.1	**Introduction……**	**73**
3.2	**Selecting Appropriate Cell Types for Experimentation…….**	**73**
3.2.1	Breast Cancer Cell Lines……	74
3.2.1.1	MCF-7 Cells……..	74
3.2.1.2	MDA-MB-231 Cells…….	74
3.2.2	SGBS Cells……....	77
3.3	**Aims of this Chapter……... **	**77**
3.4	**Optimal Seeding Density of Breast Cancer Cell Lines……**	**78**
3.4.1	Optimal Seeding Density of MCF-7 Cells……..	79
3.4.2	Optimal Seeding Density of MDA-MBA-231 Cells……	79
3.5	**The Effects of SGBS Cells on Cancer Cell Proliferation……**	**79**
3.5.1	Co-Culture: MCF-7 Cells with Pre-Differentiated SGBS Cells……...	81
3.5.2	Co-Culture: MCF-7 Cells with Mature SGBS Cells…….	81
3.5.3	Co-Culture: MDA-MB-231 Cells with Pre-Differentiated SGBS Cells...	84
3.5.4	Co-Culture: MDA-MB-231 Cells with Mature SGBS Cells……	84
3.6	**Discussion……**	**87**
3.7	**Conclusion……... **	**89**

3.1 Introduction

Breast cancer (BC) is the commonest female malignancy worldwide (WHO, 2020). Consisting of a heterogenous group of sub-types, the natural course of BC is variable, and outcomes differ markedly between these different sub-categories (Dixon and Barber, 2019). Treatment of BC is ever evolving, but the challenge of poor outcomes for patients with advanced or more aggressive disease persists.

The cancer tumour microenvironment (TME) has become an important focus of research over recent years. Adipocytes have relatively recently been recognised as an important member of the TME, secreting adipokines which influence cancer behaviour, promoting progression of the malignancy.

To further investigate the role of adipocytes in the BC TME, an $ER^+/HER2^-$ and an $ER^+/PR^-/HER2^-$ (triple negative; TN) BC cell line will be selected. $ER^+/HER2^-$ is the commonest sub-type of BC and TN BC is the most aggressive, with the poorest outcomes (Dixon and Barber, 2019). The potential for benefit is thus greatest by analysing these cancer sub-types.

Here, the effect of adipocytes on BC cell proliferation will be investigated; one of the most important factors determining outcomes in BC is the size of the malignant lesion at the time of diagnosis and treatment (Dixon and Barber, 2019); patients with larger cancers have worse outcomes. Identification of adipokines which encourage BC cell proliferation may therefore help identify targets for novel therapies.

3.2 Selecting Appropriate Cell Types for Experimentation

When experimenting with non-explant material, cell lines and cell strains are used. A cell line is an immortalised animal cell culture resulting in a purified progeny of a single cell population which can be replicated by researchers for many passages. A cell strain can likewise be passaged but is not immortal. In 1951, HeLa cells - cervical cancer cells taken from a 30-year-old patient named Henrietta Lacks - were the first human cell

line to be established by researcher George Gey (Lucey *et al.*, 2009). Today, American Type Culture Collection (ATCC®) maintains almost 4 000 human cell lines.

3.2.1 Breast Cancer Cell Lines

BC is a heterogenous group of diseases; considerable histopathological, and biomolecular differences are seen between different tumour types, and in keeping with this, a range of BC cell lines are available (Table 3.1).

3.2.1.1 MCF-7 Cells

In 1973, the Michigan Cancer Foundation's seventh attempt at establishing a BC cell line was successful. It was named Michigan Cancer Foundation 7 (MCF-7). The epithelial-like adenocarcinoma cells were taken from a metastatic pleural effusion in 69-year-old female Sister Catherine Mallon, and immortalised. The adherent cells fit a *Luminal A* molecular sub-classification pattern (Holliday and Speirs, 2011), being $ER^+/PR^+/HER2^-$. They are not particularly aggressive or invasive; they do not exhibit much migratory potential and have low metastatic potential (Figure 3.1) (Comsa *et al.*, 2015).

MCF-7 cells are now the most researched BC cell line in the world (Lee *et al.*, 2015), giving rise to more translational data than any other BC cell line (Comsa *et al.*, 2015).

3.2.1.2 MDA-MB-231 Cells

The MDA-MB-231 BC cell line was immortalised at the MD Anderson Cancer Centre, from the pleural effusion of 51-year-old Caucasian female. The cells are TN; they lack oestrogen and progesterone receptors, and HER2 is not amplified. MDA-MB-231 is a poorly differentiated, highly aggressive cancer cell line belonging to the claudin-low TN BC molecular sub-category.

Table 3.1: Molecular Subclassification of Breast Cancers and Cell Lines

Class	Descriptor	Example Cell Lines
Luminal A	• ER + • PR + / - • HER2 - • Ki67 low	MCF-7 SUM185 T47D
Luminal B	• ER + / - • PR + / - • HER2 + / - • Ki67 high	BT474 ZR-75
HER2 Enriched	• ER - • PR - • HER2 +	MDA-MB-453 SKBR3
TNBC Basal-like	• ER - • PR - • HER2 - • CK5/6 + • EGFR +	MDA-MB-468 SUM190
TNBC Claudin-low	• ER - • PR - • HER2 - • Claudin low	BT549 Hs578T MDA-MB-231 SUM1315

(Neve *et al.,* 2006; Malhotra *et al*., 2010; Subik *et al.,* 2010; Holliday and Speirs, 2011)

Figure 3.1: The Molecular Profile and Characteristics of MCF-7 Cancer Cells

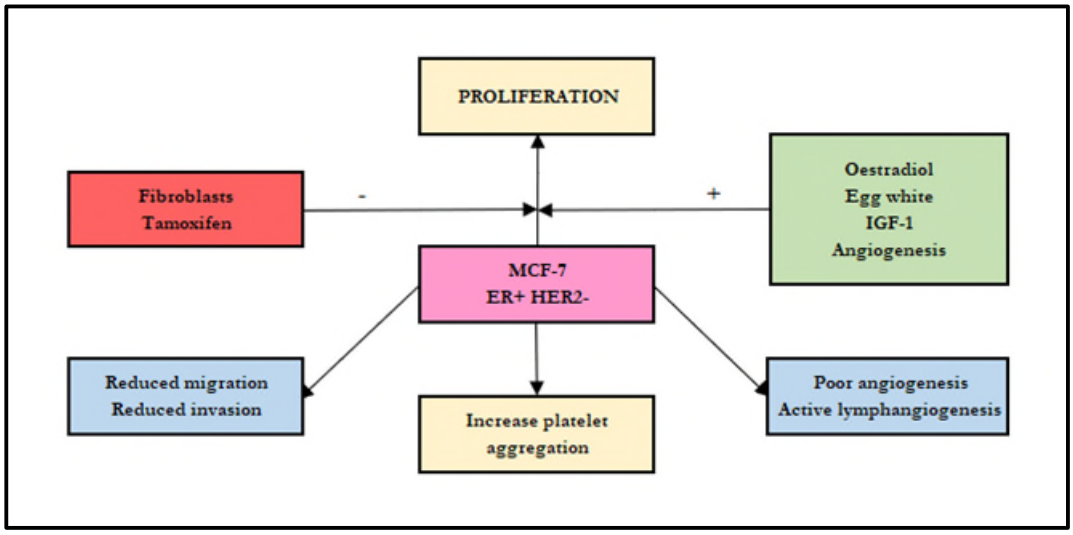

[Adapted, with permission, from (Comsa *et al.*, 2015)]

Molecular profile and characteristics of the MCF-7 BC cell line. ER+: oestrogen receptor positive, HER2-: human epidermal growth factor receptor 2 negative, IGF-1: insulin-like growth factor 1.

3.2.2 SGBS Cells

Attempts to isolate mammary preadipocytes to grow, differentiate into, and maintain as a primary cell culture of mature adipocytes for experimentation were unsuccessful until revisited again at the very end of the research period. A cell strain was thus selected.

In 2001, Wabitsch and Brenner *et al.* published their work describing the preadipocyte cell strain they had developed from the white subcutaneous adipose tissue of an infant with Simpson-Golabi-Behmel Syndrome (SGBS). The rare SGB Syndrome is X-linked and characterised by both prenatal and postnatal overgrowth. Although the syndrome is often linked to a mutation in the Glypican 3 gene, genetic analysis of the infant from whom the cells were harvested did not reveal this aberration.

Wabitsch and Brenner *et al.*'s work resulted in a cell strain which can be differentiated to >95% mature adipocytes, to at least 50 generations (Fischer-Posovszky, 2008). Differentiated adipocytes are recognised as both functionally and biochemically comparable to primary preadipocytes (Rosenow *et al.*, 2010).

3.3 Aims of this Chapter

The aims of this Chapter are to determine the:

1. Optimal seeding density of MCF-7 cells for use in the xCELLigence® RTCA® DP system
2. Optimal seeding density of MDA-MB-231 cells for use in the xCELLigence® RTCA® DP system
3. Effect on the proliferation of MCF-7 cells when co-cultured with pre-differentiated (pd-) SGBS cells, as compared to MCF-7 cells grown alone
4. Effect on the proliferation of MCF-7 cells when co-cultured with mature SGBS cells, as compared to MCF-7 cells grown alone

5. Effects on the proliferation of MDA-MB-231 cells when co-cultured with pd-SGBS cells, when compared with MDA-MB-231 cells grown alone
6. Effects on the proliferation of MDA-MB-231 cells when co-cultured with mature SGBS cells, when compared with MDA-MB-231 cells grown alone

3.4 Optimal Seeding Density of Breast Cancer Cell Line Cells

The xCELLigence® RTCA® DP system ascertains cellular proliferation rate using electrical impedance. Cells suspended in culture medium, a conductive solution, are seeded in 16-well plates which have gold microelectrodes fused to their bottom surface. Electrical impedance across the bottom of the plate is measured and, when all other factors are equal, a greater number of adherent cells results in greater impedance. In the same time period, an increase in impedance is interpreted as higher a rate of proliferation.

For xCELLigence® experimentation, optimal cell seeding density must be determined. Density must allow enough cell-cell communication such that proliferation is not hindered, but cells must not be so dense that 100% confluence is achieved too rapidly, before enough experimentation time has elapsed. Optimal density was selected as the concentration of cells which gave linear growth during the planned duration of experiments.

As previously described (Chapter Two; Section 2.2.7.1), MCF-7 and MDA-MB-231 cells were seeded, separately, in duplicate at concentrations of 10 000, 20 000, 30 000, 35 000, 40 000, 50 000, and 60 000 cells per well, in GM_{SGBS} medium. Proliferation was measured for 24-56 h.

3.4.1 Optimal Seeding Density of MCF-7 Cells

Reviewing the results of the seeding density experiment revealed an optimal cell seeding density of 30 000 cells per well (Figure 3.2).

3.4.2 Optimal Seeding Density of MDA-MB-231 Cells

Reviewing the results of the seeding density experiment revealed an optimal cell seeding density of 30 000 cells per well (Figure 3.3).

3.5 The Effect of SGBS Cells on Cancer Cell Proliferation

MCF-7 cells and MDA-MB-231 cells were each co-cultured with both pd- and mature SGBS cells:

Co-culture one:	MCF-7 cells with pd-SGBS cells
Co-culture two:	MCF-7 cells with mature SGBS cells
Co-culture three:	MDA-MB-231 cells with pd-SGBS cells
Co-culture four:	MDA-MB-231 cells with mature SGBS cells

Each co-culture experiment was performed with four technical and three biological repeats, as described previously (Chapter Two; Section 2.2.7.2). Three differing concentrations of adipocytes were used in each experiment to investigate whether a dose-dependent influence exists. Cell indices were normalised at the point of co-culture instigation. Any well where the graph morphology suggested sub-optimal growth was excluded. Analysis was undertaken with a minimum of three wells per cell concentration. Data were analysed with RTCA Software Pro and GraphPad Prism® 8.3.1.

Figure 3.2: MCF-7 Seeding Density Optimisation

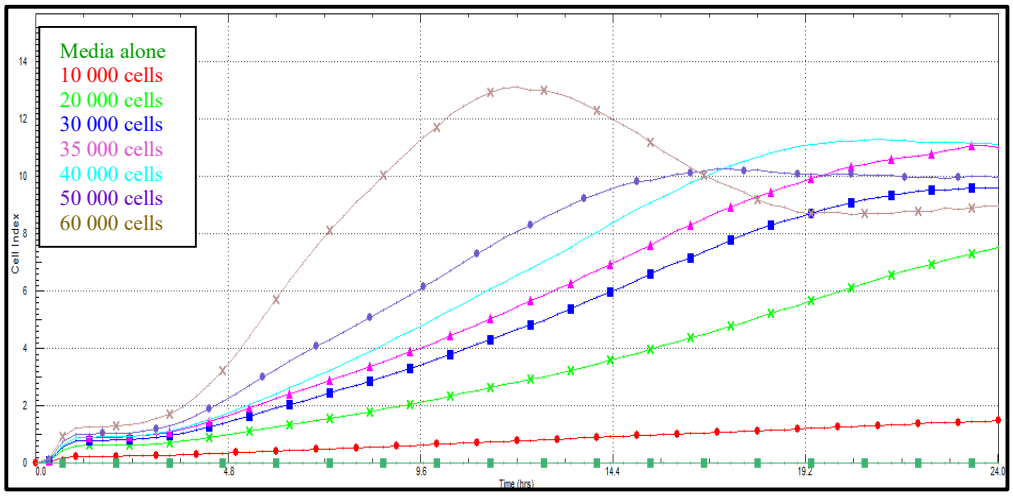

Graph to illustrate mean cell indices over time for MCF-7 cells seeded in six different densities. Readings taken every 15 min. Key as shown. Graph exported from RTCA Software Pro.

Figure 3.3: MDA-MB-231 Seeding Density Optimisation

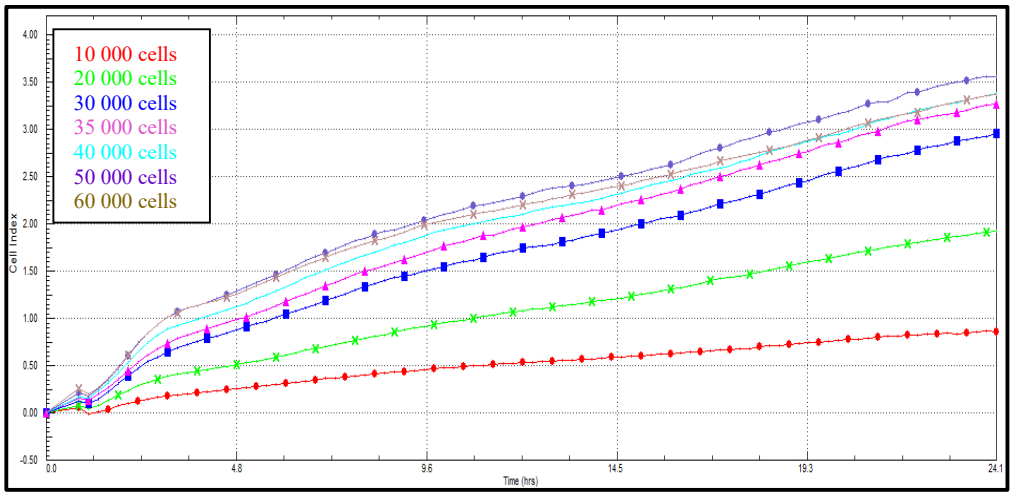

Graph to illustrate mean cell indices over time for MDA-MB-231 cells seeded in six different densities. Readings taken every 15 min. Key as shown. Graph exported from RTCA Software Pro.

3.5.1 Co-Culture: MCF-7 Cells with Pre-Differentiated SGBS Cells

When co-cultured with pre-differentiated SGBS cells, MCF-7 proliferation was significantly increased as compared to MCF-7 cells cultured alone at both 6 h ($p < 0.0001$) and 12 h ($p < 0.001$) post instigation of co-culture (Figure 3.4). Furthermore, proliferation was significantly increased as the concentration of pd-SGBS cells increased from 0 to 25 000 to 31 250 cells/well.

Interestingly, although the rate of proliferation remained significantly higher than for MCF-7 cells grown alone at both 6 h and 12 h, proliferation of MCF-7 cells co-cultured with the highest concentration of pd-SGBS (C: 41 750 cells/well) was lower than expected from the preceding trend; it was lower than the proliferation of MCF-7 in the presence of pd-SGBS B (31 250 cells/well). This may reflect a change in the response to increasing concentrations of stimuli, or it may reflect a depletion of nutrients in the media as a consequence of higher demand from a greater number of cells.

3.5.2 Co-Culture: MCF-7 Cells with Mature SGBS Cells

When co-cultured with mature SGBS cells, MCF-7 proliferation was significantly increased as compared to MCF-7 cells cultured alone at both 6 h ($p < 0.0001$) and 12 h ($p < 0.001$) post instigation of co-culture (Figure 3.5). In the displayed experiment, proliferation was significantly increased as the concentration of mature SGBS cells increased from 0 to 25 000 to 31 250 cells/well, but this was not reproduced in the repeats (Appendix A). In one repeat, the trend featured but did not reach significance.

Again, although the rate of proliferation remained significantly higher than for MCF-7 cells grown alone at both 6 h and 12 h, proliferation of MCF-7 cells co-cultured with the highest concentration of SGBS (C: 41 750 cells/well) was borderline / lower than expected from the preceding trend; it was lower than the proliferation of MCF-7 in the presence of SGBS B (31 250 cells/well) at 6 h in the displayed experiment. As with

Figure 3.4: MCF-7 Proliferation when Co-Cultured with Pre-Differentiated SGBS (Representative Experiment)

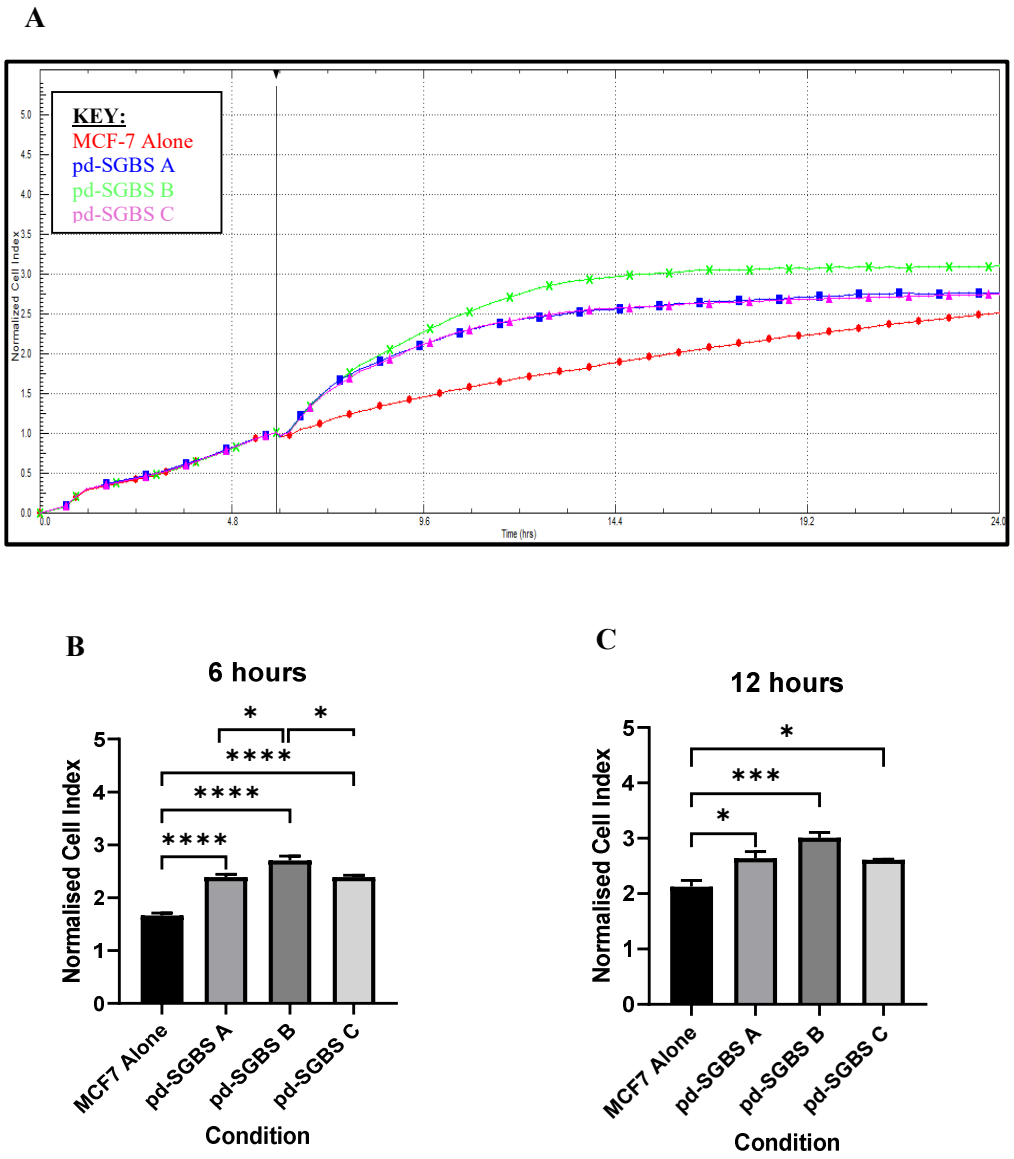

A: Graph to illustrate proliferation (as mean normalised cell indices over time) for MCF-7 cells grown in the absence and presence of pd-SGBS cells. Readings taken every 15 min. Cell indices normalised at initiation of co-culture. Key as shown; pd-SGBS A: 25 000 cells/well, pd-SGBS B: 31 250 cells/well, pd-SGBS C: 41 750 cells/well. **B & C:** Analysis of data in **A** at (**B**) 6 h and (**C**) 12 h post initiation of co-culture. Bars represent means ± SEM of the technical repeats. Significance is indicated by * for $p < 0.05$, *** for $p < 0.001$, and **** for $p < 0.0001$, as analysed by one-way ANOVA and Tukey's post hoc multiple comparison test.

Figure 3.5: MCF-7 Proliferation when Co-Cultured with Mature SGBS (Representative Experiment)

A

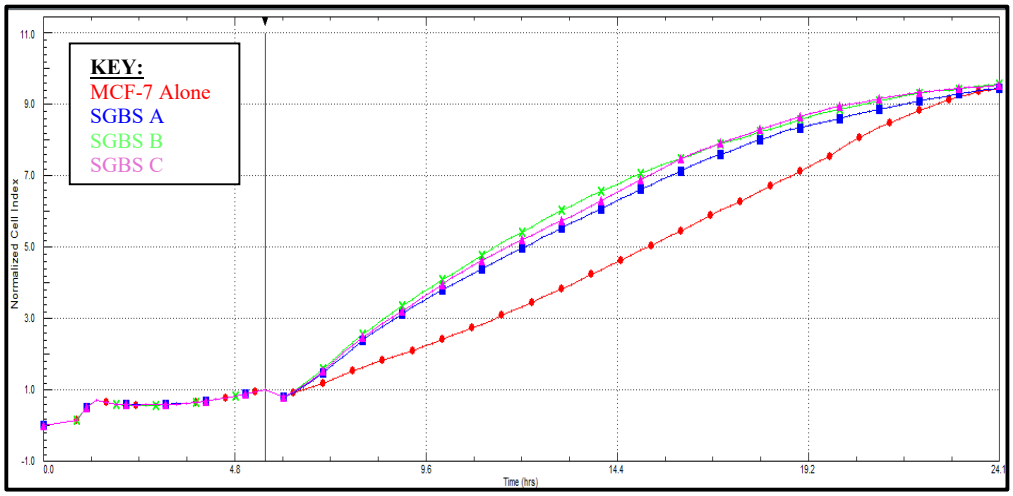

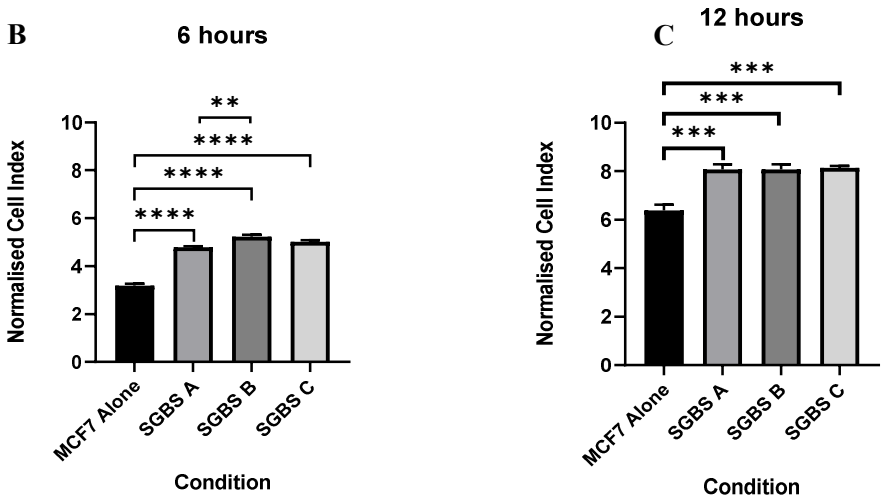

A: Graph to illustrate proliferation (as mean normalised cell indices over time) for MCF-7 cells grown in the absence and presence of mature SGBS cells. Readings taken every 15 min. Cell indices normalised at initiation of co-culture. Key as shown; SGBS A: 25 000 cells/well, SGBS B: 31 250 cells/well, SGBS C: 41 750 cells/well. **B & C:** Analysis of data in **A** at (**B**) 6 h and (**C**) 12 h post initiation of co-culture. Bars represent means ± SEM of the technical repeats. Significance is indicated by ** for $p < 0.01$, *** for $p < 0.001$, and **** for $p < 0.0001$, as analysed by one-way ANOVA and Tukey's post hoc multiple comparison test.

the pd-SGBS experiments, this may reflect a change in the response to increasing concentrations of stimuli, or it may reflect a depletion of nutrients in the media as a consequence of the higher demand from a greater number of cells.

3.5.3 Co-Culture: MDA-MB-231 Cells with Pre-Differentiated SGBS Cells

When co-cultured with pd-SGBS cells, MDA-MB-231 proliferation was significantly decreased as compared to MDA-MB-231 cells cultured alone at 6 h ($p < 0.001$), and at 12 h post instigation of co-culture ($p < 0.01$) (Figure 3.6). In the repeats (Appendix A), results were mixed (one experiment demonstrated significant decreases at 6 and 12 h, whilst the other demonstrated essentially no change). Overall, results indicate that pd-SGBS cells inhibit the proliferation of MDA-MB-231 cells.

3.5.4 Co-Culture: MDA-MB-231 Cells with Mature SGBS Cells

When co-cultured with mature SGBS cells, MDA-MB-231 proliferation was significantly increased. This increase was typically later than that seen when SGBS cells were co-cultured with MCF-7 cells (Figure 3.7).

Figure 3.6: MDA-MB-231 Proliferation when Co-Cultured with Pre-Differentiated SGBS (Representative Experiment)

A

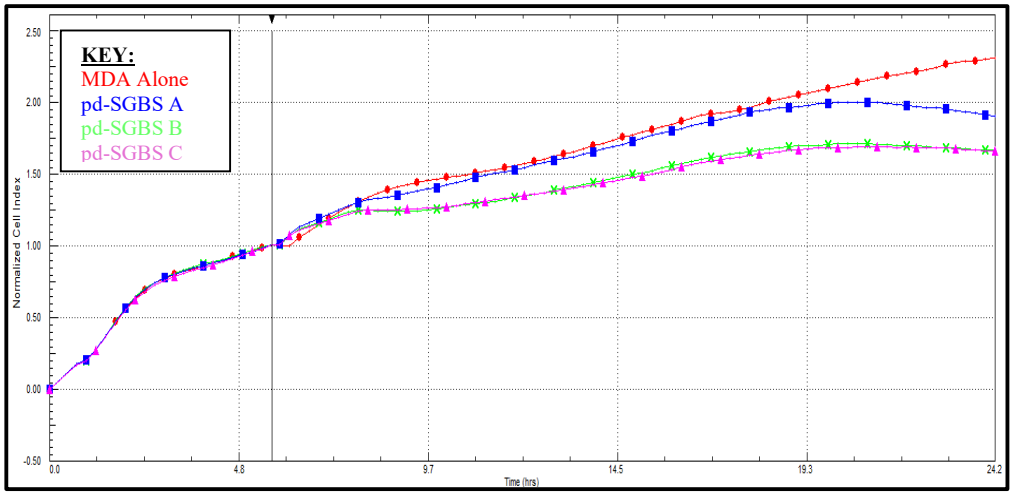

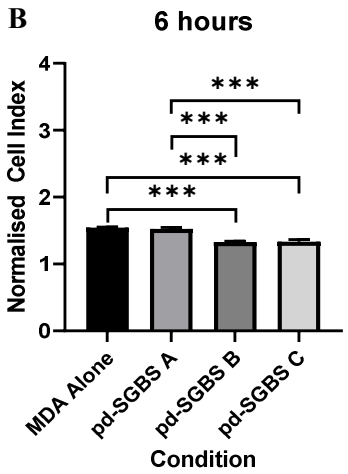

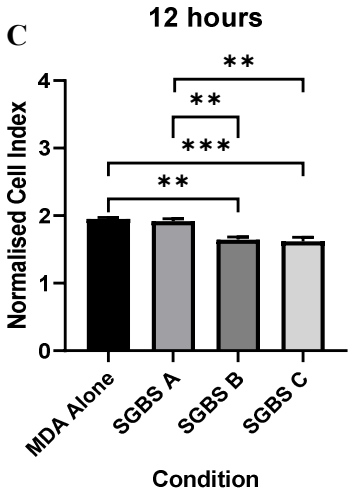

A: Graph to illustrate proliferation (as mean normalised cell indices over time) for MDA-MB-231 (MDA) cells grown in the absence and presence of pd-SGBS cells. Readings taken every 15 min. Cell indices normalised at initiation of co-culture. Key as shown; pd-SGBS A: 25 000 cells/well, pd-SGBS B: 31 250 cells/well, pd-SGBS C: 41 750 cells/well. **B & C:** Analysis of data in **A** at (**B**) 6 h and (**C**) 12 h post initiation of co-culture. Bars represent means ± SEM of the technical repeats. Significance is indicated by ** for $p < 0.01$, and *** for $p < 0.001$, as analysed by one-way ANOVA and Tukey's post hoc multiple comparison test.

Figure 3.7: MDA-MB-231 Proliferation When Co-Cultured with Mature SGBS (Representative Experiment)

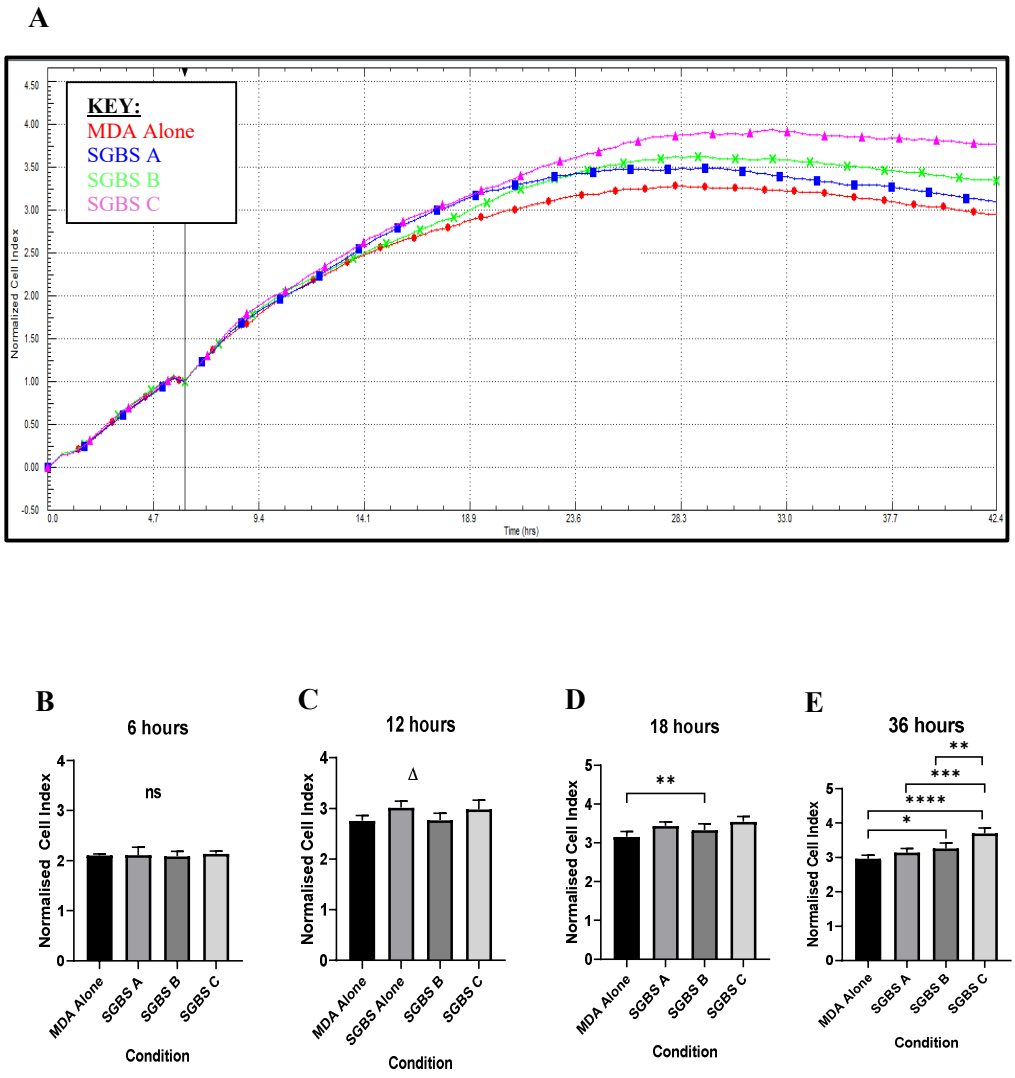

A: Graph to illustrate proliferation (as mean normalised cell indices over time) for MDA-MB-231 (MDA) cells grown in the absence and presence of SGBS cells. Readings taken every 15 min. Cell indices normalised at initiation of co-culture. Key as shown; SGBS A: 25 000 cells/well, SGBS B: 31 250 cells/well, SGBS C: 41 750 cells/well. **B, C, D, & E:** Analysis of data in **A** at (**B**) 6 h, (**C**) 12 h, (**D**) 18 h, and (**E**) 36 h post initiation of co-culture. Bars represent means ± SEM of the technical repeats. Significance is indicated by ns for *no significance*, * for $p < 0.05$, ** for $p < 0.01$, *** for $p < 0.001$, and **** for $p < 0.0001$, and Δ ANOVA $p < 0.05$ but Tukey's post hoc multiple comparison test not significant, as analysed by one-way ANOVA and Tukey's post hoc multiple comparison test.

3.6 Discussion

This Chapter aimed to identify the optimal seeding densities of MCF-7 and MDA-MB-231 cells for use in the xCELLigence® RTCA® DP system. Also, it aimed to identify the effect on the proliferation of the ER^+ BC cell line MCF-7 and the TN BC cell line MDA-MB-231 when each was co-cultured in novel proliferation experiments with pd- and mature SGBS cells, as compared to being cultured alone.

For both MCF-7 and MDA-MB-231 cells, a seeding density of 30 000 cells/well was identified. This concentration was satisfactory for the experiments conducted here.

MCF-7 cells, when co-cultured with pd-SGBS cells, had a significantly higher proliferative rate than MCF-7 cells cultured alone. Furthermore, proliferation was significantly increased as the concentration of pd-SGBS cells increased from 0 to 25 000 to 31 250 cells/well. As the concentration further increased to 41 750, proliferation increased, but not to the degree expected from the preceding increases. This may have been due to excessive strain on nutrient resources, inhibitory effects of waste chemicals, or an alteration on the nature of stimulation received when concentrations further increased.

In the literature, studies of adipocyte and cancer cell co-culture have yielded mixed results with regards to influence on proliferation. In 2003 for example, Manabe *et al.* investigated the role of (rat) pre- and mature adipocytes in the growth of BC cells, including MCF-7, in a 3D co-culture construct. By analysing bromodeoxyuridine uptake, they found that preadipocytes did not increase proliferation in the BC cell line. They performed their investigations with a single concentration of cells ($1x10^6$ preadipocytes to $3x10^5$ MCF-7 cells) however, and there is thus no range of concentrations to analyse. Manabe *et al.* (2003) experimented with an adipocyte to cancer cell ratio of 1 000 000 : 300 000 or 10 : 3. In the research conducted here, the ratio was almost 1 : 1 ([25 000 - 41 750] : 30 000 or [2.5 - 4.2] : 3). At the higher concentration and ratio in this research (4.2 : 3), increases in cell proliferation were not as high as in the lower cell concentration groups. It is possible that the mechanism by

which these results occurred were even more marked in Manabe *et al.*'s (2003) research and they thus did not see a difference.

In 2006, Kashani *et al.* published similar work on the influence of preadipocytes on the proliferation of MCF-7 cells, also in a 3D co-culture construct. Using the MTT assay measure of proliferation, they found that preadipocytes *reduced* the rate of MCF-7 proliferation. They likewise performed their experiments with a single concentration of preadipocytes ($1x10^5$ preadipocytes to $1x10^4$ MCF-7 cells; ratio of 10 : 1), and there is thus no range of concentrations to analyse.

Pre-differentiated (and mature) SGBS cells are known to have aromatase function (McInnes *et al.*, 2008). Aromatase is a critical enzyme in the conversion of androgens to oestrogens, and, as MCF-7 cells are ER^+, they respond to oestrogen stimulation. In the presence of serum, for example in foetal or new-born calf serum (Lykkesfeldt and Briand, 1986), oestrogen production may occur. Although MCF-7 cells may grow in the absence of oestrogen stimulation, their growth is increased by it (McInnes *et al.*, 2008). The mechanism by which preadipocytes failed to increase ER^+ cell growth, or inhibited ER^+ cell growth in the literature is thus unexpected but may be a reflection of the complexity of the signalling networks present and warrants further work.

When co-cultured with mature SGBS cells, MCF-7 proliferation was significantly increased as compared to MCF-7 cells cultured alone. The results achieved here are in keeping with previous published work (Manabe *et al.*, 2003; Kashani *et al.*, 2006), although the potential for a dose dependent response is a new finding and warrants further investigation. It is possible that a large contribution to this effect was made by oestrogen, however further investigation is necessary to identify other influencing factors, as research has shown that stimulatory effects of adipocytes on MCF-7 occur even in the presence of the selective oestrogen receptor modulator tamoxifen (D'Esposito *et al.*, 2012).

Results obtained for the role of pre-differentiated SGBS on the proliferative rate of MDA-MB-231 demonstrated a reduction in the rate of proliferation of the TN BC cell

line. Factors secreted by pre-differentiated adipocytes differ to those from mature, and it is thus likely that different pathways are stimulated when cells are co-cultured, with different consequential downstream effects. There is a paucity of research looking at the effect(s) of preadipocytes on MDA-MB-231 cells, and more work is needed.

When co-cultured with mature SGBS cells, MDA-MB-231 proliferation showed no early significant difference as compared to MDA-MB-231 cells cultured alone. When cultured beyond 12 h, however, statistically significant increases in proliferation were observed. Interestingly, Park *et al.* (2020) demonstrated an increase in cell proliferation at 48 and 72 h post MDA-MB-231 exposure to conditioned media from human adipose derived mesenchymal stem cell differentiated adipocytes; there was no significant difference at 24 h.

TN BC cells do not respond to oestrogen stimulation. Adipocyte mediated increased proliferation rate in a TN BC cell line thus indicates mechanisms and pathways other than the oestrogen stimulation postulated for MCF-7 cells.

3.7 Conclusion

To date, no research has been published which investigates the influence of pre-differentiated and mature SGBS adipocytes on the rate of proliferation of MCF-7 or MDA-MB-231 cancer cells. Here, it is demonstrated that pre-differentiated and mature SGBS cells exert a statistically significant stimulatory influence on the proliferation of the ER^+ BC cell line MCF-7. Mature SGBS cells do not appear to influence the proliferation of MDA-MB-231 cells by 12 h, but a longer co-culture time reveals a different dynamic. Interestingly, pre-differentiated SGBS cells inhibit the proliferation of MDA-MB-231 cells.

MCF-7 and MDA-MB-231 cells differ in their biology and consequently in their behaviour, despite both being BC cell lines. The mechanisms by which adipocytes exert

their influence on BC cells are not yet fully understood. It is known that, in addition to the ER, the two cell lines express different receptors with differing signalling cascades. These may feature in the stimulation resulting from adipokines. Because of the existence of different pathways, it is likely that the cells' sensitivities to the secreted factors here differ.

MDA-MB-231 cells are more aggressive than MCF-7 cells. It is possible that some of this increased aggressiveness is as a result of activation of a greater number of pathways prior to additional stimulation, as compared to MCF-7. In this scenario, it would be plausible for further factor stimulation from the co-cultured SGBS cells not to increase proliferation as it did to MCF-7 cells for this reason. The reduction in MDA-MB-231 proliferation requires further investigation, and investigation of the proteome secretion of pre-differentiated SGBS compared to mature.

To further investigate the results seen here, differences in cytokine secretion between peri-cancer cells and distant cells will be analysed.

CHAPTER FOUR

Differences in Cytokine Secretion and Gene Expression of Adipose Tissue and Adipocytes, Dependent upon Proximity to Cancer

Chapter Four: Differences in Cytokine Secretion and Gene Expression of Adipose Tissue and Adipocytes, Dependent upon Proximity to Cancer

Contents

4.1	**Introduction……**	**93**
4.1.1	Cytokines in the Tumour Microenvironment ……...	93
4.2	**Aims of the Chapter……...**	**93**
4.3	**Explant Culture and Proteome Array Analysis……**	**94**
4.3.1	Differences in Cytokine Secretory Profile of Peri-Tumoural Adipose Tissue Compared to Resection Margin Tissue, in Patients with ER^+ Breast Cancer …….....	95
4.3.2	Differences in Cytokine Secretory Profile of Peri-Tumoural Adipose Tissue Compared to Resection Margin Tissue, in Patients with Triple Negative Breast Cancer……...	100
4.3.3	Combined ER^+ and Triple Negative Breast Cancer Data……...	109
4.4	**SGBS and MCF-7 Cell Co-Culture Media Cytokine and Gene Analysis……...**	**109**
4.4.1	SGBS and MCF-7 Cell Co-Culture Media Cytokine Analysis……	109
4.4.2	SGBS Select Cytokine Gene Expression Analysis…….	113
4.4.2.1	SGBS Select Cytokine Gene Expression Time Course……..	113
4.4.2.2	Gene Expression Profile of SGBS Co (MCF-7) Adipocytes Compared to SGBS Alone Adipocytes……..	119
4.4.2.3	Gene Expression Profile of SGBS Co (MDA-MB-231) Adipocytes Compared to SGBS Alone Adipocytes…….	119
4.5	**Discussion……...**	**123**
4.6	**Conclusion……...**	**125**

4.1 Introduction

Malignant tumours are complex lesions which communicate with their non-malignant environment, modifying the behaviour of local cells to increase their own proliferative and metastatic capabilities; multi-directional communication must occur between many (native and recruited) cells for this to happen. Identifying important players, both cellular and chemical, in this complicated network may lead to breakthroughs for developing novel therapeutic agents and thus improve cancer survival. Over recent years, adipose tissue (AT) and adipocytes have generated much interest, previously being a grossly underappreciated component of the tumour microenvironment (TME).

4.1.1 Cytokines in the Tumour Microenvironment

Cytokines are chemical signalling molecules secreted by cells to mediate cell-cell communication. Since the discovery of the first adipose tissue derived cytokine TNF-α in the early 1990s, over 600 signalling molecules have now been identified and understanding of their role in malignancy is increasing.

4.2 Aims of the Chapter

The aims of this Chapter are to determine:

1. Whether the cytokine secretory profile of peri-tumoural adipose tissue from patients with invasive ER^+ BC differs to that of breast tissue distant to the site of malignancy
2. Whether the cytokine secretory profile of peri-tumoural adipose tissue from patients with invasive TN BC differs to that of breast tissue distant to the site of malignancy
3. Whether the cytokine secretory profile of SGBS adipocyte cells co-cultured with MCF-7 BC cells differs to that of SGBS cells grown alone

4. Whether the gene expression profile of SGBS adipocyte cells co-cultured with MCF-7 BC cells differs to that of SGBS cells grown alone
5. Whether the gene expression profile of SGBS adipocyte cells co-cultured with MDA-MB-231 BC cells differs to that of SGBS cells grown alone

4.3 Explant Culture and Proteome Array Analysis

Human breast AT samples were collected from female patients undergoing surgery for invasive ER^+ or TN BC at UHCW University Hospital. Ethical approval for the study was obtained from the Arden Tissue Bank (ATB). Patients provided written informed consent, and the tissue was collected by ATB staff. Each sample consisted of one each of *peritumoural* and *distant ('resection margin')* tissue specimens. Fresh tissue samples were processed within one hour of surgical resection. Explants were cultured, as described previously (Chapter Two; Section 2.2.1.2).

The Proteome Profiler™ Human XL Cytokine Array Kit (R&D Systems, Abingdon, United Kingdom) allows for the simultaneous assessment of 105 cytokines, chemokines, growth factors, and acute phase proteins (Appendix B). Post processing, signals are proportional to the quantity of target protein bound and observations can be made comparing cytokine quantities in different samples. Membranes were treated with serum-free media from the peri-tumoural (PT) and distant ('resection margin', RM) breast AT explants, and analyses were performed with ImageQuantTL 8.1 software.

R&D Systems® (Abingdon, United Kingdom) state each researcher should choose their own pixel density difference cut-off as the minimum level for significance between paired samples, but a difference of at least 5 000 - 8 000 pixels per inch (ppi) is required (personal communication). Here, a pixel density of 10 000 ppi was selected as the cut-off. To be able to compare cytokines between different paired samples, $\log_2$

fold change (FC) was calculated. Pixel density was changed to 1 for both PT and RM numbers if the difference between cytokine pairs was <10 000, to obtain a FC of 1 and log_2 FC of 0 to denote no difference. All differences shown on the heatmaps are, therefore, significant.

Nine fresh human breast AT samples were processed; six from patients with ER^+ disease and three from patients with TN BC (Table 4.1). PT specimens were all from within 10 mm of the tumour. Histology slides of explant tissue received back from ATB staff demonstrated healthy AT which had maintained integrity (Figure 4.1).

4.3.1 Differences in Cytokine Secretory Profile of Peri-Tumoural Adipose Tissue Compared to Resection Margin Tissue, in Patients with ER^+ Breast Cancer

Six paired (PT and RM) patient samples were processed. Each paired sample was analysed on two membranes - one for PT media and the other for RM. Pixel densities were normalised as a percentage of the mean of the (first paired) reference spots on the RM explant media membrane. Log_2 FCs were calculated for each cytokine in each paired sample and displayed graphically (Figures 4.2 and 4.3). Positive log_2 FC indicated cytokine concentrations higher in media from PT samples and negative values indicated higher concentrations in RM media.

To analyse overall change across the six samples, results for individual cytokines were analysed: cytokines which demonstrated a log_2 FC in at least three of the six samples, with the majority being positive were selected for further analysis. Calculation of median returned a majority of 0-fold change results in view of the mixed change in some samples. As this would negate the sometimes relatively substantial change seen, mean was used.

Table 4.1: Human Breast Adipose Tissue Samples Processed

Sample	Receptor Status	Grade	Tumour Size	Patient BMI	Patient Age at Surgery (Years)	Sample Distance from Tumour
ER1	ER+ HER2-	2	16 x 16 x 23 mm	22.1	53	PT: 3 mm RM: 18 mm
ER2	ER+ HER2-	2	7 x 12 x 10 mm	26.6	66	PT: 5 mm RM: 40 mm
ER3	ER+ HER2-	1	9 x 11 mm	26.7	59	PT: 2 mm RM: 20 mm
ER4	ER+ HER2-	2	15 x 8 x 12 mm	28.8	71	PT: 3 mm RM: 50 mm
ER5	ER+ HER2-	2	15 x 15 x 17 mm	30.2	75	PT: 5 mm RM: 40 mm
ER6	ER+ HER2-	3	10 x 17 x 8 mm	Unknown	57	PT: 10 mm RM: 30 mm
TNBC1	ER- PR- HER2-	3	10 x 17 x 8 mm	Unknown	73	PT: 3 mm RM:18 mm
TNBC2	ER- PR- HER2-	2	10 x 10 x 12 mm	Unknown	45	PT: 5 mm RM: 60 mm
TNBC3	ER- PR- HER2-	3	15 x 13 x 14 mm	Unknown	50	PT: 2 mm RM: 30 mm

Figure 4.1: Haematoxylin & Eosin Stained Slide of Human Breast Adipose Tissue Post 24 h Culture

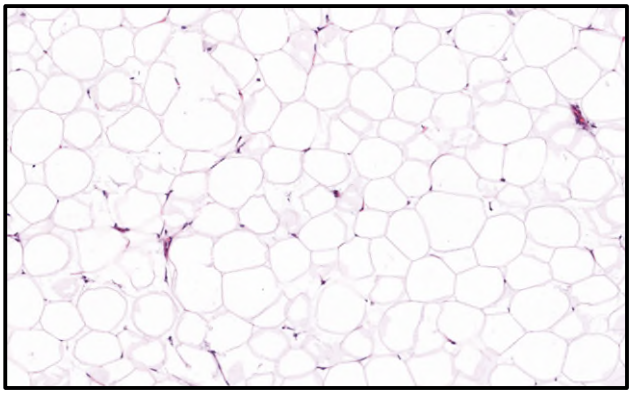

H&E stained slide of explant adipose tissue post culture to demonstrate tissue integrity.

x10 magnification.

Figure 4.2: Log_2 Fold Change of Cytokines in ER^+ Explant Media: Peri-Tumoural Tissue Compared to Resection Margin Tissue

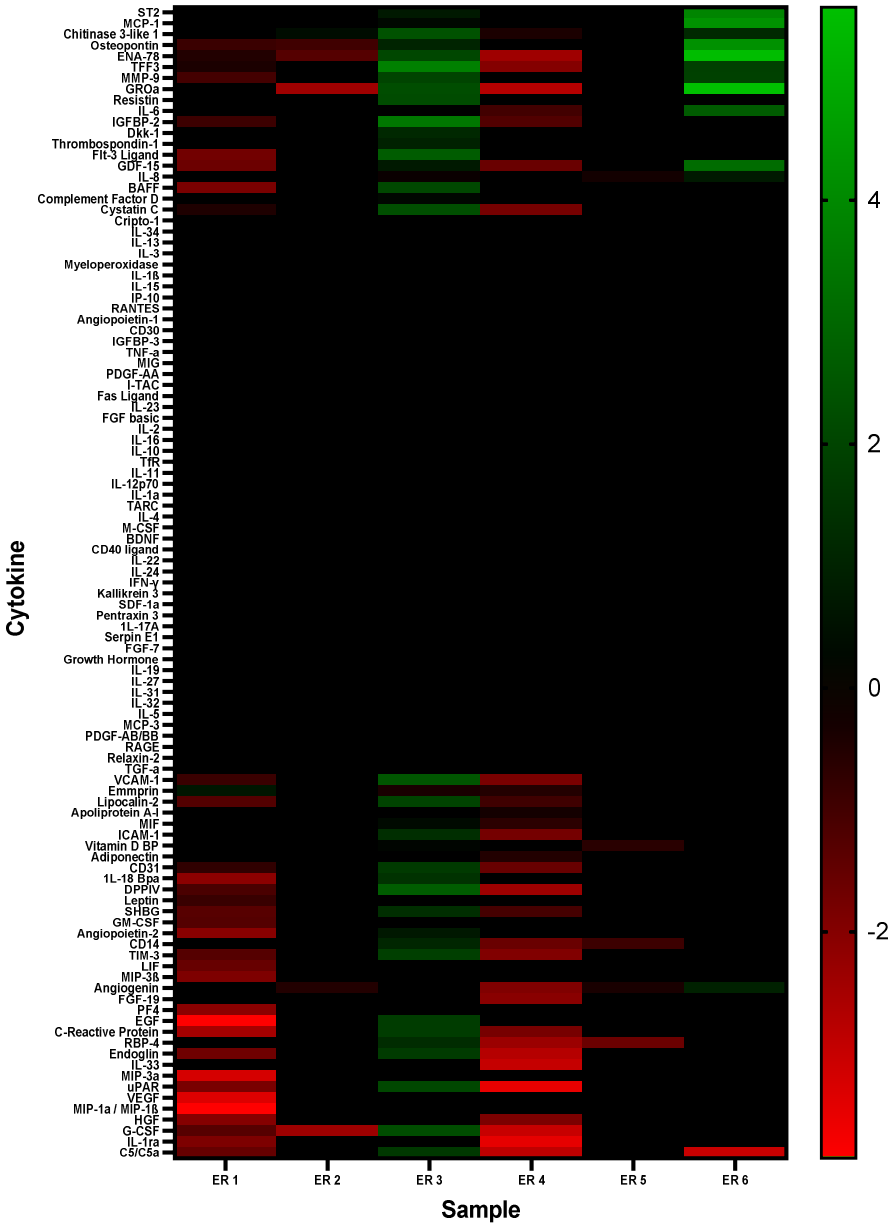

Heatmap to illustrate log_2 fold change of cytokine secretion in ER^+ explant media. Data ordered by mean change. Key as shown; green scale denotes increased levels in media from peri-tumoural (PT) tissue, red scale denotes increased levels in media from resection margin (RM) tissue, black denotes no change.

Figure 4.3: Log_2 Fold Change of Select Cytokines in ER^+ Explant Media: Peri-Tumoural Tissue Compared to Resection Margin Tissue

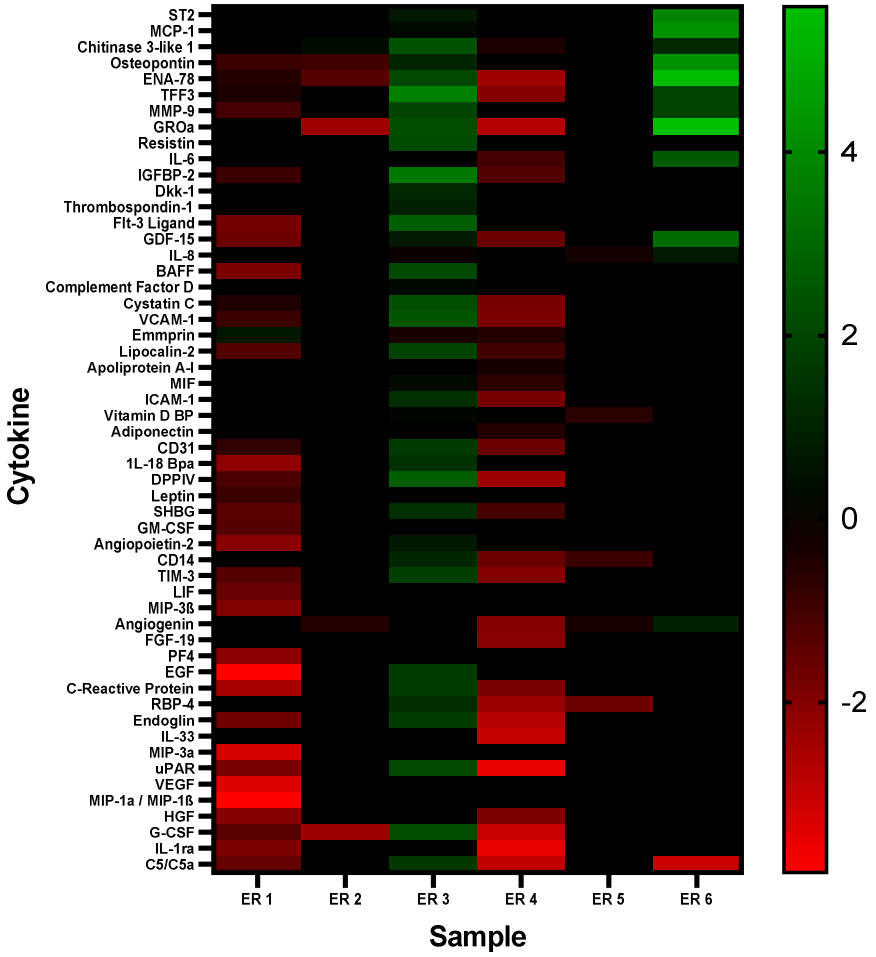

Heatmap to illustrate log_2 fold change of select cytokine secretion in ER^+ explant media; cytokines with no (significant) overall difference between PT and RM specimens removed. Data ordered by mean change. Key as shown; green scale denotes increased levels in media from peri-tumoural (PT) tissue, red scale denotes increased levels in media from resection margin (RM) tissue, black denotes no change.

Whole group analysis revealed two cytokines which were found in higher concentrations in the PT specimen when compared to the RM - Chitinase 3-like 1 (CHI3L1) and Matrix Metalloproteinase-9 (MMP-9) (Table 4.2) (mean log_2 FC 0.577863 and 0.464383 respectively). 15 cytokines were lower (range of mean log_2 FC across six specimens: -0.03941 to -0.97222). The remainder showed grossly mixed results, or no change. The difference seen in the two elevated cytokines CHI3L1 and MMP-9 was not significant, as analysed by Wilcoxon matched-pairs signed rank test (Figure 4.4)

4.3.2 Differences in Cytokine Secretory Profile of Peri-Tumoural Adipose Tissue Compared to Resection Margin Tissue, in Patients with Triple Negative Breast Cancer

In media taken from TN explants, 89 cytokines showed a significant difference between the two sample sites, although the change was not consistent across the group as a whole.

To analyse overall change across the three patients, mean log_2 FC was calculated for each cytokine and analysis was undertaken as for ER^+ samples (Section 4.3.1) (Figures 4.5 and 4.6). Cytokines were included if at least two of the three samples demonstrated a positive change in log_2 FC value.

Overall, 19 cytokines were found in higher concentrations in the PT explant media when compared to RM (range of mean log_2 FC across samples: 0.16759 to 4.92244), and two were lower (mean log_2 FC of -0.03552 and -0.15888). The remaining cytokines showed a mixed picture. Data for the top ten cytokines (Table 4.3) have been displayed in graphical format (Figure 4.7).

Table 4.2: Cytokines Increased in Peri-Tumoural ER^+ Explant Media

CYTOKINE	Alternative Name(s)	Mean Log_2 FC	Action
CHI3L1	YKL-40	0.577863	Chitinase like protein involved in antipathogen response. Acts via MAPK, ERK, Akt, and Wnt/β-catenin signalling pathways, *via* the IL-13 receptor α2 (He *et al.*, 2013)
MMP-9	CLG-4B, Gelatinase B	0.464383	Degrades extracellular matrix. Has wide ranging roles in malignancy including invasion, angiogenesis, and immune modulation of the TME (Yousef *et al.,* 2014). Associated with brain metastasis in BC (Chu *et al.,* 2019)

Table to show cytokines identified in concentrations higher in PT explant media, as compared to RM, for patients with ER+ disease. CHI3L1: Chitinase 3-like 1, MMP-9: matrix metalloproteinase-9.

Figure 4.4: Select Cytokine Secretion by Resection Margin and Peri-Tumoural Breast Tissue in Patients with ER$^+$ Breast Cancer

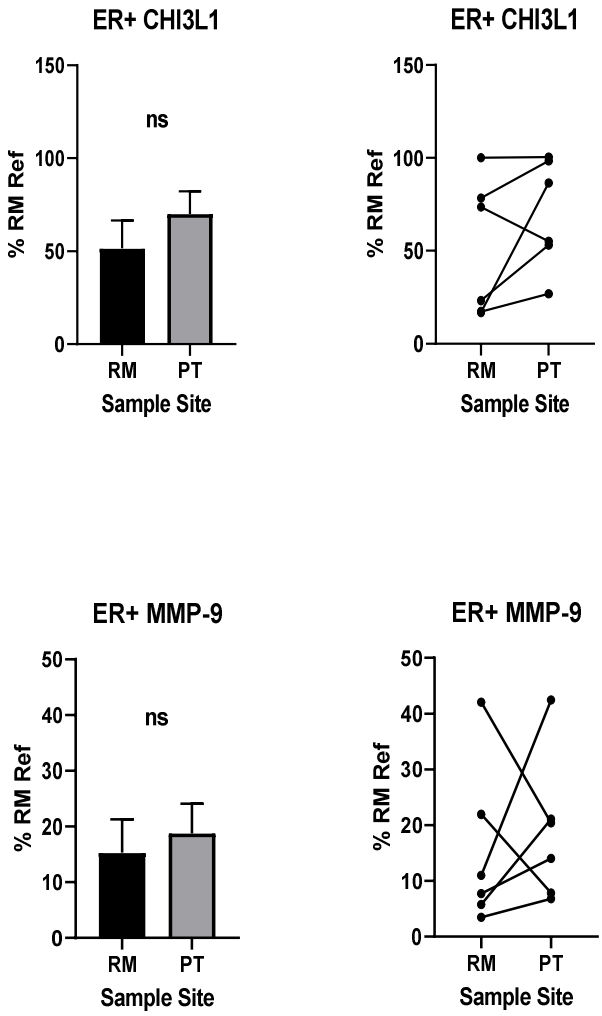

Graphs to illustrate differences in cytokine levels in ER$^+$ peri-tumoural (PT) and resection margin (RM) breast tissue explant culture media from six patients diagnosed with BC. No significance (ns) demonstrated for either cytokine, as analysed by Wilcoxon matched-pairs signed rank test. Bar graphs demonstrate normalised pixel density means ± SEM, and before-after graphs demonstrate change in normalised values of matched pairs.

Figure 4.5: Log_2 Fold Change of Cytokines in Triple Negative Explant Media: Peri-Tumoural Tissue Compared to Resection Margin Tissue

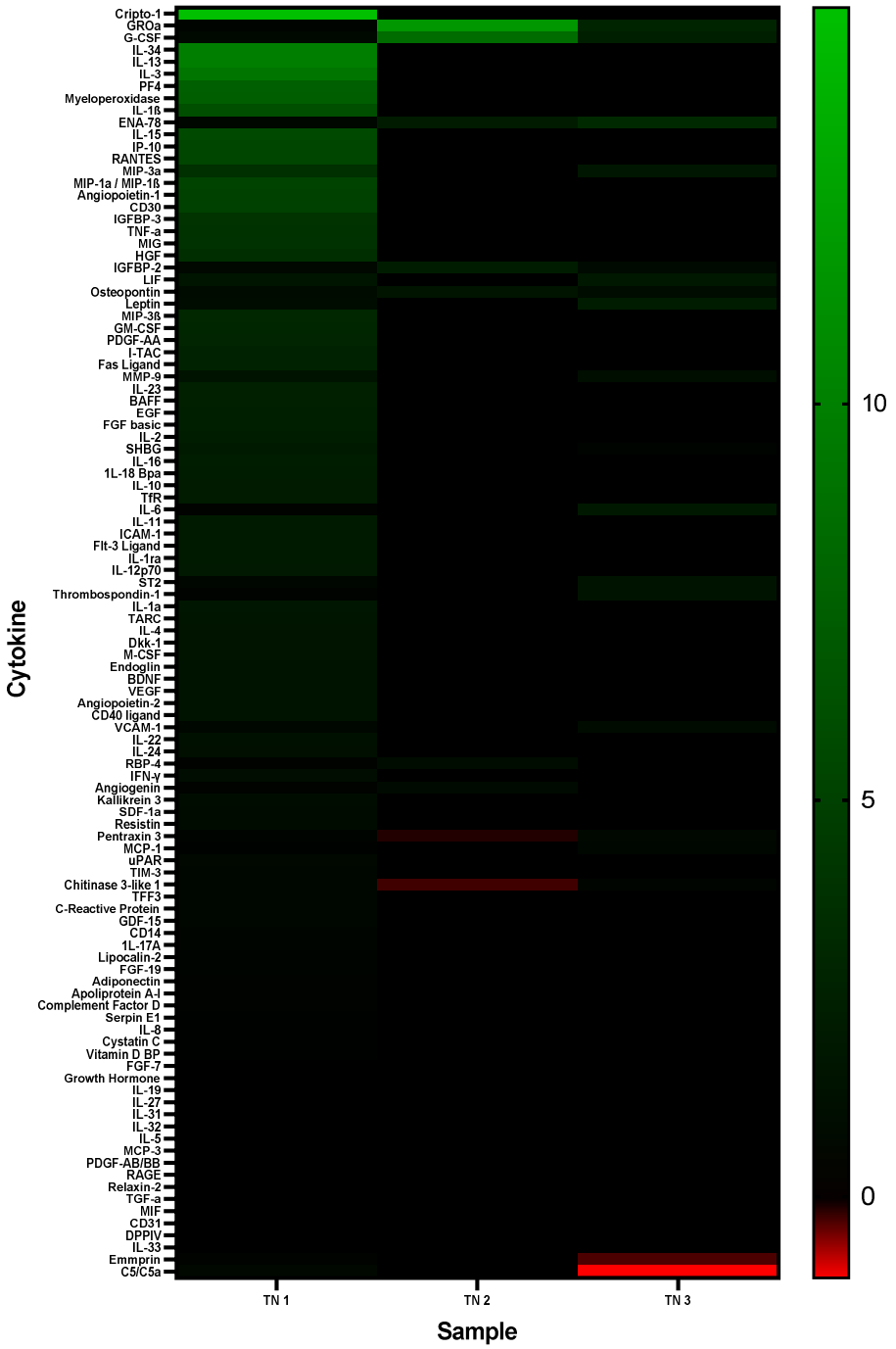

Heatmap to illustrate log_2 fold change of cytokine secretion in TN explant media. Data ordered by mean change. Key as shown; green scale denotes increased levels in media from peri-tumoural (PT) tissue, red scale denotes increased levels in media from resection margin (RM) tissue, black denotes no change.

Figure 4.6: Log_2 Fold Change of Select Cytokines in Triple Negative Explant Media: Peri-Tumoural Tissue Compared to Resection Margin Tissue

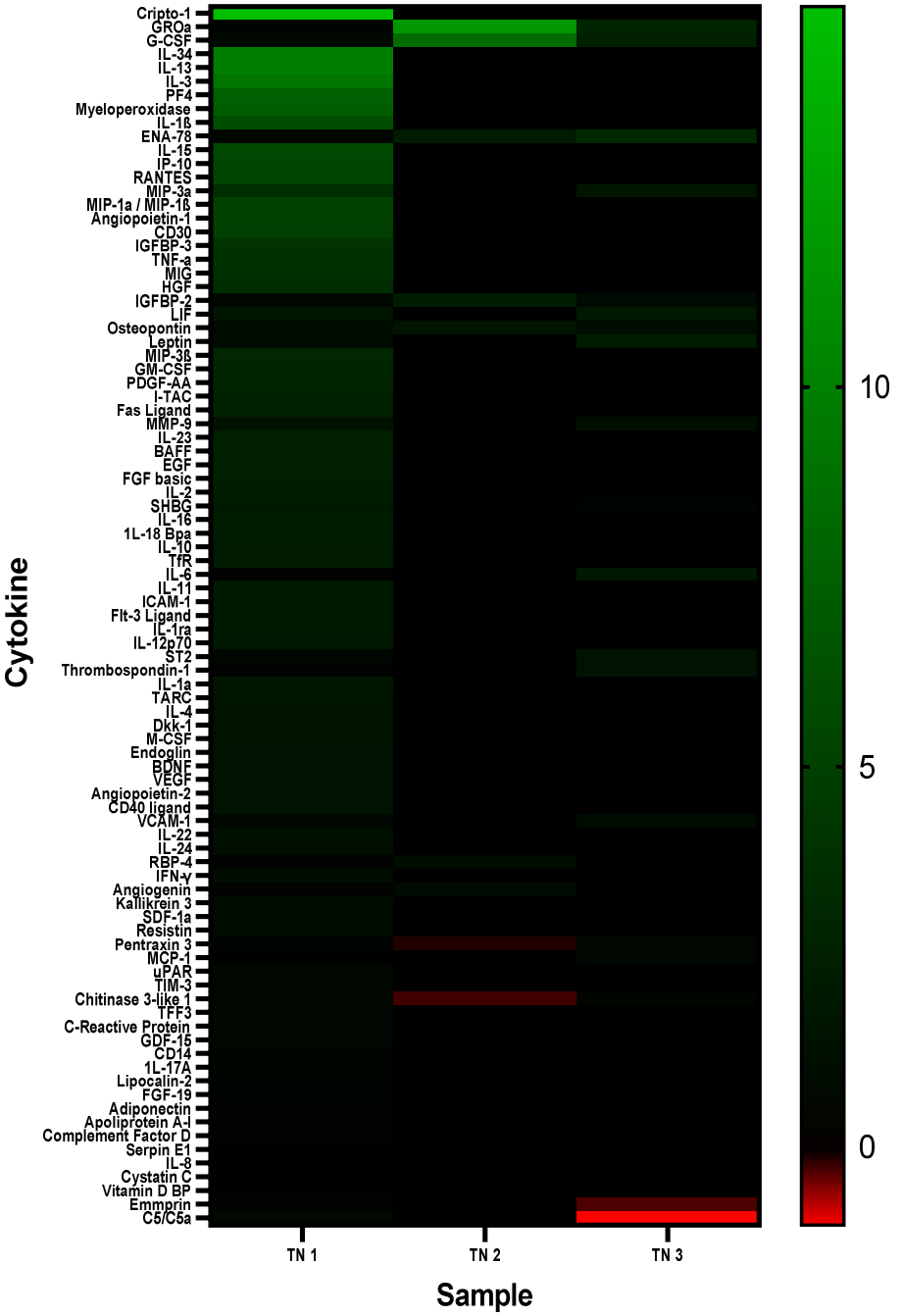

Heatmap to illustrate log_2 fold change of select cytokine secretion in TN explant media; cytokines with no (significant) overall difference between peri-tumoural (PT) and resection margin (RM) specimens removed. Data ordered by mean change. Key as shown; green scale denotes increased levels in media from PT tissue, red scale denotes increased levels in media from RM tissue, black denotes no change.

Table 4.3: Ten Most Increased Cytokines in Peri-Tumoural Triple Negative Explant Media

CYTOKINE	Alternative Name(s)	Mean Log_2 FC	Action
GROα	CXCL1, MSGA-α	4.922437	Leukocyte chemoattractant during normal homeostasis and inflammatory responses. Known role in malignant transformation of cells, angiogenesis, and metastasis (Bhat *et al.*, 2017). Upregulated in breast cancer, and higher levels associated with tumour recurrence and metastasis (Zou *et al.*, 2014)
G-CSF	CSF3	3.811303	Tumourigenic, angiogenic, and/or immunosuppressive in number of cancers including colon, non-small cell lung, glioma, bladder, and melanoma (Aliper *et al.*, 2014). Plasma levels significantly increased in patients with breast cancer, and recombinant human G-CSF increases proliferation of MCF-7 cells (Liu *et al.*, 2020)
ENA-78	CXCL5	1.917576	Neutrophil activator and regulator. Implicated in cancer growth, and angiogenesis. Promotes cancer proliferation and colonisation of metastases in bone in breast cancer (Romero-Moreno *et al.*, 2019)
MIP-3α	CCL20, LARC, Exodus-1	1.789910	Mediates leucocyte migration during inflammation. Role in several cancers, including breast, via enhancing cell proliferation and TME remodelling leading to metastasis (Kadomoto *et al.,* 2020)
IGFBP-2	-	1.168741	Known to interact with various components of the extracellular matrix and cell membrane receptors. Has fundamental roles in metabolism and also oncogenesis. Administration inhibits tumour growth and metastasis (Russo *et al.,* 2015). Promotes invasiveness of MCF-7 cells (Wang *et al.*, 2015)

Continued…

LIF	Leukaemia Inhibitory Factor	1.123134	Member of the IL-6 cytokine family and activates the JAK/STAT pathway. Promotes tumourigenesis; in BC, promotes cell cycle progression and is anti-apoptotic, via STAT3. *Via* JAK/STAT3 and PI3K/Akt/mTOR promotes invasion and metastasis (Jones *et al.*, 2018)
Osteopontin	OPN	1.063968	Bone matrix protein involved in osteoclast attachment. Known roles in various pathways involved in carcinogenesis and metastasis (Zhao *et al.*, 2018). Increases oestradiol production in adipocytes (Leitner *et al.*, 2015). Induces aggressive phenotype of BC (Li *et al.,* 2013)
Leptin	OB	1.014811	Neuroendocrine tumour acting *via* activation of JAK/STAT, JNK and MAPK signalling pathways (Housa *et al.*, 2006). Exogenous leptin stimulation of breast cells increases cellular transformation (Housa *et al.*, 2006). Treatment of malignant breast cells increases proliferative rate (Hu *et al.*, 2002)
MMP-9	CLG-4B, Gelatinase B	0.823249	Degrades extracellular matrix. Has wide ranging roles in malignancy including invasion, angiogenesis, and immune modulation of the TME (Yousef *et al.,* 2014). Associated with brain metastasis in BC (Chu *et al.,* 2019)
IL-6	-	0.674084	Important role in regulation of immune and inflammatory responses. Also acts to influence cancer cell biology (Kaur and Zhang, 2005); increase in invasiveness of BC cells. Elevated serum levels correspond to poorer prognosis in individuals with BC (Dirat *et al.*, 2011)

[CHI3L1 was also increased (mean $\log_2$ fold change 0.167593124) in PT media, but not sufficiently to feature in the top ten]

Table to show top ten cytokines identified in concentrations higher in PT explant media as compared to RM, for patients with TN disease. GROα: Growth Regulated protein α, G-CSF: Granulocyte Colony-Stimulating Factor, ENA-78: Epithelial cell derived Neutrophil Activating Peptide-78, MIP-3α: Macrophage Inflammatory Protein-3, IGFBP-2: Insulin-like Growth Factor Binding Protein-2, LIF: Leukaemia Inhibitory Factor, MMP-9: Matrix Metalloproteinase-9, IL-6: Interleukin-6.

Figure 4.7: Select Cytokine Secretion by Resection Margin and Peri-Tumoural Breast Tissue in Patients with Triple Negative Breast Cancer

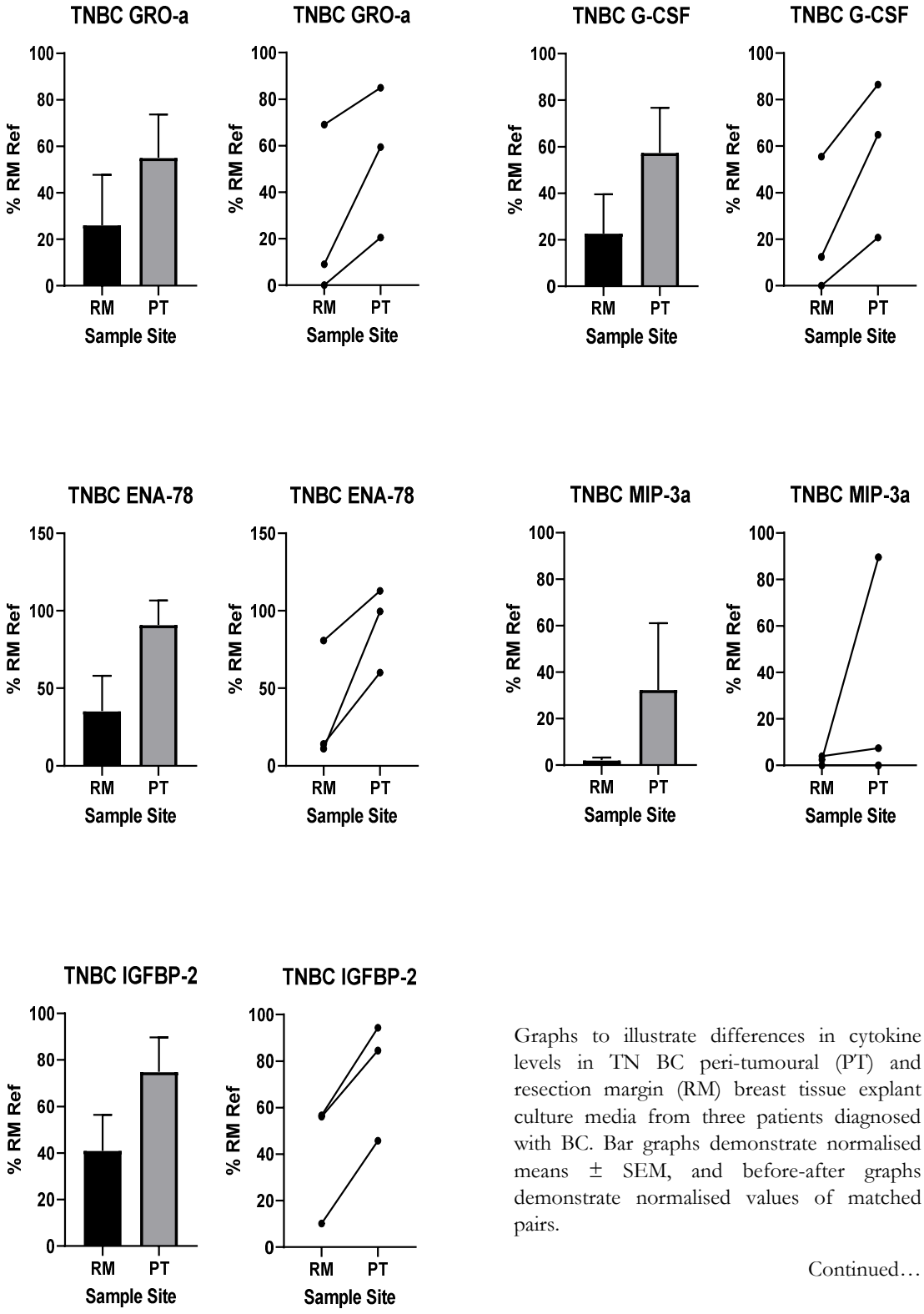

Graphs to illustrate differences in cytokine levels in TN BC peri-tumoural (PT) and resection margin (RM) breast tissue explant culture media from three patients diagnosed with BC. Bar graphs demonstrate normalised means ± SEM, and before-after graphs demonstrate normalised values of matched pairs.

Continued…

Fig4.7 (continued): Cytokine Secretion by Resection Margin and Peri-Tumoural Breast Tissue in Patients with Triple Negative Breast Cancer

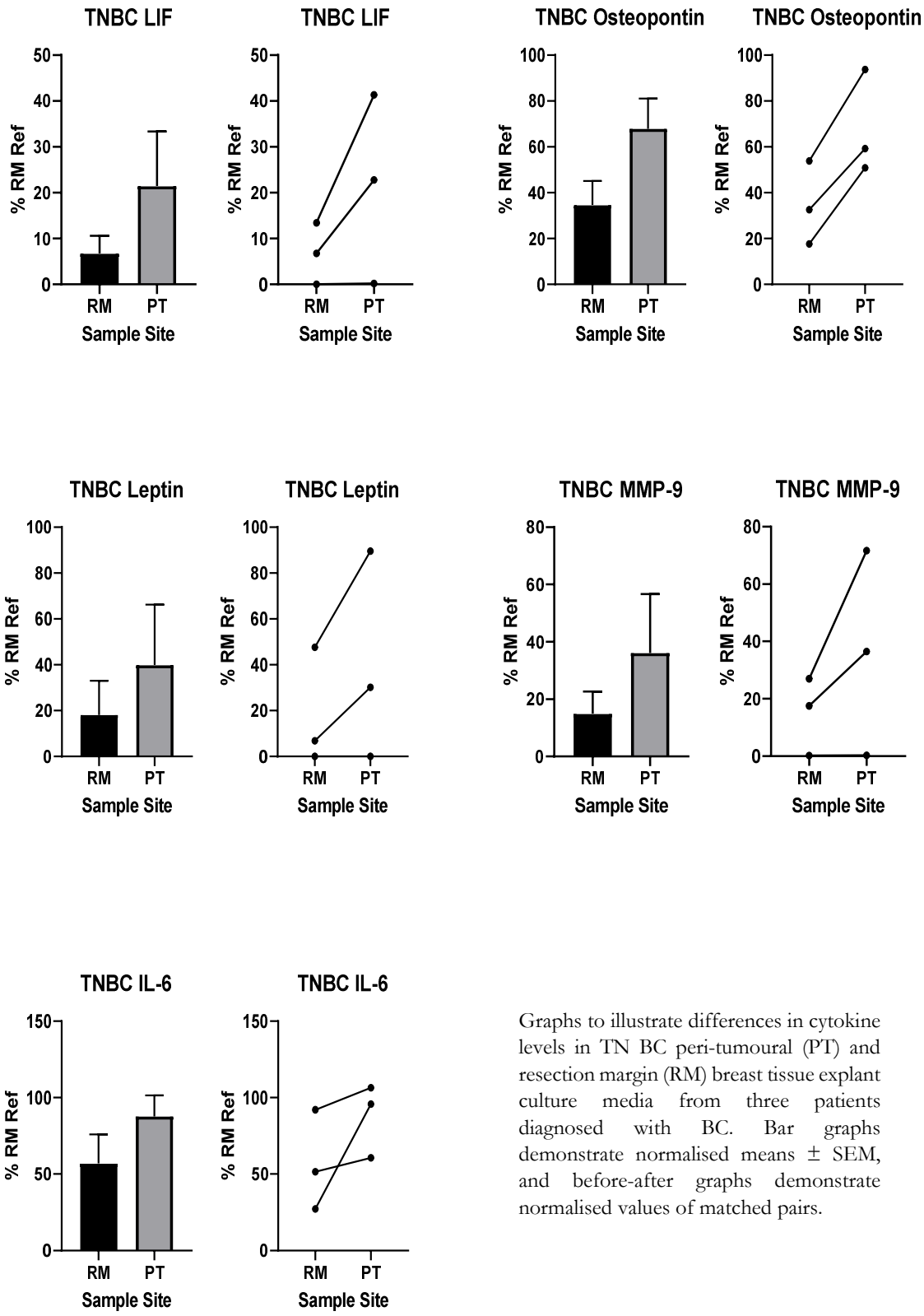

Graphs to illustrate differences in cytokine levels in TN BC peri-tumoural (PT) and resection margin (RM) breast tissue explant culture media from three patients diagnosed with BC. Bar graphs demonstrate normalised means ± SEM, and before-after graphs demonstrate normalised values of matched pairs.

4.3.3 Combined ER^+ and Triple Negative Breast Cancer Data

Data from both ER^+ and TN BC were combined (Figures 4.8 and 4.9) to investigate whether any cytokines were overall increased across the BC subtypes. Cytokines were included in analyses if a $\log_2$ FC was seen in at least five of the nine specimens, and the majority (absolute minimum of four) of these were positive (Appendix C: full data).

Seven cytokines were overall increased in the combined ER^+ and TN BC group analysis: GROα, ENA-78, G-CSF, Osteopontin, MMP-9, IGFBP-2, and Chitinase 3-like 1. This increase did not reach significance, as analysed by Wilcoxon matched-pairs signed rank test (Figure 4.10).

4.4 SGBS and MCF-7 Cell Co-Culture Media Cytokine and Gene Analysis

AT explant tissue used in the above analyses consisted of a mixed population of cell types. To investigate the specific role of adipocytes, MCF-7 BC cell line cells were co-cultured with mature SGBS cells, as previously described (Chapter Two; Section 2.2.5.1), to investigate the effects of these cancer cells on adipocyte inflammatory cytokine secretion, as assessed by the Proteome Profiler™ Human XL Cytokine Array Kit (Chapter Two; 2.2.6). Gene expression analysis was also undertaken (Chapter Two; Section 2.2.10) to compare expression of select genes between SGBS co-cultured (SGBS Co) and SGBS grown alone (SGBS Alone) cells.

4.4.1 SGBS and MCF-7 Cell Co-Culture Media Cytokine Analysis

Three paired (SGBS Co and SGBS Alone) samples were processed. Each pair was analysed on two membranes - one for the media from the SGBS Co and the other for the SGBS Alone. Pixel densities were normalised as a percentage of the mean of the (first paired) reference spots on the SGBS Alone media membrane. To analyse overall change across the three samples, mean $\log_2$ FC was calculated for each cytokine.

Figure 4.8: Log_2 Fold Change of Cytokines in ER^+ and Triple Negative Explant Media: Peri-Tumoural Tissue Compared to Resection Margin Tissue

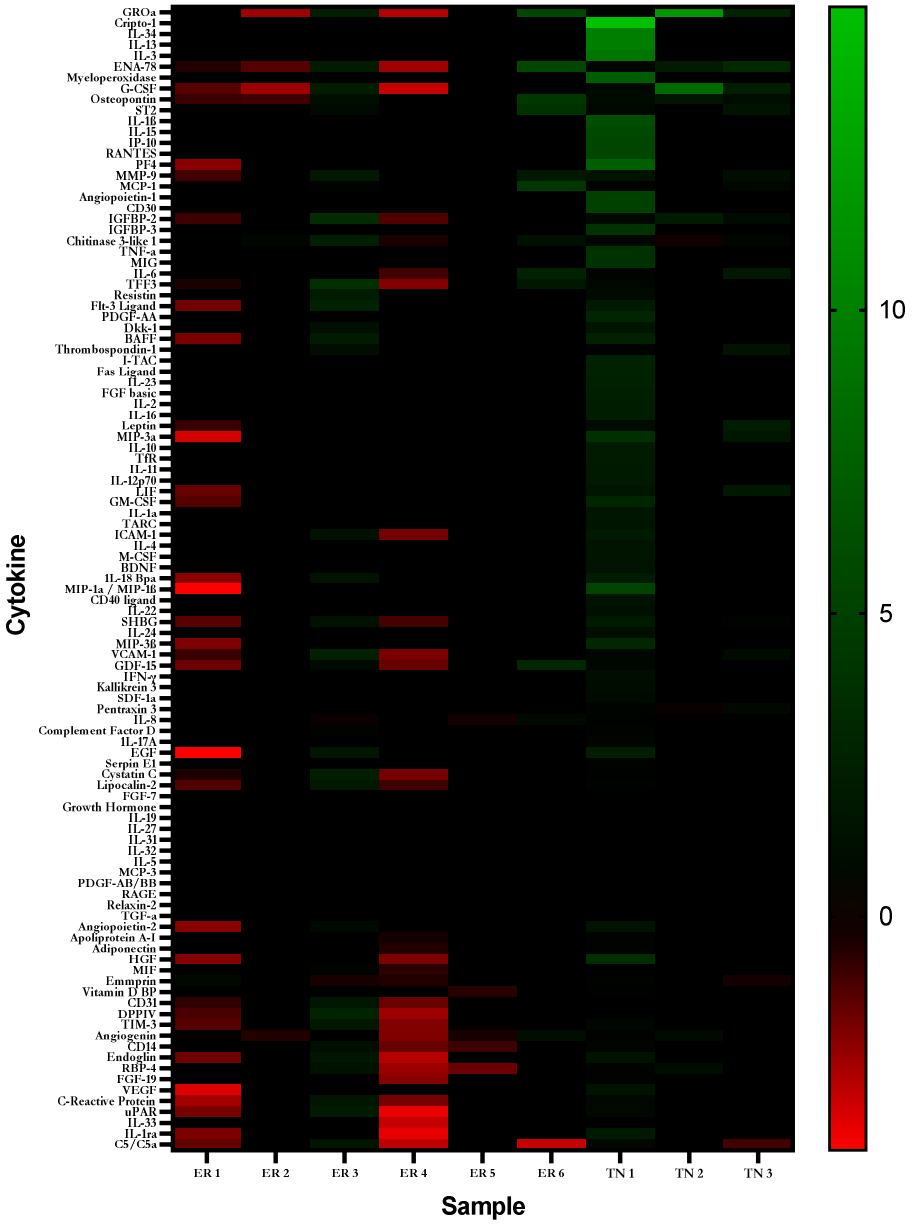

Heatmap to illustrate log_2 fold change of cytokine secretion in ER+ and TN explant media. Data ordered by mean change. Key as shown; green scale denotes increased levels in media from peri-tumoural (PT) tissue, red scale denotes increased levels in media from resection margin (RM) tissue, black denotes no change.

Figure 4.9: Log_2 Fold Change of Select Cytokines in ER^+ and Triple Negative Explant Media: Peritumoural Tissue Compared to Resection Margin Tissue

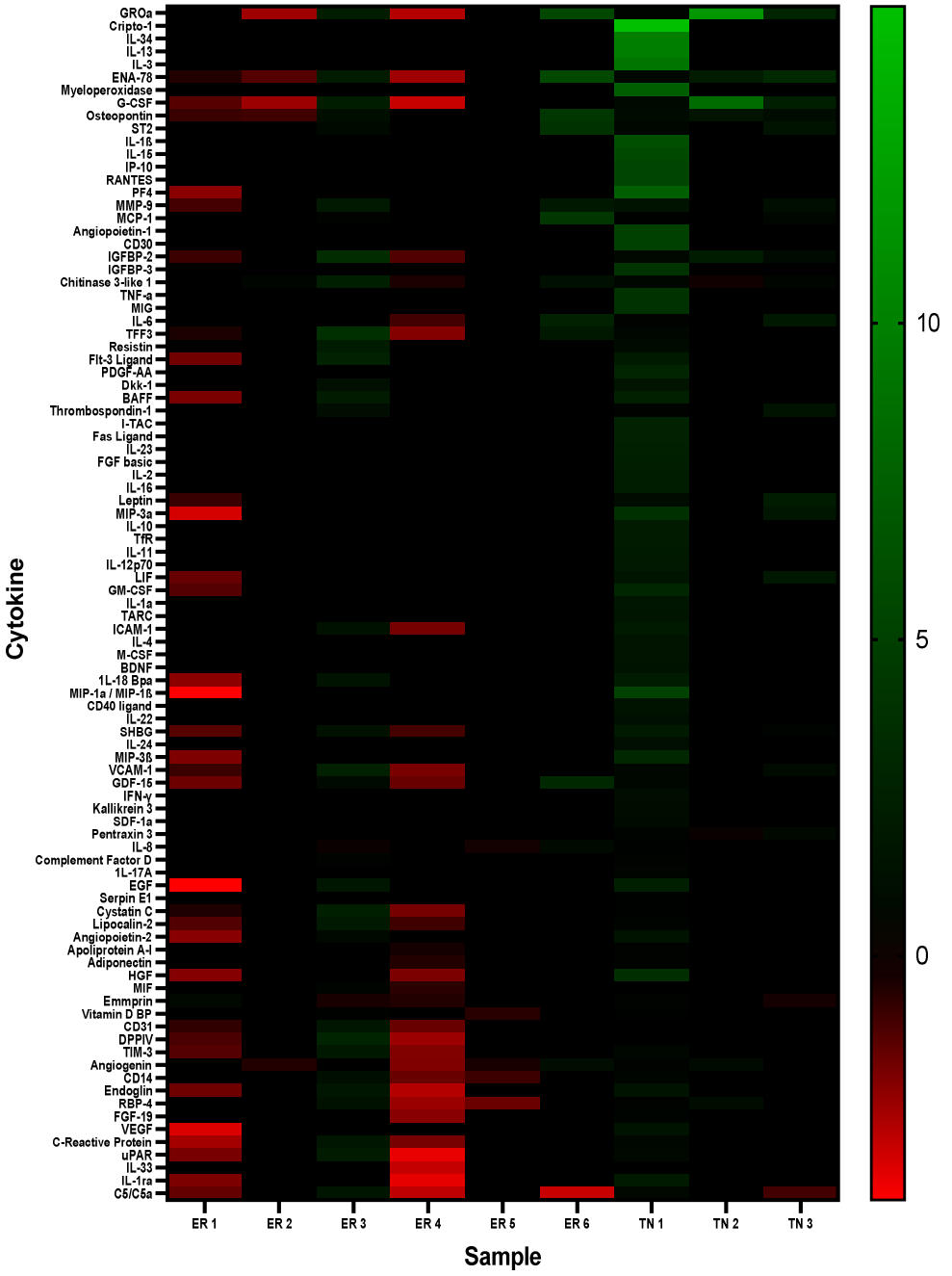

Heatmap to illustrate log_2 fold change of select cytokine secretion in TN explant media; cytokines with no (significant) overall difference between peritumoural (PT) and resection margin (RM) specimens removed. Data ordered by mean change. Key as shown; green scale denotes increased levels in media from PT tissue, red scale denotes increased levels in media from RM tissue, black denotes no change.

Figure 4.10: Select Cytokine Secretion by Resection Margin and Peri-Tumoural Breast Tissue: Combined Data for ER$^+$ and TN Samples

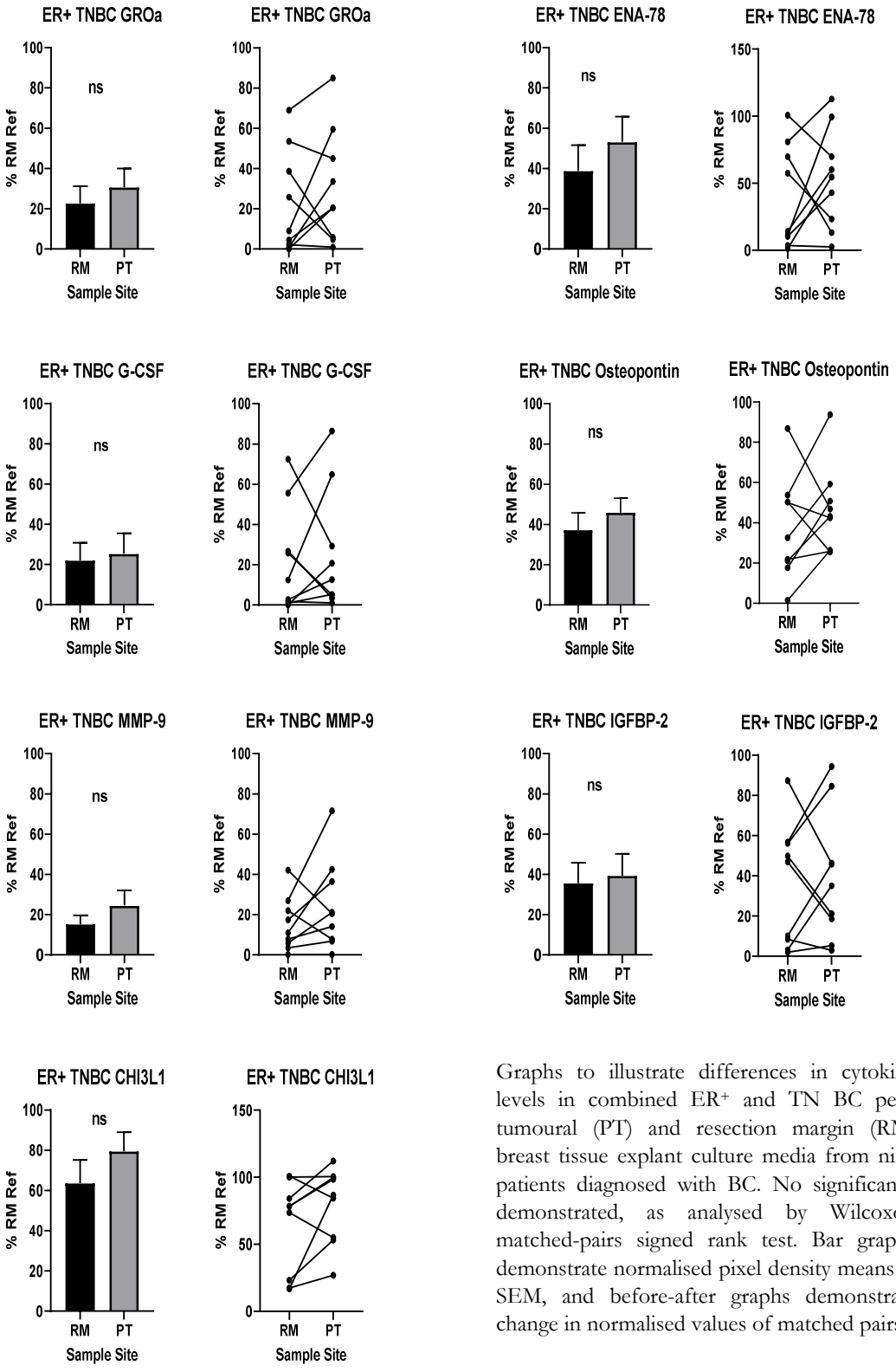

Graphs to illustrate differences in cytokine levels in combined ER$^+$ and TN BC peri-tumoural (PT) and resection margin (RM) breast tissue explant culture media from nine patients diagnosed with BC. No significance demonstrated, as analysed by Wilcoxon matched-pairs signed rank test. Bar graphs demonstrate normalised pixel density means ± SEM, and before-after graphs demonstrate change in normalised values of matched pairs.

In media taken from SGBS MCF-7 Co and SGBS Alone cultures, all cytokines showed a change (Figure 4.11). Overall, 25 cytokines were found in higher concentrations in the SGBS Co media when compared to the SGBS Alone (cytokines were considered higher if there were two or more positive FCs across the three experiments; range of mean log_2 FC across three experiments: 0.02139 to 0.69356). Statistical analysis was conducted to determine whether differences across the whole sample set were significant for the top ten cytokines (Table 4.4); no significant result for the group was seen, as analysed by paired t-test (Figure 4.12.).

4.4.2 SGBS Select Cytokine Gene Expression Analysis

Data obtained from proteome array work were interrogated, and the literature reviewed. *CHI3L1* (Chitinase 3-like 1), *CXCL8* (IL-8), *SPP1* (Osteopontin), *CST3* (Cystatin C), *CCL2* (MCP-1), *IL1RL* (ST2), *CXCL5* (ENA-78) genes were selected for investigation of expression in SGBS Co and SGBS Alone cells.

4.4.2.1 SGBS Select Cytokine Gene Expression Time Course

In order to determine normal gene expression profiles for the selected cytokines during SGBS differentiation, a time course of expression was undertaken. SGBS cells were cultured and differentiated as discussed previously (Chapter Two; Sections 2.2.2.8-10), and lysed (Chapter Two; Section 2.2.3). Cells were harvested pre-differentiation ('Day 0'), and on Days five, ten, 14, and 20. RNA was extracted (Chapter Two; Section 2.2.4), reverse transcribed (Chapter Two; Section 2.2.11), and polymerase chain reactions (PCR) undertaken (Chapter Two; Section 2.2.12).

First, gene expression was confirmed. Importantly, it was identified that the differentiation of SGBS cells is associated with marked, statistically significant, changes

Figure 4.11: Log_2 Fold Change of Cytokines in Cell Co-Culture Media: SGBS MCF-7 Co-Culture Media Compared to SGBS Alone Media

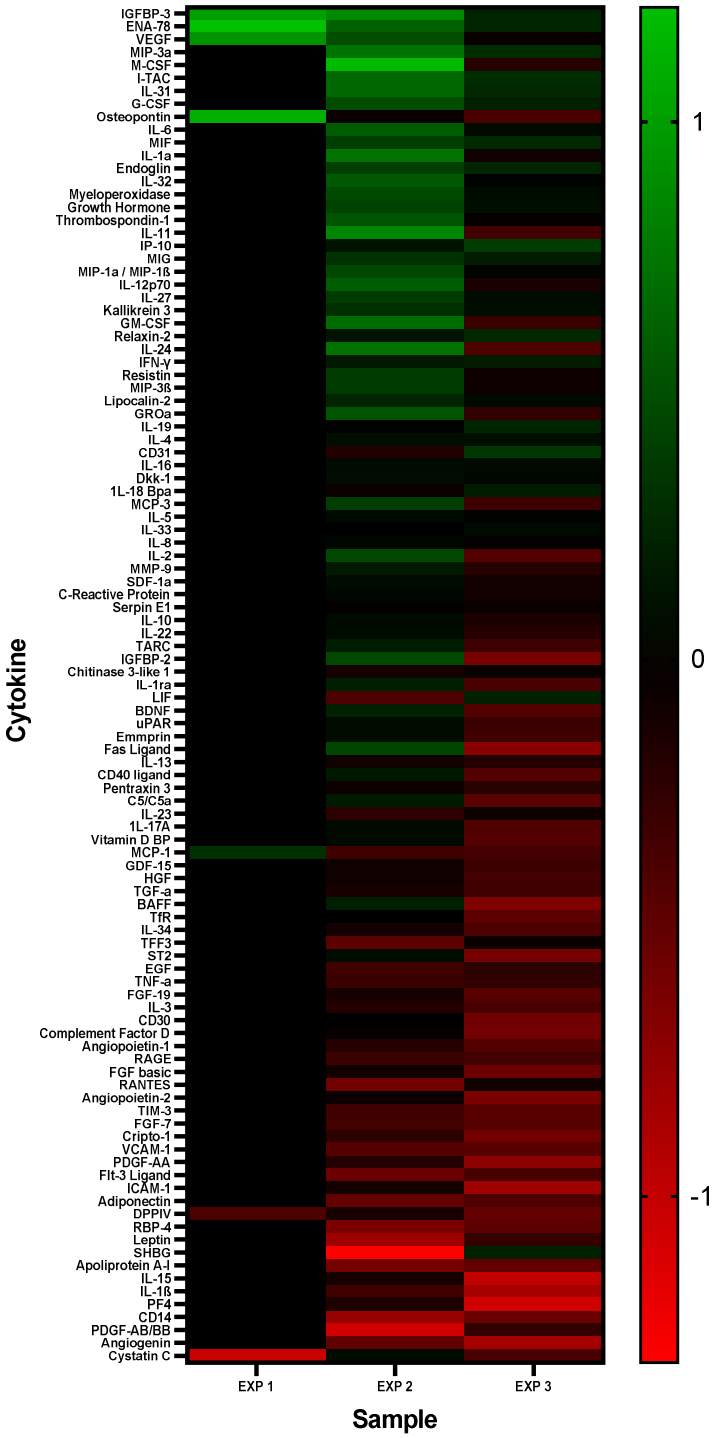

Heatmap to illustrate log_2 fold change of cytokine secretion in SGBS Co media compared to SGBS Alone media. Data ordered by mean change. Key as shown; green scale denotes increased levels in media from SGBS Co, red scale denotes increased levels in media from SGBS Alone, black denotes no change.

Table 4.4: Ten Most Increased Cytokines in SGBS Co Media

CYTOKINE	Alternative Name(s)	Mean Log_2 FC	Action
IGFBP-3	-	0.693558	Carrier and regulator of insulin-like growth factors. Important function in signalling pathways which regulate growth. Increased levels associated with increased risk of pre-menopausal BC (Burger *et al.*, 2005)
ENA-78	CXCL5	0.683778	Neutrophil activator and regulator. Implicated in cancer growth, and angiogenesis. Promotes cancer proliferation and colonisation of metastases in bone in breast cancer (Romero-Moreno *et al.*, 2019)
MIP-3α	CCL20, LARC, Exodus-1	0.332246	Mediates leucocyte migration during inflammation. Role in several cancers, including breast, via enhancing cell proliferation and TME remodelling leading to metastasis (Kadomoto *et al.,* 2020)
I-TAC	CXCL11, SCYB9B	0.312529662	Contributes to regulation of migration, and activation of immune cells (Tokunaga *et al.*, 2018). Increased expression in BC correlates with poor prognosis (Zou *et al.*, 2014). Increases proliferation, invasion, and migration of MDA-MB-231 cells *via* activation of ERK pathway (Hwang *et al.,* 2020)
IL-31	-	0.295832	Member of the IL-6 family and has role in immune regulation. Inhibits tumour growth in immunocompetent mice, no effect in immunodeficient mice (Kan *et al.,* 2020)

Continued…

G-CSF	CSF3	0.224676	Tumourigenic, angiogenic, and/or immunosuppressive in number of cancers including colon, non-small cell lung, glioma, bladder, and melanoma (Aliper *et al.*, 2014). Plasma levels significantly increased in patients with BC, and recombinant human G-CSF increases proliferation of MCF-7 cells (Liu *et al.*, 2020)
IL-6	-	0.212771	Important role in regulation of immune and inflammatory responses. Also acts to influence cancer cell biology (Kaur and Zhang, 2005); increase in invasiveness of BC cells. Elevated serum levels correspond to poorer prognosis in individuals with BC (Dirat *et al.*, 2011).
MIF	-	0.211038	Inflammatory cytokine promoting cell proliferation in MCF-7 cells *via* PI3K/Akt pathway (Richard *et al.,* 2015)
Endoglin	CD105, ENG	0.207695	Accessory receptor for TGF-β and soluble cytokine. regulates differentiation, proliferation and migration of cells. Promotes tumour angiogenesis (Nassiri *et al.*, 2011)
IL-32	-	0.207695	Inflammatory cytokine found to increases tumour growth and reduces apoptosis in BC (Hong *et al.*, 2017)

Table to show top ten cytokines identified in concentrations higher in SGBS Co media as compared to SGBS Alone. IGFBP-3: insulin-like growth factor binding protein 3, I-TAC: Interferon-inducible T cell Alpha Chemoattractant, IL-31: Interleukin-31, MIF: Macrophage Inhibitory Factor, IL-32: Interleukin-32.

Figure 4.12: Cytokine Secretion by SGBS Adipocytes Cultured Alone and in Co-Culture with MCF-7 Cells

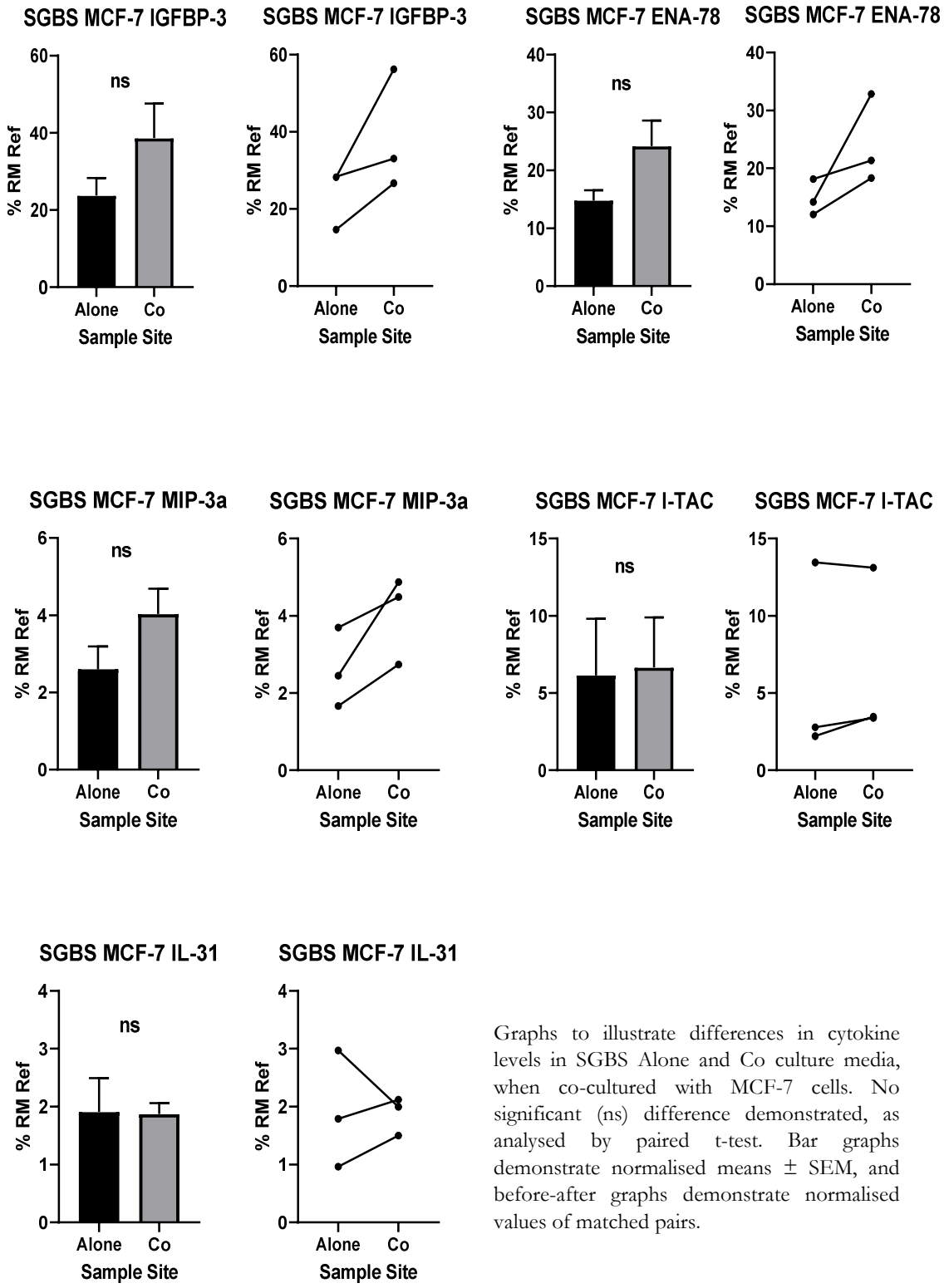

Graphs to illustrate differences in cytokine levels in SGBS Alone and Co culture media, when co-cultured with MCF-7 cells. No significant (ns) difference demonstrated, as analysed by paired t-test. Bar graphs demonstrate normalised means ± SEM, and before-after graphs demonstrate normalised values of matched pairs.

Figure 4.12 (continued): Select Cytokine Secretion by SGBS Adipocytes Cultured Alone and in Co-Culture with MCF-7 Cells

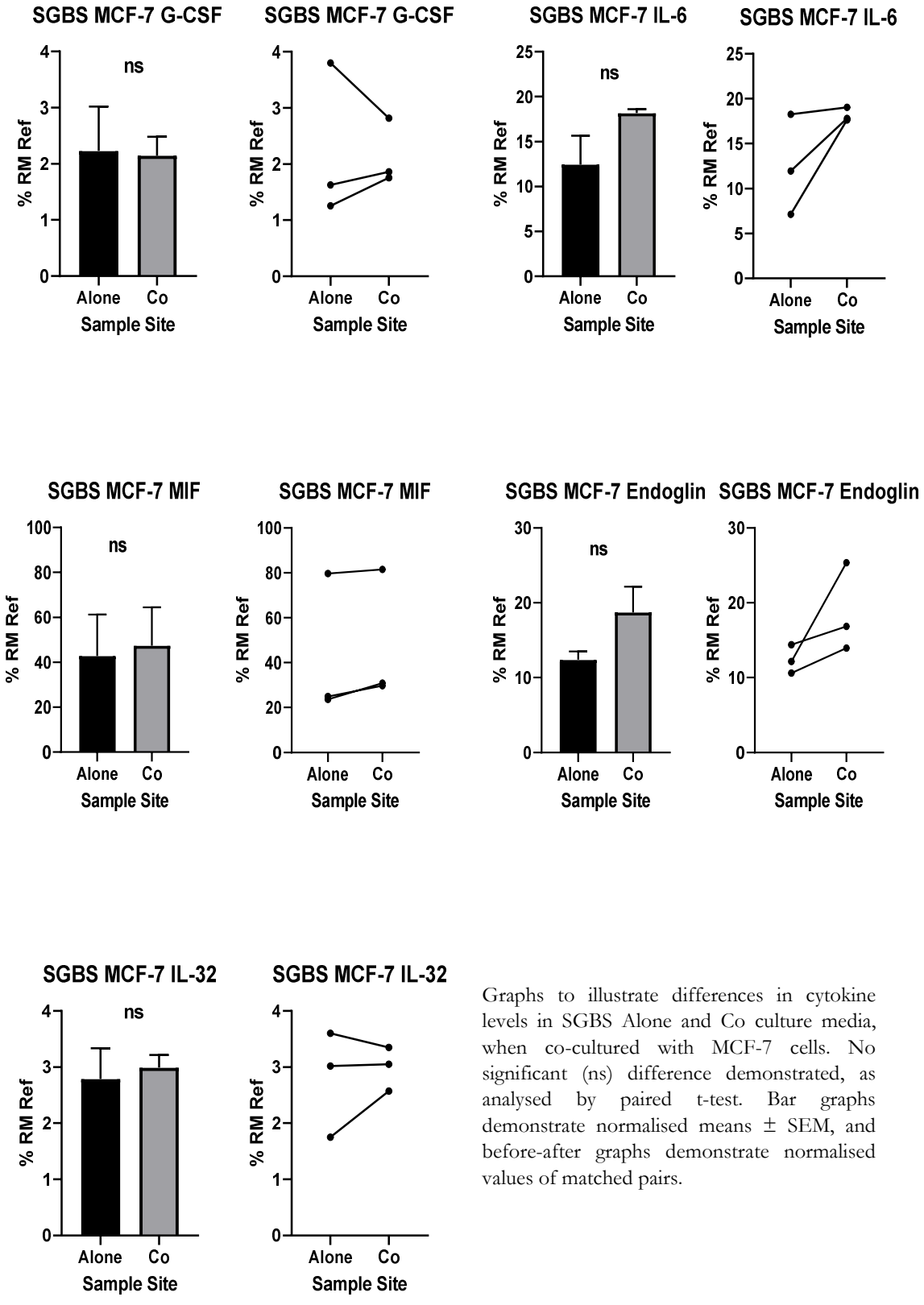

Graphs to illustrate differences in cytokine levels in SGBS Alone and Co culture media, when co-cultured with MCF-7 cells. No significant (ns) difference demonstrated, as analysed by paired t-test. Bar graphs demonstrate normalised means ± SEM, and before-after graphs demonstrate normalised values of matched pairs.

in expression of the genes analysed (PCR for CXCL8 and IL1RL did not return usable results), with the greatest change seen in the expression of CHI3L1 (Figure 4.13), as analysed by one-way ANOVA and with significance set at $p < 0.05$. Gene expression for CCL2 and CXCL was higher in pre-differentiated cells whereas expression was higher for CHI3L1, SPP1, and CST3 in mature SGBS cells.

4.4.2.2 Gene Expression Profile of SGBS Co (MCF-7) Adipocytes Compared to SGBS Alone Adipocytes

SGBS adipocytes were co-cultured with MCF-7 cells (Chapter Two; Section 2.2.5), and PCR performed (Chapter Two; Section 2.2.12) to analyse expression for the selected genes. Statistical analysis, as determined by Student's t-test with significance set at $p < 0.05$, demonstrated expression of the CHI3L1 gene to be higher in SGBS adipocytes co-cultured with MCF-7 cells, as compared to SGBS cells grown alone (Figure 4.14).

4.4.2.3 Gene Expression Profile of SGBS Co (MDA-MB-231) Adipocytes Compared to SGBS Alone Adipocytes

SGBS adipocytes were also co-cultured with MDA-MB-231 cells (Chapter Two; Section 2.2.5), and PCR performed (Chapter Two; Section 2.2.12) to analyse expression for the selected genes. Statistically significant increases, as determined by Student's t-test with significance set at $p < 0.05$, in the expressions of CHI3L1, CXCL8, CCL2, and CXCL5 were identified (Figure 4.15). (PCR for SPP1 did not return usable results).

Figure 4.13: Expression of Select Genes in SGBS Adipocytes at Different Stages of Differentiation

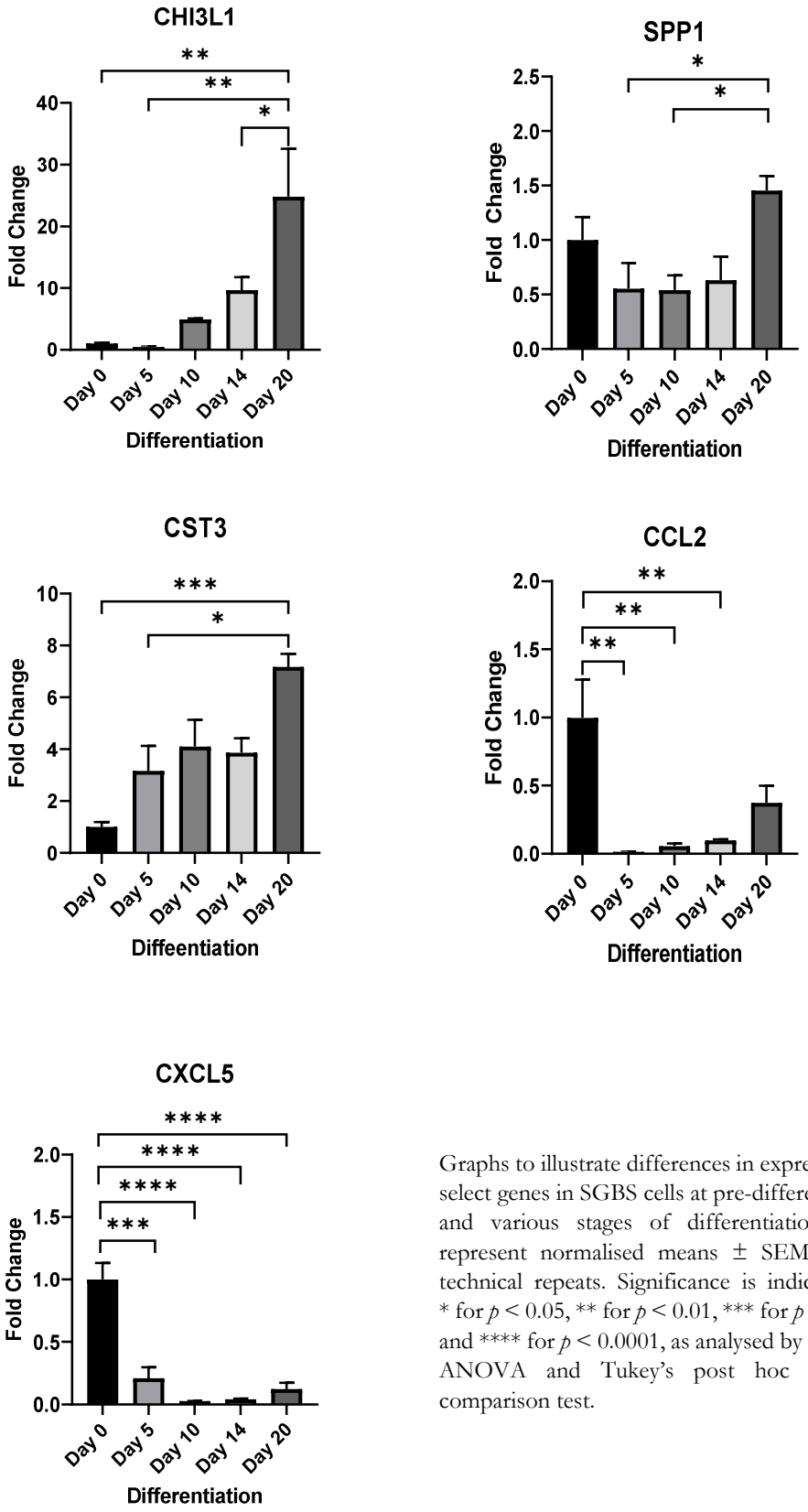

Graphs to illustrate differences in expression of select genes in SGBS cells at pre-differentiation and various stages of differentiation. Bars represent normalised means ± SEM of the technical repeats. Significance is indicated by * for $p < 0.05$, ** for $p < 0.01$, *** for $p < 0.001$, and **** for $p < 0.0001$, as analysed by one-way ANOVA and Tukey's post hoc multiple comparison test.

Figure 4.14: Expression of Select Genes in SGBS Adipocytes Cultured Alone and in Co-Culture with MCF-7 Cells

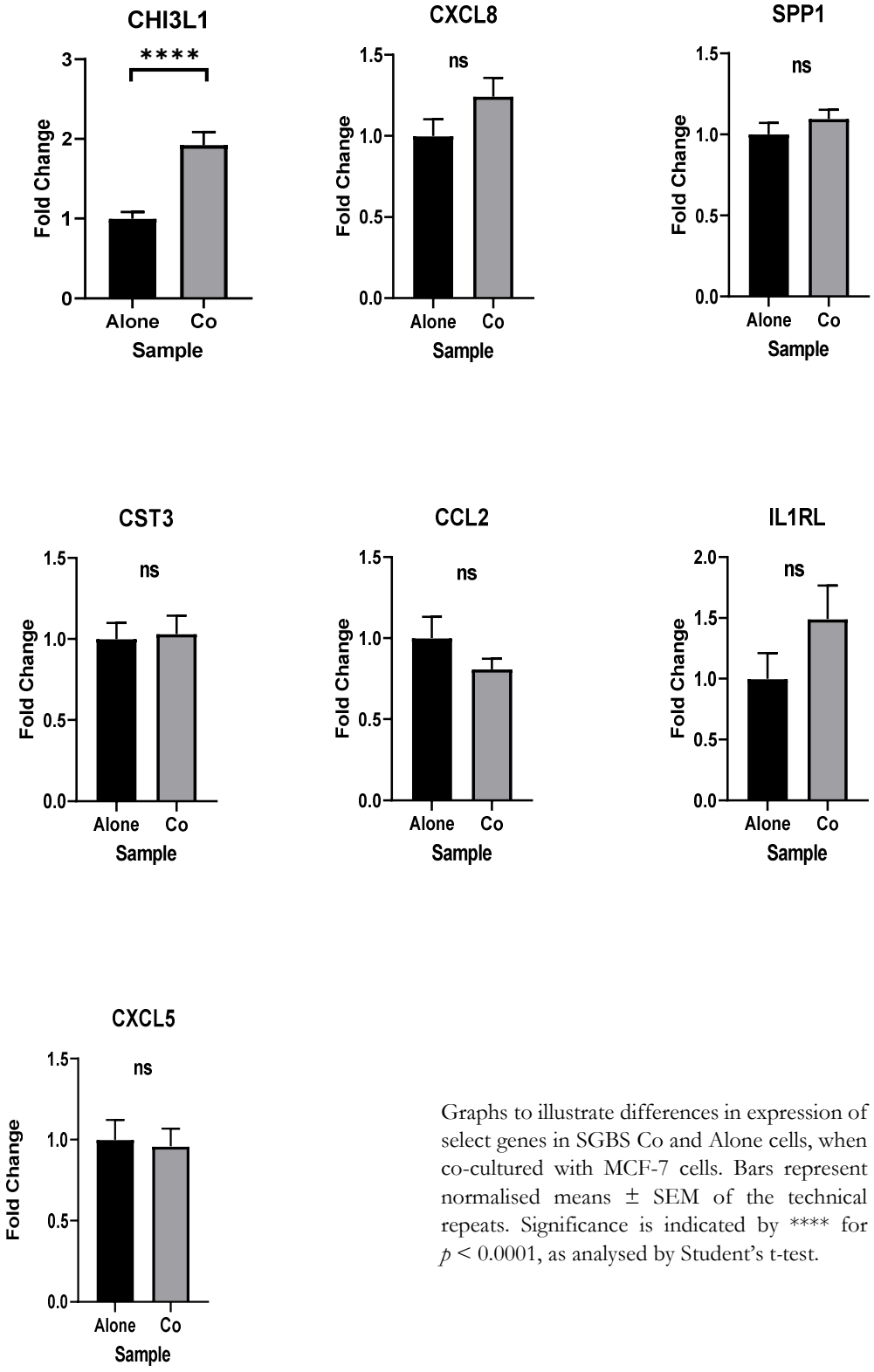

Graphs to illustrate differences in expression of select genes in SGBS Co and Alone cells, when co-cultured with MCF-7 cells. Bars represent normalised means ± SEM of the technical repeats. Significance is indicated by **** for $p < 0.0001$, as analysed by Student's t-test.

Figure 4.15: Expression of Select Genes in SGBS Adipocytes Cultured Alone and in Co-Culture with MDA-MB-231 Cells

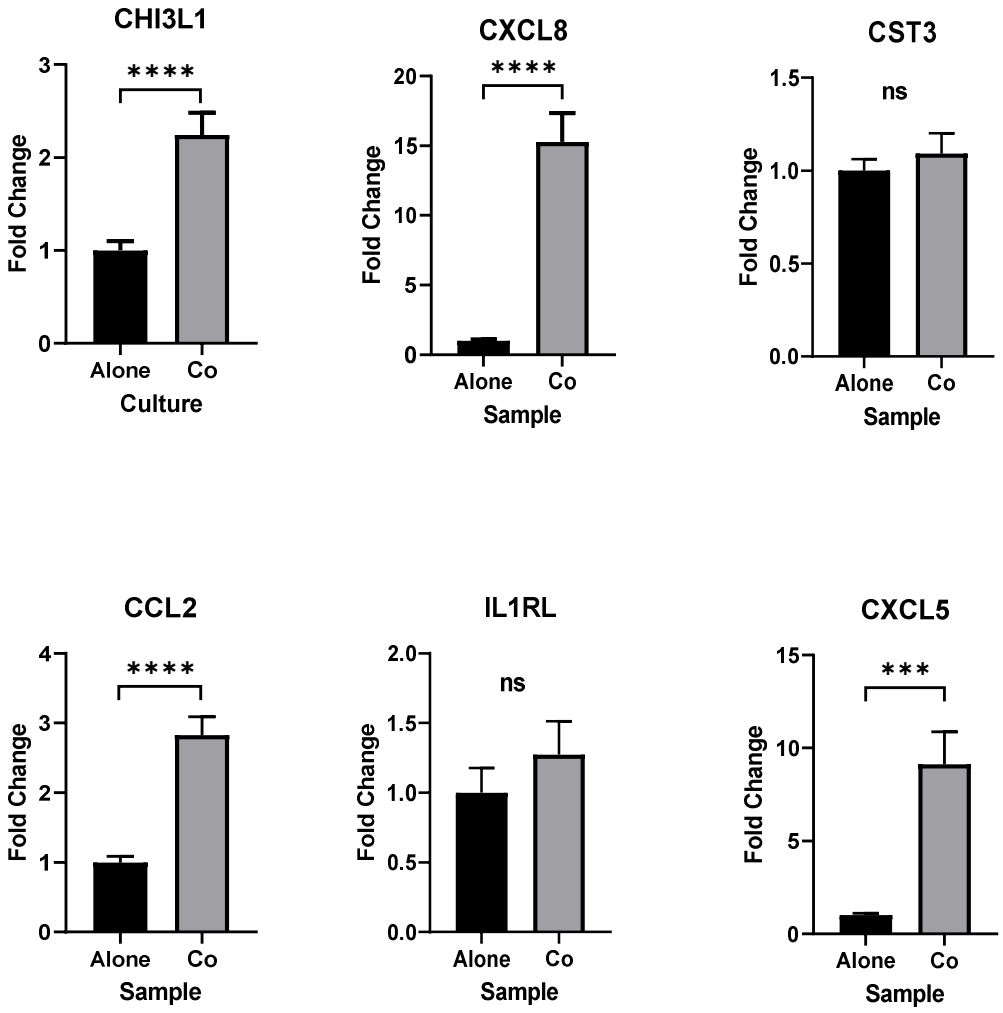

Graphs to illustrate differences in expression of select genes in SGBS Co and Alone cells, when co-cultured with MDA-MB-231 cells. Bars represent normalised means ± SEM of the technical repeats. Significance is indicated by *** for $p < 0.001$, **** for $p < 0.0001$, and ns for *no significance*, as analysed by Student's t-test.

4.5 Discussion

This Chapter has demonstrated that, in breast malignancy, cytokine secretion from AT in the TME differs to that from tissue more distant to a cancer. Differences are seen in both ER^+ and TN cancer, but these differences were not consistent across specimens in this study. Lack of consistency or uniformity of results here likely resulted from the small number of samples and the differences in tumour and patient characteristics, as well as the differences in sample distance from the tumour. Tumour characteristics which may influence cytokine secretion include the histology, size, and grade of the cancer. Patient characteristics or factors which may influence cytokine secretion include age, BMI, and other medical health issues (Horst *et al.*, 2016). Also, various additional factors are recognised as potentially influencing cytokine secretion; an individual's diet, their duration of fasting (patients are instructed not to eat for at least six hours before surgery, and differing operation times will result in different durations of starvation), and the time of day and year (Solis-Pereyra *et al.*, 1997; Horst *et al.*, 2016). Larger sample numbers would negate, or lessen the impact, of some of these factors.

Overall cytokine secretion appears to be unchanged or reduced in the tissue around an ER^+ lesion (two cytokines increased, 15 decreased, 67 mixed, and 50 unchanged) but increased in the tissue around a TN BC (18 increased, two decreased, 71 mixed, and 16 unchanged). MMP-9 and CHI3L1 were the only cytokines identified which were increased in both ER^+ and TN BC. Having been extensively researched (a simple search of "breast cancer" and MMP-9 on PubMed returned over 1 000 matches), MMP-9's role in cancer development and progression has long been recognised; it degrades extracellular matrix, and promotes invasion, angiogenesis, and immune modulation of the TME (Yousef *et al.,* 2014). CHI3L1's role in promoting angiogenesis is accepted, but its wider effects on cellular proliferation and metastases in BC are less well studied.

It is not a surprising finding that TN BC cells (and whole cancers) effect a greater change in the cells of their immediate vicinity, when compared to ER^+ malignancy.

That a difference is seen is understandable when the great heterogeneity of BC sub-types is considered. Indeed, Bareche *et al.* (2020) found that the TME within different TN BC sub-types varied, and it is therefore not surprising that the cytokine analyses here have returned differing results for the two more distinct categories. TN BC is an aggressive disease; tumours grow rapidly, and patients do less well when compared to ER^+ cancer (Dixon and Barber, 2019; Bareche *et al.*, 2020). When co-cultured with (murine) 3T3-L1 adipocytes, MDA-MB-231 had a marked inflammatory response (Nickel *et al.*, 2018). It is possible therefore that TN BC engineers a greater response from and change in the cells in its vicinity in order to promote its own growth and progression, further increasing its aggressiveness and propensity to metastasise. It is known that adipokine secretion from smaller adipocytes is lower than that from larger cells (Skurk *et al.*, 2007). In the TME, adipocytes closest to the cancer are smaller. In the less aggressive ER^+ BC, it may be that the reduction in cytokine concentrations seen in the PT explant media was because of this phenomenon. The greater aggressiveness of TN may have stimulated adipocytes with sufficient strength to maintain or increase cytokines comparatively, despite the reduced size.

When studied in isolation, the cytokine secretion and gene expression profiles of SGBS adipocytes were altered by co-culturing with BC cell line cells. 25 cytokines were identified in higher concentrations in media from SGBS Co as compared to SGBS Alone. Interestingly this was markedly more than in ER^+ PT explant media.

When gene expression analysis was undertaken, SGBS Co (MCF-7) showed a statistically significant increase in CHI3L1 expression. When SGBS Co (MDA-MB-231) cells were analysed, CHI3L1, CXCL8, CCL2, and CXCL5 were all statistically significantly upregulated. Again, cells co-cultured with the TN cancer cells displayed a greater change than those co-cultured with ER^+ cells.

Interestingly, quite marked changes occur in cytokine gene expression during SGBS adipocyte differentiation; further work is required here to understand more about differences in gene expression with maturity to better understand the potential difference effects of pre-differentiated and mature adipocytes in the TME.

4.6 Conclusion

Breast cancers influence the gene expression and secretion of adipokines from local adipocytes, and TN BC cells do this more aggressively. CHI3L1 is a cytokine which featured recurrently in findings; levels were increased in the media of ER^+ explant cultures and TN BC explant cultures, and gene expression was elevated in both SGBS Co (MCF-7) and SGBS Co (MDA-MB-231). Further work to investigate its role in the BC TME may identify it as a novel therapeutic target.

CHAPTER FIVE

CHI3L1 Stimulation of Breast Cancer Cells

CHAPTER FIVE: CHI3L1 Stimulation of Breast Cancer Cells

Contents

5.1	**Introduction……**	**128**
5.2	**CHI3L1 - An Overview…….**	**128**
5.2.1	Functions of CHI3L1……...	128
5.2.2	CHI3L1 in Cancer and in the Tumour Microenvironment ……..	129
5.2.3	CHI3L1 in the Breast and Breast Cancer……...	131
5.3	**Aims of this Chapter…….**	**132**
5.4	**CHI3L1 Stimulation of Breast Cancer Cells……**	**132**
5.4.1	MCF-7……..	133
5.4.2	MDA-MB-231……..	133
5.5	**Discussion……...**	**136**
5.6	**Conclusion……...**	**136**

5.1 Introduction

In Chapter Four, the inflammatory cytokine Chitinase 3 like-1 (CHI3L1) was identified as a cytokine of interest; levels were higher in media of ER^+ and triple negative (TN) breast cancer (BC) peri-tumoural explants, and gene expression was higher in SGBS cells co-cultured with MCF-7 and SGBS cells co-cultured with MDA-MB-231 cells, as compared to SGBS cells grown alone. The role of CHI3L1 in BC is not fully understood and it was therefore selected for further investigation of its effect, if any, on the proliferation of BC, with a view to identifying it as a potential therapeutic target.

5.2 CHI3L1 - An Overview

Produced by many cells including neutrophils, macrophages, fibroblasts, and cancer cells, CHI3L1 (YKL-40) belongs to the 18 glycosyl hydrolase (GH18) gene family (Libreros and Iragavarapu-Charvulu, 2015), and is located on Chromosome 1 (Kzhyshkowska *et al.*, 2016). The GH18 family contains both true chitinases and the chitinase-like proteins (CLPs). Chitinases cleave chitin (absent in mammals) whereas CLPs, although binding chitin, do not split it (Libreros and Iragavarapu-Charvulu, 2015); CHI3L1 has no known enzymatic activity (He *et al.*, 2013). CLPs have properties of both growth factors and cytokines (Lee *et* al., 2009; Shao *et al.*, 2009), although CHI3L1 is difficult to detect in healthy individuals.

5.2.1 Functions of CHI3L1

Members of the GH18 family have been conserved across species and through time and are now known to have important functions in antipathogen responses. CHI3L1 is secreted into the circulation as well as into third spaces (Kzhyshkowska *et al.*, 2016), triggered by an immune response (Yeo *et al.,* 2019). Its actions result in the tolerance of disease *via* the control of cell death, as well as the control of remodelling *via* IL-8 (Prakash *et al.,* 2013) and through binding collagen I, II, and III (Bigg *et al.,* 2006). Also, CHI3L1 has roles in the control of inflammation, ultimately limiting the extent of

tissue injury in the area around an insult (He *et al.*, 2013). It is also known to promote growth of cells of the stroma and increasing the migration effects of endothelial cells (Eurich *et* al., 2009).

The production of CHI3L1 is stimulated by various cytokines such as IL-1β, IL-6, IL-13, and TNF-α, and it is known to be upregulated during the inflammatory process (Libreros and Iragavarapu-Charvulu, 2015). Importantly, in certain disease states including infection and malignancy, CHI3L1 and other members of the GH18 group can become dysregulated, and the extent of this dysregulation often correlates with the severity of the disease (He *et al.*, 2013). In many disease states including acute and chronic non-infectious inflammation, diabetes mellitus, vascular disease, neurodegenerative conditions, and malignancy, CHI3L1 can be used as a diagnostic and prognostic marker (Kzhyshkowska *et al.*, 2016).

Although the exact and complete mechanism of action of CHI3L1 is not yet known, it has been demonstrated that CHI3L1 promotes inflammation by regulating Th2-like (IL-4 and IL-5 mediated) immune reactions (Lee *et al.*, 2009), and activating the MAPK, ERK, PI3K, AKT, and WNT/β-catenin signalling pathways, *via* the IL-13 receptor α2 (IL13Rα2) (Shao, 2009; He *et al.*, 2013; Kzhyshkowska *et al.*, 2016) (Figure 5.1). This receptor, in normal health, is only present in sperm (Okamoto *et al.*, 2019), but in malignancy, a correlation exists between its level of expression and invasiveness and potential for metastasis. This is true for BC (Kawakami *et al.*, 2003).

5.2.2 CHI3L1 in Cancer and in the Tumour Microenvironment

CHI3L1 is produced by several solid cancers including breast, colon, ovarian, prostate, endometrial, glioblastoma, and kidney (Hamilton *et al.,* 2015), as well as non-malignant cells of the TME such as fibroblasts and immune cells. It acts as a growth factor, stimulating proliferation of the malignancy whilst suppressing apoptosis (Eurich *et al.*, 2009; Yeo *et al.*, 2019), as well as stimulating the expression of various macrophage and

Figure 5.1: Chitinase 3-Like 1 in Cancer Progression

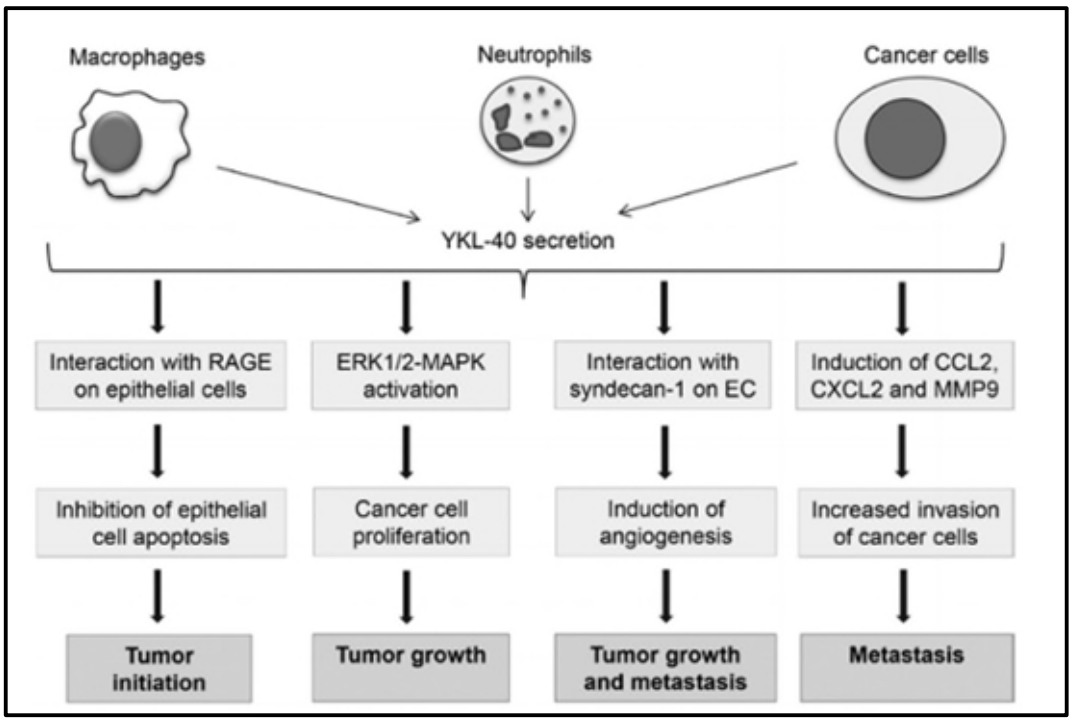

[Reproduced, with permission, from (Kzhyshkowska *et al.*, 2016)]

YKL-40: Chitinase 3-like 1 (CHI3L1). Modes of action of CHI3L1 in promoting tumour growth and progression. EC: endothelial cells.

neutrophil chemoattractants including MCP-1 and IL-8 (Libreros *et al.*, 2013). The role of CHI3L1 has been investigated in various cancers including colon, glioblastoma, and breast. In both colon cancer and glioblastoma, CHI3L1 expression increased the malignancies' proliferation as well as invasion (Kzhyshkowska *et al.*, 2016).

5.2.3 CHI3L1 in the Breast and Breast Cancer

CHI3L1 is expressed by the ductal epithelium of the breast, and levels are markedly raised during involution suggesting it has a strong role in the tissue remodelling and regression seen at the time of weaning (Scully *et* al., 2011; Libreros *et al.,* 2013). CHI3L1 expression has been identified in BC (Roslind *et al.*, 2008); cancer cells themselves, macrophages, and cancer-associated-fibroblasts have been found to secrete it (Libreros *et al.,* 2013; Cohen *et al.*, 2017), stimulating an immunosuppressing but cancer growth promoting environment.

Research has shown that CHI3L1 stimulates breast tumour angiogenesis, perhaps through its expression in smooth muscle cells which influence vascular sprouting and vascular stability (Kzhyshkowska *et al.*, 2016); when CHI3L1 expressing MDA-MB-231 cells were implanted in mice, tumours demonstrated greater vasculature (Shao, 2013). Also, when the animals were implanted with cells with CHI3L1-shRNA, malignancies had lower vessel density and overall angiogenesis (Shao *et al.*, 2009). Direct stimulation of Met-1 (murine) breast cancer cells with a physiologically relevant concentration of CHI3L1 (100 ng/ml) enhanced cell motility and migration but did not influence proliferation, and culture with knockdown of fibroblast CHI3L1 confirmed reduced cell motility (Cohen *et al.*, 2017). Culture of breast Met-1 cells with CHI3L1 resulted in significant upregulation of CCL2, CXCL1, CXCL2, IL-6, MMP-9, and Osteopontin - factors known to increase inflammation and cancer invasion (Cohen *et al.*, 2017). In glioblastoma, CHI3L1 enhanced survival of malignant cells in response to radiotherapy (Francescone *et al.,* 2011); this finding is potentially important in patients with BC as post-operative radiotherapy is a vital component of treatment for many.

Increased plasma CHI3L1 has been associated with increased risk of death from various diseases including cancer (Johansen *et* al., 2010). Many research groups have identified that raised serum or plasma levels of CHI3L1 are correlated with a poorer prognosis and reduced overall survival in many malignancies, including breast, with levels being particularly higher in advanced (including metastatic) disease (Jensen *et al.*, 2003; Shao *et al.*, 2011; Kang *et al.*, 2014).

5.3 Aims of this Chapter

The effect, if any, of directly stimulating MCF-7 and MDA-MB-231 cells with CHI3L1 is unknown. Here, to investigate whether CHI3L1 does or does not have any direct stimulatory action on these BC cell lines, xCELLigence® experiments were conducted.

The aims of this Chapter are to determine the:

1. Effect, if any, on the rate of proliferation of MCF-7 cells when cultured in the presence of CHI3L1, as compared to culturing in CHI3L1-free media
2. Effect, if any, on the rate of proliferation of MDA-MB-231 cells when cultured in the presence of CHI3L1, as compared to culturing in CHI3L1-free media

5.4 CHI3L1 Stimulation of Breast Cancer Cells

MCF-7 and MDA-MB-231 cells were each cultured in three concentrations of CHI3L1, in an xCELLigence® DP proliferation experiment, as previously described (Chapter Two; Section 2.2.8). It has been demonstrated that 100-300 ng/ml of CHI3L1 stimulate ERK and AKT pathways, and 300-500 ng/ml induce β-catenin (He *et al.,* 2013). Media were thus prepared with concentrations of 250 ng/ml, 500 ng/ml, and 750 ng/ml of CHI3L1. Trial co-cultures were undertaken without FBS-containing media for the cancer cell line; where media was FBS-free from the start, MCF-7 and MDA-MB-231 cells failed to attach, and where cells were plated in the presence of serum and left overnight to attach, washed and then cultured in serum-free media,

considerable cell death and detachment occurred over the next 24 h. The xCELLigence® experiments were thus conducted in FBS-containing media throughout (the same FBS batch was used for all experiments so as to maintain uniformity of FBS composition). Experiments were run for 24 h. Any well where the graph morphology suggested sub-optimal growth was excluded, and data were analysed with GraphPad Prism® 8.4.2.

5.4.1 MCF-7

MCF-7 cells cultured in the presence of CHI3L1 demonstrated significantly increased proliferation as compared to MCF-7 cultured in CHI3L1-free media, as analysed by one-way ANOVA (Figure 5.2). Experiments were repeated three times; the increased proliferation was seen in two (representative experiment shown; see Appendix D for full data). Increases were seen at 250 ng/ml and 750 ng/ml concentrations.

5.4.2 MDA-MB-231

MDA-MB-231 cells cultured in the presence of CHI3L1 demonstrated mixed responses with a trend towards increased proliferation when compared to MDA-MB-231 cultured in CHI3L1-free media (Figure 5.3). In view of previous findings here (Chapter Three) where increased proliferation in MDA-MB-231 when co-cultured with mature SGBS occurred later than with MCF-7 cells, this experiment was run for longer. Experiments were repeated three times; no consistency in results was demonstrated despite the longer time (representative experiment shown; see Appendix D for full data) but increases were seen in two of the three repeats. All statistically significant changes seen were for increases in proliferation; no statistically significant CHI3L1-mediated reduction in MDA-MB-231 proliferation was seen.

Figure 5.2: MCF-7 Proliferation when Cultured in the Absence and Presence of Chitinase 3-Like 1

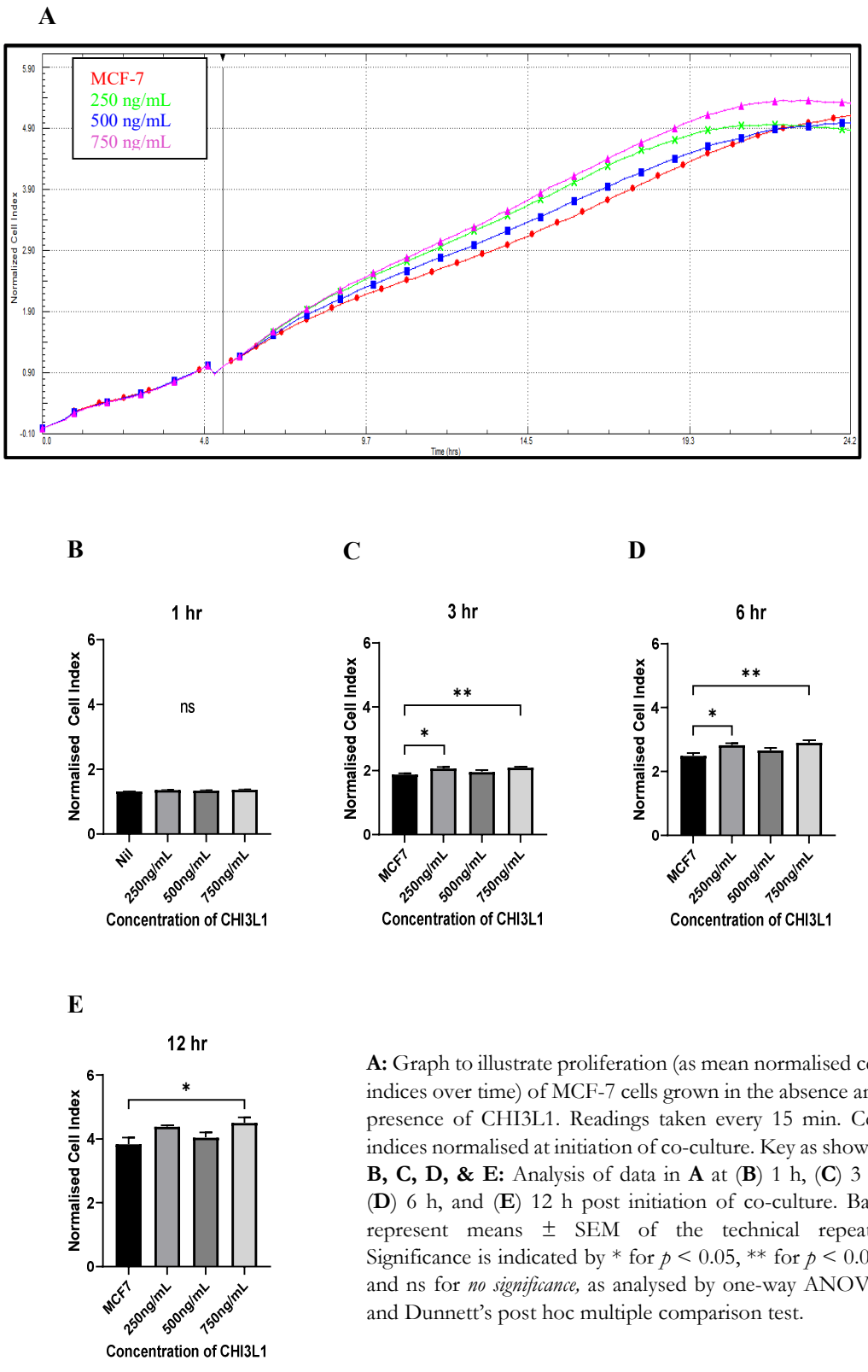

A: Graph to illustrate proliferation (as mean normalised cell indices over time) of MCF-7 cells grown in the absence and presence of CHI3L1. Readings taken every 15 min. Cell indices normalised at initiation of co-culture. Key as shown. **B, C, D, & E:** Analysis of data in **A** at (**B**) 1 h, (**C**) 3 h, (**D**) 6 h, and (**E**) 12 h post initiation of co-culture. Bars represent means ± SEM of the technical repeats. Significance is indicated by * for $p < 0.05$, ** for $p < 0.01$, and ns for *no significance,* as analysed by one-way ANOVA and Dunnett's post hoc multiple comparison test.

Figure 5.3: MDA-MB-231 Proliferation when Cultured in the Absence and Presence of Chitinase 3-Like 1

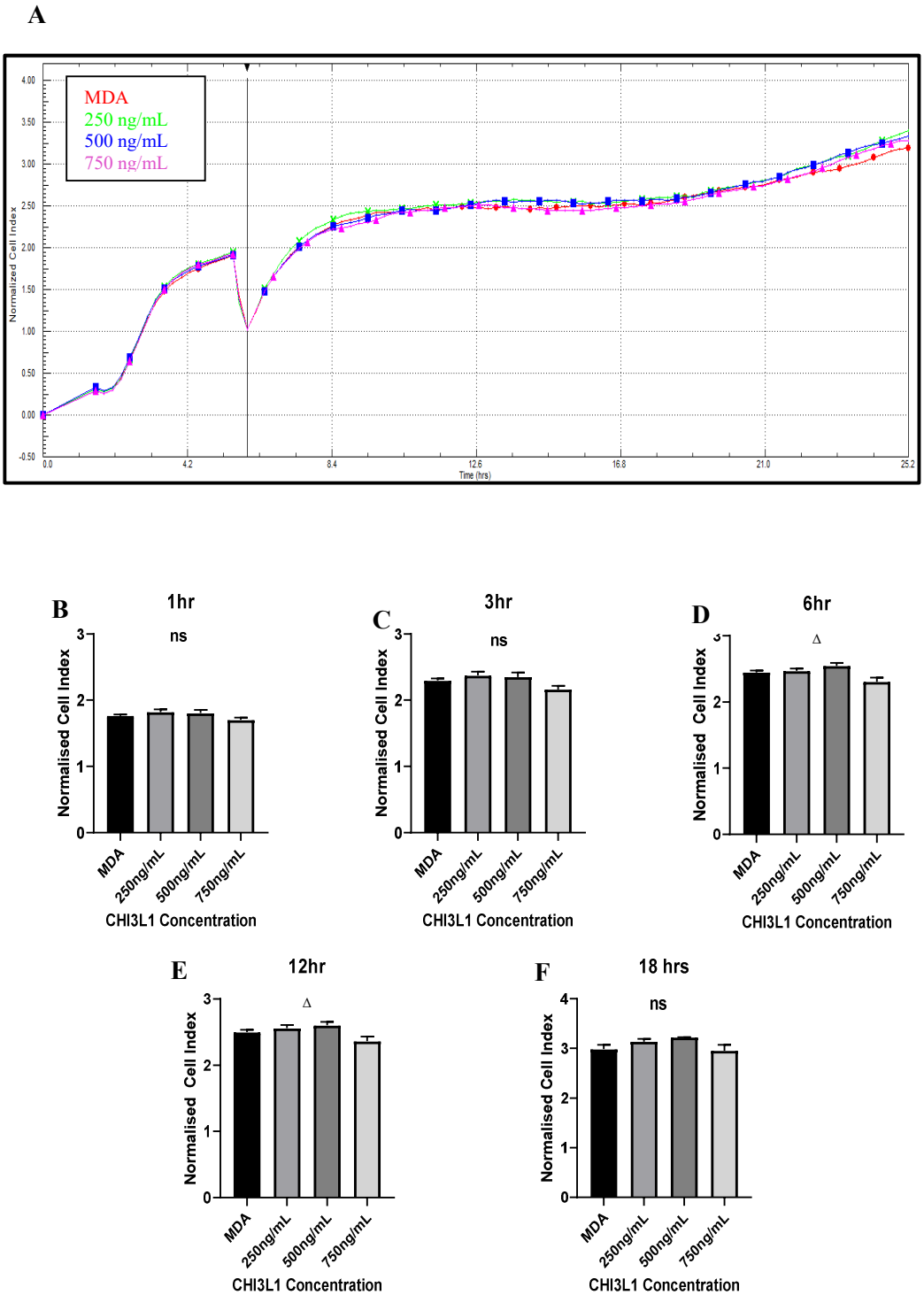

A: Graph to illustrate proliferation (as mean normalised cell indices over time) of MDA-MB-231 ('MDA') cells grown in the absence and presence of CHI3L1. Readings taken every 15 min. Cell indices normalised at initiation of co-culture. Key as shown. **B, C, D, E,** and **F:** Analysis of data in **A** at (**B**) 1 h, (**C**) 3 h, (**D**) 6 h, (**E**) 12 h, and (**F**) 18 h post initiation of co-culture. Bars represent means ± SEM of the technical repeats. Significance is indicated by ns for *no significance*, and Δ for ANOVA significant but Dunnett's not significant, as analysed by one-way ANOVA and Dunnett's post hoc multiple comparison test.

5.5 Discussion

CHI3L1 is a potent pro-inflammatory cytokine seen in many disease states, both benign and malignant. It is known to encourage the angiogenesis, motility, and metastasis of various malignancies and is pro-proliferative in some cancers. The latter effect has not been demonstrated in BC cells thus far. Here, ER^+ MCF-7 cells stimulated with CHI3L1 at concentrations known to activate its signalling pathways resulted in a significant increase in cellular proliferation. Additionally, when the TN cell line MDA-MB-231 was stimulated, an increase in proliferation was also seen. Results for MDA-MB-231 were not as marked or as definitive as for MCF-7, but the only changes demonstrated, where they occurred, were increases in proliferation; no significant decrease in proliferation occurred as a consequence of CHI3L1 stimulation.

The difference in response to CHI3L1 between MCF-7 and MDA-MB-231 is likely a consequence of different mechanisms of action between these two BC cell lines. MDA-MB-231 cells do not express IL-13 receptor α2, whereas MCF-7 cells do (Kawakami *et al.*, 2003). Presently, IL-13 receptor α2 is the only recognised receptor for CHI3L1 and thus the effects seen on MDA-MB-231 cells must be mediated via a different, as of yet unidentified, route. It may be that the concentrations of CHI3L1 selected were incompletely or intermittently stimulating this unknown pathway. More research is required to further investigate, firstly, the influence of CHI3LI on MDA-MB-231 cells and, secondly, the mechanism underlying this influence.

5.6 Conclusion

CHI3L1 stimulation of MCF-7 and MDA-MB-231 cells resulted in an increase in cellular proliferation of both, although this was statistically significant only in the former. It has known roles in angiogenesis of tumours and the results obtained here indicate that it also has activity directly stimulating cells to proliferate.

CHAPTER SIX

Discussion

Chapter Six: Discussion

Contents

6.1 General Discussion……... 139

6.1.1 General Comments: Proliferation of ER^+ and Triple Negative Breast Cancer Cell Lines in the Presence and Absence of Pre-Differentiated and Mature SGBS Adipocytes…… 140

6.1.2 General Comments: The Influence of ER^+ and Triple Negative Breast Cancer on Adipose Tissue and Adipocyte Cytokine Secretion…….. 141

6.1.3 General Comments: CHI3L1 Stimulation of MCF-7 and MDA-MB-231 Cells……. 143

6.2 Conclusion……. 144

6.3 Future Work……... 145

6.4 Clinical Implications……. 145

Chapter Six: Discussion

6.1 General Discussion

Breast cancer (BC) is the commonest female malignancy worldwide (World Health Organisation, 2020) and, with an increasing incidence (Dixon and Barber, 2019), poses a significant disease burden on individuals and health economies. After the advent of the National Health Service's Breast Screening Programme, outcomes in BC improved (Public Health England, 2019). This was due in the main to detection and treatment of malignancy at an earlier stage. The increased awareness in the population also contributed to the benefit seen. Although overall 10-year survival from BC is good at more than 75%, there remains room for improvement. Survival is not uniform across the BC sub-types; $ER^+/HER2^-$ is the most commonly diagnosed BC and carries a better prognosis than the less common but much more aggressive $ER^-/PR^-/HER2^-$ (triple negative [TN]) type. Considerable differences exist in the biology of these diseases, and it is widely accepted that BC is a heterogenous malignancy with great variation seen in the different sub-types. More work is still needed to improve understanding of BC and the differences between sub-types so that treatment, and thus outcomes, particularly for the higher risk sub-types, can be improved.

Over recent years, the tissue that sits around a cancer - the tumour microenvironment (TME) - has become an important focus of research. In many cancers, the tissue immediately around a tumour has been shown to differ from tissue distant to the disease (Balkwill *et al.,* 2012). It is accepted that cancers recruit non-malignant cells to the TME and alter the behaviour of these benign cells as well as the behaviour of locally resident non-cancerous cells, to promote tumour growth and spread. This recruitment is a complex process, requiring multi-directional communication between many different cell types.

Neglected as an important member of the TME in initial research, more attention is now being paid to adipocytes. Historically considered an inert tissue of lipid storage and insultation only, adipose tissue (AT) has been demonstrated to be incredibly dynamic (Schedin and Hovey, 2010). In the healthy state, AT has a wide-ranging role

in homeostasis, and in disease considerable change is seen. In obesity, where substantial work has been undertaken investigating the change in AT, increased numbers of hypertrophic adipocytes cause hypoxia which leads to the activation of pro-inflammatory signalling pathways along with recruitment of cells of the immune system, further compounding the issue of local hypoxia and inflammation (Lee *et al.*, 2014; Matthews and Thompson, 2016). Inflammation has been identified as a key enabler and cause of adipocyte dysfunction, with morphological change seen in cells and abnormal adipokine secretion occurring as a result. Many of the features seen in obesity mediated AT inflammation are also seen in the TME, as triggered by the malignancy.

Although much is now known about adipocytes and BC progression, the exact mechanisms by which adipocytes exert their influence are still not yet fully understood (Park *et al.,* 2020). With outcomes still poor in some sub-types of BC, and worse outcomes observed in obese patients (Protani *et al.,* 2010; Yao-Borengasser *et al.,* 2015), and because of the intimate relationship between adipocytes and BC, better understanding the action of adipocytes in the TME may be the key to improving treatment and outcome. This research aimed to further the knowledge and understanding of the role of adipocytes in the BC TME and the primary aim was to find a potential novel cytokine target for treatment.

6.1.1 General Comments: Proliferation of ER^+ and Triple Negative Breast Cancer Cell Lines in the Presence and Absence of Pre-Differentiated and Mature SGBS Adipocytes

Following optimisation experiments, the adipocyte cell strain SGBS was co-cultured in its pre-differentiated and mature forms with the ER^+ cell line MCF-7 and the TN cell line MDA-MB-231, in the xCELLigence® DP system (Chapter Three). This system assesses cellular proliferation *via* measurement of the changes in electrical impedance caused by changing numbers of cells seeded in plates embedded with sensory electrodes.

The co-culture experiments demonstrated that both pre-differentiated and mature SGBS adipocytes increase the proliferation of MCF-7 cells. Interestingly, in experiments with MDA-MB-231, proliferation was *reduced* by pre-differentiated SGBS adipocytes, but stimulated by mature SGBS adipocytes. Work by Park *et al.* (2020) demonstrated that treatment of MCF-7 and MDA-MB-231 cells with conditioned media from 3T3-L1 (murine) adipocytes and differentiated human adipose derived mesenchymal stem cell cultures increased proliferation of the BC cells via the PI3K/AKT/mTOR pathway. It is possible that (some of) the effects seen here in MCF-7 cells were mediated by activation of the same pathway. The reduced rate of proliferation of MDA-MB-231 cells caused by co-culture with pre-differentiated SGBS is a novel finding and requires further investigation, analysing the cytokine secretion profile of these cells and their interaction with the MDA-MB-231 cell line. Gene expression analyses conducted in this research demonstrated differences in pre-differentiated and mature adipocytes (Chapter Four). Investigating these (and other similar) findings further may provide further information about this inhibitory mechanism.

6.1.2 General Comments: The Influence of ER^+ and Triple Negative Breast Cancer on Adipose Tissue and Adipocyte Cytokine Secretion

To investigate how their secretion changed in the TME, cytokine levels were analysed; fresh human breast tissue (peri-tumoural [PT] and resection margin [RM]) samples from nine patients were cultured for 24 h and the resulting cytokine containing media were analysed with the Proteome Profiler™ Human XL Cytokine Array Kit (Chapter Four). The presence of 105 cytokines was compared across peri-tumoural and resection margin tissue samples.

Six specimens from patients with $ER^+/HER2^-$ disease demonstrated multiple changes in many cytokines, and whole group analyses revealed an increase in CHI3L1 and MMP-9. Specimens from three patients with TN disease were also analysed. These revealed a greater number of cytokines increased in the PT media samples (18) as compared to that in ER^+ samples, and fewer cytokine levels remaining the same across

paired RM-PT specimens. CHI3L1 and MMP-9 were amongst the cytokines increased. These experiments demonstrated the greater effects of TN BC on its surrounding tissue. It also demonstrated the persistence of those effects when AT was no longer in close proximity to cancer - cytokine secretion did not return to normal (where normal is defined as levels seen in distant tissue) despite the cancer no longer being present. This supports the recognised concept of cancer-promoting phenotypic alterations in adipocytes.

Breast tissue explants used for the cytokine analysis consisted of AT which is formed of a mixed population of cell types. Previous studies investigating adipokine secretion in AT have revealed a considerable proportion to be of non-adipocyte origin (Fain *et al.*, 2004). To further investigate the specific role of adipocytes, media from SGBS cells co-cultured with MCF-7 cells were analysed using the Proteome Profiler™ Human XL Cytokine Array. 25 cytokines were increased across the three technical repeats and no cytokine was unchanged. The remaining 80 of the 105 cytokines assessed demonstrated either a mixed pattern or were found in lower concentrations in media from the SGBS Co sample as compared to the SGBS Alone sample.

Data were interrogated, and the literature reviewed. To assess changes in gene expression profiles of SGBS cells grown alone and in co-culture with BC cell lines, the genes encoding cytokines CHI3L1/YKL-40 (gene *CHI3L1*), IL-8 (gene *CXCL8*), Osteopontin (gene *SPP1*), Cystatin C (gene *CST3*), MCP-1 (gene *CCL2*), ST2 (gene *IL1RL*), and ENA-78 (gene *CXCL5*) were selected.

First, a time course of gene expression for pre-differentiated and maturing SGBS cells was performed. This confirmed gene expression, and also revealed that *CCL2* and *CXCL5* gene expression was higher in pre-differentiated cells, as compared to mature SGBS. This gave a small insight into genetic differences between pre-differentiated and mature adipocytes, although greater work is required to further analyse the differences seen and their implications, as well as investigation of a greater number of genes.

Next, SGBS Co and SGBS Alone gene expression was analysed. In SGBS cells co-cultured with MCF-7 cells, there was a statistically significant upregulation of the *CHI3L1* gene. In SGBS cells co-cultured with MDA-MB-231 cells, there were statistically significant increases in *CHI3L1*, *CXCL8*, *CCL2*, and *CXCL5* gene expression. Interestingly, from the Proteome Array work, CHI3L1 cytokine levels were lower in SGBS Co media when compared to SGBS Alone (log_2 fold change -0.057). This was an unexpected finding and further work is necessary here. It is possible that alterations in translation, majority secretion from non-adipocyte cells, or altered secretion from adipocytes could explain this. In explant tissue, adipocytes were likely involved in a complex interplay between different cells that stimulated secretion of cytokines including CHI3L1. When cultured as a single cell population, it is possible that this complex interplay was altered, and thus this result seen. This finding highlights that although adipokines in the TME have become a recent focus of research, and there is considerable knowledge about some, much remains unknown about their influence and role in the changing dynamic of the TME.

Previous studies have demonstrated that malignancy induces change in adipokine secretion from adipocytes co-cultured with BC cell lines (Manabe *et al.*, 2003; Dirat *et al.* 2011; Lee *et al.*, 2017), and this change promotes the cancer's own growth and progression. The research here has added to this existing knowledge base, identifying potential cytokines for further research, and identifying differences between pre-differentiated and mature adipocytes, but much more work is required to further understand the role of the adipocyte in the TME.

6.1.3 General Comments: CHI3L1 Stimulation of MCF-7 and MDA-MB-231 Cells

CHI3L1 was identified as a recurrently featuring cytokine; levels were increased in the media of ER^+ explant cultures and TN BC explant cultures (and one of only two cytokines common to both), and gene expression was elevated in both SGBS Co (MCF-7) and SGBS Co (MDA-MB-231). The influence, if any, of direct stimulation of MCF-7 and MDA-MB-231 cells with CHI3L1 was thus investigated (Chapter Five).

Concentrations of CHI3L1 known to activate signalling pathways were used to stimulate the cells whilst xCELLigence® DP experiments were conducted to assess proliferation. These showed that CHI3L1 treatment of MCF-7 cells resulted in a significant increase in cell proliferation. Treatment of MDA-MB-231 yielded mixed results, with a trend towards increased proliferation, but further investigation is required to determine the exact influence of CHI3L1 on TN cells.

The mechanism of action of CHI3L1 remains unclear. Its only recognised receptor is IL13Rα2 (He *et al.,* 2013) and this receptor is not found in MDA-MB-231 cells (Kawakami *et al.*, 2003). The influence exerted on these cells is thus via a currently unknown mechanism. When Kawakami *et al.* (2003) transfected (mouse) breast tumours with IL13Rα2, they found that targeted IL-13 cytoxin treatment had a profound growth arresting effect on the cancers. The CHI3L1 / IL-33 / IL13Rα2 is thus a potentially important pathway in BC and warrants further analysis.

6.2 Conclusion

This research, conducted within the limits of 2D culturing of single cell populations, has shown that adipocytes influence the behaviour of ER^+ and TN BC cells; in ER^+ cancer cells, proliferation is increased, whereas in MDA-MB-231 cells it is increased by mature SGBS cells and decreased by pre-differentiated SGBS cells, when grown in co-culture - the latter is a novel finding. Interaction between adipocytes and cancer cells results in persisting changes even when the non-malignant tissue / cell is away from the immediate relationship of the cancer, as seen and evidenced by altered cytokine secretion between resection margin / SGBS Alone and peri-tumoural / SGBS Co samples. Marked differences are seen between the changes induced in ER^+ and TN BC. TN BC exposure appears to result in a greater shift to elevation of cytokines whereas ER^+ malignancies result in comparatively less increase, with an overall decrease. CHI3L1 is a cytokine which featured recurrently and has now been demonstrated to be a direct stimulant of ER^+ MCF-7 BC cells. This is another novel finding. It may also have stimulatory effects on MDA-MB-231 cells, but further work is required.

6.3 Future Work

The multiple interactions in the cancer TME are complex, and fuller interrogation of cellular relationships of this complicated network of cells and structural proteins requires more complex model systems. More research is now being conducted utilising 3D models simulating the structure of real tumours, and with mixed cell populations including mesenchymal stem cells. The present study has highlighted interesting initial findings - the inhibitory effects of pre-differentiated SGBS adipocytes on TN BC cells, the cytokines identified as altered in the media of PT explant tissue and SGBS Co cultures, the changes in gene expression seen in adipocytes co-cultured with cancer cells, and finally the stimulatory effects of CHI3L1 on ER^+ (and possibly TN) BC cells. Further work is required to investigate these findings in more complex systems which better model the TME so that understanding and treatment of BC can be further improved; the stimulatory effect of CHI3L1 identified here warrants further investigation as a potential new therapeutic target.

6.4 Clinical Implications

It is known that, in addition to influencing cancer growth, invasion, and metastasis, cancer-associated adipocytes increase resistance to radio- and chemotherapy (Dirat *et al.*, 2011). Also, the rate of BC recurrence is higher in patients with higher body mass index (BMI), as compared to leaner patients (Lee *et al.,* 2017). There is therefore a clear need to continue research such as that conducted here to better understand the role of adipocytes in BC.

In clinical practice, there is already a move towards greater individualised patient care. The genetics of a BC are analysed in select populations of patients to determine the potential benefit of adjuvant chemotherapy, for example. Further investigation of the findings here may allow greater patient-specific treatments to be generated, based on potentially cancer promoting cytokine aberrations in the TME. This would be particularly important for those patients who do not undergo surgical treatment; for example, those not medically fit for a general anaesthetic. In these patients, as the

cancer remains *in situ*, it continues to drive abnormal cytokine secretion encouraging its own growth. For medically unfit patients with ER^+ BC, hormone therapy may be prescribed. For those with ER^- disease, options are very limited. If patients are unfit for a general anaesthetic, they are unlikely to be fit for chemotherapy. In this patient sub-population therefore, knowledge of cancer promoting factors in the TME could reveal targets for treatment to slow cancer progression, and further work looking at the inhibitory effects of pre-differentiated adipocytes seen here could also be useful.

Studies looking at the behaviour of peri-tumoural tissue which remains *in situ* in patients who have breast conserving surgery followed by radiotherapy are required. This study has demonstrated, in keeping with previous knowledge (Hu and Polyak, 2008), that changes in peri-tumoural tissue / SGBS Co cells persist after the cancer cells (the drivers of aberration) are no longer present. Further work investigating the duration of this persistence could yield clinically important information about the safety of tissue left behind after resection. When a breast conserving operation is performed (wide local excision / "lumpectomy"), the requirement is that tumour cells are microscopically at least (*only*) 1 mm away from the edge of the specimen removed. This results in tissue with altered cytokine secretion (as demonstrated here - all PT specimens were >1 mm from the tumour) remaining *in situ*. Despite radiotherapy, recurrence rates of cancer in patients who have breast conserving surgery are up to 15% (Braunstein *et al.,* 2017). It may be that residual recruited adipocytes with persisting abnormal behaviour, confounded by the insult and inflammatory response to radiotherapy, contribute to this recurrence rate.

Finally, this research has identified CHI3L1 to be a cytokine of interest in the BC TME. The rate of proliferation of ER^+, and possibly TN, BC cells is increased when stimulated with the cytokine. BC cells MCF-7 cells express its only known receptor IL13Rα2, whereas MDA-MB-231 cells do not, indicating an unknown mechanism of action in the latter cells. When IL-13 cytotoxic treatment was applied to breast tumours, tumour growth was markedly reduced (Kawakami *et al.*, 2003). Inhibiting IL13Rα2 stimulation through IL-13 and CHI3L1 antagonism could therefore yield therapeutic benefit and this could be of particular interest in the treatment of the more aggressive TN sub-type of BC where medical treatment options are limited.

APPENDIX A

SGBS – Cancer Co-Culture Proliferation

Additional Data

MCF-7 Proliferation when Co-Cultured with Pre-Differentiated SGBS (Additional Data 1)

A

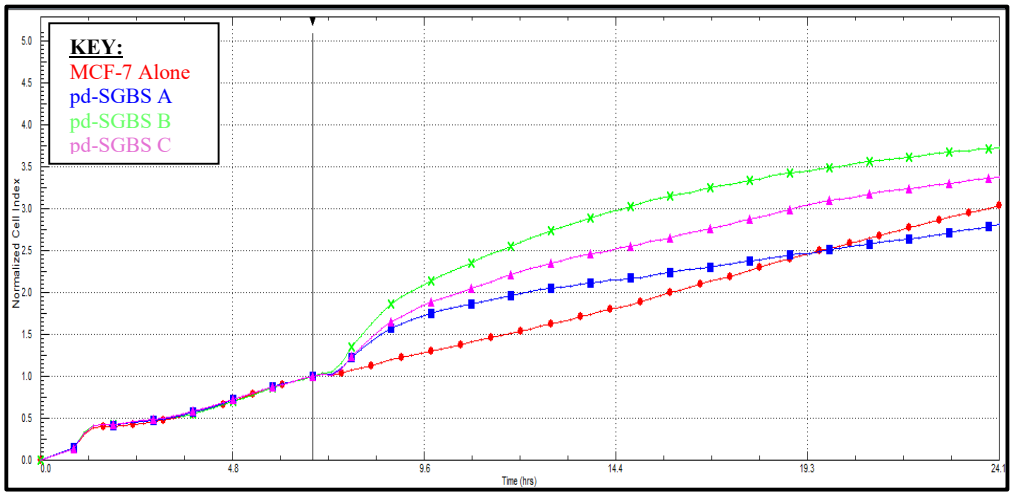

B

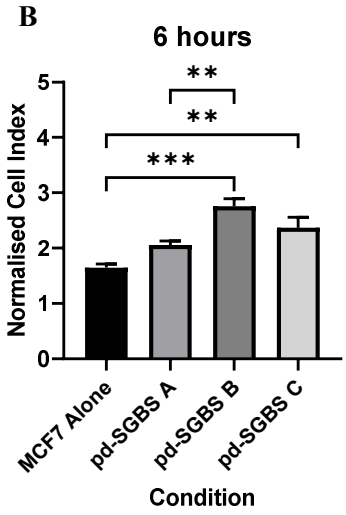

C

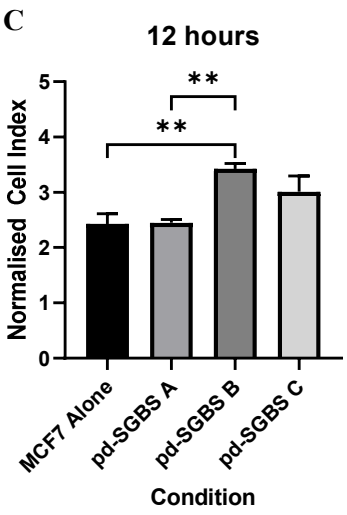

A: Graph to illustrate proliferation (as mean normalised cell indices over time) for MCF-7 cells grown in the absence and presence of pd-SGBS cells. Readings taken every 15 min. Cell indices normalised at initiation of co-culture. Key as shown; pd-SGBS A: 25 000 cells/well, pd-SGBS B: 31 250 cells/well, pd-SGBS C: 41 750 cells/well. **B & C:** Analysis of data in **A** at (**B**) 6 h and (**C**) 12 h post initiation of co-culture. Bars represent means ± SEM of the technical repeats. Significance is indicated by ** for $p < 0.01$, and *** for $p < 0.001$, as analysed by one-way ANOVA and Tukey's post hoc multiple comparison test.

MCF-7 Proliferation when Co-Cultured with Pre-Differentiated SGBS (Additional Data 2)

A

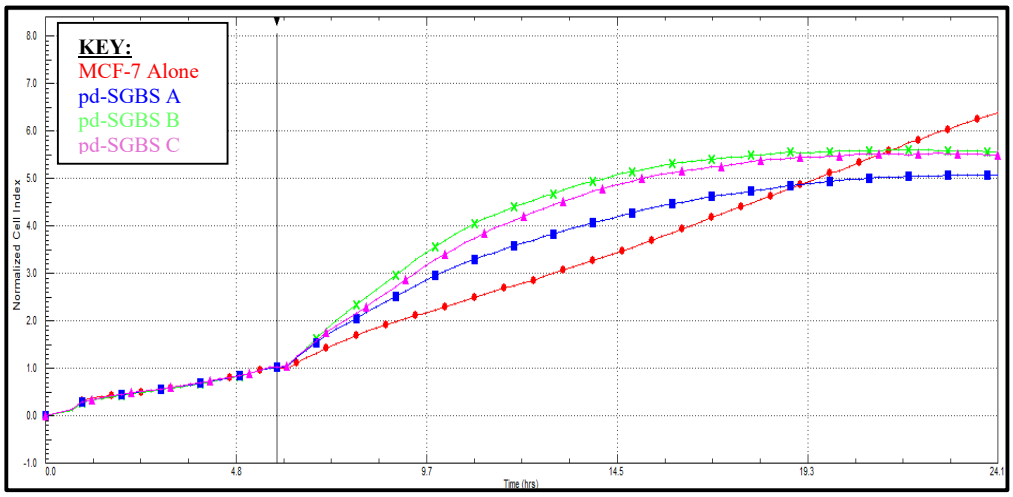

B

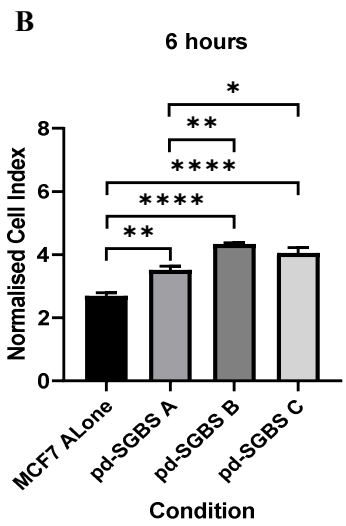

C

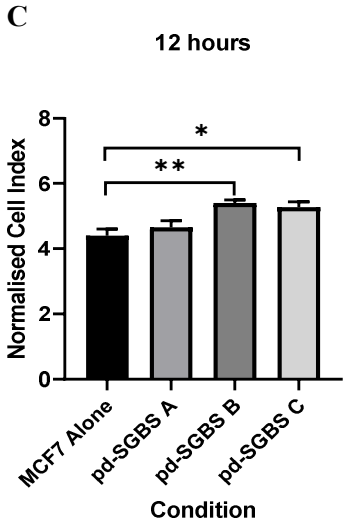

A: Graph to illustrate proliferation (as mean normalised cell indices over time) for MCF-7 cells grown in the absence and presence of pd-SGBS cells. Readings taken every 15 min. Cell indices normalised at initiation of co-culture. Key as shown; pd-SGBS A: 25 000 cells/well, pd-SGBS B: 31 250 cells/well, pd-SGBS C: 41 750 cells/well. **B & C:** Analysis of data in **A** at (**B**) 6 h and (**C**) 12 h post initiation of co-culture. Bars represent means ± SEM of the technical repeats. Significance is indicated by * for $p < 0.05$, ** for $p < 0.01$, and **** for $p < 0.0001$, as analysed by one-way ANOVA and Tukey's post hoc multiple comparison test.

MCF-7 Proliferation when Co-Cultured with Mature SGBS (Additional Data 1)

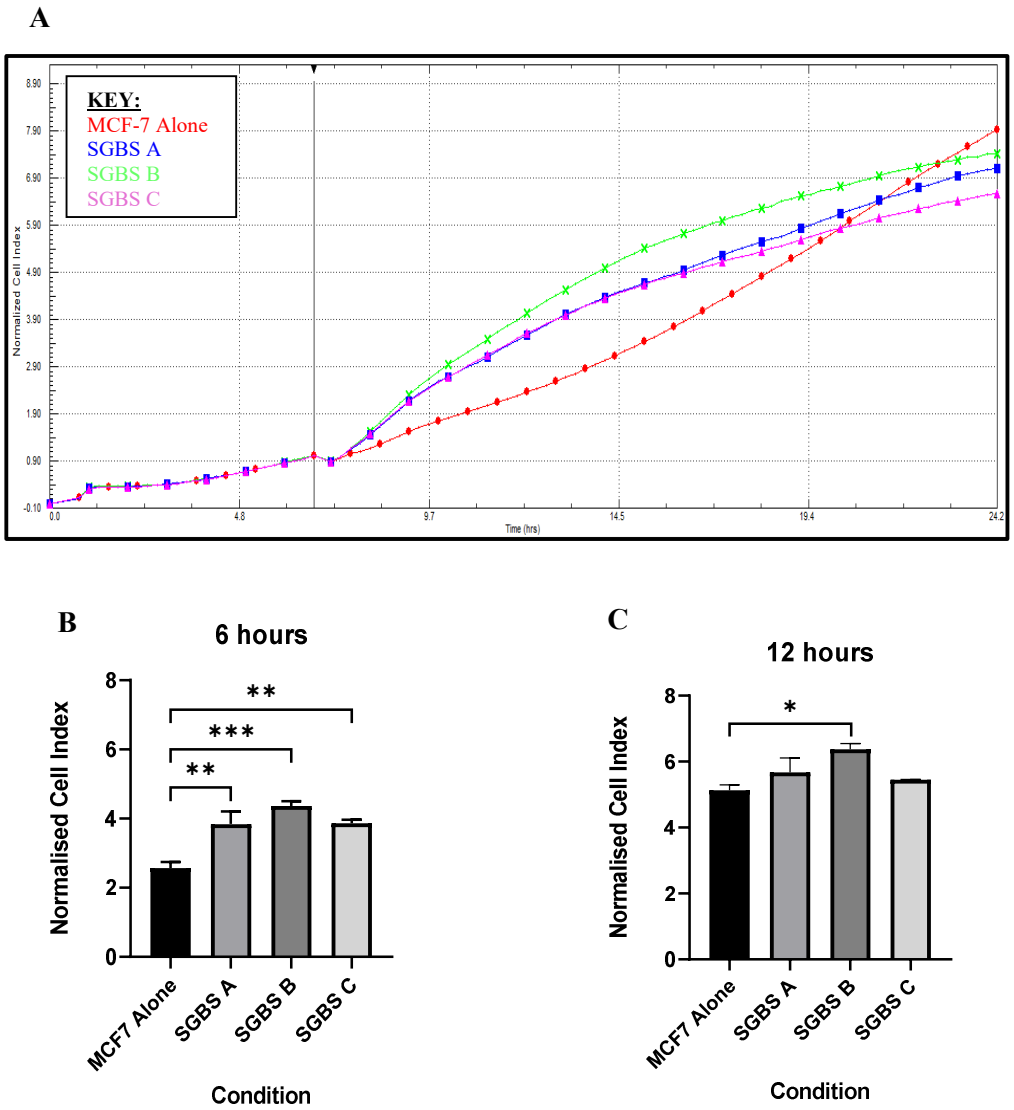

A: Graph to illustrate proliferation (as mean normalised cell indices over time) for MCF-7 cells grown in the absence and presence of SGBS cells. Readings taken every 15 min. Cell indices normalised at initiation of co-culture. Key as shown; SGBS A: 25 000 cells/well, SGBS B: 31 250 cells/well, SGBS C: 41 750 cells/well. **B & C:** Analysis of data in **A** at (**B**) 6 h and (**C**) 12 h post initiation of co-culture. Bars represent means ± SEM of the technical repeats. Significance is indicated by * for $p < 0.05$, ** for $p < 0.01$, and *** for $p < 0.001$, as analysed by one-way ANOVA and Tukey's post hoc multiple comparison test.

MCF-7 Proliferation when Co-Cultured with Mature SGBS (Additional Data 2)

A

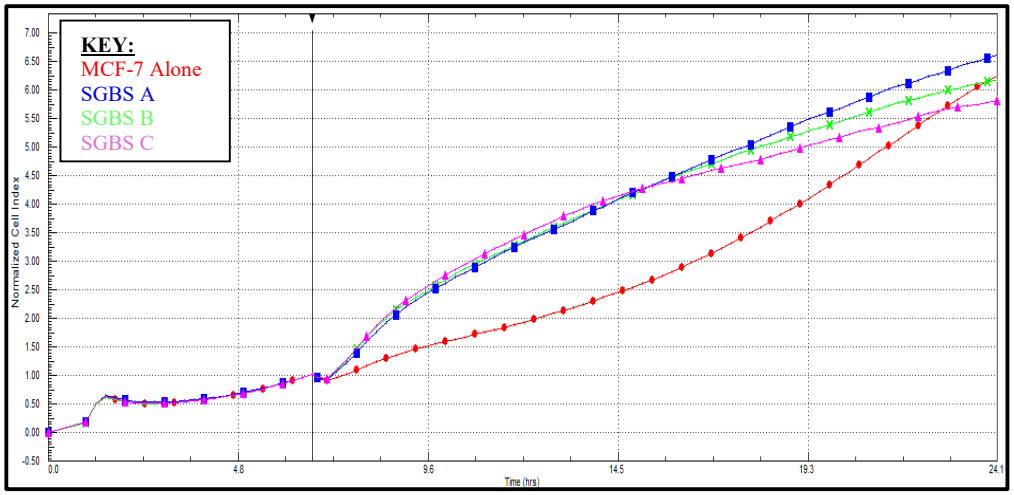

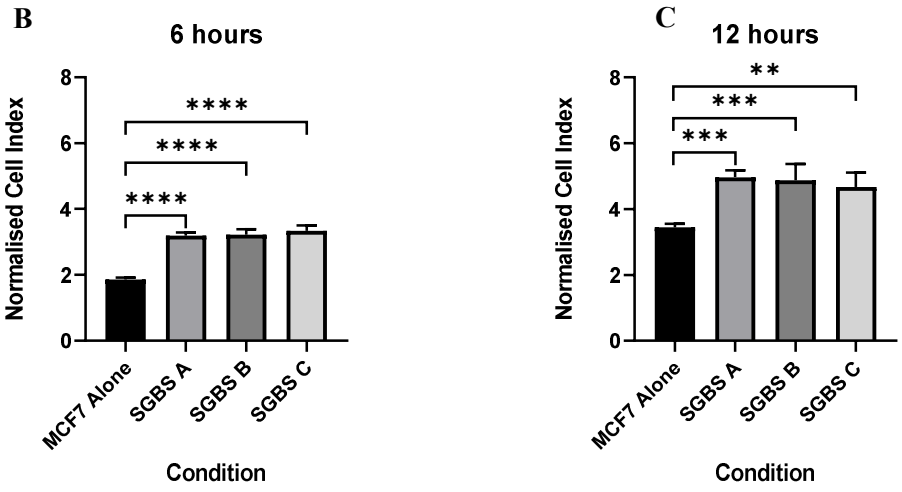

A: Graph to illustrate proliferation (as mean normalised cell indices over time) for MCF-7 cells grown in the absence and presence of SGBS cells. Readings taken every 15 min. Cell indices normalised at initiation of co-culture. Key as shown; SGBS A: 25 000 cells/well, SGBS B: 31 250 cells/well, SGBS C: 41 750 cells/well. **B & C:** Analysis of data in **A** at (**B**) 6 h and (**C**) 12 h post initiation of co-culture. Bars represent means ± SEM of the technical repeats. Significance is indicated by ** for p <0.01, *** for $p < 0.001$, and **** $p < 0.0001$, as analysed by one-way ANOVA and Tukey's post hoc multiple comparison test.

MDA-MB-231 Proliferation when Co-Cultured with Pre-Differentiated SGBS (Additional Data 1)

A

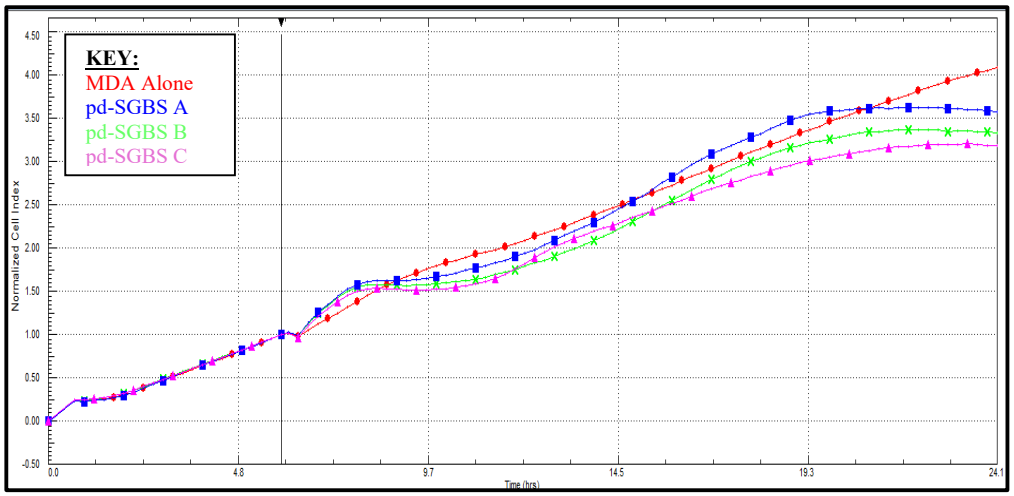

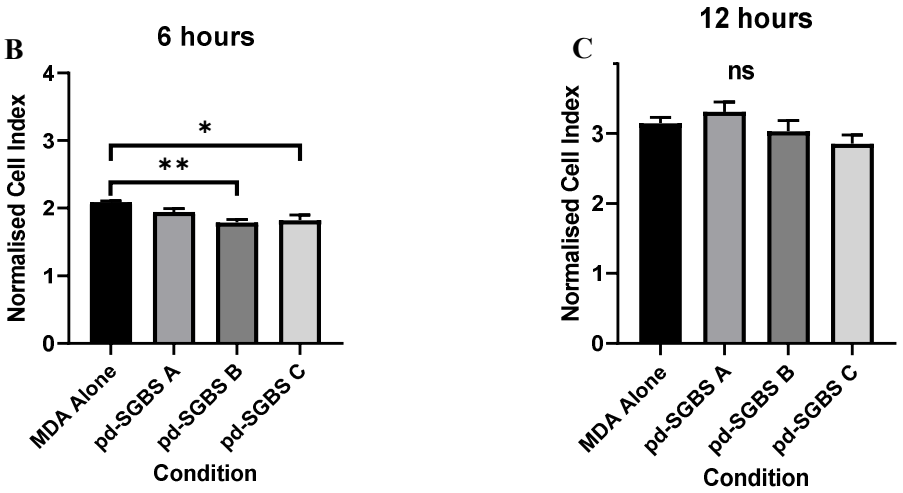

A: Graph to illustrate proliferation (as mean normalised cell indices over time) for MDA-MB-231 (MDA) cells grown in the absence and presence of pd-SGBS cells. Readings taken every 15 min. Cell indices normalised at initiation of co-culture. Key as shown; pd-SGBS A: 25 000 cells/well, pd-SGBS B: 31 250 cells/well, pd-SGBS C: 41 750 cells/well. **B & C:** Analysis of data in **A** at (**B**) 6 h and (**C**) 12 h post initiation of co-culture. Bars represent means ± SEM of the technical repeats. Significance is indicated by ns for *no significance*, * for $p < 0.05$, and ** for $p < 0.01$, as analysed by one-way ANOVA and Tukey's post hoc multiple comparison test.

MDA-MB-231 Proliferation when Co-Cultured with Pre-Differentiated SGBS (Additional Data 2)

A

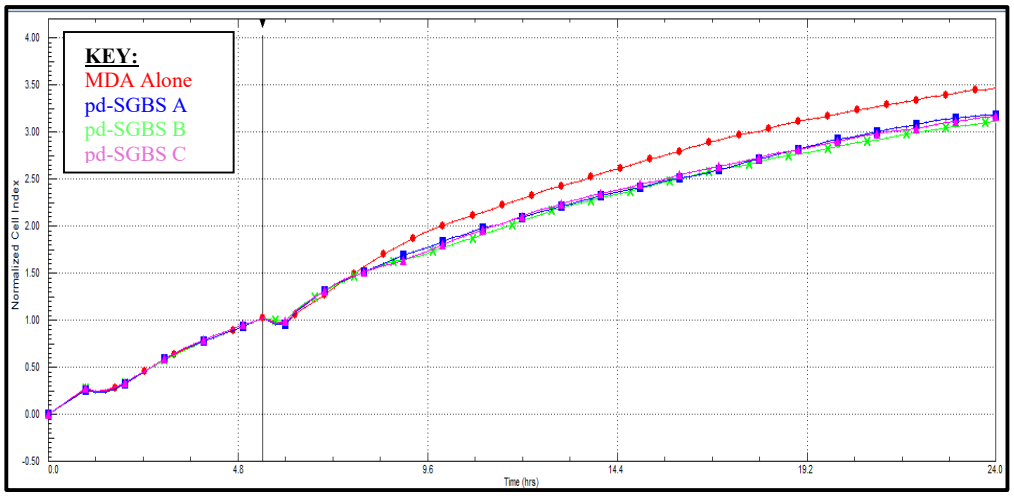

B

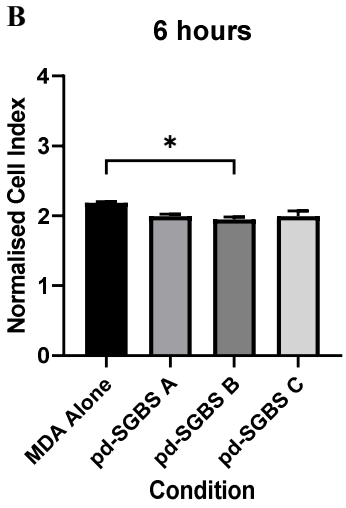

C

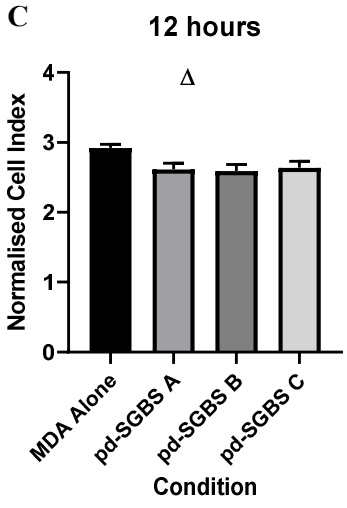

A: Graph to illustrate proliferation (as mean normalised cell indices over time) for MDA-MB-231 (MDA) cells grown in the absence and presence of pd-SGBS cells. Readings taken every 15 min. Cell indices normalised at initiation of co-culture. Key as shown; pd-SGBS A: 25 000 cells/well, pd-SGBS B: 31 250 cells/well, pd-SGBS C: 41 750 cells/well. **B & C:** Analysis of data in **A** at (**B**) 6 h and (**C**) 12 h post initiation of co-culture. Bars represent means ± SEM of the technical repeats. Significance is indicated by * for $p < 0.05$, and Δ ANOVA $p < 0.05$ but Tukey's post hoc multiple comparison test not significant, as analysed by one-way ANOVA and Tukey's post hoc multiple comparison test.

MDA-MB-231 Proliferation when Co-Cultured with Mature SGBS (Additional Date 1)

A

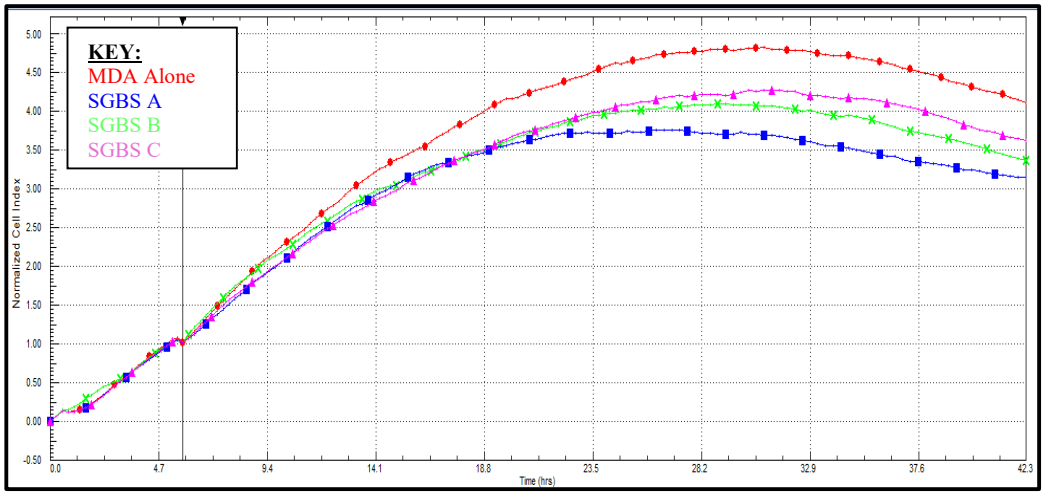

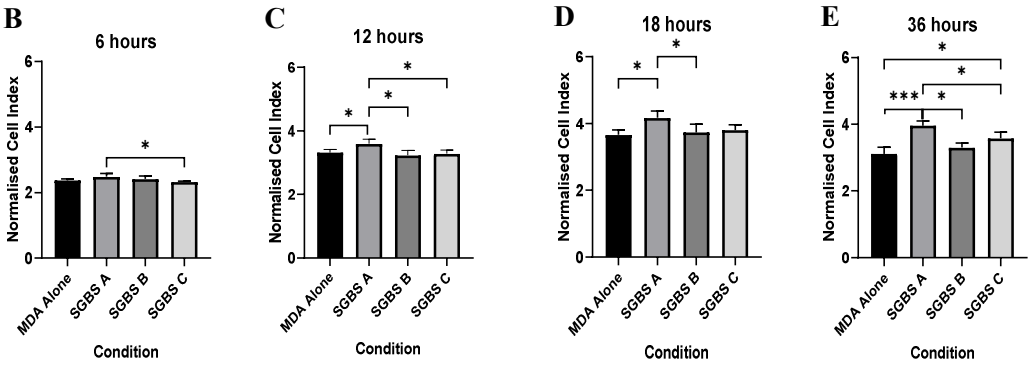

A: Graph to illustrate proliferation (as mean normalised cell indices over time) for MDA-MB-231 (MDA) cells grown in the absence and presence of SGBS cells. Readings taken every 15 min. Cell indices normalised at initiation of co-culture. Key as shown; SGBS A: 25 000 cells/well, SGBS B: 31 250 cells/well, SGBS C: 41 750 cells/well. **B, C, D, & E:** Analysis of data in **A** at (**B**) 6 h, (**C**) 12 h, (**D**) 18 h, and (**E**) 36 h post initiation of co-culture. Bars represent means ± SEM of the technical repeats. Significance is indicated by * for $p < 0.05$, and *** for $p < 0.001$, as analysed by one-way ANOVA and Tukey's post hoc multiple comparison test.

MDA-MB-231 Proliferation when Co-Cultured with Mature SGBS (Additional Data 2)

A

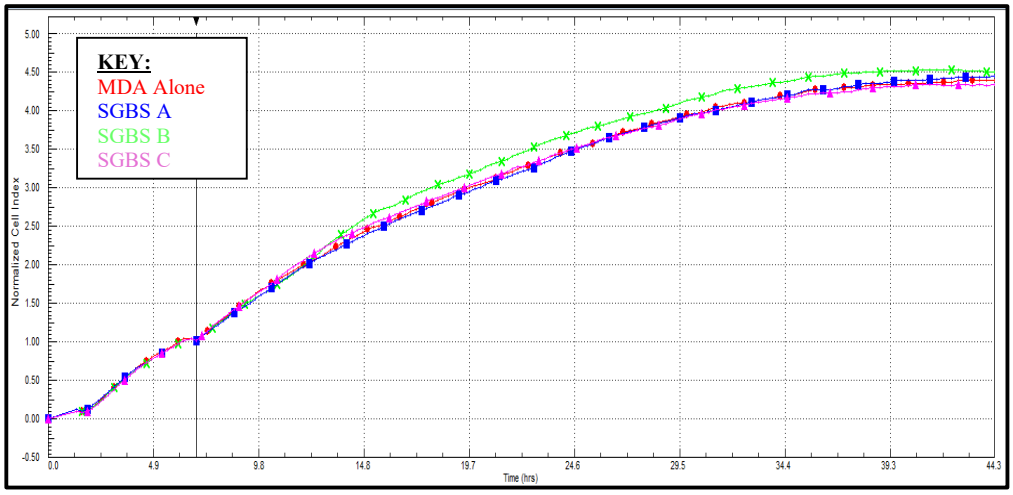

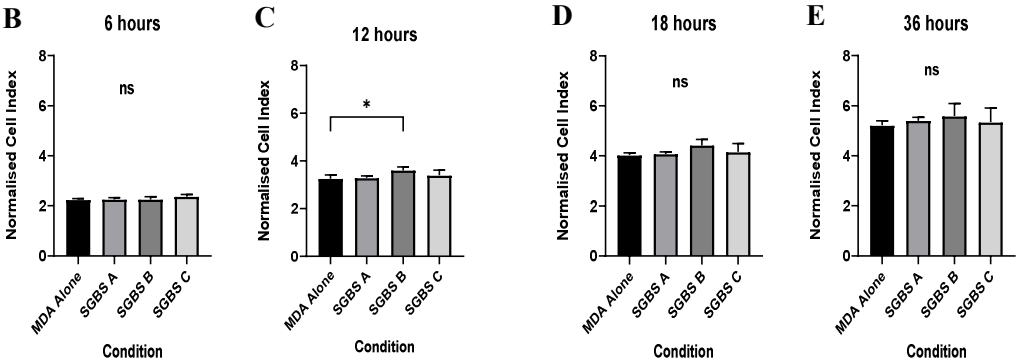

A: Graph to illustrate proliferation (as mean normalised cell indices over time) for MDA-MB-231 (MDA) cells grown in the absence and presence of SGBS cells. Readings taken every 15 min. Cell indices normalised at initiation of co-culture. Key as shown; SGBS A: 25 000 cells/well, SGBS B: 31 250 cells/well, SGBS C: 41 750 cells/well. **B, C, D & E:** Analysis of data in **A** at (**B**) 6 h, (**C**) 12 h, (**D**) 18 h, and (**E**) 36 h post initiation of co-culture. Bars represent means ± SEM of the technical repeats. Significance is indicated by ns for *no significance*, and * for $p < 0.05$, as analysed by one-way ANOVA and Tukey's post hoc multiple comparison test.

APPENDIX B

Proteome Profiler™ Human XL Cytokines

The Proteome Profiler™ Human XL Cytokine Array Kit (R&D Systems, Abingdon, United Kingdom) allows for the simultaneous assessment of 105 cytokines, chemokines, growth factors, and acute phase proteins:

Adiponectin/Acrp30	IFN-gamma	CCL2/MCP-1
Angiogenin	IGFBP-2	CCL7/MCP-3
Angiopoietin-1	IGFBP-3	M-CSF
Angiopoietin-2	IL-1 alpha/IL-1F1	MIF
Apolipoprotein A1	IL-1 beta/IL-1F2	CXCL9/MIG
BAFF/BLyS/TNFSF13B	IL-1ra/IL-1F3	CCL3/CCL4 MIP-1 alpha/beta
BDNF	IL-2	CCL20/MIP-3 alpha
CD14	IL-3	CCL19/MIP-3 beta
CD30	IL-4	MMP-9
CD31/PECAM-1	IL-5	Myeloperoxidase

CD40 Ligand/TNFSF5	IL-6	Osteopontin (OPN)
Chitinase 3-like	IL-8	PDGF-AA
Complement Component C5/C5a	IL-10	PDGF-AB/BB
Complement Factor D	IL-11	Pentraxin 3/TSF-14
C-Reactive Protein/CRP	IL-12 p70	CXCL4/PF4
Cripto-1	IL-13	RAGE
Cystatin C	IL-15	CCL5/RANTES
Dkk-1	IL-16	RBP4
DPPIV/CD26	IL-17A	Relaxin-2
EGF	IL-18 BPa	Resistin
CXCL5/ENA-78	IL-19	CXCL12/SDF-1 alpha

Endoglin/CD105	**IL-22**	**Serpin E1/PAI-1**
EMMPRIN	**IL-23**	**SHBG**
Fas Ligand	**IL-24**	**ST2/IL1 R4**
FGF basic	**IL-27**	**CCL17/TARC**
KGF/FGF-7	**IL-31**	**TFF3**
FGF-19	**IL-32 alpha/beta/gamma**	**TfR**
Flt-3 Ligand	**IL-33**	**TGF-alpha**
G-CSF	**IL-34**	**Thrombospondin-1**
GDF-15	**CXCL10/IP-10**	**TIM-1**
GM-CSF	**CXCL11/I-TAC**	**TNF-alpha**
CXCL1/GRO alpha	**Kallikrein 3/PSA**	**uPAR**

Growth Hormone (GH)	**Leptin**	**VCAM-1**
HGF	**LIF**	**VEGF**
ICAM-1/CD54	**Lipocalin-2/NGAL**	**Vitamin D BP**

[Adapted from (https://www.rndsystems.com/products/proteome-profiler-human-xl-cytokine-array-kit_ary022b)]

APPENDIX C

Differences in Cytokine Secretion Profiles of:

- **Peri-Tumoural and Resection Margin Explants**
- **SGBS Co and SGBS Alone**

Log_2 Fold Change of Cytokines in ER+ Explant Media

(Peri-Tumoural Tissue Compared to Resection Margin)

Cytokine	ER 1	ER 2	ER 3	ER 4	ER 5	ER 6
1L-17A	0	0	0	0	0	0
1L-18 Bpa	-2.1284819	0	1.4420118	0	0	0
Adiponectin	0	0	0	-0.5142171	0	0
Angiogenin	0	-0.5243398	0	-1.9495944	-0.3808089	0.9441101
Angiopoietin-1	0	0	0	0	0	0
Angiopoietin-2	-2.0827497	0	0.680152	0	0	0
Apoliprotein A-I	0	0	0	-0.3116277	0	0
BAFF	-1.8592204	0	2.0694519	0	0	0
BDNF	0	0	0	0	0	0
C5/C5a	-1.529535	0	1.6259719	-2.8966142	0	-3.0331258
CD14	0	0	1.0769231	-1.5934455	-0.9165495	0
CD30	0	0	0	0	0	0
CD31	-0.7326928	0	1.6781069	-1.5741345	0	0
CD40 ligand	0	0	0	0	0	0
Chitinase 3-like 1	0	0.3281696	2.3658323	-0.4184004	0	1.1915793
Complement Factor D	0	0	0.1814521	0	0	0
C-Reactive Protein	-2.505614	0	1.7169355	-1.8048953	0	0
Cripto-1	0	0	0	0	0	0
Cystatin C	-0.4609154	0	2.2831147	-1.7916346	0	0
Dkk-1	0	0	1.1423151	0	0	0
DPPIV	-1.1240385	0	2.6896131	-2.3776283	0	0
EGF	-3.8539732	0	1.7164725	0	0	0
Emmprin	0.6217724	0	-0.3787432	-0.5302881	0	0
ENA-78	-0.5259757	-1.299309	2.0603337	-2.4053465	0	5.4827934
Endoglin	-1.6813631	0	1.7073685	-2.7484375	0	0
Fas Ligand	0	0	0	0	0	0
FGF basic	0	0	0	0	0	0
FGF-19	0	0	0	-2.0814104	0	0
FGF-7	0	0	0	0	0	0
Flt-3 Ligand	-1.7355721	0	2.6472135	0	0	0
G-CSF	-1.3114642	-2.384367	2.2135852	-3.0109472	0	0
GDF-15	-1.6338096	0	0.7236987	-1.5909338	0	3.1224793
GM-CSF	-1.271905	0	0	0	0	0
Growth Hormone	0	0	0	0	0	0
GROα	0	-2.4165027	2.2099293	-2.7386945	0	5.5816651
HGF	-2.0142071	0	0	-1.8852776	0	0
ICAM-1	0	0	1.3178527	-1.7705234	0	0
IFN-γ	0	0	0	0	0	0
IGFBP-2	-0.91578	0	3.4313765	-1.2347769	0	0
IGFBP-3	0	0	0	0	0	0
IL-10	0	0	0	0	0	0
IL-11	0	0	0	0	0	0
IL-12p70	0	0	0	0	0	0

IL-13	0	0	0	0	0	0
IL-15	0	0	0	0	0	0
IL-16	0	0	0	0	0	0
IL-19	0	0	0	0	0	0
IL-1ra	-1.8953053	0	0	-3.4875584	0	0
IL-1α	0	0	0	0	0	0
IL-1β	0	0	0	0	0	0
IL-2	0	0	0	0	0	0
IL-22	0	0	0	0	0	0
IL-23	0	0	0	0	0	0
IL-24	0	0	0	0	0	0
IL-27	0	0	0	0	0	0
IL-3	0	0	0	0	0	0
IL-31	0	0	0	0	0	0
IL-32	0	0	0	0	0	0
IL-33	0	0	0	-2.9857715	0	0
IL-34	0	0	0	0	0	0
IL-4	0	0	0	0	0	0
IL-5	0	0	0	0	0	0
IL-6	0	0	0	-1.0019653	0	2.6343843
IL-8	0	0	-0.1554009	0	-0.3022083	0.700179
IP-10	0	0	0	0	0	0
I-TAC	0	0	0	0	0	0
Kallikrein 3	0	0	0	0	0	0
Leptin	-0.8538879	0	0	0	0	0
LIF	-1.56729	0	0	0	0	0
Lipocalin-2	-1.265471	0	1.9309035	-0.9611666	0	0
MCP-1	0	0	0.2151667	0	0	4.2489702
MCP-3	0	0	0	0	0	0
M-CSF	0	0	0	0	0	0
MIF	0	0	0.2824122	-0.6524464	0	0
MIG	0	0	0	0	0	0
MIP-1α / MIP-1β	-3.8565977	0	0	0	0	0
MIP-3α	-3.2356698	0	0	0	0	0
MIP-3β	-1.90938	0	0	0	0	0
MMP-9	-1.0402025	0	1.95287	0	0	1.8736321
Myeloperoxidase	0	0	0	0	0	0
Osteopontin	-0.8893948	-0.9783662	1.030076	0	0	4.2071974
PDGF-AA	0	0	0	0	0	0
PDGF-AB/BB	0	0	0	0	0	0
Pentraxin 3	0	0	0	0	0	0
PF4	-2.0937888	0	0	0	0	0
RAGE	0	0	0	0	0	0
RANTES	0	0	0	0	0	0
RBP-4	0	0	1.2779619	-2.349645	-1.6183814	0
Relaxin-2	0	0	0	0	0	0
Resistin	0	0	2.1712386	0	0	0
SDF-1α	0	0	0	0	0	0
Serpin E1	0	0	0	0	0	0
SHBG	-1.3255732	0	1.3180795	-1.0573746	0	0

ST2	0	0	0.7000581	0	0	3.8511869
TARC	0	0	0	0	0	0
TFF3	-0.4199602	0	3.6974845	-2.0046967	0	1.8446236
TfR	0	0	0	0	0	0
TGF-α	0	0	0	0	0	0
Thrombospondin-1	0	0	0.9493713	0	0	0
TIM-3	-1.2876931	0	1.8079004	-1.9593358	0	0
TNF-α	0	0	0	0	0	0
uPAR	-1.8336389	0	2.0446865	-3.5336129	0	0
VCAM-1	-0.879512	0	2.4920678	-1.8489858	0	0
VEGF	-3.356329	0	0	0	0	0
Vitamin D BP	0	0	0.1200077	0	-0.6301442	0

Log_2 Fold Change of Cytokines in ER+ Explant Media (Peri-Tumoural Tissue Compared to Resection Margin)

Cytokine	TN 1	TN 2	TN 3
1L-17A	0.326902	0	0
1L-18 Bpa	2.1332693	0	0
Adiponectin	0.2022666	0	0
Angiogenin	0.1627795	0.7512488	0
Angiopoietin-1	5.0013129	0	0
Angiopoietin-2	1.3865606	0	0
Apoliprotein A-I	0.1769791	0	0
BAFF	2.4350056	0	0
BDNF	1.4762614	0	0
C5/C5a	0.5476322	0	-1.0242691
CD14	0.3455308	0	0
CD30	4.9652028	0	0
CD31	0	0	0
CD40 ligand	1.3311882	0	0
Chitinase 3-like 1	0.4146653	-0.2579927	0.3461067
Complement Factor D	0.1713562	0	0
C-Reactive Protein	0.392835	0	0
Cripto-1	14.998883	0	0
Cystatin C	0.1115787	0	0
Dkk-1	1.534754	0	0
DPPIV	0	0	0
EGF	2.3906928	0	0
Emmprin	0.200764	0	-0.3073188
ENA-78	0.4817388	2.0950647	3.175924
Endoglin	1.4795433	0	0
Fas Ligand	2.5859321	0	0
FGF basic	2.3521302	0	0
FGF-19	0.250123	0	0
FGF-7	0	0	0
Flt-3 Ligand	1.9889514	0	0
G-CSF	0.6381428	8.4072159	2.3885504
GDF-15	0.3927415	0	0
GM-CSF	2.9489519	0	0

Growth Hormone	0	0	0
GROα	0.2990156	11.754105	2.7141905
HGF	3.5865002	0	0
ICAM-1	2.0078883	0	0
IFN-γ	0.9383562	0	0
IGFBP-2	0.5910693	2.1806207	0.7345332
IGFBP-3	3.9823278	0	0
IL-10	2.0808429	0	0
IL-11	2.016306	0	0
IL-12p70	1.9493316	0	0
IL-13	9.7880505	0	0
IL-15	5.6461735	0	0
IL-16	2.206018	0	0
IL-19	0	0	0
IL-1ra	1.9726898	0	0
IL-1α	1.645726	0	0
IL-1β	6.0861644	0	0
IL-2	2.2468479	0	0
IL-22	1.1890392	0	0
IL-23	2.4429485	0	0
IL-24	1.1256981	0	0
IL-27	0	0	0
IL-3	9.0653489	0	0
IL-31	0	0	0
IL-32	0	0	0
IL-33	0	0	0
IL-34	9.8127	0	0
IL-4	1.5407146	0	0
IL-5	0	0	0
IL-6	0.2085855	0	1.8136668
IL-8	0.1524483	0	0
IP-10	5.3773398	0	0
I-TAC	2.5953805	0	0
Kallikrein 3	0.9055037	0	0
Leptin	0.9116372	0	2.132796
LIF	1.6208914	0	1.748511
Lipocalin-2	0.2999213	0	0
MCP-1	0.1046257	0	0.458557

MCP-3	0	0	0
M-CSF	1.5026136	0	0
MIF	0	0	0
MIG	3.7678438	0	0
MIP-1α / MIP-1β	5.1960805	0	0
MIP-3α	3.6599848	0	1.7097473
MIP-3β	3.018031	0	0
MMP-9	1.4093113	0	1.0604371
Myeloperoxidase	7.2784108	0	0
Osteopontin	0.8008686	1.5283814	0.8626535
PDGF-AA	2.8138241	0	0
PDGF-AB/BB	0	0	0
Pentraxin 3	0.2950242	-0.138733	0.5859856
PF4	7.4009251	0	0
RAGE	0	0	0
RANTES	5.3752613	0	0
RBP-4	0.1917234	0.9247228	0
Relaxin-2	0	0	0
Resistin	0.8063621	0	0
SDF-1α	0.81758	0	0
Serpin E1	0.1524899	0	0
SHBG	1.9686042	0	0.2560566
ST2	0.4327318	0	1.4762564
TARC	1.6377092	0	0
TFF3	0.393104	0	0
TfR	2.0516989	0	0
TGF-α	0	0	0
Thrombospondin-1	0.2262662	0	1.4635707
TIM-3	0.5043321	0	0
TNF-α	3.8874309	0	0
uPAR	0.5493565	0	0
VCAM-1	0.5035619	0	0.8046272
VEGF	1.4603158	0	0
Vitamin D BP	0.1076485	0	0

Log_2 Fold Change of Cytokines in SGBS Co-Culture

(SGBS Co Compared to SGBS Alone)

Cytokine	Experiment 1	Experiment 2	Experiment 3
1L-17A	0	0.0511648	-0.4192184
1L-18 Bpa	0	-0.06823	0.1682206
Adiponectin	0	-0.5170401	-0.4038563
Angiogenin	0	-0.4997859	-0.8429798
Angiopoietin-1	0	-0.1988714	-0.4275531
Angiopoietin-2	0	-0.0670575	-0.6288729
Apoliprotein A-I	0	-0.6052602	-0.5043949
BAFF	0	0.1879338	-0.6562973
BDNF	0	0.2051329	-0.4233278
C5/C5a	0	0.1620782	-0.461299
CD14	0	-0.7712583	-0.547486
CD30	0	0	-0.5789664
CD31	0	-0.1782532	0.3418809
CD40 ligand	0	0.1425144	-0.4251363
Chitinase 3-like 1	0	-0.1114716	-0.0593876
Complement Factor D	0	-0.0376045	-0.5821226
C-Reactive Protein	0	0.0430588	-0.0987499
Cripto-1	0	-0.2328961	-0.5937809
Cystatin C	-1.041082787	0.0615055	-0.3785362
Dkk-1	0	0.0772739	0.0351482
DPPIV	-0.390251506	-0.1134879	-0.5101924
EGF	0	-0.3302917	-0.2166613
Emmprin	0	0.072296	-0.3331538
ENA-78	1.213082176	0.6038221	0.2344306
Endoglin	0	0.394628	0.2284571
Fas Ligand	0	0.4345242	-0.7040916
FGF basic	0	-0.0993601	-0.5589795
FGF-19	0	-0.1179417	-0.4441477
FGF-7	0	-0.3425259	-0.4498701
Flt-3 Ligand	0	-0.5506271	-0.3672997
G-CSF	0	0.4815531	0.1924756
GDF-15	0	-0.0825729	-0.3049543
GM-CSF	0	0.6833064	-0.3007397

Growth Hormone	0	0.4144954	0.0861312
GROα	0	0.5194667	-0.259659
HGF	0	-0.0877854	-0.3438905
ICAM-1	0	-0.1020332	-0.8162235
IFN-γ	0	0.1529858	0.1679429
IGFBP-2	0	0.448394	-0.6182668
IGFBP-3	0.993085611	0.8664351	0.2211546
IL-10	0	0.0538309	-0.1452568
IL-11	0	0.8381874	-0.346931
IL-12p70	0	0.5790153	-0.1337413
IL-13	0	-0.0913891	-0.1875798
IL-15	0	-0.1067653	-1.0030269
IL-16	0	0.0624426	0.0506144
IL-19	0	0.0058641	0.2236372
IL-1ra	0	0.1918242	-0.3710445
IL-1α	0	0.7153218	-0.0848201
IL-1β	0	-0.3363703	-0.8613694
IL-2	0	0.4462137	-0.4267069
IL-22	0	0.0674673	-0.1996258
IL-23	0	-0.2284139	-0.0783488
IL-24	0	0.7190917	-0.396923
IL-27	0	0.3759287	0.0599757
IL-3	0	-0.1837051	-0.387429
IL-31	0	0.644333	0.2431636
IL-32	0	0.5539549	0.0159019
IL-33	0	0	0.0603417
IL-34	0	-0.1020959	-0.3934407
IL-4	0	0.0826112	0.0827682
IL-5	0	0.0535428	0.0106389
IL-6	0	0.5766311	0.0616815
IL-8	0	0.038644	-0.0135868
IP-10	0	0.1092455	0.3761255
I-TAC	0	0.6554679	0.282121
Kallikrein 3	0	0.3020172	0.0815639
Leptin	0	-0.8159894	-0.282805
LIF	0	-0.402063	0.2058263
Lipocalin-2	0	0.2186965	0.0582294
MCP-1	0.295805812	-0.3245581	-0.3491449

MCP-3	0	0.3826152	-0.3110861
M-CSF	0	1.1691657	-0.2049696
MIF	0	0.3791007	0.2540144
MIG	0	0.3079728	0.1650206
MIP-1α / MIP-1β	0	0.44725	0.0143532
MIP-3α	0	0.7174015	0.2793366
MIP-3β	0	0.3656234	-0.0816572
MMP-9	0	0.1542387	-0.1888046
Myeloperoxidase	0	0.455165	0.0637084
Osteopontin	1.101908453	-0.0462633	-0.3886257
PDGF-AA	0	-0.1893905	-0.7248767
PDGF-AB/BB	0	-1.0763584	-0.2593732
Pentraxin 3	0	-0.0815969	-0.2143751
PF4	0	-0.1525474	-1.0718843
RAGE	0	-0.30307	-0.3398511
RANTES	0	-0.586508	-0.091129
RBP-4	0	-0.631084	-0.4640245
Relaxin-2	0	0.1082639	0.2417459
Resistin	0	0.3779423	-0.0786365
SDF-1α	0	0.0734581	-0.111818
Serpin E1	0	-0.0268856	-0.0525119
SHBG	0	-1.3089184	0.1998014
ST2	0	0.0742865	-0.6121493
TARC	0	0.1710625	-0.3203369
TFF3	0	-0.4757497	-0.0555465
TfR	0	0	-0.4696164
TGF-α	0	-0.1326864	-0.319893
Thrombospondin-1	0	0.5192336	-0.025264
TIM-3	0	-0.3325415	-0.4524474
TNF-α	0	-0.2946019	-0.2537946
uPAR	0	0.0700496	-0.2969869
VCAM-1	0	-0.4404302	-0.4565372
VEGF	0.938703131	0.4806717	-0.0579766
Vitamin D BP	0	0.0559379	-0.4240364

APPENDIX D

CHI3L1 Stimulation of MCF-7 and MDA-MB-231 Cells

(Additional Data)

MCF-7 Proliferation when Cultured in the Absence and Presence of CHI3L1

(Biological repeat two of three)

A

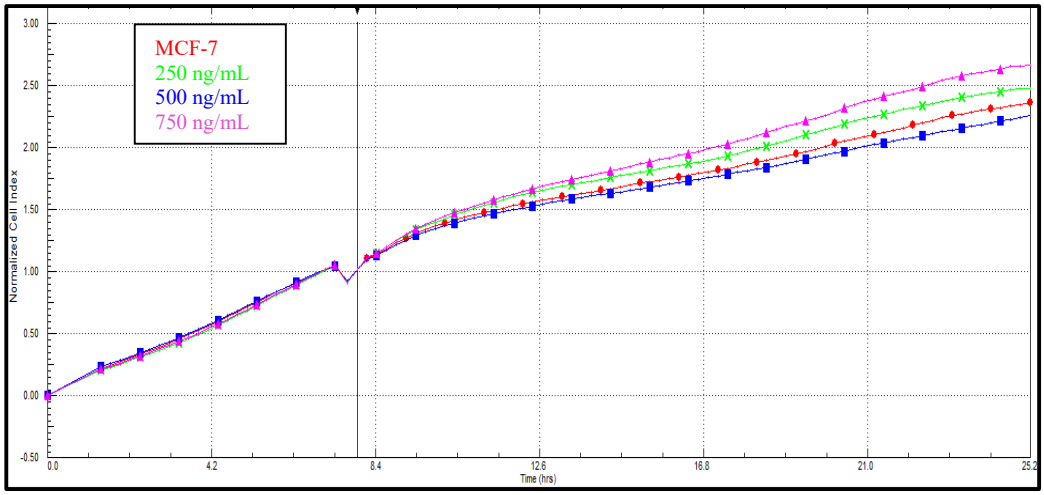

B

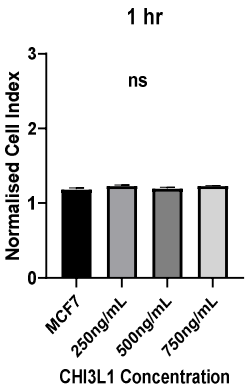

C

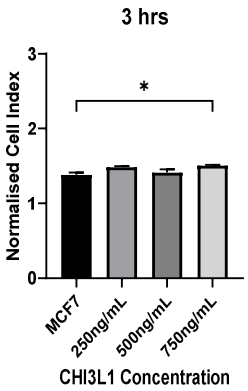

D

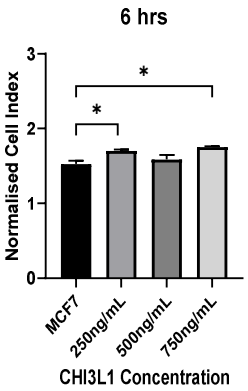

E

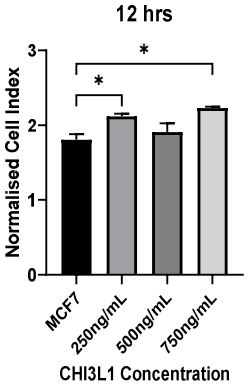

A: Graph to illustrate proliferation (as mean normalised cell indices over time) of MCF-7 cells grown in the absence and presence of CHI3L1. Readings taken every 15 min. Cell indices normalised at initiation of co-culture. Key as shown. **B, C, D, & E:** Analysis of data in **A** at (**B**) 1 h, (**C**) 3 h, (**D**) 6 h, and (**E**) 12 h post initiation of co-culture. Bars represent means ± SEM of the technical repeats. Significance is indicated by * for $p < 0.05$, and ns for *no significance*, as analysed by one-way ANOVA and Dunnett's post hoc multiple comparison test.

MCF-7 Proliferation when Cultured in the Absence and Presence of CHI3L1

(Biological repeat three of three)

A

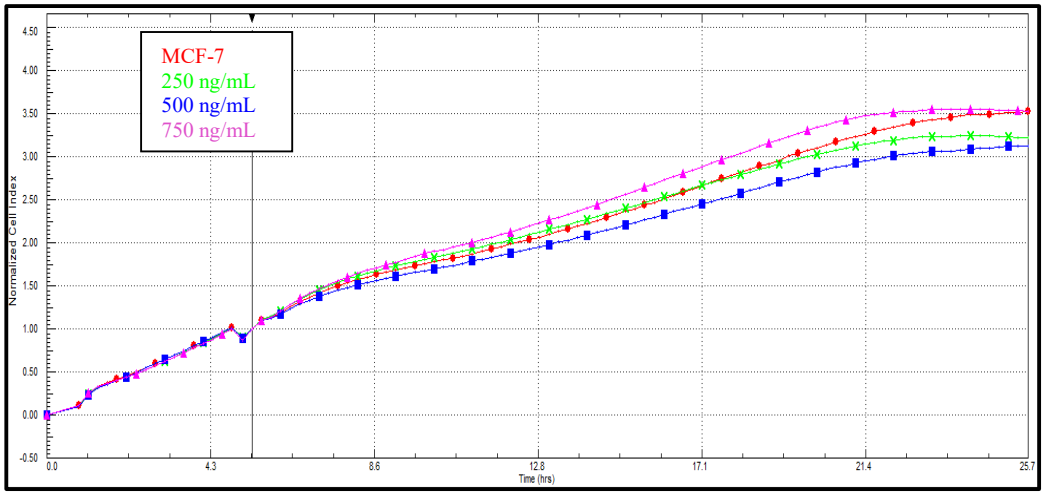

B

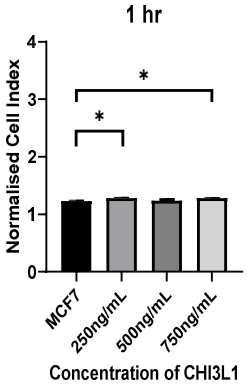

C

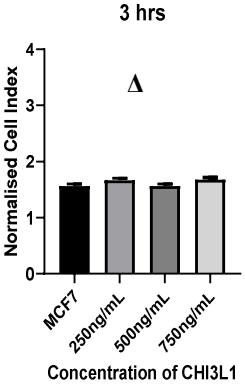

D

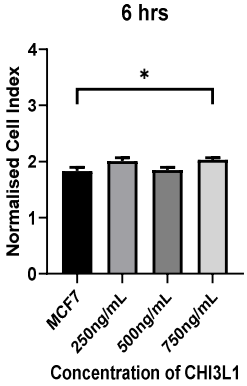

E

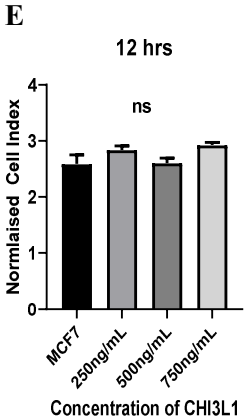

A: Graph to illustrate proliferation (as mean normalised cell indices over time) of MCF-7 cells grown in the absence and presence of CHI3L1. Readings taken every 15 min. Cell indices normalised at initiation of co-culture. Key as shown. **B, C, D, & E:** Analysis of data in **A** at (**B**) 1 h, (**C**) 3 h, (**D**) 6 h, and (**E**) 12 h post initiation of co-culture. Bars represent means ± SEM of the technical repeats. Significance is indicated by * for $p < 0.05$, and Δ for ANOVA significant but Dunnett's not significant, as analysed by one-way ANOVA and Dunnett's post hoc multiple comparison test.

MDA-MB-231 Proliferation when Cultured in the Absence and Presence of CHI3L1

(Biological repeat one of three)

A

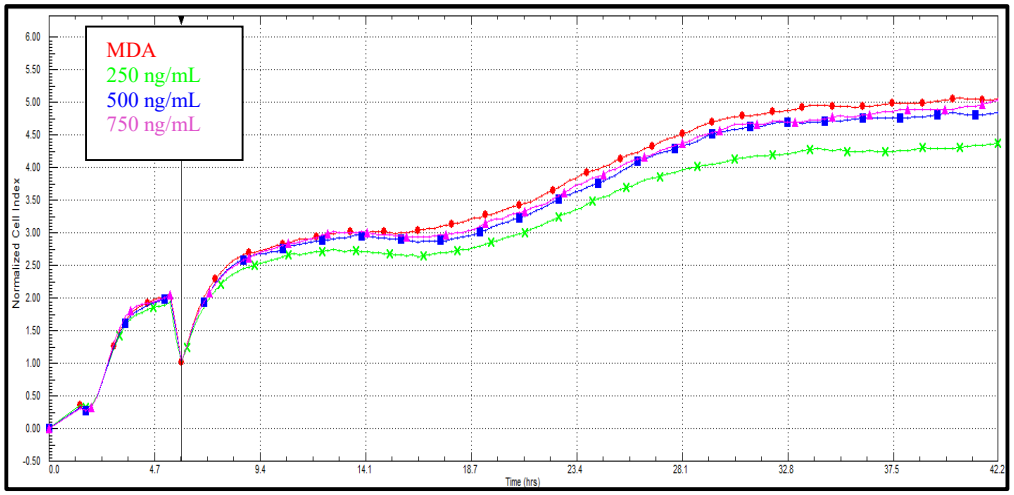

B

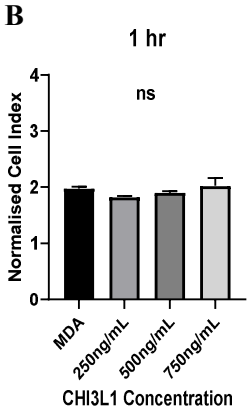

C

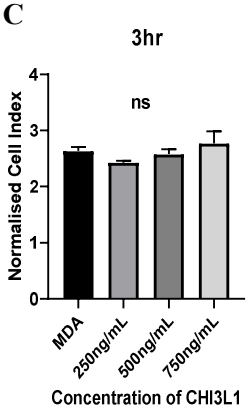

D

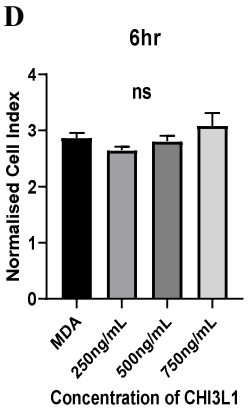

E

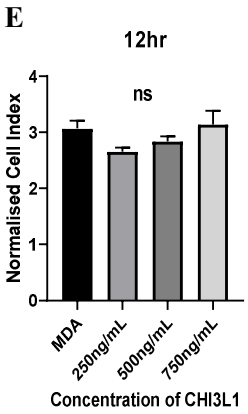

A: Graph to illustrate proliferation (as mean normalised cell indices over time) of MDA-MB-231 ('MDA') cells grown in the absence and presence of CHI3L1. Readings taken every 15 min. Cell indices normalised at initiation of co-culture. Key as shown. **B, C, D, & E:** Analysis of data in **A** at (**B**) 1 h, (**C**) 3 h, (**D**) 6 h, and (**E**) 12 h post initiation of co-culture. Bars represent means ± SEM of the technical repeats. Significance is indicated by ns for *no significance*, as analysed by one-way ANOVA and Dunnett's post hoc multiple comparison test.

MDA-MB-231 Proliferation when Cultured in the Absence and Presence of CHI3L1 (Biological repeat three of three)

A

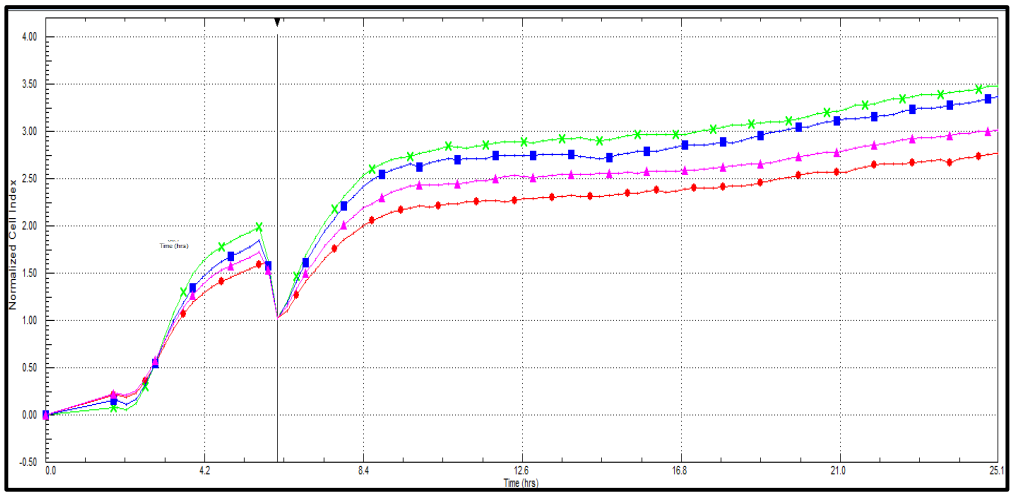

B

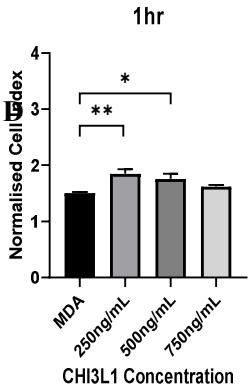

C

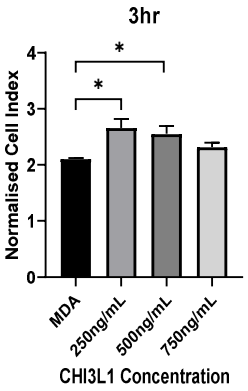

D

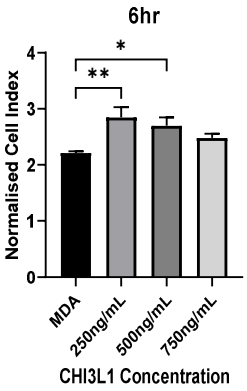

E

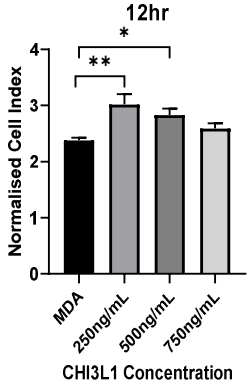

A: Graph to illustrate proliferation (as mean normalised cell indices over time) of MDA-MB-231 ('MDA') cells grown in the absence and presence of CHI3L1. Readings taken every 15 min. Cell indices normalised at initiation of co-culture. Key as shown. **B, C & D:** Analysis of data in **A** at (**B**) 3 h, (**C**) 6 h, and (**D**) 12 h post initiation of co-culture. Bars represent means ± SEM of the technical repeats. Significance is indicated by * for $p < 0.05$, and ** for $p < 0.01$, as analysed by one-way ANOVA and Dunnett's post hoc multiple comparison test.

REFERENCES

Achari AE, Jain SK. Adiponectin, a Therapeutic Target for Obesity, Diabetes, and Endothelial Dysfunction. *International Journal of Molecular Sciences,* 2017; 18: 1321 doi:10.3390/ijms18061321 (Accessed on 23.03.2018)

Alao JP. The regulation of cyclin D1 degradation: roles in cancer development and the potential for therapeutic intervention. *Mol Cancer* 2007; 6: 24 doi:10.1186/1476-4598-6-24

Aliper AM, Frieden-Korovkina VP, Buzdin A, Roumiantsev SA, Zhavoronkov A. A role for G-CSF and GM-CSF in nonmyeloid cancers. *Cancer Med* 2014; 3(4): 737-746

Badowska-Kozakiewicz AM, Patera J, Sobol M, *et al.* The Role of Oestrogen and Progesterone Receptors in Breast Cancer - Immunohistochemical Evaluation of Oestrogen and Progesterone Receptor Expression in Invasive Breast Cancer in Women. *Contemp Oncol (Pozn)* 2015; 19(3): 220-225

Balkwill FR, Capasso M, Hagemann T. The tumour microenvironment at a glance. *J Cell Sci* 2012; 125: 5591-5596

Banerjee K, Resat H. Constitutive activation of STAT3 in breast cancer cells: A review. *International Journal of Cancer* 2016; 138(11): 2570-2578

Barcellos-Hoff MH, Ravani SA. Irradiated Mammary Gland Stroma Promotes the Expression of Tumorigenic Potential by Unirradiated Epithelial Cells. *Cancer Res* 2000; 60: 1254-1260

Barchetta I, Cimini FA, Ciccarelli G, Baroni MG, Cavallo MG. *Sick fat*: the good and the bad of old and new circulating markers of adipose tissue inflammation. *J Endocrinol Invest* 2019; 42: 1257-1272

Bareche Y, Buisseret L, Grusso T. Unravelling triple-negative breast cancer tumour microenvironment heterogeneity: towards an optimized treatment approach. *J Natl Cancer Inst* 2020; 112(7): 708-719

Basen-Engquist K., Chang M. Obesity and cancer risk: recent review and evidence. *Current Oncology Reports* 2011; 13(1): 71-6

Bhat K, Sarkissyan M, Wu Y, Vadgama J. GROα overexpression drives cell migration and invasion in triple negative breast cancer cells. *Oncol Rep* 2017; 38(1):21-30

Bigg HF, Wait R, Rowan AD, *et al.* The Mammalian Chitinase-like Lectin, YKL-40, binds specifically to type I collagen and modulates the rate of type I collagen fibril formation. *J Biol Chem* 2006; 281: 21082-21095

Braunstein LZ, Taghian AG, Niemierko A, *et al.* Breast-cancer subtype, age, and lymph node status as predictors of local recurrence following breast-conserving therapy. *Breast Cancer Res Treat* 2017; 161: 173-179

Bray F, Ferlay J, Soerjomataram I, *et al.* Global Cancer Statistics 2018: GLOBOCAN Estimates of Incidence and Mortality Worldwide for 36 Cancers in 185 Countries. *Ca-Cancer J Clin* 2018; 68(6): 394-424

Burger AM, Leyland-Jones B, Banerjee K, Spyropoulos DD, Seth AK. Essential roles of IGFBP-3 and IGFBP-rP1 in breast cancer. *Eur J Cancer* 2005; 41: 1515-1527

Cancer Research UK. Undated. Breast cancer statistics. Accessed at URL: https://www.cancerresearchuk.org/health-professional/cancer-statistics/statistics-by-cancer-type/breast-cancer on 01.11.2019

Cancer Research UK. 2017. Breast screening. Accessed at URL: https://www.cancerresearchuk.org/about-cancer/breast-cancer/getting-diagnosed/screening/breast-screening on 01.11.2019

Carroll JS. Mechanisms of Oestrogen Receptor (ER) Gene Regulation in Breast Cancer. *Eur J Endocrinol* 2016; 175: R41-49

Carter JC, Church FC. Mature breast adipocytes promote breast cancer motility. *Exp Mol Pathol* 2012; 92: 312-317

Choe SS, Huh JY, Hwang IJ, Kin JI, Kim JB. Adipose tissue remodelling: its role in energy metabolism and metabolic disorders. *Front Endocrinol (Lausanne)* 2016; 7: 30 doi:10.3389/fendo.2016.00030 (Accessed on 15.02.2020)

Choi J, Cha YJ, Koo JS. Adipocyte Biology in Breast Cancer: From Silent Bystander to Active Facilitator. *Prog Lipid Res* 2018; 69: 11-20

Christodoulatos GS, Spyrou N, Kadillari J, Psallida S, Dalamaga M. The role of adipokines in breast cancer: current evidence and perspectives. *Curr Obes Rep* 2019; 8: 413-433

Christopoulous PF, Msaouel P, Koutsilieris M. The role of the insulin-like growth factor-1 system in breast cancer. *Mol Cancer* 2015; 14: 43 doi:10.1186/s12943-015-0291-7 (Accessed on 18.03.2018)

Chu D-T, Phuong TNT, Tien NLB, *et al.* The effects of adipocytes on the regulation of breast cancer in the tumour microenvironment: an update. *Cells* 2019; 8: 857 doi:10.3390/cells8080857

Cichon MA, Degnim AC, Visscher DW, *et al.* Microenvironmental Influences that Drive Progression from Benign Breast Disease to Invasive Breast Cancer. *J Mammary Gland Biol Neoplasia* 2010; 15: 389-397

Cohen N, Shani O, Raz Y, *et al.* Fibroblasts drive an immunosuppressive and growth-promoting microenvironment in breast cancer via secretion of Chitinase 3-like 1. *Oncogene* 2017; 36: 4457-4468

Colcotta F, Allavena P, Sica A, Garlanda C, Mantovani A. Cancer-related inflammation, the seventh hallmark of cancer: links to genetic instability. *Carcinogenesis* 2009; 30(7): 1073-1081

Comsa S, Cimpean AM, Raica M. The Story of MCF-7 breast cancer cell line: 40 years of experience in research. *Anticancer Res* 2015; 35: 3147-3154

Couldrey C, Moitra J, Vinson C, *et al.* Adipose tissue: a vital in vivo role in mammary gland development but not differentiation. *Dev Dyn* 2002; 223: 459-488

D'Esposito V, Passaretti F, Hammarstedt A, *et al.* Adipocyte-released insulin-like growth factor-1 is regulated by glucose and fatty acids and controls breast cancer cell growth in vitro. *Diabetologia* 2012; 55: 2811-2822

Dirat B, Bochet L, Dabek M, *et al.* Cancer-associated adipocytes exhibit an activated phenotype and contribute to breast cancer invasion. *Cancer Res* 2011; 71(7): doi:10.1158/0008-5472.CAN-10-3323

Divella R., De Luca R., Abbate I, *et al.* Obesity and cancer: the role of adipose tissue and adipo-cytokines-induced chronic inflammation. *Journal of Cancer* 2016; 7(15): 2346-59

Dixon JM, Barber MD. (Eds.) 2019. A Companion to Specialist Surgical Practice: Breast Surgery. 6th Edition. London: Elsevier

Dominiak A, Chelstowska B, Olejarz W, Nowicka G. Communication in the cancer microenvironment as a target for therapeutic interventions. *Cancers* 2020; 12: 1232 doi:10.3390/cancers12051232

Ellis H, Mahadevan V. 2010. *Clinical Anatomy.* 12th Edition. Singapore: Wiley-Blackwell

Engelman JA, Luo J, Cantley LC. The evolution of phosphatidylinositol 3-kinases as regulators of growth and metabolism. *Nat Rev Genet* 2006; 7: 606-619

Esquivel-Velazquez M, Ostoa-Saloma P, Placios-Arreola MI, *et al.* The Role of Cytokines in Breast Cancer Development and Progression. *J Interferon Cytokine Res* 2015; 35(1) doi.org/10.1089/jir.2014.0026

Eurich K, Segawa M, Toei-Shimizu S, *et al.* Potential role of chitinase 3-like-1 in inflammation-associated carcinogenic changes of epithelial cells. *World J Gastroenterol* 2009; 15(42) 5249-5259

European Collection of Authenticated Cell Cultures. 2017. Cell line profile: MDA-MB-231. Accessed at https://www.phe-culturecollections.org.uk/media/133182/mda-mb-231-cell-line-profile.pdf in February 2019

Fain JN, Madan AK, Hiler ML, Cheema P, Bahouth SW. Comparison of the release of adipokines by adipose tissue, adipose tissue matrix, and adipocytes from visceral and subcutaneous abdominal adipose tissues of obese humans. *Endocrinology* 2004; 145(3): 2273-2282

Feng Y, Spezia M, Huang S, *et al.* Breast cancer development and progression: risk factors, cancer stem cells, signalling pathways, genomics, and molecular pathogenesis. *Genes and Diseases* 2018; 5: 77-106

Fischer-Posovszky P, Newell FS, Wabitsch M, *et al.* Human SGBS cells - a unique tool for studies of human fat cell biology. *Obesity Facts* 2008; 1: 184-189

Francescone RA, Scully S, Faibish M, *et al.* Role of YKL-40 in the angiogenesis, radioresistance, and progression of glioblastoma. *J Biol Chem* 2011; 286(17): 15332-15343

Friedman J. Leptin at 20: an overview. *Int J Endocrinol* 2014; 223: T1-T8

Gallagher E, LeRoith D. Obesity and diabetes: the increased risk of cancer and cancer-related mortality. *Physiological Reviews* 2015; 95(3): 727-48

Gao D, Rahbar R, Fish E. CCL5 activation of CCR5 regulates cell metabolism of breast cancer cells. *Open Biol* 2016; 6: 160122 doi.org/10.1098/rsob.160122

Ghaben AL, Scherer PE. Adipogenesis and Metabolic Health. *Nat Rev Mol Cell Biol* 2019; 20: 242-258

Guerrero-Zotano A, Mayer IA, Arteaga CL. PI3K/AKT/mTOR: role in breast cancer progression, drug resistance, and treatment. *Cancer Metastasis Rev* 2016; 35(4): 515-524

Guille A, Chaffanet M, Birnbaum D. Signalling pathway switch in breast cancer. *Cancer Cell Int* 2013; 13: 66 doi:10.1186/1475-2867-13-66

Gunter MJ, Hoover DR, Yu H, *et al.* Insulin, insulin-like growth factor-1, and risk of breast cancer in postmenopausal women. *J Natl Cancer Inst* 2009; 101: 48-60

Hajer GR, van Haeften TW, Visseren FLJ. Adipose tissue dysfunction in obesity, diabetes, and vascular diseases. *Eur Heart J* 2008; 29(24): 2959-71

Hamilton G, Rath B, and Burghuber O. Chitinase-3-like-1/YKL-40 as marker of circulating tumor cells. *Trans Lung Cancer Res* 2015; 4(3): 287-291

Hanahan D, Weinberg RA. The Hallmarks of Cancer. *Cell* 2000; 100: 57-70

Hanahan D, Weinberg RA. Hallmarks of Cancer: The Next Generation. *Cell* 2011; 144: 646-674

Harvey AJ. 2019. 'Overview of cell signalling pathways in cancer' in Badve S, Kumar GL (Eds.) *Predictive biomarkers in oncology*. Switzerland: Springer, pp 167-182

He CH, Lee CG, Dela Cruz, *et al*. Chitinase 3-like 1 regulates cellular and tissue responses via IL-13 receptor α2. *Cell Rep* 2013; 4(4): 830-841

Hicks DG, Kulkarni S. HER2+ Breast Cancer. Review of Biologic Relevance and Optimal Use of Diagnostic Tools. *Am J Clin Pathol* 2008; 129: 267-273

Hocevar BA, Howe PH. Mechanisms of TGF-beta-induced cell cycle arrest. *Miner Electrolyte Metab* 1998; 24(2-3): 131-135

Holliday DL, Speirs V. Choosing the right cell line for breast cancer research. *Breast Cancer Res* 2011; 13(14): 215

Hong JT, Son DJ, Lee CK, *et al*. Interleukin 32, inflammation and cancer. *Pharmacol and Therapeut* 2017; 174: 127-137

Horst RT, Jaeger M, Smeekens SP, *et al*. Host and Environmental Factors Influencing Individual Human Cytokine Responses. *Cell* 2016; 167(4): 1111-1124

Housa D, Housova J, Vernerova Z, Haluzik M. Adipocytokines and Cancer. *Physiol Res* 2006; 5(3): 233-44

Hovey RC, Aimo L. Diverse and Active Roles for Adipocytes During Mammary Gland Growth and Function. *J Mammary Gland Biol Neoplasia* 2010; 15: 279-290

Hoy AJ, Balaban S, Saunders DN. Adipocyte-Tumor Cell Metabolic Crosstalk in Breast Cancer. *Trends Mol Med* 2017; 23(5): 381-392

Hu M, Polyak K. Molecular characterisation of the tumor microenvironment in breast cancer. *Eur J Cancer* 2008; 44(18): 2760-2765

Hu X, Juneja SC, Mahile NJ, Cleary MP. Leptin - a growth factor in normal and malignant breast cells and for normal mammary gland development. *J Natl Cancer Inst* 2002; 94: 1704-11

Human Protein Atlas. 2020. Breast cancer. Accessed at URl: https://www.proteinatlas.org/learn/dictionary/pathology/breast+cancer+2 on 06.06.2020

Hwang HJ, Lee Y-R, Kang D, *et al.* Endothelial cells under therapy-induced senescence secrete CXCL11, which increases aggressiveness of breast cancer cells. *Cancer Lett* 2020; 490: 100-110

Inman JL, Robertson C, Mott JD, *et al.* Mammary gland development: cell fate specification, stem cells and the microenvironment. *Development* 2015; 142: 1028-42

Iqbal N, Iqbal N. Human epidermal growth factor receptor 2 (HER2) in cancers: overexpression and therapeutic implications. *Mol Biol Int* 2014; 852748

Javed A, Lteif A. Development of the Human Breast. *Semin Plast Surg* 2013; 27: 5-12

Jensen BV, Johansen JS, and Price PA. High levels of serum HER-2/neu and YKL-40 independently reflect aggressiveness of metastatic breast cancer. *Clin Can Res* 2003; 9: 4423-4434

Jiramongkol Y, Lam EW-F. Multifaceted Oncogenic Role of Adipocytes in the Tumour Microenvironment. *Adv Exp Med Biol* 2020; 1219: 125-142

Johansen JS, Bojesen SE, Tybjaerg-Hansen A, Mylin AK, Price PA, Nordestgaard BG. Plasma YKL-40 and total and disease-specific mortality in the general population. *Clin Chem* 2010; 56(10): 1580-91

John Hopkins Medicine Pathology [John Hopkins University]. 2020. Breast Cancer & Pathology. Accessed at URL: https://pathology.jhu.edu/breast/staging-grade on 02.08.2020

Jones SA, Jenkins BJ. Recent insights into targeting the IL-6 cytokine family in inflammatory diseases and cancer. *Nat Rev Immunol* 2018; (12): 773-789

Kadomoto S, Izumi K, Mizokami A. The CCL20-CCR6 axis in cancer progression. *Int J Mol Sci* 2020; 21: 5186 doi:10.3390/ijms21155186

Kan T, Feldman E, Timaner M, *et al.* IL-31 induces antitumor immunity in breast carcinoma. *J Immunother Cancer* 2020; 8: e001010 doi.1136/jitc-2020-001010

Kang EJ, Jung H, Woo OH, Park KW, Woo SU, Yang DS, *et al.* YKL-40 expression could be a poor prognostic marker in the breast cancer tissue. *Tumour Biol* 2014; 35(1): 277-86

Karastergiou K, Mohamed-Ali V. The autocrine and paracrine roles of adipokines. *Mol Cell Endocrinol* 2010; 318: 69-78

Kashani IR, Barbarestani M, Etesam F, *et al.* Human preadipocytes inhibit proliferation of MCF-7 Breast Cancer Cell Line. *Acta Medica Iranica* 2006; 44(5): 291-298

Kaur T, Zhang Z-F. Obesity, breast cancer and the role of adipocytokines. *Asian Pacific J Cancer Prev* 2005; 6: 547-552

Kawakami K, Kawakami M, Puri RK. Specifically targeted killing of interleukin-13 (IL-13) receptor-expressing breast cancer by IL-13 fusion cytotoxin in animal model of human disease. *Mol Cancer Ther* 2003; 3: 137-147

Kim HS, Jung M, Choi SK, *et al.* IL-6-mediated cross-talk between human preadipocytes and ductal carcinoma in situ in breast cancer progression. *J Exp Clin Cancer Res* 2018; 37(1): 200 doi:10.1186/s13046-018-0867-3 (Accessed on 16.04.2020)

Kzhyshkowska J, Yin S, Liu T, *et al.* Role of chitinase-like proteins in cancer. *Biol Chem* 2016; 397(3): 231-47

Lazebnik Y. Comment: What are the hallmarks of cancer? *Nat Rev Cancer* 2010; 10: 232:233

Lee AV, Oesterreich S, Davidson NE. MCF-7 Cells - changing the course of breast cancer research and care for 45 years. *J Natl Cancer Inst* 2015; 107(7): 1-4

Lee CG, Hartl D, Lee GR, *et al.* Role of breast regression protein 39 (BRP-39)/chitinase 3-like-1 in Th2 and IL-13-induced tissue responses and apoptosis. *J Exp Med* 2009; 206(5): 1149-1166

Lee J, Hong BS, Ryu HS, *et al.* Transition into inflammatory cancer-associated adipocytes in breast cancer microenvironment requires microRNA regulatory mechanism. *PLoS One* 2017; 12(3): e0174126

Lee YS, Kim J-w, Osborne O, *et al.* Increased adipocyte O_2 consumption triggers HIF-1α, causing inflammation and insulin resistance in obesity. *Cell,* 2014; 157(6): 1339-52

Lehr S, Hartwig S, Sell H. Adipokines: a treasure trove for the discovery of biomarkers for metabolic disorders. *Proteomics Clin Appl* 2012; 6: 91-101

Leitner L, Jurets A, Itariu BK, *et al.* Osteopontin promotes aromatase expression and estradiol production in human adipocytes. *Breast Cancer Res Treat* 2015; 154: 63-69

Levy DE, Lee C-k. What does Stat3 do? *The Journal of Clinical Investigation* 2002; 109: 1143-8

Li C, Uribe DJ. Clinical characteristics of different histological types of breast cancer. *British Journal of Cancer* 2005; 93 (9): 1046-52

Li NY, Weber CE, Mi Z, *et al.* Osteopontin upregulates critical epithelial-mesenchymal transition transcription factors to induce an aggressive breast cancer phenotype. *J Am Coll Surg* 2013; 217(1): 17-26

Liberti MV, Locasale JW. The Warburg Effect: How Does it Benefit Cancer Cells? *Trends Biochem Sci* 2016; 41(3):2 11-218

Libreros S, Garcia-Areas R, and Iragavarapu-Charyulu V. CHI3L1 plays a role in cancer through enhanced production of pro-inflammatory/pro-tumorigenic and angiogenic factors. *Immunol Res* 2013; 57(0): 99-105

Libreros S, Iragavarapu-Charyulu V. YKL-40/CHI3L1 drives inflammation on the road of tumor progression. *J Leukoc Biol* 2015; 98(6): 931-936

Liu L, Wang M, Ma ZB, *et al.* The role of adiponectin in breast cancer: a meta-analysis. *PLoS One* 2013; 8(8): e73183

Liu L, Liu Y, Yan X, Zhou C, Xiong X. The role of granulocyte colony-stimulating factor in breast cancer development: A review. *Mol Med Rep* 2020; 21: 2019-2029

Lucey BP, Nelson-Rees WA, Hutchins GM. Henrietta Lacks, HeLa Cells, and Cell Culture Contamination. *Arch Pathol Lab Med* 2009; 133: 1463-7

Lykkesfeldt AE, Briand P. Indirect mechanism of oestradiol stimulation of cell proliferation of human breast cancer cell lines. *Br J Cancer* 1986; 53: 29-35

Ma Y, Ren Y, Dai Z-J, *et al.* IL-6, IL-8 and TNF-α levels correlate with disease stage in breast cancer patients. *Adv Clin Exp Med* 2017; 26(3): 421-426

Macias H, Hinck L. Mammary Gland Development. *Wiley Interdiscip Rev Biol* 2012; 1(4): 533-57

Maffini MA, Soto AM, Calabro JM, Ucci AA, Sonnenschein C. The stroma as a crucial target in rat mammary gland carcinogenesis. *J Cell Sci* 2003; 117: 1495-1502

Makki J. Diversity of breast carcinoma histological subtypes and clinical relevance. *Clinical Medicine Insights: Pathology* 2015; 8: 23-31

Malhotra GK, Zhao X, Band H, Band V. Histological, molecular and functional subtypes of breast cancers. *Cancer Biol Ther* 2010; 10(10): 955-960

Manabe Y, Toda S, Miyazaki K, Sugihara H. Mature adipocytes, but not preadipocytes, promote the growth of breast carcinoma cells in collagen gel matrix culture through cancer-stromal cell interactions. *J Pathol* 2003; 201: 221-228

Matthews SB, Thompson HJ. The obesity-breast cancer conundrum: an analysis of the issues. *Int J Mol Sci* 2016; 17: 989 doi:10.3390/ ijms17060989 (Accessed on 15.03.2018)

Mauer J. Versatile functions for IL-6 in metabolism and cancer. *Trends Immunol* 2015; 36(2): 92-101

McGuire A, Brown AL, Malone C, McLaughlin R, Kerin MJ. Effects of Age on the Detection and Management of Breast Cancer. *Cancers* 2015; 7: 908-929

McInnes KL, Brown KA, Knower KC, *et al.* Characterisation of aromatase expression in the human adipocyte cell line SGBS. *Breast Cancer Res Treat* 2008; 12(3): 429-35

Miller DM, Thomas SD, Islam A, *et al.* c-Myc and cancer metabolism. *Clin Cancer Res* 2012; 18(20): 5346-53

Mitri Z, Constantine T, O'Regan R. The HER2 receptor in breast cancer: pathophysiology, clinical use, and new advances in therapy. *Chemother Res Pract* 2012; 743193

Moore KL, Dalley AF. 1999. Clinically Oriented Anatomy. 4th Edition. London: Lippincott Williams & Wilkins, pp 72-79

Nassiri F, Cusimano MD, Scheithauer BW, *et al.* Endoglin (CD105): A review of its role in angiogenesis and tumor diagnosis, progression and therapy. *Anticancer Res.* 2011; 31: 2283-2290

National Cancer Institute. Undated. Cancer: A Historic Perspective. Accessed at URL: https://training.seer.cancer.gov/disease/history/ on 26.07.2020

Neve RM, Chin K, Fridlyand J, *et al.* A collection of breast cancer cell lines for the study of functionally distinct cancer subtypes. *Cancer Cell* 2006; 10(6): 515-527

Nickel A, Blucher C, Al Kadri O, *et al.* Adipocytes induce distinct gene expression profiles in mammary tumor cells and enhance inflammatory signalling in invasive breast cancer cells. *Sci Rep* 2018; 8: 9482

Office for National Statistics (UK). 2016. Incidence of, and mortality from, malignant neoplasm of breast in England, 2004-2014. Accessed at URL: https://www.ons.gov.uk/peoplepopulationandcommunity/healthandsocialcare/conditionsanddiseases/adhocs/007864incidenceofandmortalityfrommalignantneoplasmofbreastinengland2004to2016 on 04.07.2020

Office for National Statistics (UK). 2019. Cancer survival in England: adults diagnosed between 2013 and 2017 and followed up to 2018. Accessed at URL: https://www.ons.gov.uk/peoplepopulationandcommunity/healthandsocialcare/conditionsanddiseases/bulletins/cancersurvivalinengland/stageatdiagnosisandchildhoodpatientsfollowedupto2018 on 04.07.2020

Okamoto H, Yoshimatsu Y, Tomizawa T, *et al.* Interleukin-13 receptor α2 is a novel marker and potential therapeutic target for human melanoma. *Sci Rep* 2019; 9(1): 1281 doi: 10.1038/s41598-019-39018-3

Ouchi N, Parker JL, Lugus JJ, Walsh K. Adipokines in inflammation and metabolic disease. *Nat Rev Immunol* 2011; 11(2): 85-97

Pallegar NK, Christian SL. 2020. Adipocytes in the Tumour Microenvironment. In: Birbrair A (Ed.). *Tumour Microenvironment Advances in Experimental Medicine and Biology*. Chan: Springer

Park J, Kang S-E, Ahn KS, *et al.* Inhibition of the PI3-AKT-mTOR pathway suppresses the adipocyte-mediated proliferation and migration of breast cancer cells. *J Cancer* 2020; 11: 2552-2559

Picon-Ruiz M, Chendong P, Drews-Elger K, *et al.* Interactions between adipocytes and breast cancer cells stimulate cytokine production and drive Src/Sox2/miR-302b-mediated malignant progression. *Cancer Res* 2016; 76(2): 491-504

Prakash M, Bodas M, Prakash D, *et al.* Diverse pathological implications of YKL-40: answers may lie in 'outside-in' signalling. *Cell Signal* 2013; 25: 1567-1573

Protani M, Coory M, Martin JH. Effect of obesity on survival of women with breast cancer: systematic review and meta-analysis. *Breast Cancer Res Treat* 2010; 123: 627-635

Public Health England. 2018. Blog: PHE Screening. Breast screening performance report shows we are detecting cancers early but uptake is falling. Accessed at URL: https://phescreening.blog.gov.uk/2018/02/06/breast-screening-performance-report-shows-we-are-detecting-cancers-early-but-uptake-is-falling/ on 19.07.2020

Pujol E, Proenza AM, Roca P, Liado I. Changes in mammary fat pad composition and lipolytic capacity throughout pregnancy. *Cell Tissue Res* 2006; 323: 505-511

R&D Systems. 2017. Proteome Profiler™ Array Human XL Cytokine Array Kit: Package Insert; Array Procedure. Minneapolis: Bio-Techne, pp 6-7

Richard V, Kindt N, Saussez S. Macrophage migration inhibitory factor involvement in breast cancer (Review). *Int J Oncol* 2015; 47: 1627-1633

Romero-Moreno R, Curtis KJ, Coughlin TR, *et al.* The CXCL5/CXR2 axis is sufficient to promote breast cancer colonization during bone metastasis. *Nat Commun* 2019; 10: 4404 doi:10.1038/s41467-019-12108-6

Rosenfeld S. Are the somatic mutation and tissue organisation field theories of carcinogenesis incompatible? *Cancer Inform* 2013; 12: 221-229

Rosenow A, Arrey TN, Bouwman FG, *et al.* Identification of novel human secreted proteins by using SGBS cells. *J Proteome Res* 2010; 9(10): 5389-5401

Roslind A, Knoop AS, Jensen M-B, *et al.* YKL-40 protein expression is not a prognostic marker in patients with primary breast cancer. *Breast Cancer Res Treat* 2008; 112: 275-285

Russo VC, Azar WJ, Yau SW, Sabin MA, Wether GA. IGFBP-2: the dark horse in metabolism and cancer. *Cytokine Growth Factor Rev* 2015; 26(3): 329-46

Rutkowski JM, Davis KE, Scherer PE. Mechanisms of obesity and related pathologies: the macro- and microcirculation of adipose tissue. *FEBS J* 2009; 276(20): 5738-46

Rybinska I, Agresti R, Trapani A, Tagliabue E, Triulzi T. Adipocytes in Breast Cancer, the Thick and Thin. *Cells* 2020; 9(560): 1-22

Saely CH, Geiger K, Drexel H. Brown versus white adipose tissue: a mini-review. *Gerontology* 2012; 58(1): 15-23

Schedin P, Hovey RC. Editorial: The mammary stroma in normal development and function. *J Mammary Gland Biol Neoplasia* 2010; 15: 275-277

Scully S, Yan W, Bentley B, *et al.* Inhibitory activity of YKL-40 in mammary epithelial cell differentiation and polarization induced by lactogenic hormones: a role in mammary tissue involution. *PLoS One* 2011; 6(10): e25819

Sethi G, Sung B, Aggarwal BB. TNF: a master switch for inflammation to cancer. *Front Biosci* 2008; 13: 5094-5107

Shah R, Rosso K, Nathanson SD. Pathogenesis, Prevention, Diagnosis and Treatment of Breast Cancer. *World J Clin Oncol* 2014; 5(3): 283-298

Shao R, Hamel K, Petersen L, Cao QJ, Arenas RB, Bigelow C, *et al.* YKL-40, a secreted glycoprotein, promotes tumour angiogenesis. *Oncogene* 2009; 28: 4456-4468

Shao R, Cao QJ, Arenas RB, Bigelow C, Bentley B, Yan W. Breast cancer expression of YKL-40 correlates with tumour grade, poor differentiation, and other cancer markers. *Br J Cancer* 2011; 105(8): 1203-9

Shao R. YKL-40 acts as an angiogenic factor to promote tumor angiogenesis. *Front Physiol* 2013; 4(133): 1-9

Shao Y, Zhao F-Q. Emerging evidence of the physiological role of hypoxia in mammary gland development and lactation. *J Anim Sci Biotechnol* 2014; 5: 9 doi:10.1186/2049-1891-5-9

Siriwardhana N, Layman R, Karwandyar A, *et al.* Inflammatory cytokines link obesity and breast cancer. *J Metabolic Synd* 2012; 1: 102 doi:10.4172/2167-0943. 1000102

Skandalakis J. 2009. 'Embryology and Anatomy of the Breast' in: Shiffman M. (Ed.) *Breast Augmentation*. Heidelberg: Springer Berlin, pp3-24 Accessed at https://doi.org/10.1007/978-3-540-78948-2_1 on 23.11.2019

Skurk T, Alberti-Huber C, Herder C, *et al.* Relationship between adipocyte size and adipokine expression and secretion. *J Clin Endocrinol Matab* 2007; 92(3): 1023-1933

Solis-Pereyra B, Aattouri N, Lemonnier D. Role of food in the stimulation of cytokine production. *Am J Clin Nutr* 1997; 66: 521-525

Sondka Z, Bamford S, Cole CG, *et al.* The COSMIC cancer gene census: describing genetic dysfunction across all human cancers. *Nat Rev Cancer* 2018; 18: 696-705

Sonnenschein C, Soto AM. Somatic mutation theory of carcinogenesis: why it should be dropped and replaced. *Mol Carcinog* 2000; 29(4): 205-11

Soto AM, Sonnenschein C. One hundred years of somatic theory of carcinogenesis: Is it time to switch? *Bioessay* 2014; 36(1): 118-120

Stenkula KG, Erlanson-Albertsson C. Adipose cell size: importance in health and disease. *Am J Physiol Regul Integr Comp Physiol* 2018; 315: R284-R295

Stephens PJ, Tarpey PS, Davies H, *et al.* The landscape of cancer genes and mutational processes in breast cancer. *Nature* 2012; 486: 400-403

Subik K, Lee J-F, Baxter L, *et al.* The expression patterns of ER, PR, HER2, CK5/6, EGFR, Ki-67 and AR by immunohistochemical analysis in breast cancer cell lines. *Breast Cancer: Basic and Clinical Research* 2010; 4: 35-41

Tokunaga R, Zhang W, Naseem M, *et al.* CXCL9, CXCL10, CXCL11/CXCR3 axis for immune activation - a target for novel cancer therapy. *Cancer Treat Res* 2018; 63: 40-47

Toren P, Mora BC, Venkateswaran V. Diet, obesity, and cancer progression: are adipocytes the link? *Lipid Insights* 2013; 6: 37-45

Travis RC, Key TJ. Oestrogen exposure and breast cancer risk. *Breast Cancer Res.* 2003; 5: 239-247

Trayhurn P, Wood S. Adipokines: inflammation and the pleiotropic role of white adipose tissue. *Br J Nutr* 2004; 92(3): 347-55

Vasconcellos R, Medrado NV, Mileib R, *et al.* Behaviour of adipocytes in the mammary niche during pregnancy and lactation. *J Stem Cell Res Ther* 2019; 5(1): 1-6

Wabitsch M, Brenner RE, Melzner I, *et al.* Characterization of a human preadipocyte cell strain with high capacity for adipose differentiation. *Int J Obes* 2001; 25: 8-15

Wang C, Gao C, Meng K, Qiao H, Wang Y. Human adipocytes stimulate invasion of breast cancer MCF-7 cells by secreting IGFBP-2. *PLoS One* 2015; 10(3): e0119348 doi:10.1371/journal.pone.0119348

Wang F, Gao S, Chen F, *et al.* Mammary Fat of Breast Cancer: Gene Expression Profiling and Functional Characterization. *PLoS One* 2014; 9(10): e109742 doi:10.1371/journal.pone.0109742

Wang X, Yang L. Tumour necrosis factor and cancer, buddies or foes? *Acta Pharmacol Sin* 2008; 29(11): 1275-1288

Wang Y, Attane C, Milhas D, *et al.* Mammary adipocytes stimulate breast cancer invasion through metabolic remodeling of tumor cells. *J Cl Insight* 2017; 2(4): e87489

Warburg O. The Metabolism of Carcinoma Cells. *Cancer Res* 1925; 9(1): 148-163

Wensveen FM, Valentic S, Sestan M, *et al.* The "big bang" in obese fat: events initiating obesity-induced adipose tissue inflammation. *Eur J Immunol* 2015; 45: 2446-2456

World Cancer Research Fund. 2018. Breast cancer statistics. Accessed at URL: https://www.wcrf.org/dietandcancer/cancer-trends/breast-cancer-statistics on 09.08.2020

World Health Organisation. © 2018. *Obesity and overweight* [online]. Available from: http://www.who.int/news-room/fact-sheets/detail/obesity-and-overweight (Accessed on 15.03.2018).

World Health Organisation. 2020. Breast Cancer: prevention and control. Accessed at URL: https://www.who.int/cancer/detection/breastcancer/en/ on 09.08.2020

World Obesity Federation. © 2015. *How is obesity measured?* [online]. Available from: https://www.worldobesity.org/data/cut-points-used/ (Accessed on 23.03.2018)

Wu Q, Li B, Li Z, *et al.* Cancer-associated adipocytes: key players in breast cancer progression. *J Haematol Oncol* 2019; 12: 95 doi:10.1186/s13045-019-0778-6

Yao-Borengasser A, Monzavi-Karbassi B, Hedges RA, *et al.*, Adipocyte hypoxia promotes epithelial-mesenchymal transition-related gene expression and estrogen receptor-negative phenotype in breast cancer cells. *Oncol Rep* 2015; 33: 2689-2694

Yeo IJ, Lee C-K, Han S-B, *et al.* Roles of chitinase 3-like 1 in the development of cancer, neurodegenerative diseases, and inflammatory diseases. *Pharmacol Ther* 2019; 209: 107394 doi:10.1016/j.pharthera.2019.107394

Yousef EM, Tahir MR, S-Pierre Y, *et al.* MMP-9 expression varies according to molecular subtypes of breast cancer. *BMC Cancer* 2014: 14: 609 doi: 10.1186/1471-2407-14-609

Zagotta I, Dimova EY, Debatin K-M, *et al.* Obesity and inflammation: reduced cytokine expression due to resveratrol in a human *in vitro* model of inflamed adipose tissue. *Front Pharmacol* 2015; 6: 79 doi: 10.3389/fphar.2015.00079

Zewdu A, Casadei L, Pollock RE, Braggio D. Adipose Tumour Microenvironment. *Adv Exp Med Biol* 2020; 1226: 73-86

Zhao Y, Zhang X, Zhao H, *et al*. CXCL5 secreted from adipose tissue-derived stem cells promotes cancer cell proliferation. *Oncol Lett* 2018; 15: 1403-1410

Zou A, Lambert D, Yeh H, *et al*. Elevated CXCL1 expression in breast cancer stroma predicts poor prognosis and is inversely associated with expression of TGF-β signalling proteins. *BMC Cancer* 2014; 14: 781